The detection by conductivity of the effect of protein tagging on immobilisation within monolith columns and development of a novel free sialic acid detector

Thesis submitted for the degree of
Doctor of Philosophy

By
Vincent O'Shea B.Sc.

Supervised by
Brendan O'Connor B.Sc., Ph.D
School of Biotechnology
&
Prof Brett Paull B.Sc., Ph.D
School of Chemical Sciences

Dublin City University
Ireland
November 2009

Declaration

I hereby certify that this material, which I now submit for assessment on the programme of study leading to the award of Degree of Doctor of Philosophy, is entirely my own work, that I have exercised reasonable care to ensure that the work is original, and does not to the best of my knowledge breach any law of copyright, and has not been taken from the work of others save and to the extent that such work has been cited and acknowledged within the text of my work.

Signed: _____ (Candidate) ID No.: _____ Date: _____

Acknowledgments

Firstly I'd like to thank both my supervisors, Brendan and Brett for having such faith in me. I don't think I could have been luckier when it came to support received from "up high"

Thanks to Mick, Paul, Roisin and Damian, for being there for all the day to day problems, questions and guidance. Words can't express my gratitude for all the help you have provided me whether I knew about it or not!

Thirdly, thanks to Damien, Ken, Kuba, Mary and Ruth and everyone else in the School of Biotech who I ran into over the last four years, lads it's been emotional!

Thanks to my family, whose constant and unwavering support I can always rely on.

To Aileen, by far the best part of the Ph.D.

Finally I would like to dedicate this thesis to Dad, who despite not being with us, I know would be proud.

Table of Contents:

List of Figures

List of Tables:

Abstract

The effect of the addition of affinity and immobilisation tags on (i) the production (ii) the purification and (iii) the orientation-specific immobilisation onto activated surfaces of model proteins is reported in this study. Green Fluorescent Protein (GFP) was used as a model protein allowed for the ease of comparison of these effects due to its ability to be directly monitored and quantified by fluorescence. The immobilisation of GFP using several different methods has been investigated and compared. These included (i) direct chemical immobilisation by covalent methods taking advantage of the inherent reactivity of lysine and cysteine residues, (ii) the well-characterised biological specific recognition/immobilisation between biotin and streptavidin, (iii) the biological affinity tag of 'Strep-TagII' for a mutated streptavidin known as 'Streptactin' and (iv) a combination of both methods by biotin functionalising lysine and cysteine tagged proteins.

Several activated surfaces have been studied for the immobilisation of these proteins, including 96-well plates, and monolithic columns. This works reports on the optimisation of the production and photo-activation of monolith capillary columns as potentially useful surfaces for the immobilisation of protein bio-ligands. The monitoring and quantification of the immobilisation of protein onto monolithic columns by the contactless conductivity detection (C^4D) method also formed an important part of this study. Finally, initial work is reported here on the potential generation of a biologically active and novel biosensor for the online and direct quantification of free sialic acid in monolith capillary columns using both C^4D and fluorescence detection.

Chapter 1: Introduction

1. Introduction

The orientated immobilisation of proteins on any surface requires careful consideration. The inherent variety of factors which make up a properly folded and active protein is considerable. To immobilise a biomolecule without disrupting these factors and for it to remain active is a significant challenge. For this study a model protein (Green Fluorescent Protein) was chosen, which will enable the determination of the effect the addition of tags will have on protein immobilisation.

1.1: Green Fluorescent Protein

1.1.1: Introduction

Green fluorescent protein (GFP) was first described in the early sixties when it was co-purified with the aequorin protein from the jellyfish *Aequorea victoria*. (Osamu Shimomura *et al.*, 1962) It took another twelve years before the close relationship between these two proteins was fully established. (Morise *et al*., 1974) In a hugely labour intensive process some 30,000 specimens of *Aequorea victoria* were processed, which enabled the purification, crystallisation and partial characterisation of the protein. This allowed the determination of the excitation and emission spectra of this unique protein for the first time. Initial excitation spectra were defined at 280nm, 400nm, and 480nm. These spectra are broadly in line with the currently accepted spectra for wild-type GFP (wtGFP) namely 280nm, 395nm and 475nm. The emission spectrum of 509nm corresponds exactly with the present day emission value given for wtGFP. (Yang *et al.*, 1996)

GFP has been widely used for at least 20 years as a protein tag or label because of its unique properties. It is a spontaneously fluorescent protein, requiring only correct protein folding to fluoresce. As outlined by (Morise *et al*., 1974) its role is to transduce the blue chemiluminescence of aequorin to green light. It is perfectly evolved to do this as one of its excitation peaks (475nm) is nearly identical to the emission peak of aequorin (470nm). The reason *Aequorea victoria* has evolved this complicated two-protein system to produce green fluorescent light is not yet fully understood. Despite this seemingly inefficient mechanism this system seems to be widespread in the phylum Cnidaria. (Matz *et al.*, 1999)

To date, it remains unresolved as to exactly why these organisms fluoresce, or why green emission holds an advantage over the primary blue emitters. It has been proposed

that fluorescent proteins in coral are acting as a protective barrier against UV light from the sun. Salih and co-workers have shown that corals which are in shallower waters have a greater diversity of fluorescent proteins than coral in deeper and darker waters (Salih *et al*., 2000) It is proposed that they may protect resident symbiotic organisms that produce energy by photosynthesis This may not fully explain the presence of fluorescent proteins in jellyfish but may give an important clue to the functions of these unique molecules.

1.1.2: Structure of GFP

In 1996 two papers were published which elucidated the crystal and molecular structure of GFP. Both groups described GFP as consisting of 238 amino acids, molecular weight of 30kDa and confirmed the protein as having two excitation spectra of 395nm and 475nm and an emission spectra of 508nm. The protein folds in the shape of a cylinder, comprising 11 strands of β-sheet which protects a central α-helix (Ormo *et al*., 1996). These groups have also determined that the protein folds to a molecule which is 42Å long and 24Å in diameter. This structure has been referred to as the "β-can". (Figure 1.1)

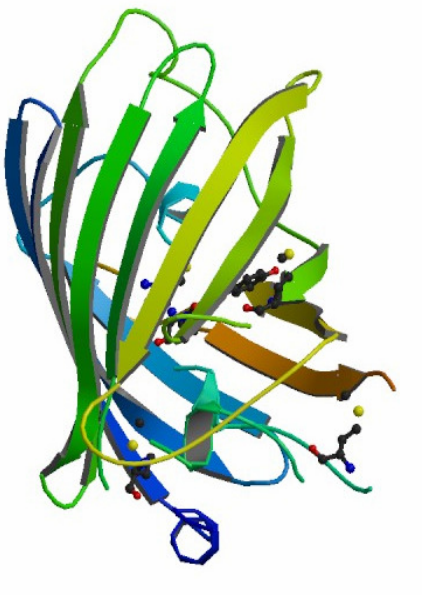

Figure 1.1: Green Fluorescent Protein structure submitted to Protein Data bank by Ormo, M., Remington, S.J. (PDB I.D.: 1ema)

Two β-can structures can combine to form a dimer structure (Yang *et al*., 1996). The structure uploaded to **http://www.rcsb.org/pdb/home/home.do** by this group shows the

outlined dimer structure under the PDB I.D. 1GFL. In the dimer structure the monomers are associated in a twisted head to tail orientation via hydrophilic contacts along with several hydrophobic contacts (Zacharias and Tsien 2006). In this dimer structure there is a 25Å separation between the two fluorophores of the GFP monomers (Youvan and Michel-Beyerle, 1996). To date, GFP is the only fluorescent protein known that is not an obligate homo-oligomer in its natural state.

There are several residues which are reported to be involved in this dimerisation; the best studied are A206, L221 and F223. These residues have been changed both singly and in combination by site directed mutagenesis, mainly to positively charged residues such as A206K, L221K and F223R. These mutations have eliminated the formation of a dimer molecule. (Zacharias *et al.*, 2002a) Of course oligomerisation is important when it comes to using GFP to monitor protein localisation, expression or fluorescent resonance energy transfer (FRET). As dimerisation of GFP can have a seriously deleterious effect on all these processes, ((David A. Zacharias and Roger Y. Tsien, 2005) recommend that at least one of the mutations outlined above should be used in all GFP expression constructs as they do not effect the function of the protein apart from the homo-affinity of GFP. This is achieved by mutating smaller neutral amino acids such as alanine to positively charged amino acid residues such as lysine or arginine. The inhibition of dimerisation by electrostatic interactions is vital as protein folding and protein-protein interactions are measured by fluorescence. Any additional fluorescence due to dimerisation can give an increased signal and false positives.

The most vital component of the structure of GFP is the protection it affords the fluorophore forming residue, which is securely protected within the β-can structure. Yang and co-workers (1996) describe the cylindrical fold of GFP as “remarkable” and describe how the β-sheets are fitted to each other like the staves of a barrel and form a regular pattern of hydrogen bonds, which may account for the protein’s stability against denaturation. The α-helices then cap both ends of the protein and, as such, the chromophore forming residues are completely protected from the bulk solvent (Yang *et al*., 1996). The initial half of the polypeptide is made up of three anti-parallel strands, the central helix, followed by three further anti-parallel strands. The backbone then crosses the ‘bottom’ of the molecule, which forms the second half of the β-can structure in a five stranded ‘Greek Key’ motif. The ‘top’ of the molecule is capped by three short, helical segments, and by short, much distorted, helical segment caps at the bottom of the cylinder (Ormo *et al*., 1996).

GFP is used as a tag to monitor protein location by fluorescent microscopy. If GFP can be engineered to be more fluorescent it can potentially be used for localisation studies. It has been determined that the smallest possible domain in GFP required for fluorescence is amino-acids 7-229 (Li *et al.*, 1997). Consequently this means that only 15 amino acid residues can be deleted from the wtGFP without losing fluorescence. N-terminal deletions of the amino acids 2-8 completely remove fluorescence. By mutation it has been established that replacing the Glutamic acid at position 7 with other amino acids greatly reduces GFP fluorescence. Conversely at the C-terminus of the GFP protein mutation of residue 229 is tolerated as the protein will still fluoresce regardless of the amino acid residue present at that position.

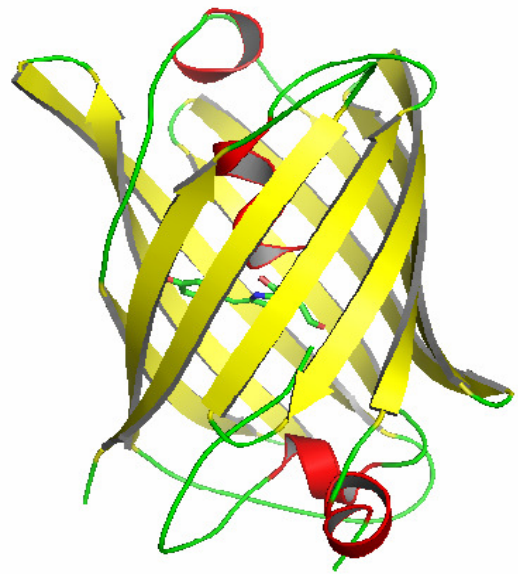

Figure 1.2: Colour coded structure of GFP. Yellow = β-sheet, Red = α-helix, Green = Loop. Submitted to Protein Data bank by Ormo, M., Remington, S.J. (PDB I.D.: 1ema)

The wild type Ile229 can be replaced with any other amino acid without a noticeable loss of fluorescence. Through a series of well defined mutations (Li *et al.*, 1997) replaced the negatively charged glutamic acid residues at positions 6 and 7 with either a single or double mutation of a neutral amino acid (Alanine) or a positive amino acid. (Lysine) They found that if either residues were mutated the fluorescence of the wtGFP stayed the same. When both residues were changed to either neutral or positively charged amino acids the fluorescence was lost. They also mutated these residues to a negatively charged aspartic acid. This mutation also reduced the fluorescence of the protein by up to 70%. This led Li and his co-workers to suggest that glutamic acid residues at positions 6 and 7 are not only required for their negative charge but for

maintaining specific contacts within the wild type protein. The same group focused on mutating the Isoleucine residue at position 229. As Isoleucine has a hydrophobic character they mutated this residue to (i) another hydrophobic residue (Leucine), (ii) a positively charged residue (Lysine) and (iii) a negatively charged residue (Aspartic Acid). The relative fluorescence of these mutants displayed no significant difference from the wild type. This group also made deletions and insertions in the two largest loops of the protein. Both of these actions resulted in the complete abolition of fluorescence (Li *et al*., 1997).

From these examples alone, it can be seen that GFP's major function is the protection its tertiary structure gives to the chromophore forming residues. The protein is non-fluorescent in its unfolded state, and has evolved to protect the chromophore from the surrounding solvent and produce an environment within the "β-can" to produce fluorescence. Hence, while this protein, once folded is extremely stable and resistant to denaturation agents, heat and extreme pH, any unfolding will lead to a loss of fluorescence. GFP has therefore been used successfully in folding studies, when fused downstream from a protein (Cabantous *et al*., 2008), and in solubility studies, where the respective strengths and weakness of Guanidine and Arginine were compared in relation to the solubilisation of insoluble particles (Tsumoto *et al*., 2003).

1.1.3: The chromophore of GFP

The structure of the GFP chromophore had been initially suggested by (Shimomura, 1979). This was later confirmed by (Cody *et al*., 1993). Later, (Prasher *et al*., 1992) managed to clone the wtGFP gene into *E. coli*,. However they were not successful in creating fluorescent colonies. As it was not known at this stage if the chromophore required co-factors and it was assumed that bacterial cells did not have the required cellular machinery to produce this effect.

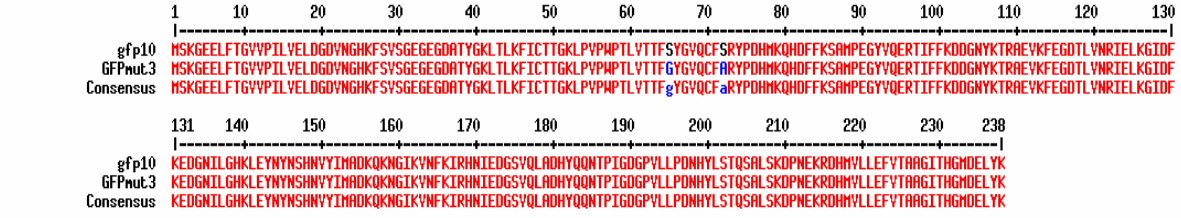

Figure 1.3: Sequence alignment between original GFP clone, (Prasher *et al*., 1992) and GFPmut3 used in this study.

In 1994 (Chalfie *et al*., 1994) described for the first time that the eukaryotic GFP could be expressed in both prokaryotic and other eukaryotic systems to produce fluorescence without the need for specialised co-factors or ligands

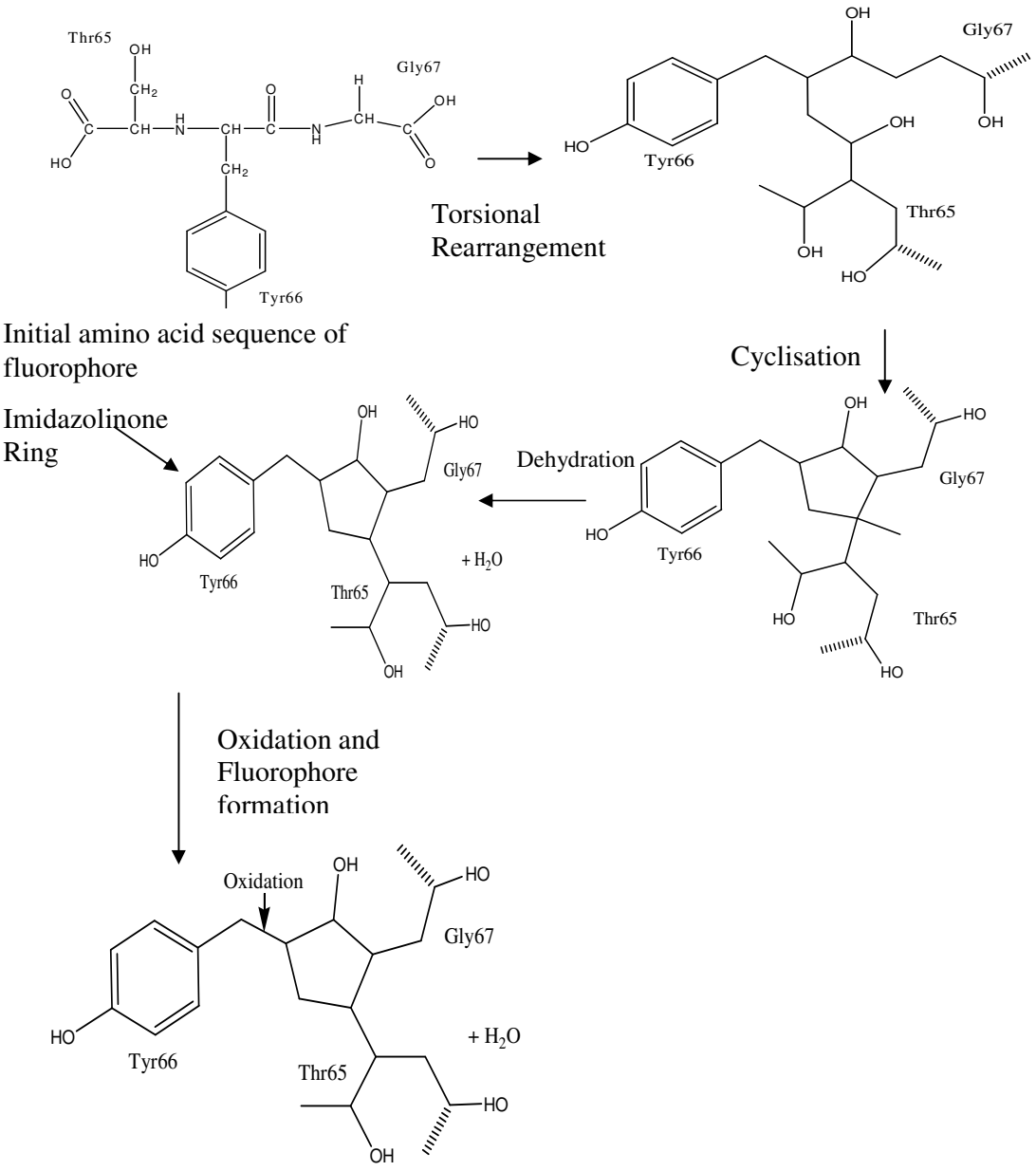

Figure 1.4: The chromophore formation of eGFP mutant. (Reid and Flynn, 1997)

In the 15 years since this paper was published there has been an explosion in the amount of reported work on this protein and the uses for its non-toxic auto-fluorescence. (Sheridan and Hughes, 2004, Zacharias *et al.*, 2002b, Cabantous *et al.*, 2008, Cabantous *et al.*, 2005, Cha *et al.*, 2000, Chalfie *et al.*, 1994, Gorokhovatsky *et al.*, 2003) GFP

fluorescence has now been reported in a wide variety of organisms from the simplest bacterial systems to mammals including pigs, rabbits and mice. Its use has revolutionised fluorescent microscopic imaging allowing us to visualise the inner workings of many different types of cells. The properties of this protein are reliant on a triple amino acid protected securely in the hydrophobic environment in the centre of the proteins 'β-can' structure (Yang *et al.*, 1996).

The amino acid sequence twists to bring the carboxyl carbon of Thr65 and the amino nitrogen of Gly67 into close proximity (Tsien, 1998). A nucleophilic reaction between these two atoms, followed by the loss of a water molecule results in the creation of an imidazolin-5-one heterocyclic ring system. (Figure 1.4) Fluorescence is then generated by oxidation of the imidazoline ring with Tyr66 and maturation of a fluorescent species. The green fluorescent protein fluorophore exists in two states. A protonated form, which is the predominant state, has an excitation maximum at 395nm, and a less prevalent, unprotonated form that absorbs 475nm. Despite the excitation wavelength, however, fluorescence emission has a maximum peak at 509nm.

The internal environment and residues adjacent to these amino acids play a vitally important role in the formation of this fluorophore. One side of the chromophore faces a large cavity that occupies a volume of 135$Å^3$.(Ormo *et al.*, 1996) Four water molecules are located in this cavity, which form a chain of hydrogen bonds joining the side chains of Glu222 and Gln69. The cavity might also temporarily accommodate the O_2 which dehydrogenates the α-β bond of Tyr66. (Ormo *et al*., 1996) There is also a complicated network of polar interactions between the protein structure and the chromophore. The amino acids His148, Thr203 and Ser205 all form hydrogen bonds with the phenolic hydroxyl. The carbonyl of the imidazolinone ring interacts with Arginine at position 96 and Glutamine at position 94, and Glu222 forms a hydrogen bond with the side chain of Thr65. An in-depth study of Arg96 indicated that the residue may be essential for the formation of the fluorophore by activating the S65 carbonyl for nucleophilic attack or by directly de-protonating the G67 backbone amide and may help catalyse the initial ring closure.(Wood *et al*., 2005) This study went on to indicate that R96 tunes the GFP spectral properties by stabilising the de-protonated form of the mature chromophore. The R96 steric properties may inhibit conformation of the Y66 side chain and pre-organise the backbone of the chromophore-forming residues to align them for ring cyclisation. Also the R96 residue electrostatic interactions may favour the G67 nitrogen de-protonation and stabilise any intermediates in the cyclisation reaction.

1.1.4: Green Fluorescent Protein Mutations

For a protein of such significance many mutations have been made to improve its performance. It will not be possible to outline all mutants, but Table 1.1 outlines the most common.

Table 1.1: Selected Mutations and associated changes of properties for Green Fluorescent Protein

Selected Mutations in GFP

Mutation	*Effect*	*Selected References*
Chromophore Mutations		
S65T, S65G, S65A	Increase in fluorescence Slight Red Shift	(Heim *et al*., 1994)
Y66W, Y66H, Y66F	All mutants 'blue shift' to one extent or another depending on aromatic ring	(Ormo *et al.*, 1996, Palm *et al.*, 1997, Cubitt *et al.*, 1995
Mutations effecting the Chromophore		
Q69M, Q69K	Cause an 1nm to 2nm red shift	(Griesbeck *et al*., 2001)
T203F, T203H, T203Y	Increase the excitation and emission spectra up to 20nm	(Ormo *et al*., 1996)
Folding Mutations		
Y145F	Improves brightness	(Heim and Tsien, 1996)
M153T	Improves folding at 37^{o}C	(Crameri *et al*., 1996)
V163A	Improves yield of correctly folded protein	(Siemering *et al*., 1996)
F64L	Improves brightness	(Patterson *et al*., 1997)
F99S	Improves folding at 37^{o}C	(Crameri *et al*., 1996)

1.2. Protein Immobilisation

1.2.1 Introduction:

The orientated immobilisation of proteins onto any surface often proves to be a difficult and complicated process. The large variety of components which make up a properly folded and active protein is considerable. This variety is derived from the twenty basic amino acids of which all proteins are composed, each containing its own unique chemical functional group, continuing to the quaternary structure of the correctly folded protein and finally to any post-translational modifications. All these factors play a vital role in the formation and function of a protein. For these reasons the chemical immobilisation of 'active' proteins has proven to be a challenging field.

1.2.2 Immobilisation methods:

The classical immobilisation of protein in a non-covalent, non-orientated manner has been used for many years. Common techniques such as passive absorption onto hydrophobic surfaces like nitrocellose membranes and polystyrene and electrostatic immobilisation onto polylysine surfaces are well characterised and studied. These immobilisation technique's major advantages are that they do not require any additional coupling reagents or protein modification. They do have some significant disadvantages though: because they are not covalent interactions the immobilisations can be weak and reversible. The immobilisation of proteins onto hydrophobic surfaces can lead to conformational problems which could lead to denaturation. Finally, limited control over the immobilisation process often leads to steric hindrance problems. For these reasons these simple if effective methods do not have the required sensitively or refinement for the current requirements of this study.

Large scale protein immobilisation techniques were focused on chemistries and methods which were borrowed from DNA microchips. (Macbeath *et al.*, 1999) are recognised as the first published attempts at the formation of a large scale protein immobilisation experiment using a slide spotter normally used for DNA spotting. In the reported experiment glass slides were functionalised with maleimide groups. Three molecules, biotin (recognised by streptavidin), a derivative of digoxigenin (recognised

by mouse monoclonal antibody DI-22) and a synthetic pipecolyl α-ketomaide (recognised by human immunophilin FKBP12) were immobilised on these slides by Michael addition. This reaction is characterised by the addition of a nucleophilic group across a double bond (Mather *et al.*, 2006). The interaction between the bait and their determined probe was finally determined by Cy5-labelled antibodies.

This experiment was soon followed by further attempts to immobilise large numbers of different proteins on solid surfaces without denaturating them. The use of a Schiff's base reaction to covalently immobilise proteins involved the reaction between immobilised aldehydes with primary amines. (Macbeath and Schreiber, 2000) Proteins may contain a variable number of lysine residues (which contain an amine moiety on their side chains) as well as the α-amine at their NH_2-termini. This means proteins can immobilise in many different orientations. While this method may have little to no effect on the activity of a protein which has multiple active sites, an unfortunate covalent immobilisation event involving a lysine residue within the active site of a protein which only has a single site may destroy the activity of that protein due to steric hindrance. Ultimately this method of immobilisation did prove successful. Nearly 11,000 distinct protein G spots were placed on a functionalised glass slide, with one reactive spot being picked out using Cy5 fluorescence (Macbeath and Schreiber, 2000).

There have also been attempts to immobilise proteins on slides by non-covalent methods. (Khan *et al.*, 2006) used a double histidine tag separated by 11 amino acids to increase the affinity and reduce a single tag's rapid dissociation with great success. This method proved successful in both chip based assays and Surface Plasma Resonance (SPR) applications. A double histidine tag immobilisation method was also used to immobilise antibodies on slide surfaces, this time without the amino acid spacer sequence (Cornelia Steinhauer *et al.*, 2006). The advantage of this method is that there is no need for protein pre-purification as purification and immobilisations steps can take place simultaneously. The addition of a histidine tag to either the N or C-terminal can result in a more orientated immobilisation event compared to relying on covalent immobilisation using inherent residues. Conversely these tags do display some disadvantages, namely the fact that the immobilisation is non-covalent, and as such protein leaching can occur.

1.2.3 Covalent Immobilisation Chemistries:

When more stable protein immobilisations are required the use of covalent chemistry such as Michael addition and Schiff base chemistry is most widely prevalent. One of the major advantages of this highly stable method of immobilisation is that like passive absorption and electrostatic methods it may be performed without any additional modifications to the protein. This is most commonly achieved by taking advantage of the inherent lysine and cysteine residues within the proteins amino acid sequence both of which, have nucleophilic side chains. Lysine's side chain has an amino functional group while cysteine's has a thiol functional group. Both of these nucleophilic groups provide ideal chemical structure for several types of covalent immobilisation.

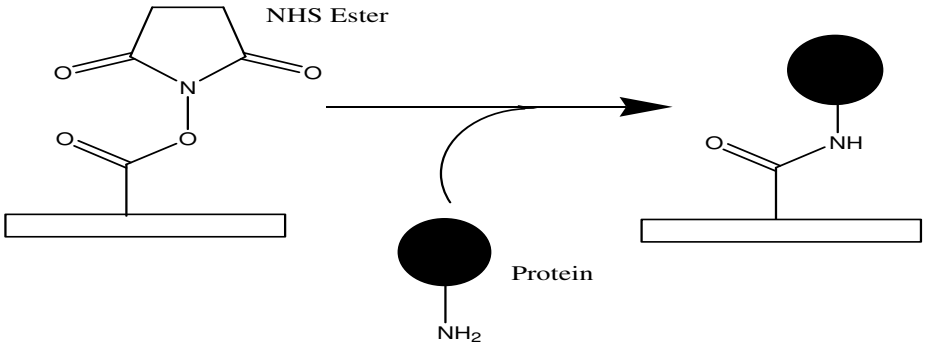

Figure 1.5: Ester Reaction with amine residue of protein for immobilisation. NHS is N-hydroxysuccimide.

As outlined in Figure 1.5, lysine residues are used to react with immobilised esters. The most commonly used of these esters is N-hydroxysuccimide (NHS) which forms a stable amide bond when reacted. Biomolecules to be immobilised by this method should be dissolved in a low ionic strength buffer before being passed over the functionalised surface. The efficiency of this reaction depends on several different factors such as pH, the amount of time given to the reaction, the protein concentration and the ionic strength of the buffer. (Rusmini *et al*., 2007) A slight disadvantage of this method is that NHS esters are relatively unstable in aqueous buffers, and attachment of proteins in these conditions can compete with ester hydrolysis. The second major method of covalent immobilisation is using inherent cysteine residues within the proteins structure.

The thiol group of cysteine amino acids reacts by conjugate addition with α-β-unsaturated carbonyls (maleimide is a perfect example of such a structure) to form a stable thioester bond.

The amines of lysine can also react with maleimides but at physiological pH's maleimide groups favour addition with thiols. The pH's involved are well characterised, maleimide will react 1000 times more readily with the thiol group of cysteines at pH 6.5-7.5 than with the amine group of lysines. This is due to the fact that amines are protonated at such pHs. (**www.piercenet.com**, Instructions for EZ-Link Maleimide-PEG11-Biotin)

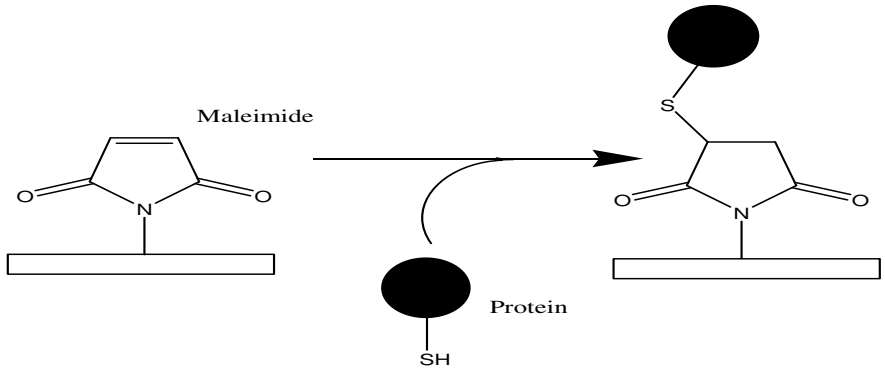

Figure 1.6: Diagrammatic representation of thiol based immobilisation of proteins

One of the major advantages of this method of covalent immobilisation is that cysteines are essential for the correct folding of many proteins tertiary structure. Cysteines are normally found in pairs within the proteins interior forming cystines though oxidation which stabilises the protein's folding though a disulfide bond. As such free cysteines are not as common an amino acid residue in the majority of proteins compared to lysines. This means that if all exterior cysteines save one can be removed or a cysteine added where there were no inherent cysteine residues previously, covalent immobilisation by the reaction with maleimide can be presumed to be orientation specific. This methodology of course depends on the characteristics of each individual protein. This method of immobilisation has been most clearly demonstrated by the addition of a five cysteine tag to either the N or C-terminal of GFP and immobilised on maleimide functionalised surfaces. (Ichihara *et al*., 2006)

Epoxide functionalised surfaces have also been used to immobilise proteins by their nucleophilic residues. As discussed previously, the most effective and well used nucleophilic residues are the amine groups of lysines and the thiols of cysteines. The

advantage of this method of immobilisation is that they are stable to hydrolysis at neutral pH which allows for relatively easy handling. Their disadvantage is

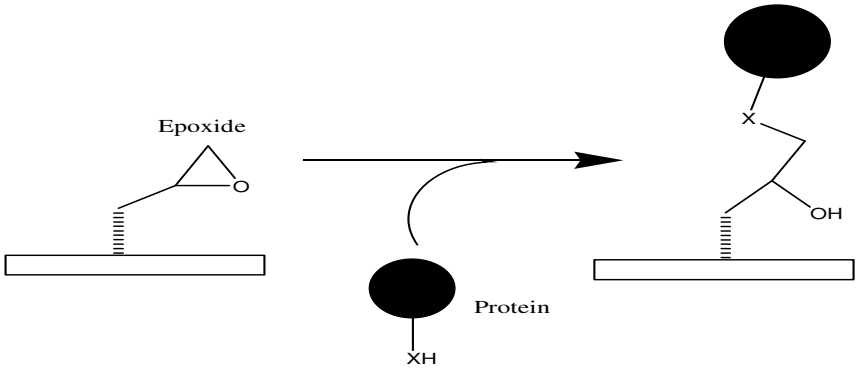

Figure 1.7: Representation of the immobilisation of proteins using immobilised epoxide groups. X = nitrogen or sulphur atoms

that this reaction can result in slow reaction times and incomplete coupling. It has been shown that the immobilisation reaction proceeds at a faster rate if the biomolecule has already been immobilised hydrophobically on the epoxy surface. This may not always be an ideal immobilisation method. For example agarose which has been functionalised with epoxy residues has shown very little immobilisation at high and low ionic strength conditions. It is thought that this is due to the lack of a hydrophobic immobilisation step. Aldehyde groups may be used to immobilise proteins with exposed α-amine groups or lysine ε-amines. The amine group's reaction with the aldehyde produces an imide with the surface functionalised aldehyde. This can then be reduced to form a secondary amine linkage (Wong *et al.*, 2009), (Fig1.8).

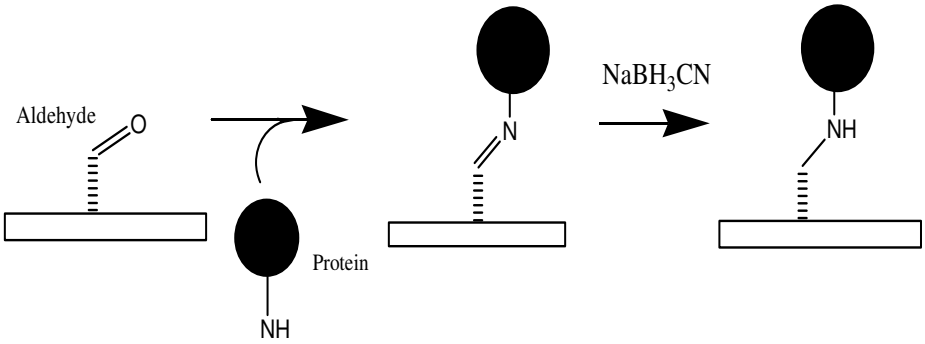

Figure 1.8: Graphic representation of the immobilisation of proteins on aldehyde functionalised surfaces.

All these methods suffer from certain disadvantages. They all rely on the covalent immobilisation of amino acids already present within the protein structure. As there is no way to determine exactly where these amino acids are within the protein, a potentially heterogeneously orientated population of immobilised proteins may be presented on a surface. Due to this fact many protein surfaces suffer from a high level of inactivity due to incorrectly orientated biomolecules. Secondly using amine or in some case carbonyl groups for immobilisation can disrupt the protein folding due to the loss of the electrostatic charges of these functional groups. Finally, all these methods depend on a high level of purity of the immobilised biomolecules. A major loss in sensitivity would occur if large amounts of impurities or containment proteins were immobilised instead of the target molecule. At a small scale this degree of purification does not form a major barrier. However, the unique properties of scaled-up production of biomolecules often present a significant challenge.

Several other methodologies for the immobilisation of biomolecules have been proposed. The most common of these is the 'Staundinger reaction', named after the German chemist who first described the reaction. The Staundinger 'ligation' method was first introduced in 2000 (Saxon and Bertozzi, 2000). It is known as a ligation rather than a reaction as the two reacting groups (an azide and a phosphine) are covalently attached to each other compared to the Staundinger reaction where the molecules are not covalently linked. The ligation is based on the functionality of the azide group (see Fig. 1.9). Azides are not present in living biological systems. They do not react with water, are resistant to oxidation and are mild electrophiles, they do not react with amines or any other biological nucleophiles and are stable at physiological temperatures. They are however susceptible to reduction by free thiols. Because of these qualities they have become used in many covalent immobilisation methods. The Staundinger ligation was first used to label cells and proteins. At room temperature and in the presence of water the coupling of an azide and a phosphine forms an amide bond. The first use of this method was published soon after. (Soellner *et al*., 2003) The ε-amino of the first lysine of ribonuclease S' (RNase S') was replaced with an azido group. A glass slide, was treated with PEG, which had succimidyl ester termini for 2hours followed by diphenylphosphinomethanethiol in dimethylformamide for 2hrs. This treatment resulted in a surface with a bound phosphinothioester. Immobilised RNase S' was then tested in two ways. Firstly the ribonucleolytic activity was tested with a fluorescent substrate. Secondly, it was tested by using immunostaining. The

immunostaining was preformed with rabbit anti-RNaseA IgG, which was subsequently probed with an Alexa Fluor 488-conjugated secondary antibody. Using both these methods it was determined that there was a 51% yield of successfully coupled protein, with 81% of the immobilised protein being active. This was compared to immobilisation of the PEG linker to amine functionalised slides, which had a similar percentage of the protein immobilised but the activity dropped to 6%. This clearly showed this immobilisation method had potential for protein immobilisation. One of the challenges is that to achieve site-specific immobilisation a method must be found to add an azide to the protein of interest, in the correct position. The most likely method to achieve this is enzymatically.

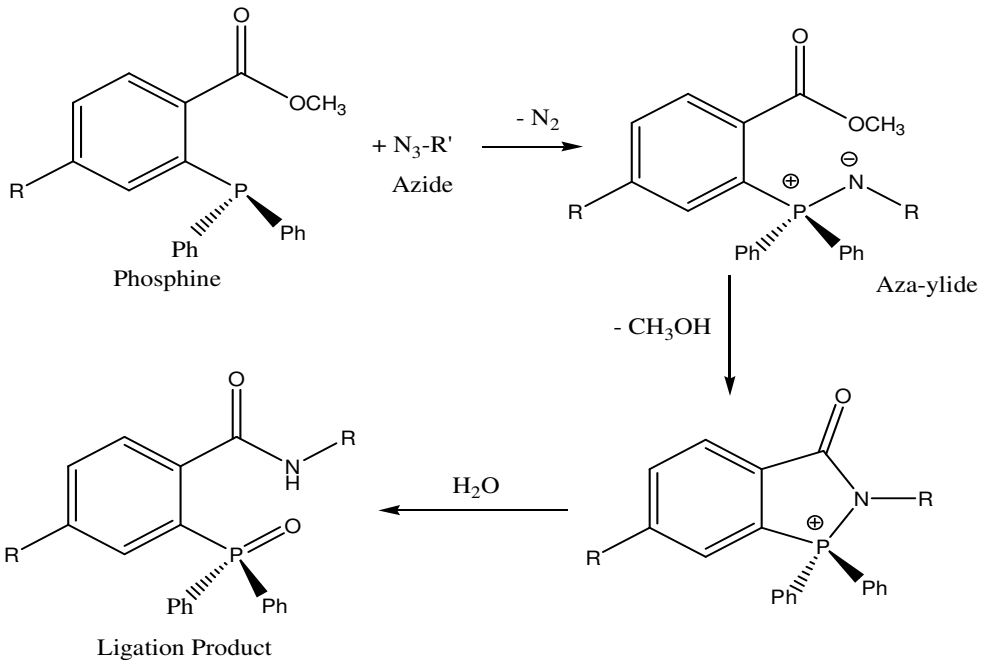

Figure 1.9: Reaction scheme for a 'Staundinger Reaction'. Where R' may be a protein

One of the first to suggest using Staudinger ligations for large scale protein microarray immobilisation was (Watzke *et al*., 2006). An azide group was placed on the C-terminus of a protein by expressed protein ligation (EPL). This method allows for a chemically synthesised C-terminal element to be fused to a recombinant N-terminal protein using intein protein splicing elements (Severinov and Muir, 1998). The 'tagged' protein was then immobilised onto a phosphine functionalised glass slide. The major drawback of

this method for protein immobilisation was the requirement for expressed protein to be modified prior to immobilisation. The following year (Kalia *et al.*, 2007) used the same method to immobilise Bovine Pancreatic Ribonuclease onto a self-assembled gold monolayer rather than a glass slide. As the C-termini azide group is inert to any other biological functional groups present in the protein it was found that the protein was immobilised in a directed manner and it retained its activity.

Another immobilisation method that has become relatively popular is known as "click chemistry". This term was introduced in 2001 (Hartmuth C. Kolb *et al.*, 2001). It was initially used to describe the construction of large complex chemical structures from smaller simpler structures, copying the methods nature uses. When "click chemistry" is referred to in the context of protein immobilisation, it refers to a 1,3-Dipolar cycloadditon. (Figure 1.10) This reaction was referred to in the above paper as the "cream of the crop" when it came to click chemistry. The initial definitions of these reactions were very specific *i.e.* they had to be modular, wide in scope, high yield, generate no toxic by-products which must be able to be purified by non-chromatographic methods. As well as these tight controls, the process was required to take place under simple reaction conditions. They must be generated from easily available starting reagents, the reaction must take place in no solvent or a solvent that is non-toxic and the product must be easily purified. These strict criteria for the 1,3-Dipolar cycloaddition has ensured that this is an effective method for the immobilisation of proteins onto solid surfaces.

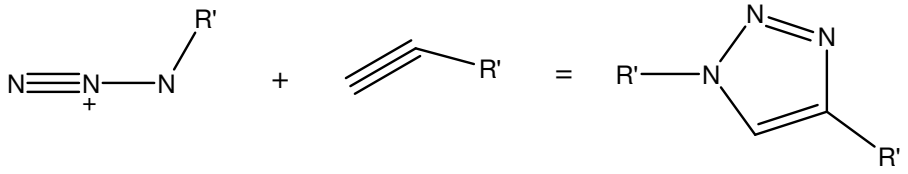

Figure 1.10: A reaction scheme for 1,3-Dipolar cylcoaddition, where R' is a protein.

As the addition of azides and alkynes to proteins is relatively easy and does not affect either protein structure, stability or function they may be used to effectively immobilise proteins with either an azide or alkyne functionalised surface. This reaction is irreversible and quantitative and made more efficient by the addition of Cu(I) species which catalyse the reaction (Wang *et al.*, 2003).

Proof of concept of this method was provided when GFP was covalently immobilised by the addition of four amino acids on the C-terminal end of the protein sequence. The enzyme "protein farnesyltransferase" recognises this amino acid sequence only when present at the C-terminus of a protein and adds an azide functional group to the biomolecule of interest by protein prenylation. The protein was then covalently immobilised on agarose beads with an alkyne functional group (Duckworth *et al*., 2006).

A covalent method of protein immobilisation has also been investigated for use with monolithic columns. Monolithic columns have in recent years found use as a stationary phase in capillary electrophoresis. They are typically composed of a single piece of porous material rather than the more commonly used particulate stationary phase. Further information can be found in Section 1.4. This immobilisation method was first introduced by (Tripp *et al*., 2000). Using porous monolith disks they functionalised the pores by filling the monolith with a reactive monomer (EDMA) and heating. This allows the monomer to be anchored to the pore surface by the radicals already present from the monolith production method. The monomer used in this case was 4,4-dimethyl-2-vinyl-2-oxazolin-5-one (Vinyl Azlactone). They then passed amine

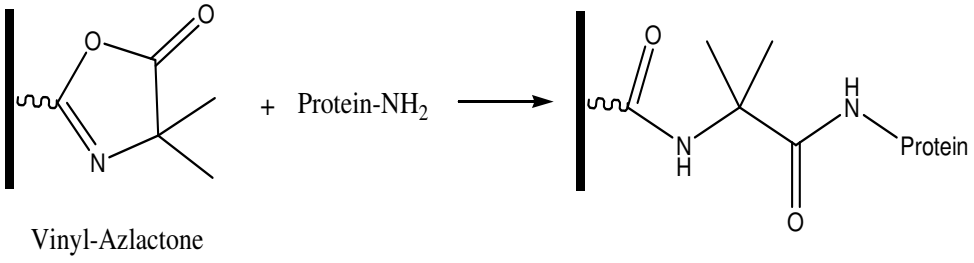

Figure 1.11: Vinyl-azlactone protein immobilisation reaction.

groups though this monolith disk and using gas chromatography determined that 50% of the groups were consumed within the first minute. This result held true over a range of solvents. This process was called "Reactive Filtration" and was intended to remove unwanted products from chemical reactions. Other groups saw this as a method to covalently immobilise proteins using their inherent amine residues. Examples include the immobilisation of trypsin (Peterson *et al*., 2003), Green Fluorescent Protein (Stachowiak *et al*., 2006), Horseradish Peroxidase, (Logan *et al*., 2007) and fluorescently labelled BSA. (Connolly *et al*., 2007)

1.3 Bio-affinity Immobilisation

1.3.1: Introduction:

One of the most well known and well studied methods of immobilising biomolecules is the use of the interaction between Avidin or Streptavidin and biotin. This biorecognition event is not based on covalent interactions but is founded mainly on hydrogen bonding and hydrophobic interactions (Wilchek *et al*., 2006). Ultimately, this interaction is one of the strongest reported non-covalent biological interactions with an average dissociation constant of $K_D = 10^{-15}$M.

1.3.2: Structure and Biotin Binding:

Avidin was originally isolated from egg white, while Streptavidin is secreted by *Streptomyces avidinii*. Streptavidin was first cloned in 1986 (Argarana *et al*., 1986) and expressed in 1989. (Sano and Cantor, 1990) The more complex eukaryotic avidin was first sequenced in 1995. (Wallen *et al*., 1995) Amazingly, for these two proteins, one from a eukaryotic source the other from a prokaryotic both are structurally and functionally almost identical. Despite structural similarities the amino acid sequences of both these proteins have only a 41% similarity while the identity percentage is 30% (Olli *et al*., 1999). They have similar secondary, tertiary and quaternary structures, which are resistant to high temperatures and extremes of pH. These proteins are also resistant to degradation by proteolytic enzymes. Both Avidin and Streptavidin are composed of four identical monomeric subunits. Each of these monomers is composed of eight stranded anti-parallel β-barrels. The interaction of these monomers in the relation to the binding of biotin has been described as a "dimer of dimers". The first monomeric subunit plays an important structural role in the binding of biotin by the fourth subunit and *vice versa.*

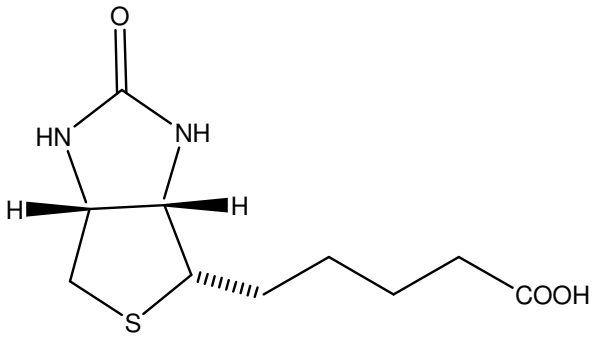

Figure 1.12: The structure of Biotin

The same interaction occurs between monomeric subunits two and three (Laitinen *et al*., 2006). Therefore each monomer in the dimer is required for the efficient binding of biotin by the corresponding subunit in the pair. The residue involved in this functional interplay is tryptophan in both cases but they are located in slightly different areas of both proteins. In avidin the Trp110 plays a vital role in the biotin binding pocket of the neighbouring subunit, while Trp120 plays a similar role in streptavidin. The binding of biotin takes place at one end of each monomeric structure, so each fully folded quaternary streptavidin or avidin structure can bind up to four biotin molecules. It has been shown that the binding of a biotin molecule to a monomeric avidin or streptavidin has a dissociation constant of $K_D=10^{-7}$M, whereas the binding of biotin to a tetrameric protein restores the dissociation constant to its wild type value ($K_D =10^{-15}$M.) (Laitinen *et al*., 2006). This may indicate that the quaternary structure of the proteins plays a vital role in the extremely tight binding of the protein to its ligand.

The crystal structure of streptavidin without bound biotin and a streptavidin biotin complex have been studied to try and determine the method by which biotin binds to the protein. The relatively high amounts of hydrophilic contact residues initially form hydrogen bonds with the biotin molecule. Secondly, there are several aromatic residues in the binding area, which provide a hydrophobic environment for the binding to take place (Weber *et al*., 1989). These interactions in themselves do not fully explain the unusually high affinity for biotin that this protein exhibits. There is evidence that that once the biotin has been bound initially to the protein, the conformation of several loops of the Avidin and Streptavidin proteins change, in such a way that may indicate a lid closing over the biotin, enclosing the biotin within the monomeric avidin/streptavidin structure (Gonzalez *et al*., 1997). As well as this, in the absence of the ligand five water molecules take the place of the biotin in the biotin binding pocket and take the shape

and hydrogen binding capacity of biotin. (Weber *et al.*, 1989) The interface between the first and third monomeric subunits is maintained by three hydrophobic interactions and Van Der Waals in Avidin, while in Streptavidin polar amino acids play an important role. The interaction between the first and fourth monomers in both proteins is maintained by about two dozen hydrogen bonds. (Figure 1.13) Finally, as outlined previously the third monomer-monomer interaction in Avidin and Streptavidin is between the first and second monomer and third and fourth monomer. These interactions are maintained by tryptophan residues and play an important role in the binding of biotin (Laitinen *et al.*, 2007).

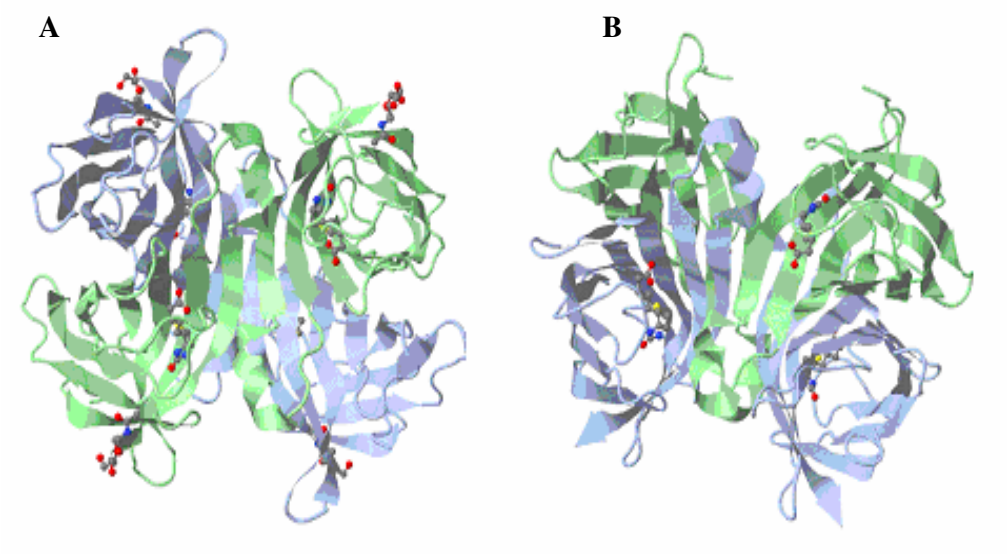

Figure 1.13: A: Molecular structure of Avidin. PDB accession code: 2avi, **B:** Molecular structure of Streptavidin, PDB accession code: 1mk5

The tight binding between Biotin and Avidin/Streptavidin has been employed in a wide range of immobilisation protocols. It has been used to bind biotinylated liposomes to streptavdin functionalised agarose beads (Yang *et al.*, 1998), glycoproteins to micro well plates, (Cordiano *et al.*, 1995) viruses to sol gels (Riccardi Cdos *et al.*, 2006) and to purify biotinylated proteins (Rybak *et al.*, 2004). The search for orientation specific immobilisation of proteins was also studied using this interaction. Using site directed mutagenesis all the inherent cysteines in streptavidin were removed and an additional tag with a single cysteine residue was added to the terminal of the protein. This tagged protein was then immobilised to maleimide functionalised surfaces by the previously

outlined thiol based immobilisation protocol. (Reznik *et al.*, 2001) These examples are only a small sample of the wide range of uses for this very important biological interaction.

Due to the fact that this is such a well characterised interaction a number of companies have produced biotinylated products. The most prominent of these companies is Pierce Chemicals which provides a wide range of biotinylation molecules. These molecules take advantage of some of the covalent reactions outlined previously to add a biotin molecule to proteins, marketed under the EZ-Link® trademark.

A: NHS-PEO_{12}-Biotin

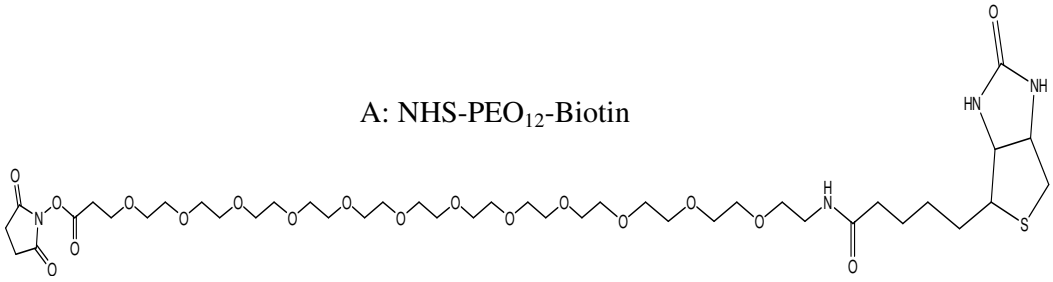

B: Maleimide-PEO_{11}-Biotin

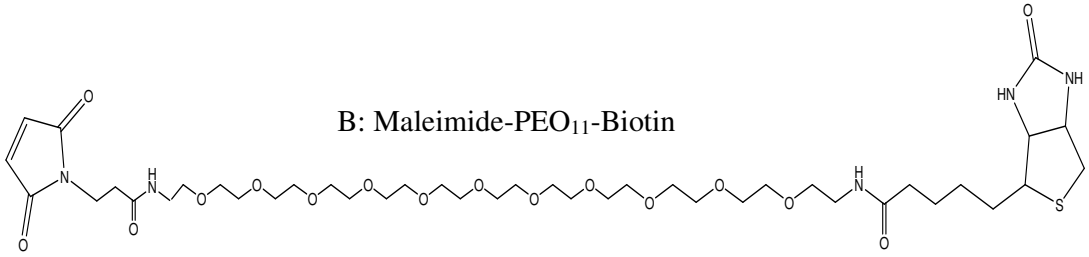

Figure 1.14: Biotin Spacer Linkers supplied by Pierce Chemical Limited.

Further work has been carried out to broaden the scope of this interaction, including groundbreaking work on biological mimics of biotin outlined in Section 1.3.3

1.3.3: Streptactin and Strep-tagII:

The initial work which led to the development of the 'Strep tag' was first outlined when a tag was engineered at the C-terminus of the V_H domain of antibodies (Schmidt and Skerra, 1993). This tag allowed for the detection of an antibody by commonly used techniques such as Western Blots by a streptavidin-alkaline phosphatase conjugate. The 'Strep Tag' is a nine amino acid sequence (Ala-Trp-Arg-His-Pro-Gln-Phe-Gly-Gly) which displays an affinity toward Streptavidin but not to Avidin and was initially only found to work reproducibly at the C-terminal of proteins. As well as being used for immobilisation this tag is used as an affinity tag to purify proteins produced as Strep-tag fusions in different expression systems. Because this tag does not have as strong an interaction with streptavidin as wild type biotin, it can be competitively eluted with biotin analogs such as desthiobiotin (Voss and Skerra, 1997).

To determine exactly how this interaction works (Schmidt *et al*., 1996) undertook crystallisation studies of streptavidin with a bound Strep-Tag. They reported that the tag interacts with several residues of Streptavidin's flexible loop, including residues 43, 45, 51, 52 and 54. This flexible group has been studied extensively and is thought to be one of the major factors contributing to the high affinity for biotin these molecules possess. Once the ligand is bound, this loop changes confirmation to 'close' over the binding site and lock the ligand in place (Weber *et al*., 1989). This group continued to determine further Streptavidin residues which form hydrogen bonds to the Strep tag, namely residues 23, 37, 84, 88, 90 and 128. One of the most important of these interactions is how the C-terminal Gly-Gly moiety of the Strep-Tag interacts through a series of bonds to the protein through a salt bridge at Arganine residue 84. It is interesting to note that this is such a specific interaction that the Strep-Tag has been shown not to interact with the closely related Avidin. The mechanism of this interaction (relying largely on C-terminal residues) sheds light on why this tag works only at the C-terminal end of proteins.

In order to improve this tag the same group used a synthetic peptide spot assay to develop a second immobilisation tag which does not have a 'C-terminal' limitation. And succeeded in developing a second tag which they named as Strep-TagII (Schmidt *et al*., 1996). This tag has the following sequence; (Asn-Trp-Ser-His-Pro-Gln-Phe-Glu-Lys) and showed a lower affinity for streptavidin (K_D =13μM) than the original Strep tag but could be used at either the N or C-terminal end of fusion proteins. To overcome the

problem of lower affinity, streptavidin itself underwent several rounds of mutagenesis to increase the affinity for this new tag. The focus once again fell on the flexible loop of the protein. As outlined previously, this flexible loop plays a vital role in the binding both of the biotin molecule and the Strep-Tag amino acid sequence. By comparing the crystal structures of both streptavidin which has not bound to the Strep-TagII and streptavidin having bound to Strep-TagII, attention was drawn to residues 44-47 (Glu-Ser-Ala-Val) of the flexible loop. (Voss and Skerra, 1997) The crystal structures show that in wild-type streptavidin the loop is "disordered" without the presence of a ligand, but once biotin is complexed to the binding site, the loop "closes" to protect this site. (Voss and Skerra, 1997) continued by mutating the residues from positions 44-47 in the protein.

	44	*45*	*46*	*47*
Wild Type Streptavidin:	Glu	Ser	Ala	Val
Mut1	Val	Thr	Ala	Arg
Mut2	Ile	Gly	Ala	Arg

Table 1.2: Substitutions made to the flexible loop of Streptavidin (Voss and Skerra, 1997)

By immobilising the wild type and mutated streptavidin in a sandwich assay on a capture membrane the efficiency of binding was determined. Antibodies against streptavidin were first immobilised, followed by the streptavidin. This was then probed with a Strep-tagII labelled alkaline phosphatase. The mutations outlined were found to have a K_D value for the Strep-TagII of ~1μM. This was a significantly tighter binding for the tag than the previously determined K_D value with wt-Streptavidin of 13μM. A change in confirmation of the flexible loop was seen as the cause of this change in the dissociation co-efficient. Within the mutated streptavidin molecules the flexible loop had changed into an almost opposite orientation, which gives a larger peptide access to the active site. Oddly, the mutations do not interact with the Strep-TagII peptide in any way (Korndorfer and Skerra, 2002). It appears that these mutations stabilised the loop and removed the need for the protein to change confirmation (Voss and Skerra, 1997).
While this system has a lower affinity for its ligand when compared to wt-streptavidin, it has a much higher affinity for the engineered Strep-TagII when compared to the wild-type. This mutated protein has been available commercially as Strep-Tactin from IBA

(http://www.iba-go.com/). As the addition of an eight amino acid tag to a proteins N or C-terminus is a relatively easy task, this broadens the usefulness of this biological system.

1.4: Monolithic Columns

The first modern rigid monoliths emerged at the start of the 1990's. They were initially used as an alternative stationary phase for HPLC alongside the popular particulate stationary phase. They provided a good alternative to particulate based systems because a monoliths high porosity allows for low back-pressures which in turn allows separations to be run at high flow rates allowing for faster separations

1.4.1 Introduction to Monolithic Columns:

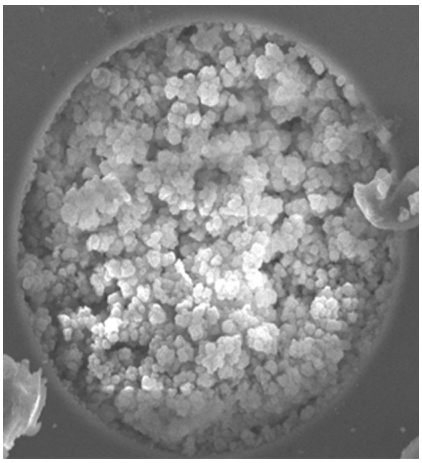

Figure 1.15: Structure of a Ethylene dimethacrylate monolithic column (Connolly *et al*., 2007)

Monoliths have been described by (Frantisek, 2006) as "a single large particle of porous material." Monoliths have their porous structure generated during their preparation. Their internal structure is defined by countless inter connected pores of different sizes. While their structurally rigidity is achieved by cross-linked monomers. The creation of monolithic structures is defined by a liquid reaction creating a solid porous structure, through the cross-linking of monomers within the presence of a non-reactive solvent. As the initial reaction is 'liquid' it requires the use of a mold and therefore monolithic structures have been formed in a wide range of shapes and structures including rods, membranes, discs, fibres and columns. They have been constructed out of various materials, the most common are agarose monoliths, silca monoliths, Cryogels and GMA(Glycidyl methacrylate) or EDMA (Ethylene dimethacrylate) monoliths.(Rangan Mallik, 2006) Functionalised monoliths in many different forms are now commercially

available. BIA separations alone now provides nearly fifty distinct monolithic columns. (**http://www.biaseparations.com**) The significant increase in the popularity of monolith structures can be explained by this sheer variety, which allows for a wide range of separation and affinity chromatography techniques.

1.4.2: Formation of monolithic columns:

Monolithic columns are formed by radical polymerisation or co-polymerisation of monomers within a mould to generate the porous monolith structure. Normally, this is achieved by adding a reactive monomer, a cross-linking monomer, a porogen and an initiator to the mould. Traditionally, the reaction was then started by heating the polymerisation mixture. More recently the use of photo-initiators and UV light as a method of forming monoliths has become popular (Yu *et al*., 2001). This has lead to an increased speed of monolith formation, and the ability to form monoliths at room temperature. A disadvantage of this technique is that one has to rely on UV transparent moulds, monomers and porogens (Lee *et al*., 2004). The use of UV light to generate monolithic structure also has an advantage in that it can be used to make focused monolithic "sections" within capillary columns. When using the original thermal-initiator methods, a complete monolith column has to be generated. By using UV light and masking certain areas where one does not want monoliths to form, distinct sections of monolith can be formed within a column.

One of the most vital aspects of monolith production is the control of pore size and pore formation. This parameter is mainly dictated by the porogen and the cross-linked monomer used in the formation reaction (Stulik *et al*., 2006). These investigators carried out an in-depth study on the effects on pore size and the amount of protein immobilised within a GMA/EDMA monolith (Homola *et al.*, 1999). Under different polymerisation conditions the amount of protein immobilised was determined. These polymerisation conditions included varying the temperature of monolith initiation. It was found that in a range of temperatures between 55°C and 80°C the greatest amount of immobilised protein achieved was at 80°C. A change in the ratio between the structural monomer and the cross-linking monomer was also studied. As a decrease in the cross-linking monomer meant a corresponding decrease in the rigidity of the monolithic structure a cross-linking content of 16% v/v to the rest of the monolithic mixture was

recommended. The final area of interest in this study was the concentration of porogen which would give the greatest surface area, but which would not have deleterious effect on the characteristic monolith low back pressures. For ultra-fast immunoextraction it was determined that a 60% (v/v) would be the optimum concentration of porogen. This produced a large enough surface area for protein immobilisation without causing a huge increase in the back pressure of the column (Jiang *et al*., 2005). The porogen to use is also an important consideration which has to be investigated and is considered one of the most important features of a monolithic preparation (Figure 1.16). For example (Lee *et al*., 2004) varied the ratios of two different porogens. The primary porogen used in these experiments was 1-decanol, with varying concentrations of cyclohexanol added. The pores formed when 1-decanol was the lone porogen were narrow and symmetrical with a maximum pore size of 2.2µm. When the ratio of porogen was changed to 2:1 1-decanol to cyclohexanol the average pore size dropped to 0.66µm. These investigators went on to report that while the column with the smaller pores is more resistant to flow, both columns can withstand pressures of up to 25megapascals (MPa).

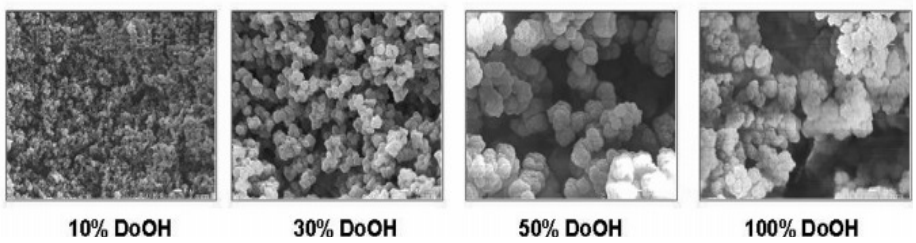

Figure 1.16: The effect of porogen concentration on monolithic structure. Image from(Jiang *et al*., 2005). DoOH = Decanol.

1.4.3.: Different types of monolith

As previously mentioned monolithic structures can be composed of many functional monomers, each with different properties. The most commonly used, and the best researched are the following;

1.4.3.1: Glycidyl methacrylate (GMA) and Ethylene dimethacrylate (EDMA) monoliths:

Methacrylate based monoliths have are most commonly used in affinity chromatography due to their inherent functional groups. Monoliths composed of these functional monomers and cross-linkers contain epoxy groups which can be used to immobilise ligands as outlined previously (Figure 1.7). An added benefit is the ease of use of these materials and the fact that by changing porogens, porogen concentrations and the cross-linker to monomer ratio the properties of these monoliths can be significantly changed (Rangan Mallik, 2006).

1.4.3.2: Agarose Monoliths:

Agarose has been used for many years as a method to separate biomolecules and its use as a monolith structure has been well documented (Walters, 2008). These monoliths are characterised by having large pores which are 20 to 200μm in diameter. The advantages of these monoliths are the low amounts of non-specific binding and their stability over a wide range of pH's. They are inhibited by having a low inherent strength, large pores which limits amount of ligand immobilisation area and their susceptibility to high temperatures (Rangan Mallik, 2006).

1.4.3.3: Silica Monoliths:

Silica monoliths have become popular because of the use of silica particles in HPLC. They are characterised by having good mechanical strength but a major weakness is the complex preparation required and their tendency to shrink after they are formed (Rangan Mallik, 2006). The preparation of silica monolith columns consists of six separate steps. After acid and base catalysis the reactive alkoxysilanes polymerise. This reaction generates the gel. This gel then separates into two separate domains i.e. a solid and liquid phase. These phases continue to react with each other to give the final formed monolith structure in a process called 'syneresis'. This syneresis reaction results in the shrinkage commonly associated with silca monoliths, but it also expels the liquid from the pores. These monoliths then have to be aged and dried. Finally, if these columns are to be used for affinity chromatography then the surfaces will have to be modified. The

pore size and structure of these monoliths are reliant on the thermodynamics and kinetics of the formation reaction. Therefore, the initial reaction mixture has to be very well defined (Rieux *et al*., 2005).

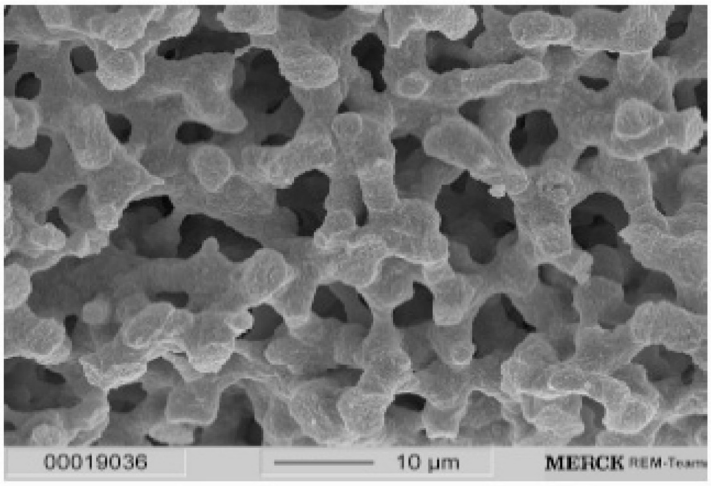

Figure 1.17: Typical structure and pore morophology of a fused silca monolith. Picture from (Rangan Mallik, 2006)

1.4.3.4: Cyrogels:

These monoliths are defined by their large pore sizes more commonly known as marcopores. The most common way to produce these monoliths is by mixing of acrylamide, allyl glycidly ether, and N,N'-methylene *bis*-(acrylamide). TEMED and

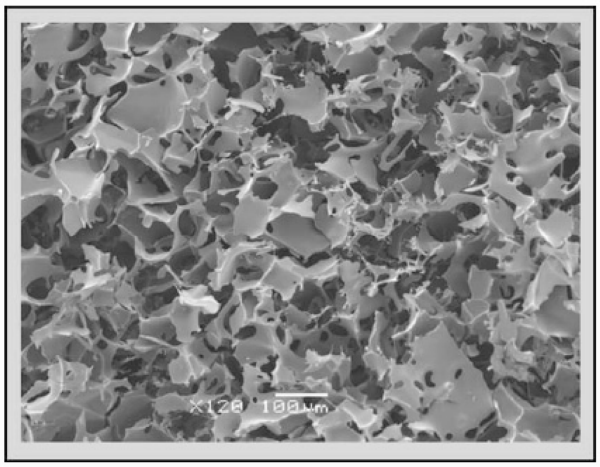

Figure 1.18: The structure and pore morophology of cyrogels: Illustration from (Rangan Mallik, 2006)

ammonium persulfate are used as initiators. The key to the formation of cyrogels as the name suggests is to perform the polymerisation at low temperatures, typically with the monomers dissolved in the aqueous phase below -10°C. The pores of the monolith are formed by the ice-crystals which are formed at this low temperature. Once the structure is formed the temperature is slowly increased to above freezing, allowing the ice to melt revealing the pores which are typically 10-100μm in diameter (Rangan Mallik, 2006).

1.4.4.: Affinity Monolith Chromatography:

Monolithic columns were first introduced as a new stationary phase in HPLC and Capillary Electrophoresis methods. More recently, many groups are using these structures as a stationary phase for affinity chromatography (Rangan Mallik, 2006). An important breakthrough in use of monoliths as a stationary phase is the control of surface chemistry of these surfaces by photografting. Many monolithic surfaces are hydrophobic when initially formed. This is not ideal for many proteins as many will be immobilised in a non-specific manner through hydrophobic interactions. A problem may also arise as many proteins with hydrophobic cores can be relatively easily denatured. The most common method to overcome this problem is to photograft a hydrophilic molecule onto the surface of the monolith. This provides a hydrophilic surface which can then be further modified to display reactive moieties for the covalent immobilisation of affinity ligands. (Stachowiak *et al*., 2006) have described that photo grafting of poly-(ethylene glycol) methacrylate (PEGMA) onto the monolithic surface reduced non-specific protein immobilisation in poly(butyl methacrylate-*co*-ethylene dimethacrylate) monolithic columns by as much as 98%. This group went on to immobilise protein in distinct zones along a capillary monolithic column using photografting techniques and the reactive monomer 2-vinyl-4,4-dimethylazlactone.

A number of groups have made progress with immobilising ligands on monolithic surfaces. (Bedair and Oleschuk, 2006) have immobilised the lectin Concanavalin A onto glycidyl methacrylate/ethylene dimethacrylate monoliths using the Schiff base method. This was then used as a pre-concentrator on a nanoelectrospray emitter for the glycoprotein of Ribonuclease B before detection by mass spectrometry. (Ostryanina *et al.*, 2002) immobilised protein and peptide ligands onto monolith supports known as Convective Interaction Media (CIM) discs (www.biaseperations.com) to fractionate

antibodies from the serum of rabbits. By using several CIM discs in series they were able to form a column which was highly selective. Peptide ligands have also been immobilised onto GMA monoliths for the study of interactions with plasminogen activators. These activators are highly important for the dissolving of blood clots and may play an important part in the treatment of heart disease (Vlakh *et al.*, 2004).

Other commonly used ligand for immobilisation on monolithic structures is Proteins A, G and L. These proteins have long been used in conventional immobilisation techniques and have made the transition to affinity chromatography monolithic columns. (Berruex *et al.*, 2000) proposed the name High Performance Monolith Chromatography (HPMC) for the capture of polyclonal bovine IgG and a recombinant human antibody to CIM discs which had immobilised Protein A, G and L. (Gupalova *et al.*, 2002) immobilised different forms of Protein G onto CIM discs to study their different binding characteristics to blood IgG's and blood serum albumin, while (Luo *et al.*, 2002) used immobilised Protein A and L-histidine to purify IgG from blood serum. It was found that the immobilised Protein A monolith columns retained functionally for six months, a considerable lifespan for a biologically functionalised surface.

Also of considerable interest is the transfer of immobilised metal affinity chromatography (IMAC) to monolithic supports. A successful example of this method was the creation of a Cryogel with a functionalised Cu^{2+} surface. As cryogel's have large pore sizes due to their method of formation, *E.coli* cells could potentially be captured by these monolithic columns. This method was found to give an 80% recovery of *E.coli* cells when eluted with 10mM Imidazole or 20mM EDTA. (Arvidsson *et al.*, 2002) (Cheeks *et al.*, 2009) then compared the purification of histidine tagged viral vectors by commercially available CIM discs and lab-made cryogels. They determined that the performance of CIM discs were superior in many ways to cyrogels especially in capture, concentration and elution capacity.

As a potential method for affinity chromatography the use of monolithic columns has just begun to be explored. The benefit of using monolithic systems is that interactions between an immobilised ligand and an analyte can be relatively easily monitored. This becomes more evident when using macromolecules such as proteins, DNA or viruses where monoliths have an inherent higher capacity than traditional chromatographic supports (Peterka *et al.*, 2006).

1.5: Capacitively Coupled Contactless Detection (C^4D)

1.5.1: Introduction to C^4D:

Absorbance at 280nm and fluorescence methods have long been used in capillary electrophoresis to detect peaks of eluted analytes. While these methods are ideal for a wide range of species they do have some limitations, the most important of which is the fact that not all analytes either absorb UV light or possess a fluorescent functionality. There is a continuing search for a non-invasive, easy to use detectors for these species. The focus of this search has been on electrochemical detection techniques, such as amperopmetry, potentionmetry and conductometry. Conductometry may be less sensitive than the other two methods but can be used for the broadest range of analytes (Guijt *et al*., 2004). Because of this conductivity detection in capillary electrophoresis has received a lot of attention over the past decade.

1.5.2: Capacitively Coupled Contactless Conductivity Detection:

Conductivity detectors were used as far back as the 1970's. These methods involved contact conductivity detection, where the detectors were in direct contact with background electrolytes (BGEs). This is not an ideal situation as depending on the BGE reactions can occur with the electrodes of the detector. This leads to reduced reproducibility, loss of detection signal or electrode fouling.

It was not until 1998 that further progress was made with this type of detection system. Two groups independently published a conductivity detection system for capillary electrophoresis. (Fracassi Da Silva and Do Lago, 1998) and (Zemann *et al.*, 1998) both used painted silver rings on a fused silca capillary to act as electrodes. Zemann and his colleagues went a step further and used stainless steel syringe needles to form electrodes. Both these systems, where the electrodes are not in direct contact with the solution to be measured, have become known as capacitively coupled contactless conductivity detection (C^4D) systems.

The use of the two syringe needles as electrodes for this system effectively "free" the detection of the conductivity within the capillary to any point. In this case as the needles were slightly larger than the capillary the detector cell was able to be moved to any

point on the capillary. The use of silver paint "locks" the detection to the area of the capillary between the two electrodes.

In these initial papers the electrodes, which form cylindrical capacitors were separated by 1mm in (Fracassi Da Silva and Do Lago, 1998) and by 2mm in (Zemann *et al.*, 1998). It is within this detection window that the conductivity of the solution within the capillary is measured. To do this an AC voltage is applied to one of the electrodes at constant amplitude. Applying an oscillation frequency causes a capacitive transition between the actuator electrode and the liquid inside the capillary. Passing through the gap between the electrodes, a second capacitive transition between the solution within the capillary and the pick-up electrode takes place (Figure 1.19). The generated electric current is indirectly proportional to the resistance or directly proportional to the conductance of the solution within the detector window(Scaronolínová *et al.*, 2006). By using suitable electronics, the conductivity of the electrolyte in the detection gap can be determined.

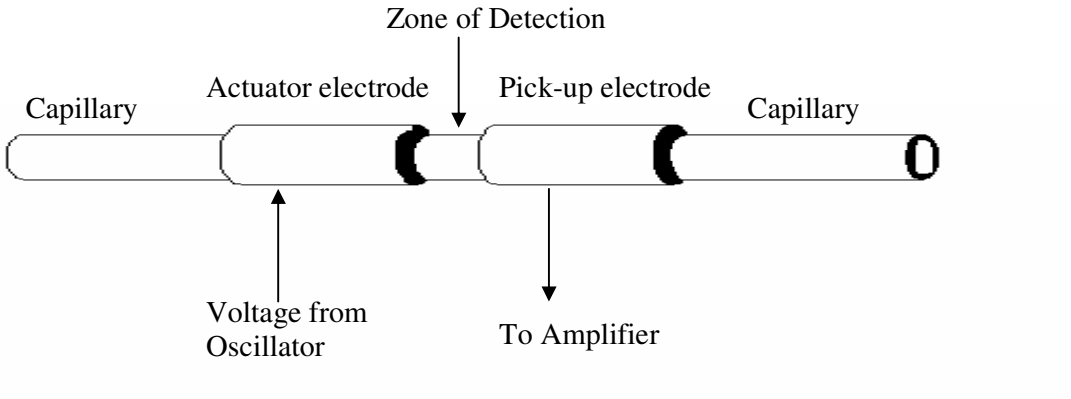

Figure 1.19: General Structure of C4D cell

When different species in aqueous solution pass the detector, the conductivity of the solution is the only parameter which undergoes a change. Permittivity and permeability of aqueous solution are usually negligible and can be considered to remain constant for this case. Any changes in the detector window registered by the pick-up electrode are therefore related to changes in the conductivity of the solution in the cell, rather than the changes in any other parameter (Guijt *et al.*, 2004).

For modern detection cells the electrodes are kept at a constant distance within a grounded housing. The electrodes are usually separated by a thin metal sheet to reduce

cross capactivity and noise. When designing these detection cells parameters such as length of the electrodes as well as distance between them are important (Zemann, 2003). An alternating current (AC) is preferred over a direct current (DC) so as to minimise the polarisation of the electrodes. AC current also reduces the electrochemical reactions on the electrode surfaces, and to minimise interference of the DC current with the detection electronics.(Guijt *et al*., 2004) Taking all of these detection advances a commercially available conductivity detector was launched in 2004. This conductivity detector is marketed under the trade name "TraceDec", and is available from Istech. (**www.istech.at**)

.

.

1.6: A Sialic Acid Binding Protein: SiaP

1.6.1: Introduction to Sialic Acid:

Sialic acid is a generic term to describe a family of related nine-carbon sugars. These sugars are most commonly presented at the terminal positions via C2 to position 3 or 6 of the previous sugar or to position eight of a previous sialic acid. The most abundant and best-studied sialic acid is N-Acetylneuraminic acid (Neu5Ac) as it is found most commonly in nature. (Severi *et al*., 2007) The special features of sialic acid are its amide group at carbon 5 and its carboxyl group at position 1.

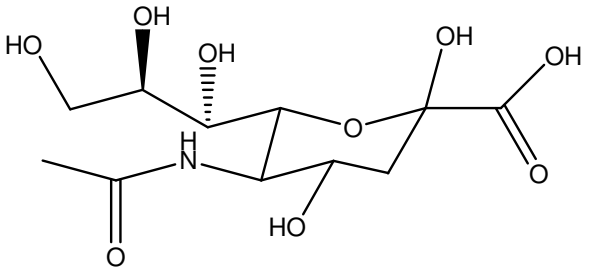

Neu5Ac

Figure 1.20: Structure of N-Acetylneuraminic Acid. (Neu5Ac)

The importance of Sialic acids within biological systems cannot be understated. After nucleotides and proteins, carbohydrates have become known as the "third language of life" (Schauer, 2004). Because these molecules are positioned at the terminus of the sugar structures which cover a cells' surface they play a vital role in almost all biological events, most importantly intercellular adhesion and cell signalling, (Severi *et al*., 2007) As well as this many infectious microorganisms also recognise sialic acid as a cell adhesion point. The study of sialic acid has recieved great interest in the last 20 years when its importance and structural diversity became fully known. Its importance in neuronal transmission, ion transport, reproduction, differentiation and protection are only now being understood. Its effect on disease states such as infections and inflammations, cancer and neurological, cardiovascular, endocrinological and autoimmune diseases as well as auto-immune and genetic disorders are even more wide-spread and studied (Traving and Schauer, 1998).

Within large scale bioreactors and biotechnology processes the production of correctly folded and formed glycoproteins is of vital importance. The sialylation of glycoproteins has such an effect on the structure and function it can lead to vast differences on the

safety and efficacy of the product (Geyer and Geyer, 2006). A rapid and efficient method to measure and determine the amount of sialylation of a glycoprotein product would therefore be of great use to the biotechnology industry. The growth of the biopharmaceutical industry relies on the production of new and novel compounds, and only now is the importance of correctly glycosylated products being realised. Combined with stricter controls by safety authorities the ability to quickly and correctly define the level of glycosylation within a biopharmaceutical product will lead to increased growth in the sector.

1.6.2: Introduction to *Haemophilus influenzae*:

The bacterium *Haemophilus influenzae* is a gram negative rod which was first isolated in 1892. It is a major cause of disease, such as septicaemia, meningitis, otitis and acute respiratory tract infections. (Severi *et al*., 2005) It was also the first organism to have its entire genome sequenced in 1995. (Fleischmann *et al*., 1995) It is an opportunistic pathogen and is adapted to infect and colonise humans. To protect itself from its host's immune systems and to increase its pathogenicity the bacterium has developed a complicated layer of sugars presented on its surface. This lipopolysaccharide (LPS) has been shown to effectively "hide" the bacterium from the host immune system. (Severi *et al*., 2005)

1.6.3: Sialic Acid use in *Haemophilus influenzae*:

The LPS in *H. influenzae* is a highly complex structure and is vitally important for the virulence of the organism (Schweda *et al*., 2007). Despite this, in a clinical test of 24 isolates which are thought to represent the genetic diversity of this bacterium, terminal sialic acid was found in the vast majority of samples (Bauer *et al*., 2001). By knock out mutations it has been determined that if sialic acid is not present on the LPS of the bacterium its ability to survive in human serum is greatly reduced (Hood *et al*., 1999). As *H. influenzae* does not have the cellular machinery to produce sialic acid all molecules displayed within the LPS have been scavenged from the surrounding environment. It has also been shown that *H. influenzae* can use sialic acid as a rich source of both carbon and nitrogen for metabolism (Vimr *et al*., 2000).

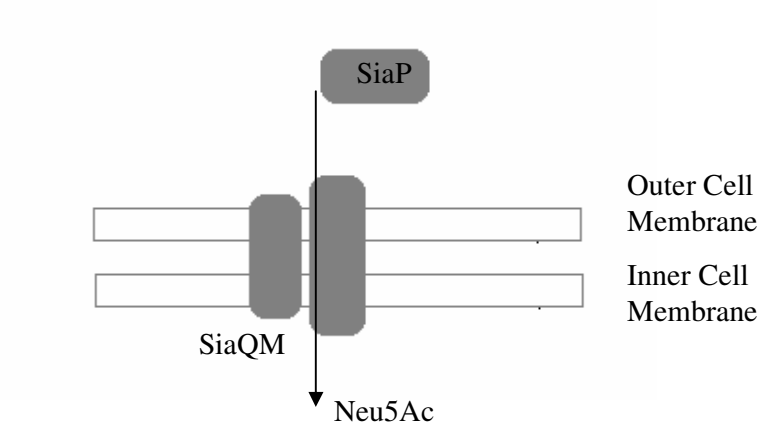

Figure 1.21: Simplified representation of the sialic acid TRAP system in *H. influenzae* (Allen *et al.*, 2005).

Much work has been done to discover the transport system the bacterium uses to acquire 'free' sialic acid. A tripartite ATP-independent periplasmic transporter (TRAP) has been deduced to be the method by which *H. influenzae* acquires this vital sugar. (Severi *et al*., 2005, Allen *et al*., 2005) As outlined by (Allen *et al.*, 2005) these TRAP transporters consist of three unique proteins, namely an extracellular solute receptor (ESR) and two distinct membrane proteins which transport the molecule of choice across the membrane. Within *H. influenzae* these proteins are expressed from two genes, the ESR protein is expressed from gene HI0146 and is known as SiaP, while the membrane transport proteins are expressed from gene HI0147 and are known as SiaQM.

1.6.4: Importance of SiaP within *Haemophilus influenzae*:

The initial work on SiaP was first carried out in 2005, where the effect on the organism of knocking out both the HI0146 and HI0147 genes were determined. (Severi *et al*., 2005) This study showed that the deletion of either of these genes removed the ability of *H. influenzae* to use sialic acid in either the decoration of its LPS or use it as a carbon or nitrogen source. Due to the fact that its LPS was not decorated with the hosts own sialic acid the ability of *H. influenzae* to survive within blood serum was found to be greatly reduced.

Also shown in this landmark paper was the binding efficiency of SiaP for sialic acid. By over-expressing and purifying SiaP from *E.coli* cells the molecular mass of the protein was determined to be 34kDa. By measuring the change in the fluorescence of SiaP

before and after sialic acid binding it was shown that the K_d was 0.12μM. This is an extremely high affinity constant.

A more in-depth study of the protein was released in 2006. (Muller *et al*., 2006) In this study the structure of SiaP was resolved to 1.7Å in an unbound form and to 2.2Å in a bound form. It was determined that SiaP has two α/β domains connected by three segments of the protein and separated by a large cleft. Domain I is composed of the residues 1-124 and 213-252, and contains a 5-stranded β-sheet, with which are packed with six α-helices.

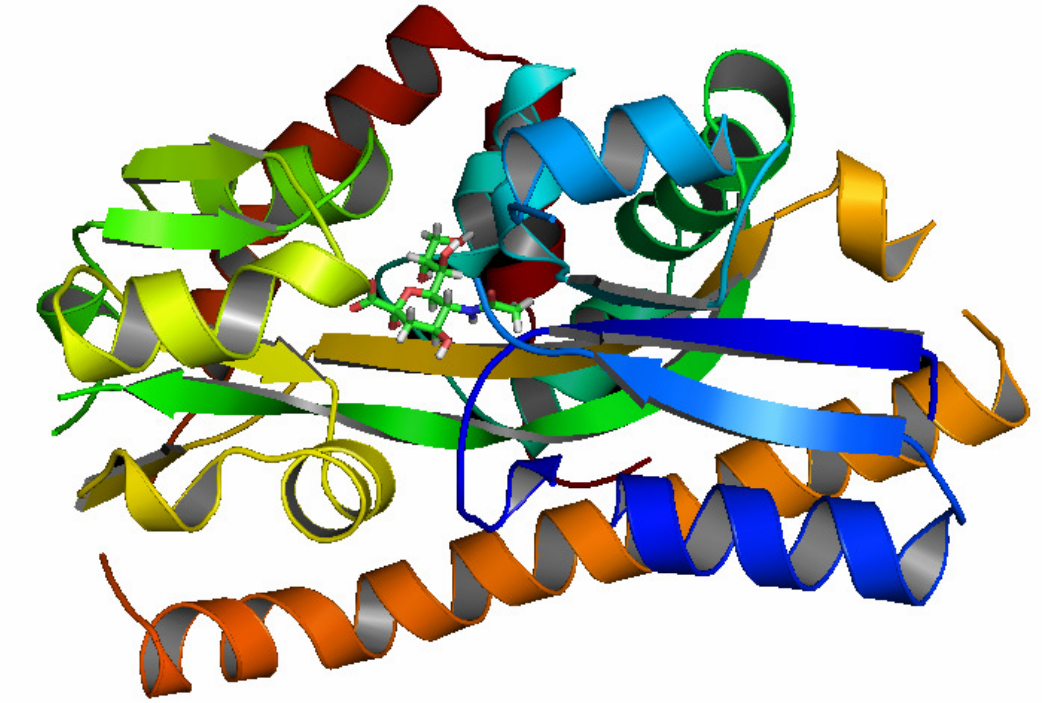

Figure 1.21: Structure of SiaP with bound Sialic Acid. PBD No: 3b50 (Johnston *et al.*, 2008).

Domain II is composed of residues 125-212 and 253-306 and has a 6-stranded β-sheet surrounded by 3 α-helices. The C-terminus of the molecule forms a pair of α-helices that folds along the base of the molecule and folds against both domains (Muller *et al*., 2006).

This protein folding pattern allows for a rotation of 25-31° around a hinge between the residues Thr127-Arg128, Ile211-Leu212 and Glu254-Lys255. This rotation only occurs when the sialic acid ligand is bound. Both domains effectively close around the bound ligand and this rotation is the cause of the highly specific interaction and tight binding between SiaP and sialic acid. The ligand binds within the cleft between the two domains

and its carboxylate group forms a salt bridge to Arg147 and a polar interaction Asn187 (Muller *et al.*, 2006).

It is thought that the binding of sialic acid to SiaP is initiated by the interaction of the carboxylate group of the ligand and the conserved Arg47 residue in domain II of the protein. The full coordination of the carboxylate also includes an interaction with Arg127 which is within the hinge region and the formation of this interaction could be involved in triggering the hinge movement of the protein. Once the hinge movement has occurred the domain I interactions with the ligand can form, binding the ligand tightly (Muller *et al.*, 2006).

1.7: Outline of this Thesis:

The study of orientation specific immobilisation of active proteins onto novel surfaces was one of the initial aims of this project. Green Fluorescent Protein was determined to be an ideal model protein candidate for initial tagging studies. It was hoped that by using the protein's inherent fluorescence the optimum tagging strategy and a successful and reproducible method of immobilisation onto a number of functionalised surfaces could be explored. Once initial tagging and orientation specific immobilisation parameters were elucidated, it was hoped to transfer these processes to a more biologically significant biomolecule.

The position of Sialic acid on the terminal end of carbohydrates, present on glycoproteins makes it an ideal target for the biopharmaceutical industry. SiaP has a high binding efficiency for sialic acid. If this protein can be positioned in the correct orientation this will provide a valuable method for the rapid and accurate analysis of Sialic acid levels in biological systems and industrial processes. By utilising monolithic columns and C^4D it is hoped to establish a quick and un-complicated method to determine biological interactions.

Chapter 2: Materials and Methods

2.1 Abbreviations:

bp	Base pair
BSA	Bovine Serum Albumin
BUMA	Butyl methacrylate
C^4D	Capacitively Coupled Contactless Conductivity Detection
DAP	2,2-Dimethoxy-2-Phenylacetophenone.
dH_20	Deionised water
DMSO	Dimethyl sulphoxide
DNA	Deoxyribonucleic acid
dNTP	Dexoyribonucleotide Triphosphate
EDMA	Ethylene Glycol dimethacrylate
EDTA	Ethylenediaminetetra acetic acid
IMAC	Immobilised metal affinity chromatography
IPTG	Isopropyl-β-*D*-thiogalactopyranoside
LB	Luria Bertani
MCS	Multiple cloning site
MOPS	3-(N-Morpholino)propanesulfonic acid
O.D.	Optical Density
ORF	Open reading frame
PAGE	Polyacrylamide gel electrophoresis
PCR	Polymerase chain reaction
PEEK	Polyetheretherketone
PEGMA	Polyethylene Glycol Methacrylate
PIPES	Piperazine-1,4-bis(2-ethanesulfonic acid)
SDS	Sodium dodecyl sulphate
TEMED	N,N,N,N'-tetramethyl ethylenediamine
TFA	Trifluoroacetic Acid
Tris	Tris (hydroxymethyl) amino acid
UV	Ultraviolet light
w/v	Weight per volume
XGAL	5-bromo-4-chloro-3-indolyl-β-D-galactopyranoside

2.2 Bacterial Strains, Primer Sequences and Plasmids:

The bacterial strains, primer sequences and plasmids used in this study are outlined in Tables 2.1, 2.2 and 2.3 respectively.

Table 2.1: Bacterial Strains

Strain	Genotype	Features	Source
Escherichia coli			
BL21 (DE3)	F^-, *dcm ompT hsd*$S_B(r_B\text{-}m_B)$gal lon λ(DE3 [lacI lacUV5-T7 gene l indl sam7 nin5])	Protease deficient High transformation efficiency Expression host	Novagen
XL10-Gold	Tet^r Δ(*mcrA*)183 Δ(*mcr*CB-*hsd*SMR-mrr)173 *end*A1 *sup*E44 *thi*-1 *rec*A1 *gyr*A96 *rel*A1 lac Hte [F'*pro*AB *lac*I^qZ ΔM15 Tn10 (Tet^r)Amy Cam^r]	High transformation efficiency Expression host	Stratagene

Table 2.2*:* Primer Sequences (Synthesised by Sigma-Aldrich, U.K.)

Primer Name	**Primer Sequence**	**Tm**
F. Primer ***Bsp*HI**-GFP	5' CCCCC**TCATGA**GTAAAGGAGAAGAACTTTTCACTGGA 3'	66^{o}C
F. Primer ***Bam*HI**-GFP	5' CCCCCC**GGATCC**ATGAGTAAAGGAGAAGAACTTTTCACT GGA 3'	69^{o}C
F.Primer *Bam***HI** Lysine tag-GFP	5'CCCCCC**GGATCC***AAGAAAAAGAAAAAG*ATGAGTAAAGGAGAAG AACTTTTCACTGGA 3'	70^{o}C
F. Primer *Bam***HI** Cysteine tag-GFP	5' CCCCCC**GGATCC***TGTTGCTGTTGCTGTTGC*ATGAGTAAAGGAG AAGAACTTTTCACTGGA 3'	74^{o}C
F. Primer ***Bam*HI** *StrepII tag*-GFP	5'CCCCCC**GGATCC***TGGAGCCACCCGCAGTTCGAAAAA*ATGAGTAA AGGA GAAGAACTTTTCACTGGA 3'	76^{o}C
F. Primer Phosphorylation-GFP	5' P'TAGAAGCTTAATTAGCTGAGCTTG 3'	66°C
R. Primer ***Bgl*II**-GFP	5'CCCCC**AGATCT**TTTGTATAGTTCATCCATGCCATGTGTAATC CCA 3'	68^{o}C
R. Primer ***Hind*III**-GFP	5' CCCCCC**AAGCTT**CTATTTGTATAGTTCATCCATGCCATGTGT 3'	67^{o}C
R. Primer ***Hind*III** *Lysine tag*-GFP	5'CCCCCC**AAGCTT**CTA*CTTTTTCTTTTTCTTTTT* GTATAGTTCATCC ATGCCATGTGT 3'	69^{o}C
R. Primer ***Hind*III** *Cysteine tag*-GFP	5'CCCCCC**AAGCTT**CTA*GCAACAGCAACAGCAACA*TTTGTATAGTT CATCCATGCCATGTGT 3'	73^{o}C
R. Primer ***Hind*III** *StrepII tag* -GFP	5'CCCCCC**AAGCTT**CTATTT*TTCGAACTGCGGGTGGCTCCATTT* GT ATAGTTCATCCATGCCATGTGT 3'	75^{o}C
R.Primer Phosphorylation-cysteine residue-GFP	5' P'ACATTTGTATAGTTCATCCATGCC 3'	66°C

Restriction sites appear in **bold** and underlined. Inserted tags are in *italics*

Table 2.3: Plasmids generated in this study

Plasmid	Description	Source
pCR2.1	PCR Cloning Vector: Amp^R, Km^R, lacZα	Invitrogen
pQE30	Amp^R, Expression vector for N-terminally tagged $(His)_6$ proteins, T5 promoter/lac operon	Qiagen
pQE60	Amp^R, Expression vector for C-terminally tagged $(His)_6$ proteins, T5 promoter/lac operon	Qiagen
pQE30-Xa	Amp^R, Expression vector for N-terminally tagged $(His)_6$ and FXa Protease site, T5 promoter/lac operon	Qiagen
pUC18	Cloning vector: Plac, amp^R, lacZα, ColE1 origin	Amersham
pRV	Cloning vector in use in lab: Amp^R , Ptac.	Roman-Vaas (2005)
pBK-miniTn7gfp2	Original source of GFP gene	Koch, B(2001)
pRV5 Derived Vector		
pVOS1	pRV5 containing GFP, with a C-terminal histidine tag	This Study
pQE30 Derived Vectors		
pVOS2	pQE30 containing GFP	This Study
pVOS3	pQE30 containing GFP with a C-terminal lysine tag added by PCR	This Study
pVOS4	pQE30 containing GFP with a C-terminal cysteine tag added by PCR	This Study
pVOS5	pQE30 containing GFP with a C-terminal Strep-TagII added by PCR	This Study
pVOS12	pQE30 containing GFP with a C-terminal single cysteine residue added by PCR	This Study
pQE60 Derived Vectors		
pVOS9	pQE60 containing GFP with a N-terminal lysine tag added by PCR	This Study

pVOS10	pQE60 containing GFP with a N-terminal cysteine tag added by PCR	This Study
pVOS11	pQE60 containing GFP with a N-terminal Strep-tagII added by PCR	This Study

pQE30-Xa Derived Vectors

pVOS2-Xa	pQE30-Xa containing GFP	This Study
pVOS3-Xa	pQE30-Xa containing GFP with a C-terminal lysine tag added by PCR	This Study
pVOS4-Xa	pQE30-Xa containing GFP with a C-terminal cysteine tag added by PCR	This Study
pVOS5-Xa	pQE30-Xa containing GFP with a C-terminal StrepII tag added by PCR	This Study
pVOS6-Xa	pQE30-Xa containing GFP with a N-terminal lysine tag added by PCR	This Study
pVOS7-Xa	pQE30-Xa containing GFP with a N-terminal cysteine tag added by PCR	This Study
pVOS8-Xa	pQE30-Xa containing GFP with a N-terminal Strep-tagII added by PCR	This Study

2.3. Media:

All chemicals and reagents were obtained from Sigma-Aldrich unless otherwise stated. Microbiological media were obtained from Cruinn Diagnostics Limited. Sterilisation was achieved by autoclaving at 121^{o}C and 15lb/in^{2} for 20 minutes.

Luria Bertani Broth (LB)

Tryptone	10 g/L
NaCl	10 g/L
Yeast Extract	5 g/L

The solution was adjusted to pH 7.0 with NaOH and sterilised by autoclaving. For solid LB agar, 15 g/L Technical Agar No.3 (Oxoid) was included.

2.4: Solutions and Buffers:

Tris-EDTA Buffer (TE Buffer)

Tris-HCl	10 mM
Na_2-EDTA	1 mM
pH	8.0

50x Tris Acetate EDTA (TAE) Buffer

Tris	242 g/L
Glacial Acetic Acid	57.1ml/L
EDTA	100 ml/L (of 0.5 M stock)
pH	8.0

The solution was diluted to 1X with dH_20 before use.

Solutions for the 1-2-3 Method of Plasmid Preparation

Solution 1:

Glucose	50mM
Na_2-EDTA	10mM
Tris-HCl	25mM

Solution 2:

NaOH	200mM
SDS	1% (w/v)

Solution 3:

Potassium Acetate	3M
pH	4.8

To 60 ml of 5 M potassium acetate, 11.5ml of glacial acetic acid and 28.5ml of dH_2O were added. The resulting solution was 3M with respect to potassium and 5M with respect to acetate.

TB Buffer for Competent Cell Production

PIPES	10mM
$CaCl_2$	15mM
KCl	250mM
pH	6.7

The pH was adjusted with KOH and $MnCl_2$ was then added to give a final concentration of 55mM. The solution was filter sterilised by passing through a 0.2µm filter and stored at 4°C.

DNA Gel Loading Dye (6x)

Bromophenol Blue	0.25% (w/v)
Xylene Cyanol	0.25% (w/v)
Ficoll (Type 400)	15% (w/v)

This dye was made in dH_2O and stored at room temperature following autoclaving. On a 1% agarose gel, bromophenol blue and xylene cyanol migrate with the 300 bp and 4000 bp fragments respectively.

Lysis Buffer for Protein Purification

NaH_2PO_4	50mM
NaCl	300mM
Imidazole	10mM
pH	8.0

Sample Buffer for SDS-PAGE

Glycerol	50%(v/v)
SDS	2% (w/v)
2-Mercaptoethanol	5% (v/v)
Bromophenol Blue	0.1% (w/v)
Tris-HCl, pH6.8	62.5mM

For native PAGE, SDS and 2-mercaptoethanol were omitted and replaced with the equivalent volume of H_2O.

SDS-PAGE Running Buffer (5X)

Tris-HCl	125mM
Glycine	960mM
SDS	0.5% (w/v)

For native PAGE, SDS was omitted.

Resin Binding Buffer

Sodium Phosphate	20mM
NaCl	500mM
Imidazole	20-40mM
pH	7.4

The optimal imidazole concentration is protein dependent.

Resin Elution Buffer

Sodium Phosphate	20mM
NaCl	500mM
Imidazole	40-250mM
pH	7.4

The optimal imidazole concentration for elution is protein dependent.

Stripping Buffer for IMAC Resins

Sodium Phosphate	20mM
NaCl	500mM
EDTA	50mM
pH	7.4

Recharging Buffer for Nickel Resins

$NiSO_4$	100mM

Coomassie Blue Stain (for 400mls)

Coomassie Blue (R-250)	1g
Methanol	160ml
dH_20	200ml
Acetic Acid	40ml

Coomassie Blue De-Stain Solution (400mls)

Methanol	160ml
dH_20	200ml
Acetic Acid	40ml

Phosphate Buffered Saline (PBS) 1X

NaCl	137m
NaH_2PO_4	4.3mM
KCl	2.7mM
K_2HPO_4	1.5mM
pH	7.4

For PBST, the detergent Tween-20 was added to a final concentration of 0.1%(v/V)

1M HEPES (4-(2-hydroxyethyl)-1-piperazineethanesulfonic acid) Buffer

238.3g HEPES in 500mls dH_20

The pH was adjusted by the addition of NaOH and brought to 1L with dH_20. This was sterilised by autoclaving.

	Stock Concentration	Storage Temperature	Final Concentration	Storage Buffer
Ampicillin	100mg/ml	-20°C	100µg/ml	Water
Gentamicin	50mg/ml	-20°C	10-20µg/ml	Water
Tetracycline	50mg/ml	-20°C	10-20µg/ml	50% Ethanol
Chloramphenicol	50mg/ml	-20°C	20-30µg/ml	100% Ethanol
Kanamycin	50mg/ml	-20°C	20-30µg/ml	Water
Streptomycin	100mg/ml	-20°C	50µg/ml	Water
IPTG	1M	-20°C	1mM	Water
XGAL	50mg/ml	-20°C	50µg/ml	Di-Methyl Formide

Table 2.4: Antibiotics and other chemicals preparation and storage

2.5 Enzymes

All restriction endonucleases and T4 DNA ligase were obtained from New England Biolabs or Promega. RED*Taq* was obtained from Sigma-Aldrich. Phusion High-Fidelity DNA Polymerase was obtained from New England Biolabs. Enzymes were used with their relevant buffers according to the manufacturers instructions.

2.6 Storing and culturing bacteria

Strains were stored as glycerol stocks. A 0.75ml aliquot of a late log phase culture was added to 0.75ml of sterile 80% glycerol in a microfuge tube. This was then mixed and stored at –20°C. A duplicate set of long-term stocks was stored at –80°C. Where hosts were harbouring plasmids, the appropriate antibiotics were added to the stock medium. Working stocks were stored on plates at 4°C.

2.7 Isolation and purification of DNA

2.7.1 Isolation of plasmid DNA

Two procedures for the isolation of plasmid DNA were employed. The 1-2-3 method was routinely used to yield high quality DNA. The Genelute plasmid miniprep Kit (Sigma) was used to prepare consistently pure and super coiled plasmid DNA, mostly for the purpose of DNA sequencing.

2.7.2: Plasmid preparation by the 1-2-3 method:

This method is adapted from a previously outlined procedure (Birnboim and Doly, 1979) which utilises the selective alkaline denaturation of high molecular weight chromosomal DNA. Circular plasmid DNA remains double stranded. A 1.5ml volume of overnight bacterial culture was transferred to a microfuge tube and centrifuged at 13,000rpm for 5 minutes to collect the cells. The supernatant was discarded and the cell pellet resuspended in 0.2ml of Solution 1 (Section 2.4). Alternatively, bacterial growth can be removed from an LB agar culture plate with a sterile loop and resuspended in 0.2ml of Solution 1. The resuspension was left for 5 min at room temperature. 0.2ml of Solution 2 was added the tube was mixed by inversion and placed on ice for 5 min. 0.2ml of Solution 3 was added the tube mixed by inversion and placed on ice for 10 minutes. Chromosomal DNA was pelleted by centrifugation at 13,000rpm for 10 minutes. The supernatant was transferred to a new microfuge tube with 0.4ml of phenol chloroform isoamylalcohol (25:24:1) and mixed by brief vortexing. After centrifugation at 13,000rpm for 5 minutes the mixture is separated into an upper aqueous and lower organic layer. The aqueous layer was removed to a new microfuge tube with an equal volume of isopropanol and mixed by inversion. The tube was left at room temperature for 5 minutes and then centrifuged at 13,000rpm for 20 minutes to pellet the plasmid DNA. The pellet was washed with 70% ethanol and then dried briefly in a SpeedVac (Savant) vacuum centrifuge. The plasmid DNA was resuspended in 50µl of TE buffer and 1µl of ribonuclease A was added to digest co-purified RNA. Plasmid DNA was stored at 4°C

2.7.3: Plasmid preparation using the GenElute plasmid miniprep kit

This method was followed as outlined in the GenElute plasmid miniprep kit (Sigma Aldrich). Bacterial growth was taken off an LB agar culture plate with a sterile loop and resuspended in 200µl of the supplied resuspension solution. This sample was vortexed to thoroughly resuspend the cells. Cells were lysed by adding 200µl of the supplied lysis solution and the contents were mixed by gentle inversion until the mixture becomes clear. 350µl of the neutralisation/binding solution was added and mixed by inversion. The cell debris was pelleted by centrifugation at 13,000rpm for 10 minutes. A GenElute miniprep-binding column was inserted into a provided micro centrifuge tube. 500µl of column preparation solution was added to each miniprep column and centrifuged at 13,000rpm for 1 minute. The flow through liquid was discarded. The cleared supernatent from the neutralisation step was added to the prepared miniprep column and centrifuged at 13,000rpm for 1 minute. The flow through was discarded. 750µl of wash solution was added to the column and centrifuged at 13,000rpm for 1 minute. The flow through was discarded and the column recentrifuged at 13,000rpm for five minutes to remove excess ethanol. The column was then transferred to a new collection tube and plasmid DNA eluted by adding 100µl elution buffer or TE buffer was to the column. The collection tube was centrifuged at 13,000rpm for 1 minute. This eluent was then used or stored at –20^{o}C.

2.8 Agarose gel electrophoresis for DNA characterisation

DNA was analysed by running on agarose gels in a horizontal gel box. Agarose was added to 1X TAE buffer to the required concentration (typically 0.7% w/v) and dissolved by boiling. The solution was poured into plastic trays and allowed to set with a plastic comb fitted to generate sample wells. TAE buffer was used as the running buffer. Loading dye was incorporated into DNA samples to facilitate loading and to indicate DNA migration during electrophoresis. Mini-gels were run at 120 Volts for 20-30 minutes or until the tracker dye had well separated. Gels were stained by immersing in a bath of ethidium bromide for 20min. Gels were visualised on a UV transilluminator coupled with an image analyser to capture the image. On every gel 0.5µg of 1Kb Plus DNA Ladder (Invitrogen) was run as a molecular size marker.

2.9 Isolation of DNA

2.9.1 Purification of DNA from PCR reaction

200µl of TE Buffer was added to the PCR reaction. 200µl of phenol solution was added, vortexed and centrifuged at 13,000rpm for five minutes. The supernatant was removed and placed in a sterile micro-centrifuge tube. The volume of supernatant removed was measured and a volume of 3M sodium acetate equal to one tenth of this was added (e.g. 300 µl supernatent; add 30µl sodium acetate) and vortexed. To this, twice the total volume of isopropanol was added, the solution was hand inverted and centrifuged at 13,000rpm for thirty minutes. The isopropanol was carefully removed without disturbing the pellet and to this supernatent 100µl of 70% ethanol was added followed by centrifugation at 13,000rpm for five minutes. The ethanol supernatant was removed without disturbing the pellet. Open micro-centrifuge tubes were placed in a vacuum dryer for five minutes to remove any remaining ethanol. The pellet was resuspended in 45µl of TE Buffer, for five to ten minutes. The plasmid DNA was then stored at 4°C for future use.

2.9.2 Purification of DNA from agarose gel

When pouring an agarose gel for use in DNA purification 1µl of SybrSafe (Invitrogen) was added to 30µl of agarose. This allows for the visualisation of the DNA without using UV light or staining with ethidium bromide, thereby increasing the efficiency of DNA purification. The DNA was purified from agarose gels using HiYield™Gel/PCR DNA Extraction Kit. (RBC Bioscience) The kit was used according to the manufactures instructions. The gel slice was excised with a sterile scalpel, transferred into a sterile micro-centrifuge tube and weighed. 500µl of DF buffer (contained in HiYield™ kit) was added to up to 300mg of agarose gel and mixed by vortexing. The gel slice was then incubated at 50^{o}C for 10-15 minutes until completely dissolved. During incubation the microfuge tube was inverted every 2-3minutes. A DF column was placed into a collection tube and up to 800µl from the incubation was transferred. This was centrifuged at 13,000rpm for 30seconds. The flow through was discarded and the DF column was replaced in the collection tube. 500µl of wash buffer was added to the DF

column and centrifuged at 13,000rpm for 30seconds. The flow through was once again discarded and the column replaced into the collection tube. The column was centrifuged for 5 minutes at 13,000rpm to remove any remaining buffer. The dried column was then transferred into a clean micro-centrifuge tube and 30µl of elution buffer or TE buffer was added to the centre of the column. After allowing to stand for five minutes, the column was centrifuged for two minutes at 13,000rpm to elute the purified DNA. This was then stored at 4^{o}C.

2.10: Preparation of high efficiency competent cells

This method is based on a method developed by (Inoue *et al.*, 1990). A 250ml flask containing 100ml of LB broth was inoculated from an overnight culture. This culture was incubated at 37°C, shaking at 220rpm, until an O.D.$_{600nm}$ of 0.5 was recorded. When the cells reached this Optical Density, they were transferred to an ice water bath to stop growth. The cooled broth was then transferred to two sterile centrifuge tubes and pelleted in a cooled Beckman J2-21 centrifuge for five minutes at 4,500rpm. The supernatant was then discarded and the pellet re-suspended in 80mls of TB buffer, which was then incubated on ice for 10 minutes. This suspension was then centrifuged as previously. The supernatant was discarded and 15mls of TB buffer was used to re-suspend the pellet. DMSO was added slowly to give a final concentration of 7%. After incubation on ice for 10 minutes the cells were aliquotted into cooled microfuge tubes and flash frozen in liquid ethanol and stored at –80^{o}C.

2.11 Transformation of high efficiency competent cells

Competent cells, prepared according to the procedures outlined in section 2.10 were allowed to thaw on ice. A 200µl aliquot of cells was mixed gently with a 1-5µl DNA/ligation mixture and incubated on ice for 30 minutes. The cells were heat shocked at 42°C for 30seconds and then transferred back onto ice for 2minutes. Using aseptic technique, 800µl of LB broth was added. The cells were incubated at 37°C for 1hour. A 100µl aliquot of the resulting transformation mixture was plated on an appropriate selective media and the plates were incubated at 37°C overnight. `

2.12 Determining cell efficiency

Competent cell efficiency is defined in terms of the number of colony forming units obtained per µg of transformed plasmid DNA. A 25ng/µl stock of pUC18 plasmid DNA was diluted to 250pg/µl, 25pg/µl and 2.5pg/µl. An aliquot of 2µl from each dilution was transformed as described above in section 2.11. The transformation efficiency was calculated from the number of colonies obtained, taking into account the dilution factor and the fraction of culture transferred to the spread plate.

2.13 Polymerase chain reaction

PCR reactions were carried out using a Hybrid PCR Express Thermocycler.

Standard Phusion PCR Reaction Mixture:

Templete DNA	1µl
Primers	0.5µl of each
Buffer (5X)	4µl
dNTPs (10mM each)	4µl
dH_2O	9µl
Phusion Taq Polymerase (1:5 dilution)	1µl

Standard PCR Program:

Stage 1: Denaturation:	98oC for 30seconds	
Stage 2: Denaturation:	98^oC for 10seconds	50 Cycles
Annealation:	65^oC for 30seconds	
Extension:	72^oC for 90seconds	
Stage3: Final Extension:	77^oC for 10minutes	

2.14 DNA sequencing

Recombinant clones and potential mutants were verified by DNA sequencing. Eurofins MWG Operon provided commercial sequencing services and samples were sent as soluble plasmid DNA in TE buffer.

2.15 Over expression of proteins in *E.coli*

100ml of LB broth was inoculated with 1ml of an overnight culture of *E.coli* that has been transformed with an expression plasmid. The appropriate selective antibiotics were included in the overnight culture to ensure that contaminating bacterial growth was inhibited. The culture was incubated at 37°C, and 220rpm, until an $O.D._{600}$ of 0.5 was reached. IPTG was added to a final concentration of 50µM to induce expression. The temperature was reduced to 30°C to aid protein production and was incubated overnight. The culture was centrifuged at 5,000rpm for 5minutes (Beckman JA-14 rotor) to pellet the cells. The supernatent was discarded and the pellets were resuspended in binding buffer and stored at 4°C.

2.15.1 Preparation of cleared lysate

The resuspended cells were lysed with a 3mm micro-tip sonicator (Sonics & Materials Inc.) using 2.5seconds, 40kHz pulses for 30 seconds. The cell debris was removed by centrifugation at 4,000rpm for 20min at 4°C (Beckman JA-20 rotor). The cleared lysate was then passed through a 0.2µm filter and transferred to a fresh universal container and stored at 4°C.

2.16 Immobilised Metal Affinity Chromatography (IMAC)

Immobilised Metal Affinity Chromatography (IMAC) was used to purify recombinant proteins fused to a 6 residue Histidine tag. This interaction is based on the coordinated binding of histidine residues to immobilised divalent cationic metal ions, such as nickel.

2.16.1: IMAC using Ni-NTA resin

Histidine tagged proteins were purified by gravity flow over a Ni-NTA resin. A 1ml aliquot of Nickel Sepharose High Performance (GE Healthcare) was poured into a 0.7 x 10cm column and allowed to settle. The column was washed with five column volumes of distilled water to remove the 20% ethanol storage buffer and equilibrated with five-column volumes of binding buffer. The pre-treated lysate protein sample (Section 2.15.2) was then applied to the column. Five column volumes of binding buffer (Section 2.4) containing 10mM imidazole were applied to the column as a wash buffer. This was followed by passing five column volumes of binding buffer (Section 2.4) containing 60mM imidazole to remove any containment proteins. His-tagged proteins were purified by passing five column volumes of elution buffer containing 250mM imidazole. Samples of each protein fraction were analysed by SDS-PAGE. (Section 2.20) Protein concentration was determined by the BCA assay. (Section 2.18)

2.17 Regenerating and cleaning of nickel resin

The nickel resin was regenerated and cleaned as outlined in the GE Healthcare handbook. Briefly summarised the used resin was poured into a column and washed with 2 column volumes dH_2O, followed by two column volumes of 50%(v/v) ethanol. The resin was then stripped with two column volumes of 100mM EDTA, pH8.0. Remaining impurities were removed with two column volumes of 200mM NaCl, followed by two column volumes of dH_2O. Hydrophobically bound proteins and lipoproteins were removed by washing with ten column volumes of 30% isopropanol for 30 minutes, followed by ten column volumes with water. The resin was then recharged by adding two column volumes of 100mM $NiSO_4$. The resin was washed again with two column volumes of dH_2O, before transfer to a sterile universal, where it was stored in 20% ethanol.

2.18: Protein quantification by BCA assay

The bicinchonic acid (BCA) assay described by (Smith *et al.*, 1985) was utilised to quantify total protein in the range of 20-2,000 μg/ml. All samples were diluted to within

the range of the assay and added in triplicate to 150µl of BCA reagent (Sigma), and incubated at 37°C for two hours. Absorbance was read at 570nm. A standard curve was generated using bovine serum albumin (BSA) as the reference protein. Protein concentration was determined from this standard curve.

2.19 Sodium Dodecyl Sulfate Polyacrylamide Gel Electrophoresis (SDS-PAGE)

Proteins were analysed by sodium dodecyl sulphate-polyacrylamide gel electrophoresis (SDS-PAGE) according to their size, as outlined by (Laemmli, 1970).

2.19.1 Preparation of SDS gels

12% separating gels and 4% stacking polyacrylamide gels were prepared as outlined in Table 2.5. Gels were poured in an ATTO vertical mini electrophoresis system (MSC). TEMED and APS were added directly before the gels were poured. The separating gel was poured first up to 2cm below the limit of the plates. The separating gel was layered with 200µl of isopropanol and left for to polymerise.

Table 2.5: Solution for the preparation of 12% SDS Gels

Solution	**12% Separating Gel**	**4% Stacking Gel**
1.5M Tris-HCl, pH8.8	1.625ml	/
0.5M Tris-HCl, pH6.8	/	0.625ml
dH_20	2.207ml	1.538ml
Acrylamide/Bis-acrylamide 30%/0.8%(w/v)	2.6ml	0.335ml
10%(w/v) Ammonium Persulphate	32.5µl	12.5µl
20%(w/v) SDS	32.5µl	12.5µl
TEMED	3.25µl	2.5µl

After polymerisation, the isopropanol was removed by washing with distilled water and TEMED was added to the stacking gel, which was poured over the separating gel immediately. A comb was placed into the liquid stacking gel immediately to form sample wells in the polymerised gel.

2.19.2 Running of SDS-PAGE gels

Once the gels were polymerised the comb and gasket were removed from the now solid gels and placed in an ATTO vertical gel box. The gels were fitted into the gel box at an angle to minimise the creation of air bubbles between the buffer and the bottom of the gels. The gels were then completely submerged with 1X Running Buffer (Section 2.4) and the wells washed using a Pasteur Pipette to remove any residual un-polymerised acrylamide. Prepared samples (section 2.20.3) were loaded into the gel by deposition into the gel wells. Typically, the gels were run at 60mA per two gels for 50min or until the dye front reached the end of the gel. The standards used in SDS-PAGE gels were purchased from either Sigma Aldrich or New England Biolabs (NEB) The banding patterns are outlined in Tables 2.7 and 2.8 respectively.

2.19.3 Sample preparation for SDS-PAGE

10µl of a protein sample was added to 10µl of SDS sample buffer (Section 2.4) in a microfuge tube. (Section 2.4). Samples were then boiled for five minutes and applied to wells

2.19.4 SDS-PAGE gel staining

SDS-PAGE gels were stained by two different methods. For quick analysis and staining gels were incubated in Coomassie Blue stain (Section 2.4) for 1hour with agitation. The gels were then de-stained with multiple washes of Coomassie Blue de-staining solution (Section 2.4) until proteins are visible as blue bands on a colourless background. For a more sensitive analysis the Silver staining method was used as described by (Blum *et al.*, 1987) , and outlined in Table 2.6

Table 2.6: Silver Stain method for SDS-PAGE Gels

Step	Duration	Reagent (total volume of each 100mls)
Fixing	60minutes-Overnight	30% Ethanol, 10% Acetic Acid
Wash	15minutes	20% Ethanol
Wash	15minutes	dH_2O
Sensitise	1minute	0.1% (w/v) $Na_2S_2O_3$
Rinse	2 x 20 seconds	dH_2O
Silver Stain	20minutes	0.1% $AgNO_3$, 70µl of 37% (v/v) Formaldehyde stock
Rinse	2 x 20 seconds	dH_2O
Development	Until bands appear	3% Na_2CO_3, 50µl of 37% Formaldehyde stock, 0.002% (w/v) $Na_2S_2O_3$
Stop	5minutes	50g/L Trizma Base, 2.5% Acetic Acid (v/v)

SDS-PAGE protein markers were purchased from NEB (www.neb.com) or Sigma-Aldrich (www.sigmaaldrich.com)

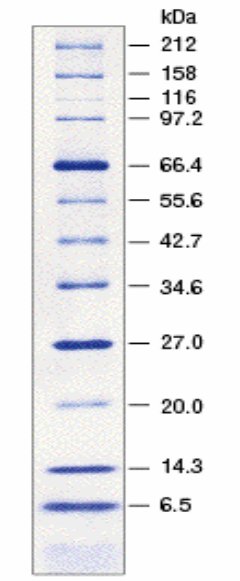

Figure 2.1: NEB BroadRange Protein Marker

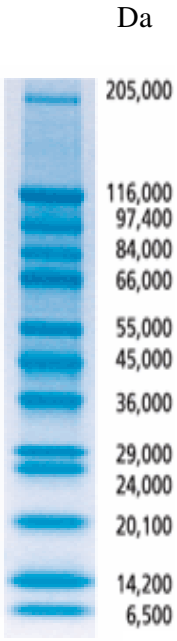

Figure 2.2: Sigma Wide Range Marker

2.20 Immobilisation of tagged GFP on MaxiSorp white plates

50µl of 5µg/ml Streptavidin was immobilised in each well of a NUNC MaxiSorp white plate and immobilised overnight at 4°C. The wells were blocked with 150µl of 2.5% BSA in PBS for one hour. The wells were then washed four times with PBS. 50µl of 50mg/ml biotinylated protein was immobilised for an hour at room temperature. The plate was washed four times with PBST, followed by four washes of PBS. 100µl of PBS was added to each well and the fluorescence was read at an excitation wavelength of 475nm and an emission wavelength of 509nm to determine the level of GFP immobilisation.

2.21 Biotinylation of GFP

When using a NHS-biotin linker it was vital that the protein was not dissolved in a buffer containing amine. When attempting to biotinylate a GFP with a maleimide-biotin

linker it was important that the buffer contained no sulfhydryls. A 5 to 20 fold molar excess of reagent to protein was used. The protein solutions contained at least a concentration of 2 mg/ml. The quantity in millimoles of reagent to achieve 20-fold molar excess was initially calculated.

$$\text{ml protein} \times \frac{\text{mg protein}}{\text{ml protein}} \times \frac{\text{mmol protein}}{\text{mg protein}} \times \frac{\text{20mmol Biotin Reagent}}{\text{mmol protein}} = \text{mmol Biotin Reagent}$$

The amount of the stock 250mM biotinylation reagent to add to the reaction was then calculated as outlined below.

$$\text{mmol Biotin Reagent} \times \frac{1{,}000{,}000\mu\text{l}}{\text{L}} \times \frac{\text{L}}{250\text{mmol}} = \mu\text{l Biotin Reagent stock solution}$$

For biotinylation using the NHS-biotin linker the reaction took place in an amine free buffer at pH 7.2-8.0. The required volume of the stock biotin reagent was added to the protein solution. The reaction was incubated on ice for two hours. An identical procedure was used for the biotinylation of GFP using Maleimide-biotin linker. The buffer conditions were different and took place in a sulfhydryl-free buffer at pH 6.5-7.5. Any remaining unreacted biotin reagent was removed by dialysis into PBS.

2.22 Dialysis of biotinylated reagent

Dialysis tubing was prepared by boiling in dH_2O containing 2% (w/v) sodium carbonate for half an hour. The tubing was rinsed with dH_2O and stored in 20% ethanol at 4°C until required. To perform dialysis the required length of dialysis tubing was washed with dH_2O to remove any residual ethanol, one end was closed and the protein solution was placed within the dialysis tubing and sealed. This sample was placed in 500mls of PBS pH7.4 and agitated for three hours at room temperature. The dialysis tubing was removed and the PBS pH7.4 was replaced. The dialysis tubing was replaced within the PBS and agitated overnight at room temperature. The biotinylated protein solution was removed from the dialysis tubing and stored at 4°C for immobilisation on monolithic columns (Section 2.23) and NUNC MaxiSorp white plates (Section 2.20)

2.23 Preparation of Monolithic Columns

Monolithic columns are most commonly used in High Performance Liquid Chromatography (HPLC). Monoliths differ from particle based columns as they are composed of a single piece porous material. This is discussed in Section 1.4.

2.23.1 Vinylisation of 100µm I.D. U.V. transparent silca column

The vinylisation method employed was based on a protocol described by (Ericson *et al.*, 1997) A section of transparent silica column was cut from the parent roll. The flow rate of the pump (Knauer Wellchrom K-120) was set to 10µl/min. The column was plumbed to a pump primed with acetone and rinsed for five minutes, then dried with nitrogen at room temperature for ten minutes. 0.2mol/L NaOH was pumped through the column at for thirty minutes, followed by washing with water for five minutes. 0.2mol/L HCl was passed through the column for five minutes and once more rinsed with water at for five minutes. This was followed by rinsing with acetone for five minutes. The cleaned column was dried with nitrogen for ten minutes. The capillary was then filled with a solution of 50% w/v of 3(trimethoxysilyl)propyl methacrylate in acetone until all air was expelled. The capillary was sealed at either end and immersed in a water bath at 60˚C for twenty hours. The capillary was finally rinsed with acetone at 10µl/min for five minutes, dried with nitrogen and stored until required for further work.

To fill a capillary with vinylisation reagents, a 433µl PEEK loop was filled with the reagents using a hand syringe. One end of the loop was connected to the pump and the other end to the capillary. In this way contamination of the pump with reactive reagents was avoided.

2.23.2 Creation of monolithic columns

Monolithic columns were produced as outlined by (Lee *et al.*, 2004)

		W/V	
EDMA:	0.1522ml	16%	} 40%
BUMA:	0.2679ml	24%	
Decanol:	0.7238ml	60%	
DAP:	4mg	1% with respect to monomers	

Sections of 12cm column were cut from the vinylised UV transparent monolithic parent column (Section 2.22.1). DAP was added to a microfuge tube before the other components were added. The mixture was vortexed for 5-10 minutes and then centrifuged at 13,000rpm for ten minutes. The supernatant was degassed by bubbling nitrogen through the solution. The vinylised column was filled by capillary action and sealed at either end. The columns were placed in a Spectra Linker Crosslinker and irradiated three times with 9,999μJ/cm^2 of UV light. The monolith was washed with methanol at 1μl per minute for thirty minutes. The columns were then stored until required.

2.23.3 Benzophenone immobilisation on monolithic columns

50mg of benzophenone was dissolved in 1ml of methanol, vortexed well and centrifuged for ten minutes. The supernatant was degassed with nitrogen for five minutes. The pump was primed with methanol, then using a 1ml syringe, PEEK tubing was filled with the degassed benzophenone in methanol. The monolithic column was attached to the PEEK tubing. Benzophenone solution was injected onto the column at 1μl per minute so that the monolithic column was filled with benzophenone solution. The column was sealed at either end and irradiated three times with UV light (1 dose = 9999x100μJ/ cm^2). After UV irradiation the column was washed with methanol to remove any unreacted benzophenone.

2.23.4 PEGMA immobilisation on monolithic columns

Monoliths from the previous benzophenone immobilisation step were washed with water to remove any residual methanol. 36μl of PEGMA was added to 1ml of water, vortexed and de-gassed by bubbling nitrogen through the solution. PEEK tubing was

filled with PEGMA solution and attached to the flow splitter while the monolith was connected to the opposite end of the PEEK tubing. The PEGMA solution was pumped through the monolith column at 1µl/min until the column was filled. The column was sealed at either end and irradiated three times with UV light (1 dose = 9999x100µJ/ cm^2). After the UV doses, the columns were washed with water and stored.

2.23.5 Vinyl-Azlactone photografting method

Vinyl-Azlactone (4,4-dimethyl-2-vinylazlactone)	0.144ml
T-Butanol:	0.75ml
dH_2O**:**	0.25ml
Benzophenone:	2.2mg

Benzophenone was placed in a microfuge tube before the other components were added. Before addition T-butanol was gently warmed to 45°C in a water bath. The solution was vortexed to dissolve the benzophenone, then centrifuged for ten minutes at 13,000rpm to pellet any containments. The supernatant was transferred to a separate eppendorf and de-gassed with nitrogen. All PEEK tubing and connectors, which were in contact with vinyl azlactone, were washed with a solution of acetronitrile with 1% trifluoroacetic acid (TFA), to remove any contaminating proteins or amino acids. The pump was primed with methanol before three microtight sleeves (Sigma Aldrich) were placed on the pegalated column. PEEK tubing was filled with the Vinyl-Azlactone solution and connected to the flow splitter in the system. The monolith was plumed in and the vinyl-azlactone was pumped through the column at 1µl/min until the monolith was full. The monolith was disconnected and sealed at either end. The micro-tight sleeves were positioned on the monolith such that there was a gap of 1cm between each sleeve. The column was placed in a light columnator and given three doses of UV light (1 dose = 9999x100µJ/ cm^2). The sleeves were then removed and the column plumed to the flow splitter and washed for twenty minutes at 1µl/min with methanol. The pump was then primed with water and the column washed at 1µl/min for half an hour. Finally the column was washed with 10mM HEPES buffer at pH 7.4. Using a Trace-Dec detector the column was scanned at 1mm increments to produce a baseline conductivity scan.

2.23.6 Immobilisation of protein on monoliths

A pump (Knauer Wellchrom K-120) was primed with 10mM HEPES, pH7.4 and monoliths with zones of grafted vinyl-azlactone were washed for half an hour. The C^4D (capacitively coupled contactless conductivity detector) was placed on the column and the baseline reading was taken while 10mM HEPES pH7.4, was flowing through the column. PEEK tubing was filled with a 1mg/ml protein sample in 10mM HEPES pH7.4, and connected to the flow splitter, which was in turn connected to the monolith. The protein was pumped through the monolith column at 1µl/min for three hours. 1M ethanolamine pH7 was pumped over the column at 1µl/min for one hour to block any un-reacted vinyl-azlactone. The monolith was then removed from the PEEK tubing and washed overnight with 10mM HEPES. The trace-dec reading of the column was taken with the C^4D detector and compared to the original baseline.

Chapter 3: Cloning, Purification and Immobilisation of tagged Green Fluorescent Protein

3.1 Cloning and Tagging of Green Fluorescent Protein

3.1.1: Overview:

This section describes the addition of purification and immobilisation tags to a model protein; Green Fluorescent Protein (GFP). GFP was chosen as a model protein due to its inherent fluorescence, which can be utilised to monitor its expression, purification and immobilisation. A GFP mutant (GFPmut3) was used in this study, which was first described in 1996 (Cormack *et al.*, 1996) and is notable for its more efficient folding in *E.coli* bacterial systems and increased fluorescence when compared to wild type. It will be referred to as GFP below.

The tags which were to be added to GFP can be divided into two distinct groups.

- Purification tag
- Immobilisation tags

The purification tag consisted of a six residue histidine sequence. This histidine tag will allow for the purification of the protein of interest by standard immobilised metal affinity chromatography (IMAC) protocols (Section 2.16).

The immobilisation tags were further subdivided into two groups.

- Immobilisation tags
    - Covalent Immobilisation Tags
        - Lysine Tag
        - Cysteine Tag
    - Bio-affinity Immobilisation Tag
        - Strep-TagII

Lysine and cysteine residues were chosen as suitable amino acids for covalent immobilisation reactions due to their respective nucleophilic amine and thiol functional groups (Figures 1.5 and 1.6) A bio-affinity immobilisation tag was provided by Strep-TagII (Section 1.3.3). This tag consists of an eight amino acid sequence which is a biological mimic of biotin. Immobilisation tags were added to GFP by the use of either the forward or reverse primers during PCR.

To determine the effects of protein tagging on further downstream processes such as expression, purification and immobilisation, GFP was cloned into *E.coli* expression vectors, which placed the purification or immobilisation tags at either the N or C-termini or in tandem at a single termini. The addition and position of the tags in relation to the level of protein expression within *E.coli* will be the focus of section 3.2. The immobilisation of tagged GFP on different surfaces and the effects the alternate

tags have on levels of immobilised protein will be outlined in section 3.3 and section 3.4.

3.1.2 Generation of C-terminal Histidine Tagged GFP Expression Vector

GFP was initially cloned into an in house *E.coli* expression vector pRV (Figure 3.1.1), to facilitate its expression with a C-terminal histidine tag.

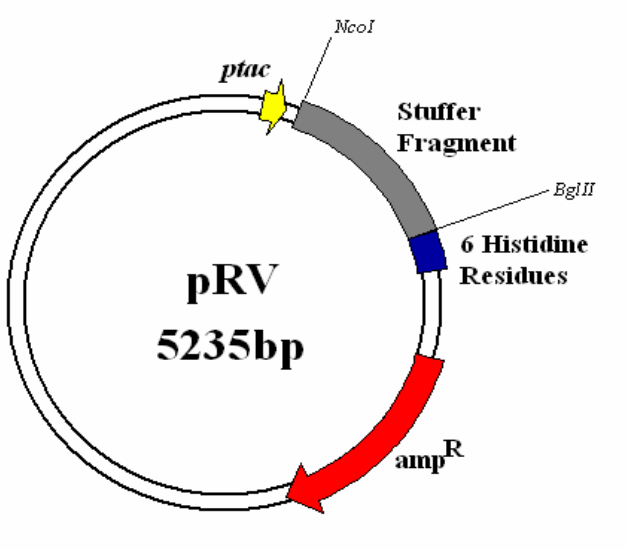

Figure 3.1.1: pRV *E.coli* Expression Vector
The pRV expression vector contains the following features. The multiple cloning site (MCS) is located before the $(His)_6$ amino acid sequence (blue) which facilitates the C-terminal tagging of a protein with the purification tag. Expression was under the control of the ptac promoter/*lac* operon (yellow). The *bla* gene that encodes beta-lactamase confers the bacteria with ampicillin resistance (red).

5'atg agt aaa gga gaa gaa ctt ttc act gga gtt gtc cca att ctt gtt gaa tta gat ggt gat gtt aat ggg cac aaa ttt tct gtc agt gga gag ggt gaa ggt gat gca aca tac gga aaa ctt acc ctt aaa ttt att tgc act act gga aaa cta cct gtt **cca tgg** cca aca ctt gtc act act ttc ggt tat ggt gtt caa tgc ttt gcg aga tac cca gat cat atg aaa cag cat gac ttt ttc aag agt gcc atg ccc gaa ggt tat gta cag gaa aga act ata ttt ttc aaa gat gac ggg aac tac aag aca cgt gct gaa gtc aag ttt gaa ggt gat acc ctt gtt aat aga atc gag tta aaa ggt att gat ttt aaa gaa gat gga aac att ctt gga cac aaa ttg gaa tac aac tat aac tca cac aat gta tac atc atg gca gac aaa caa aag aat gga atc aaa gtt aac ttc aaa att aga cac aac att gaa gat gga agc gtt caa cta gca gac cat tat caa caa aat act cca att ggc gat ggc cct gtc ctt tta cca gac aac cat tac ctg tcc aca caa tct gcc ctt tcg aaa gat ccc aac gaa aag aga gac cac atg gtc ctt ctt gag ttt gta aca gct gct ggg att aca cat ggc atg gat gaa cta tac aaa tag 3'

Figure 3.1.2: The DNA sequence of GFPmut3. The chromophore forming sequence is highlighted in green. Underlined sections are standard PCR Primer sites. Sequence highlighted in bold is an *Nco*I restriction site.

As illustrated in figure 3.1.1. DNA amplified by PCR can be cloned into the MCS of pRV as an *Nco*I-*Bgl*II fragment. However restriction analysis on GFPmut3 revealed an internal *Nco*I restriction site (figure 3.1.2), thus preventing this enzyme being utilised. However *BspH*I generates a compatible cohesive end, to *Nco*I. GFP does not have an internal *BspH*I site and therefore this restriction enzyme could be used in a cloning strategy for the tagging of GFP. The primers illustrated in figure 3.1.3. were designed for the amplification by PCR of the GFP gene as a *BspH*I-*Bgl*II 717bp fragment from pBk-miniTn7gfp2 (Table 2.3). The restricted PCR product was ligated with the expression vector pRV (which was restricted with *Nco*I-*Bgl*II) to generate the expression vector pVOS1 (see figure 3.1.5)

Forward Primer:

5' C CCC CTC ATG AGT AAA GGA GAA GAA CTT TTC ACT GGA 3'

BspHI

Reverse Primer:

5' CC CCC AGA TCT TTT GTA TAG TTC ATC CAT GCC ATG TGT AAT CCC A 3'

BglII

Figure 3.1.3: The forward and reverse primers used for the generation of an *E.coli* expression vector; pVOS1, which expresses a C-terminal Histidine tagged GFP.

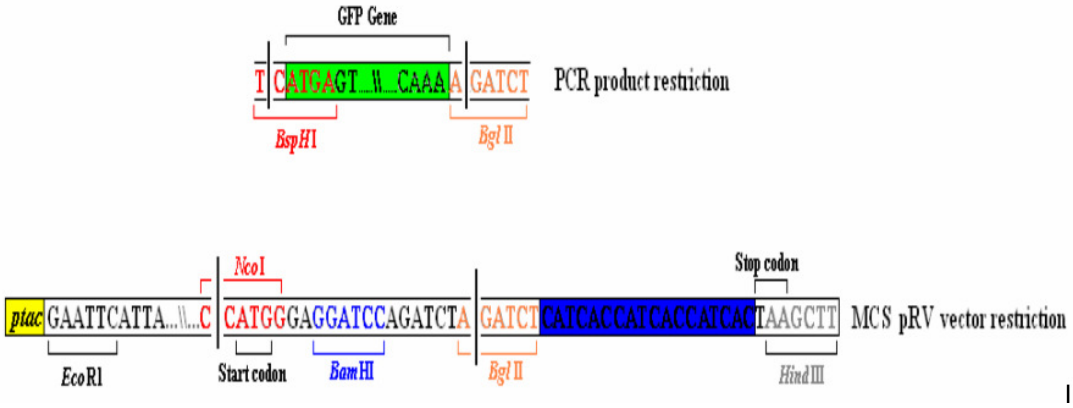

Figure 3.1.4: Schematic of the *BspH*I/*Bgl*II restricted GFP PCR product, amplified by forward and reverse primers illustrated in figure 3.1.3. and the schematic of the MCS of the pRV vector restricted by *Nco*I/*Bgl*II. The point of restriction is indicted by a black line.

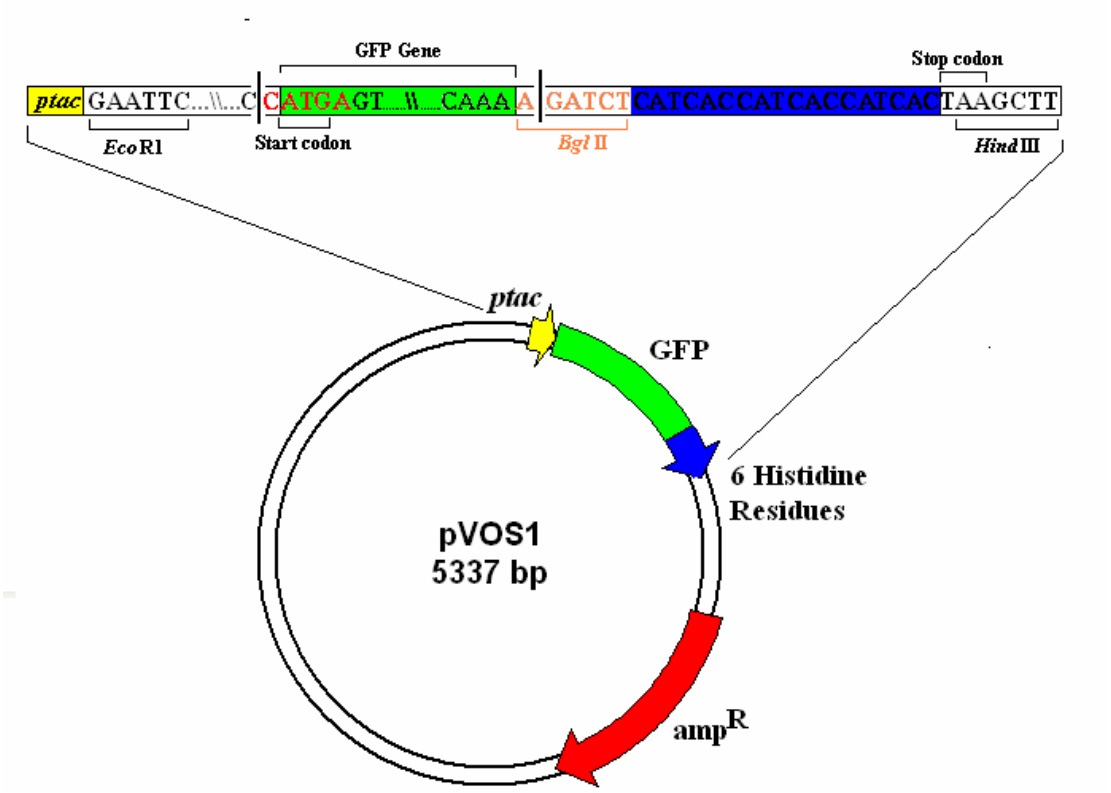

Figure 3.1.5: Schematic of the vector pVOS1, an *E.coli* expression vector which will express a C-terminal histidine tagged GFP. GFP amplified by PCR as a *BspH*I-*Bgl*II fragment was ligated with the *NcoI-BglII* restricted pRV to generate pVOS1

The ligation mix was used to transform XL10-Gold competent *E.coli* cells. (Section 2.11) Following transformation, clones were initially screened by examining for fluorescence. Plasmid DNA was prepared from fluorescing colonies; vectors were verified by restriction analysis and subsequently by sequencing. Restriction analysis for pVOS1 is illustrated in figure 3.1.6. During the cloning procedure the vector borne *Nco*I site was destroyed by ligation with the *BspH*I restriction site. Hence restriction analysis was performed with *EcoR*I and *Bgl*II restriction enzymes.

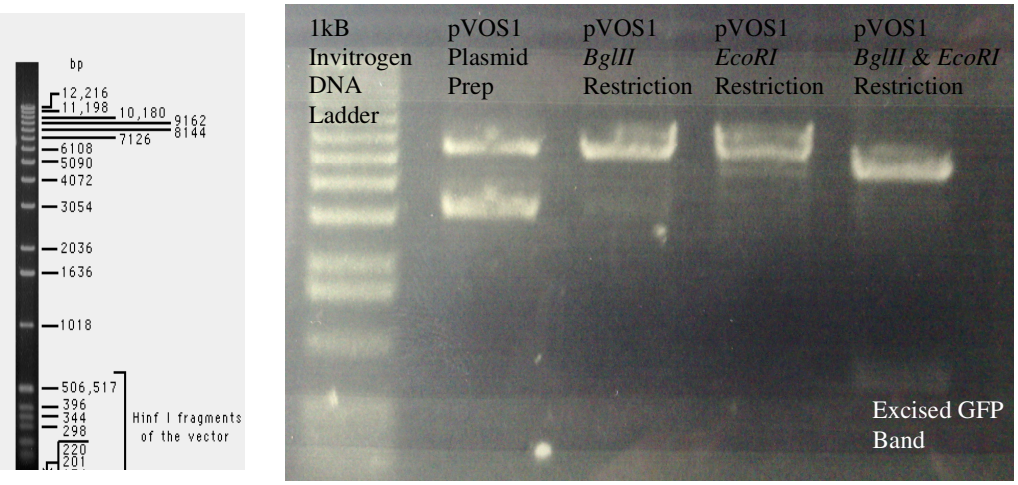

Figure 3.1.6: DNA Agarose Gel displaying restriction analysis of pVOS1 confirming the insertion of GFP within the expression vector. Single digest reactions linearise the pVOS1, while a double digest with *Bgl*II and *EcoR*I excises the GFP DNA insert. The *EcoR*I restriction enzyme was used for restriction analysis as the ligation of *Nco*I and *BspH*I cohesive ends destroyed both restriction enzyme sites.

The sequence confirmed pVOS1 vector was then used as the template vector for all future cloning reactions. Subsequent clones are formed by inserting GFP into the pQE-30, pQE-30Xa and pQE-60 *E.coli* expression vectors available from Qiagen.

3.1.3: Generation of N-terminal Histidine Tagged GFP Expression Vector

GFP was cloned into an *E.coli* expression vector pQE30 (available from Qiagen), to facilitate its expression with an N-terminal His tag.

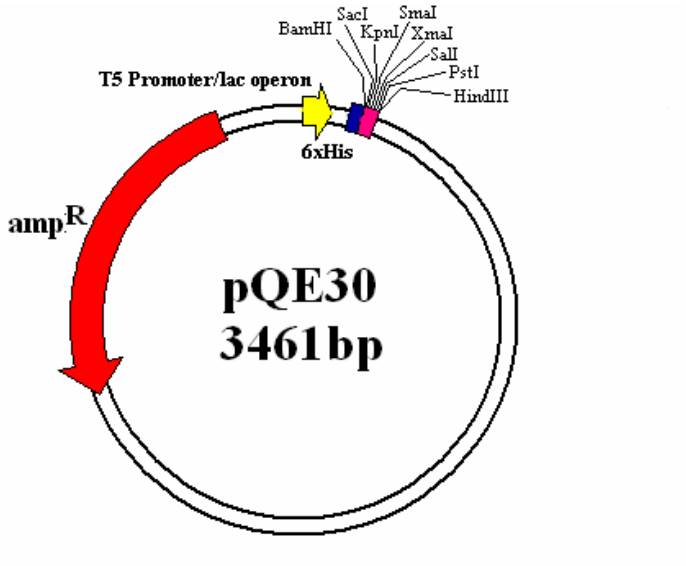

Figure 3.1.7: pQE30 (Qiagen)
The expression vector pQE30 has the MCS located after the $(His)_6$ amino acid sequence (blue) which facilitates the N-terminal tagging of a protein with the purification tag. Expression was under the control of the T5 promoter/*lac* operon (yellow). An ampicillin resistance gene is also present on the plasmid (red)

The primers illustrated in figure 3.1.8. were designed for the amplification by PCR of the GFP gene as an *BamH*I /*Hind*III 717bp fragment. The restricted PCR product was ligated with the *BamH*I /*Hind*III restricted expression vector pQE30 to generate the expression vector pVOS2 (see figure 3.1.10)

Forward Primer:
5' CCC CCC **GGA TCC** AGT AAA GGA GAA GAA CTT TTC ACT GGA 3'
BamHI

pVOS2 Reverse Primer:
5' CCC CCC **AAG CTT** CTA TTT GTA TTT GTA TAG TTC ATC CAT GCC ATG TGT 3'
HindIII

Figure 3.1.8: The forward and reverse primers used for the generation of an *E.coli* expression vector; pVOS2, which expresses an N-terminal Histidine tagged GFP.

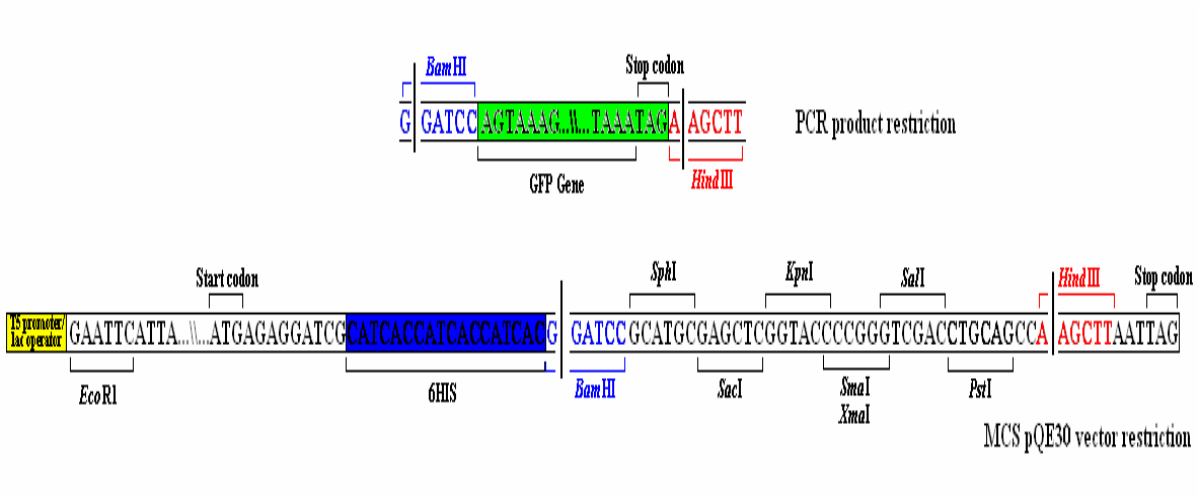

Figure 3.1.9: Schematic of the *BamH*I /*Hind*III restricted GFP PCR product, amplified by forward and reverse primers illustrated in figure 3.1.8. and the schematic of the MCS of the pQE30 vector restricted by *BamH*I /*Hind*III. The point of restriction is indicted by a vertical black line.

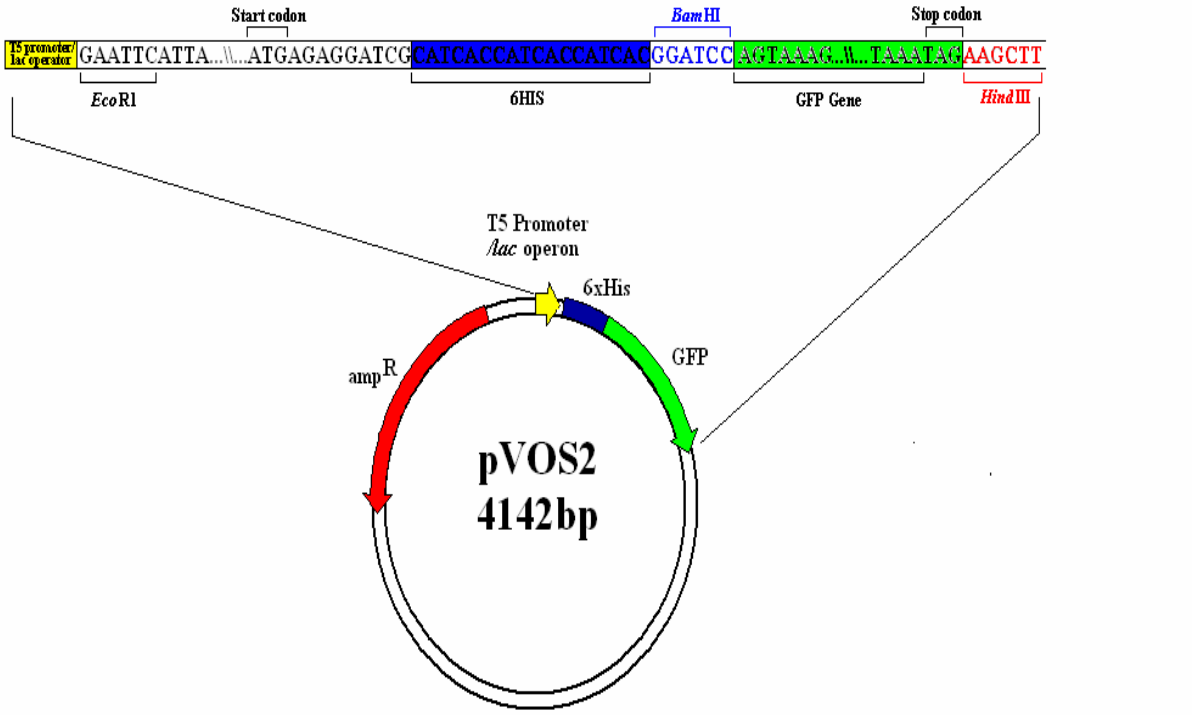

Figure 3.1.10: Illustration of the vector pVOS2. An *E.coli* expression vector which will express an N-terminal histidine tagged GFP. GFP was amplified by PCR as a *BamH*I /*Hind*III fragment and ligated with the *BamH*I /*Hind*III restricted pQE30 vector, to generate pVOS2.

The ligation was transformed into XL10-Gold competent *E.coli* cells. Following transformation, clones were initially screened by examining for fluorescence. Plasmid DNA was prepared from fluorescing colonies; vectors were verified by restriction analysis and subsequently by sequencing.

3.1.4: Generation of N-terminal Histidine Tagged GFP Expression Vector, with an N-terminal FXa protease site:

GFP was cloned into an *E.coli* expression vector pQE30-Xa (available from Qiagen), to facilitate its expression with a N-terminal histidine tag and FXa protease site. The FXa protease site facilitates the removal of the histidine affinity tag after purification viva specific digestion by FactorXa protease.

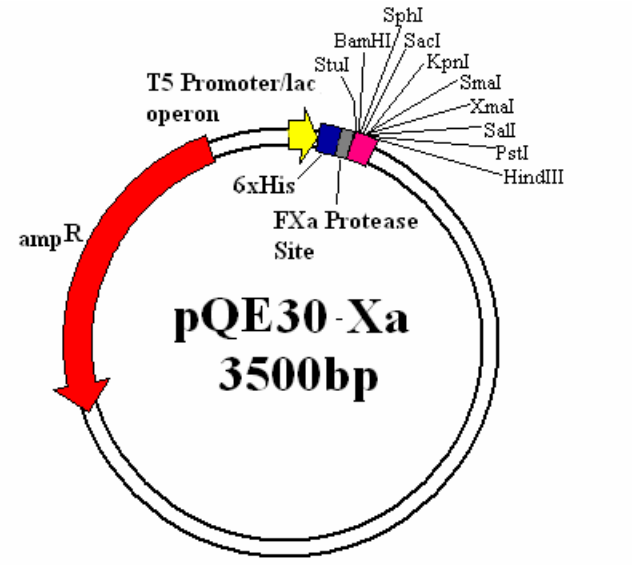

Figure 3.1.11: pQE30-Xa (Quigen)
The expression vector pQE30-Xa has the MCS located after the $(His)_6$ amino acid sequence (blue) which facilitates the N-terminal tagging of a protein with the purification tag. A FactorXa protease site is present after the Histidine tag but prior to the MCS. Expression was under the control of the T5 promoter/*lac* operon (yellow). An ampicillin resistance gene is also present on the plasmid (red)

The primers illustrated in figure 3.1.12. were designed for the amplification by PCR of the GFP gene as a *BamH*I /*Hind*III 717bp fragment. The restricted PCR product was ligated into the *BamH*I /*Hind*III restricted expression vector pQE30-Xa to generate the expression vector pVOS2-Xa (see figure 3.1.13)

Forward Primer:

5' CCC CCC **GGA TCC** AGT AAA GGA GAA GAA CTT TTC ACT GGA 3'

BamHI

pVOS2-Xa Reverse Primer:

5' CCC CCC **AAG CTT** CTA TTT GTA TAG TTC ATC CAT GCC ATG TGT 3'

HindIII

Figure 3.1.12: The forward and reverse primers used for the generation of an *E.coli* expression vector; pVOS2-Xa, which expresses an N-terminal Histidine tagged GFP. A FactorXa protease site is present after the Histidine tag but prior to the MCS.

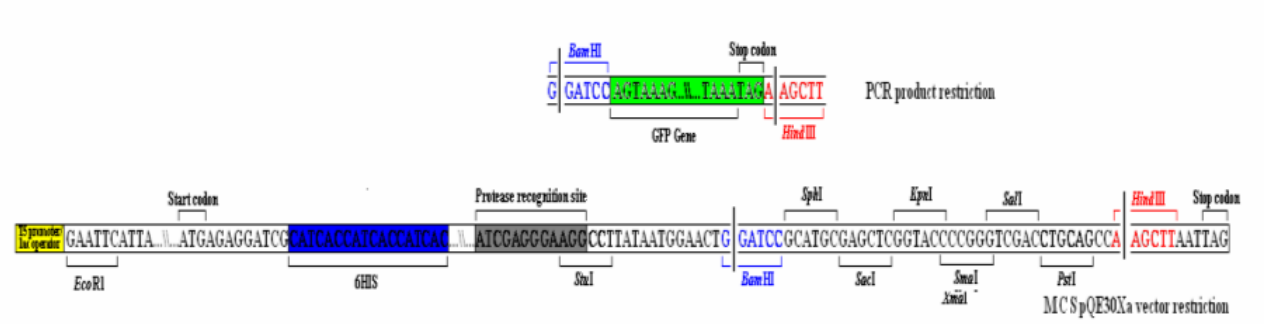

Figure 3.1.13: Schematic of the *BamH*I /*Hind*III restricted GFP PCR product, amplified by forward and reverse primers illustrated in figure 3.1.12. and the schematic of the MCS of the pQE30-Xa vector restricted by *BamH*I /*Hind*III. The point of restriction is indicted by a black line and break in the sequence.

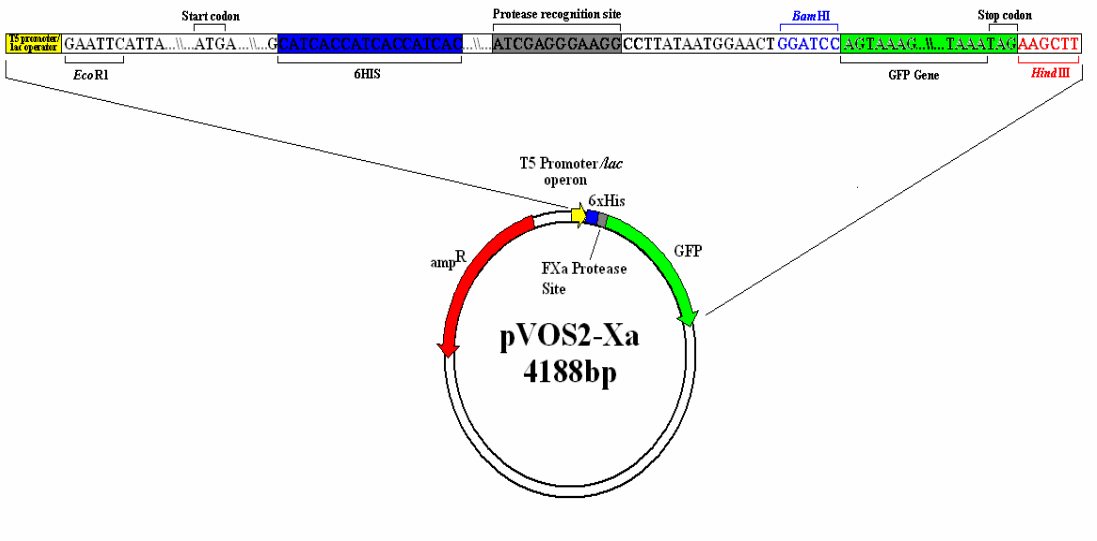

Figure 3.1.14: Illustration of vector pVOS2-Xa. An *E.coli* expression vector which will express an N-terminal histidine tagged GFP. GFP amplified by PCR as a *BamH*I /*Hind*III fragment was ligated with *BamH*I /*Hind*III restricted vector pQE30-Xa, to generate pVOS2-Xa.

The ligation was transformed into XL10-Gold competent *E.coli* cells. Following transformation, clones were initially screened by examining for fluorescence. Plasmid DNA was prepared from fluorescing colonies; vectors were verified by restriction analysis and subsequently by sequencing.

3.1.5: Generation of N-terminal Histidine Tagged GFP Expression Vectors, with a C-terminal immobilisation tag

The cloning strategy for the addition of a C-terminal immobilisation tag to GFP was based on the cloning strategy employed for the creation of pVOS2 (see figure 3.1.9) For the PCR reaction the forward primer remained constant, however the reverse primer differed depending on the immobilisation tag added, illustrated by figure 3.1.15.

Forward Primer:
5' CCC CCC **GGA TCC** AGT AAA GGA GAA GAA CTT TTC ACT GGA 3'
BamHI

pVOS3 Reverse Primer:
5' CCC CCC **AAG CTT** CTA *CTT TTT CTT TTT CTT TTT* GTA TAG TTC ATC CAT GCC ATG TGT 3'
HindIII *Lysine Tag*

pVOS4 Reverse Primer:
5' CCC CCC **AAG CTT** CTA *GCA ACA GCA ACA GCA ACA* TTT GTA TAG TTC ATC CAT GCC ATG TGT 3'
HindIII *Cysteine Tag*

pVOS5 Reverse Primer:
5' CCC CCC **AAG CTT** CTA *TTT TTC GAA CTG CGG GTG GCT CCA* GTA TAG TTC ATC CAT GCC ATG TGT 3'
HindIII *Strep-TagII*

Figure 3.1.15: The forward and reverse primers used for the amplification of a C-terminal immobilisation tagged GFP and generation of expression vectors pVOS3, pVOS4 and pVOS5.

The primers illustrated in figure 3.1.15. were designed for the amplification of the GFP gene as an *BamH*I /*Hind*III fragment by PCR. This PCR product was ligated into the *BamH*I /*Hind*III restricted expression vector pQE30 to generate the *E.coli* expression vectors pVOS3, pVOS4 and pVOS5 (see figure 3.1.16)

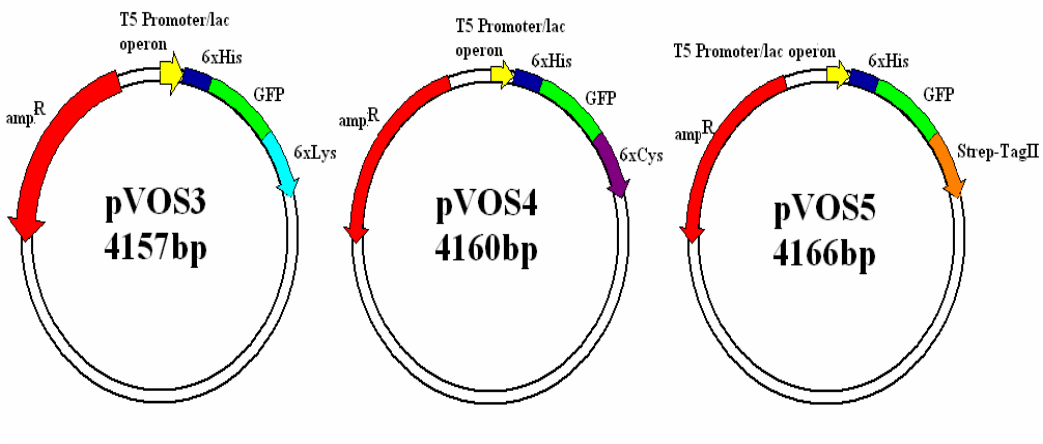

Figure 3.1.16: Schematic of vectors pVOS3, pVOS4 and pVOS5.
E.coli vectors for the expression of N-terminal purification tagged and C-terminal immobilisation tagged GFP. GFP was amplified by PCR using an identical forward primer and unique reverse primers. PCR products and the pQE-30 vector were restricted with *BamHI-HindIII* and ligated.

Each ligation was transformed into XL10-Gold competent *E.coli* cells. Following transformation, clones were initially screened by examining for fluorescence. Plasmid DNA was prepared from fluorescing colonies; vectors were verified by restriction analysis and subsequently by sequencing.

3.1.6: Generation of a Protease cleavable N-terminal Histidine Tagged GFP Expression Vectors, with a C-terminal immobilisation tag

The cloning strategy for the addition of a C-terminal immobilisation tag (6XLysine, 6XCysteine or Strep-TagII) to GFP was based on the cloning strategy employed for the creation of pVOS2-Xa (see figure 3.1.13) The FXa protease site facilitates the removal of the histidine affinity tag after purification viva specific digestion by FactorXa protease. For the PCR reaction the forward primer remained constant, however the reverse primer differed depending on the immobilisation tag added, illustrated by figure 3.1.17.

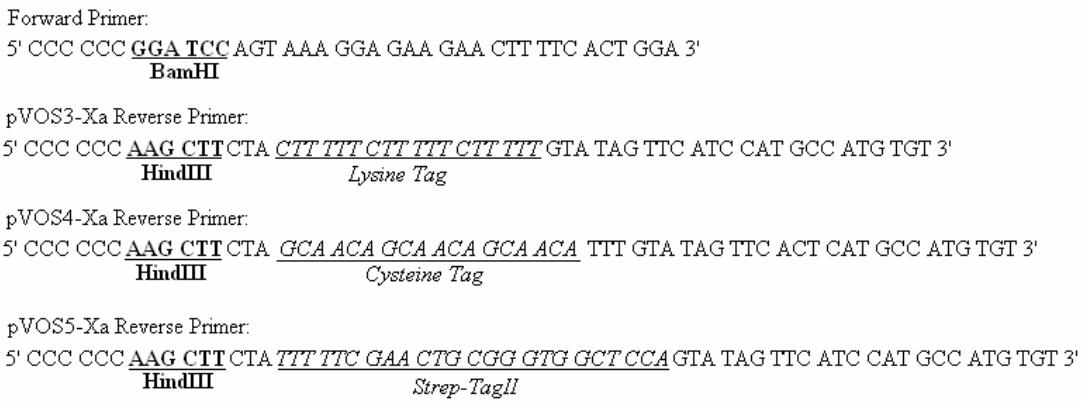

Figure 3.1.17: The forward and reverse primers used for the amplification of the C-terminal immobilisation tagged GFP and generation of expression vectors pVOS3-Xa, pVOS4-Xa and pVOS5-Xa.

The primers illustrated in figure 3.1.17. were designed for the amplification by PCR of the GFP gene as an *BamH*I /*Hind*III fragment. This PCR product was ligated into the *BamH*I /*Hind*III restricted expression vector pQE30-Xa to generate the *E.coli* expression vectors pVOS3-Xa, pVOS4-Xa and pVOS5-Xa (see figure 3.1.13)

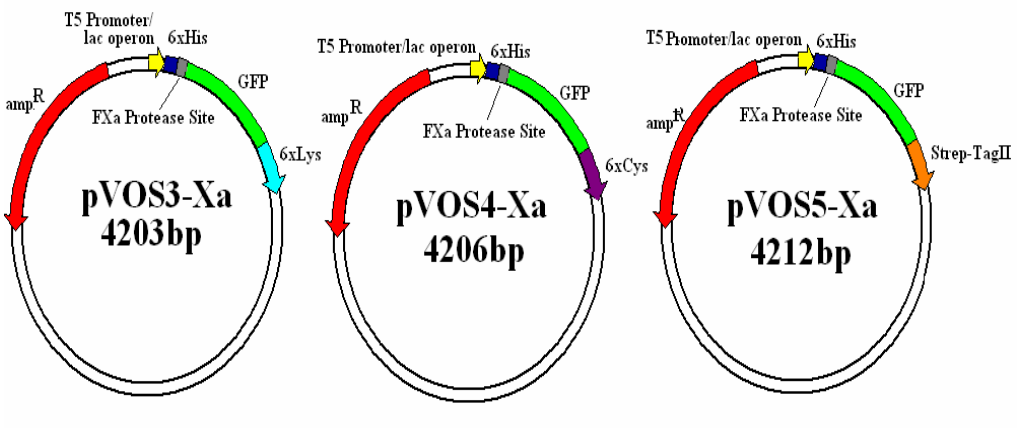

Figure 3.1.18: Schematic of vectors; pVOS3-Xa, pVOS4-Xa and pVOS5-Xa
E.coli vectors for the expression of N-terminal purification tagged and C-terminal immobilisation tagged GFP. A FactorXa protease site is present after the purification tag but prior to GFP. The GFP gene was amplified by PCR using an identical forward primer and unique reverse primers. PCR products and the pQE30-Xa vector were restricted with *BamHI-HindIII* and ligated.

Each ligation was transformed into XL10-Gold competent *E.coli* cells. Following transformation, clones were initially screened by examining for fluorescence. Plasmid DNA was prepared from fluorescing colonies; vectors were verified by restriction analysis and subsequently by sequencing.

3.1.7: Generation of a Protease cleavable N-terminal Histidine Tagged GFP Expression Vectors, with a tandem N-terminal immobilisation tag

The cloning strategy for the addition of an N-terminal immobilisation and purification tag to GFP was based on the cloning strategy employed for the creation of pVOS2-Xa (see figure 3.1.13) For the PCR reaction the reverse primer remained constant, however the forward primer differed depending on the immobilisation tag added, illustrated by figure 3.1.19.

Reverse Primer:
5' CCC CCC **AAG CTT** CTA TTT GTA TAG TTC ATC CAT GCC ATG TGT 3'
HindIII

pVOS6-Xa Forward Primer:
5' CCC CCC **GGA TCC** *AAA AAG AAA AAG AAA AAG* ATG AGT AAA GGA GGA GGA CTT TTC ACT GGA 3'
BamHI *Lysine Tag*

pVOS7-Xa Forward Primer:
5' CCC CCC **GGA TCC** *TGT TGC TGT TGC TGT TGC* ATG AGT AAA GGA GGA GGA CTT TTC ACT GGA 3'
BamHI *Cysteine Tag*

pVOS8-Xa Forward Primer:
5' CCC CCC **GGA TCC** *TGG AGC CAC CCG CAG TTC GAA AAA* ATG AGT AAA GGA GGA GGA CTT TTC ACT GGA 3'
BamHI *Strep-TagII*

Figure 3.1.19: The forward and reverse primers used for the amplification of the N-terminal purification and immobilisation tagged GFP and generation of expression vectors pVOS6-Xa, pVOS7-Xa and pVOS8-Xa.

The primers illustrated in figure 3.1.19. were designed for the amplification by PCR of the GFP gene as an *BamH*I */Hind*III fragment. This PCR product was ligated into the *BamH*I */Hind*III restricted expression vector pQE30-Xa to generate the *E.coli* expression vectors pVOS6-Xa, pVOS7-Xa and pVOS8-Xa (see figure 3.1.20)

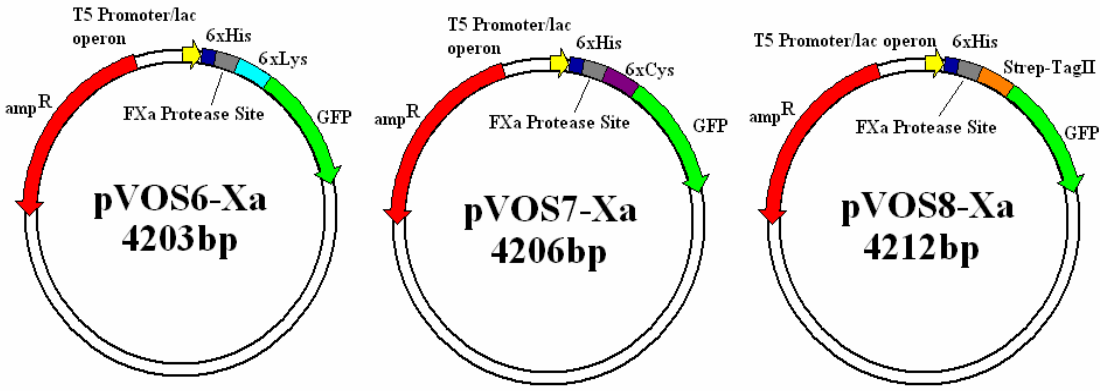

Figure 3.1.20: Schematic of vectors; pVOS6-Xa, pVOS7-Xa and pVOS8-Xa.
E.coli vectors for the expression of N-terminal purification and immobilisation tagged GFP. A FactorXa protease site is present after the purification tag but prior to the immobilisation tag. GFP was amplified by PCR using unique forward primers and an identical reverse primer. PCR products and the pQE30-Xa vector were restricted with *BamHI-HindIII* and ligated.

Each ligation was transformed into XL10-Gold competent *E.coli* cells. Following transformation, clones were initially screened by examining for fluorescence. Plasmid DNA was prepared from fluorescing colonies; vectors were verified by restriction analysis and subsequently by sequencing.

3.1.8: Generation of C-terminal purification tagged GFP expression vector, with an N-terminal immobilisation tag

GFP was cloned into an *E.coli* expression vector pQE60 (available from Qiagen), to facilitate its expression with a C-terminal histidine tag. This cloning strategy differed from the original C-terminal tagging illustrated in section 3.1.2 as it is expressed from a T5 promoter/*lac* operon compared to a *ptac* promoter present in pRV. For the PCR reaction the reverse primer remained constant, however the forward primer differed depending on the immobilisation tag added, illustrated by figure 3.1.22.

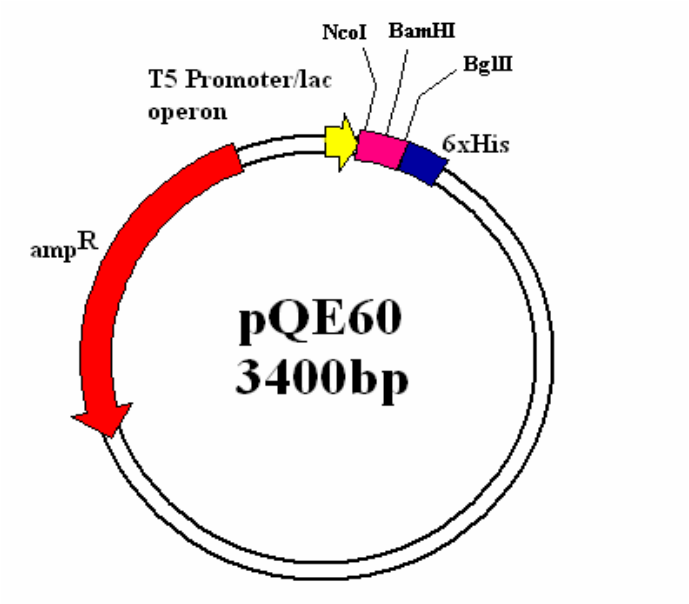

Figure 3.1.21: pQE60 (Qiagen)
The expression vector pQE60, contains the following features. The MCS is located before the $(His)_6$ amino acid sequence, which facilitates the C-terminal tagging of a protein with the purification tag. Expression is under the control of the T5 promoter/*lac* operon (yellow). The *bla* gene that encodes beta-lactamase confers the bacteria with ampicillin resistance (red)

Reverse Primer:

5' CC CCC **AGA TCT** TTT GTA TAG TTC ATC CAT GCC ATG TGT AAT CCC A 3'

BglII

pVOS9 Forward Primer:

5' CCC CCC **GGA TCC** *AAG AAA AAG AAA AAG AAA* ATG AGT AAA GGA GAA GAA CTT TTC ACT GGA 3'

BamHI *Lysine Tag*

pVOS10 Forward Primer:

5' CCC CCC **GGA TCC** *TGT TGC TGT TGC TGT TGC* ATG AGT AAA GGA GAA GAA CTT TTC ACT GGA 3'

BamHI *Cysteine Tag*

pVOS11 Forward Primer:

5' CCC CCC **GGA TCC** *TGG AGC CAC CCG CAG TTC GAA AAA* ATG AGT AAA GGA GAA GAA CTT TTC ACT GGA 3'

BamHI *Strep-TagII*

Figure 3.1.22: Primers used for the amplification of N-terminal immobilisation and C-terminal purification tagged GFP and the creation of *E.coli* expression vectors; pVOS9, pVOS10 and pVOS11.

The primers illustrated in figure 3.1.22. were designed for the amplification by PCR of the GFP gene as an *BamH*I/*Bgl*II fragment. This PCR product was ligated into the *BamH*I / *Bgl*II restricted expression vector pQE60 to generate the *E.coli* expression vectors pVOS9, pVOS10 and pVOS11 (see figure 3.1.23)

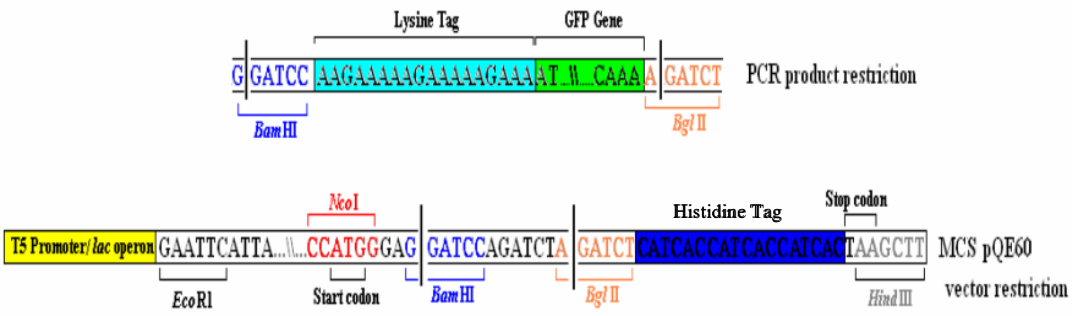

Figure 3.1.23: Schematic of the *BamH*I/*Bgl*II restricted GFP PCR product, amplified by the pVOS9 forward and reverse primers illustrated in figure 3.1.22. and the schematic of the MCS of the pQE60 vector restricted by *BamH*I/*Bgl*II. The point of restriction is indicted by a black line and break in the sequence.

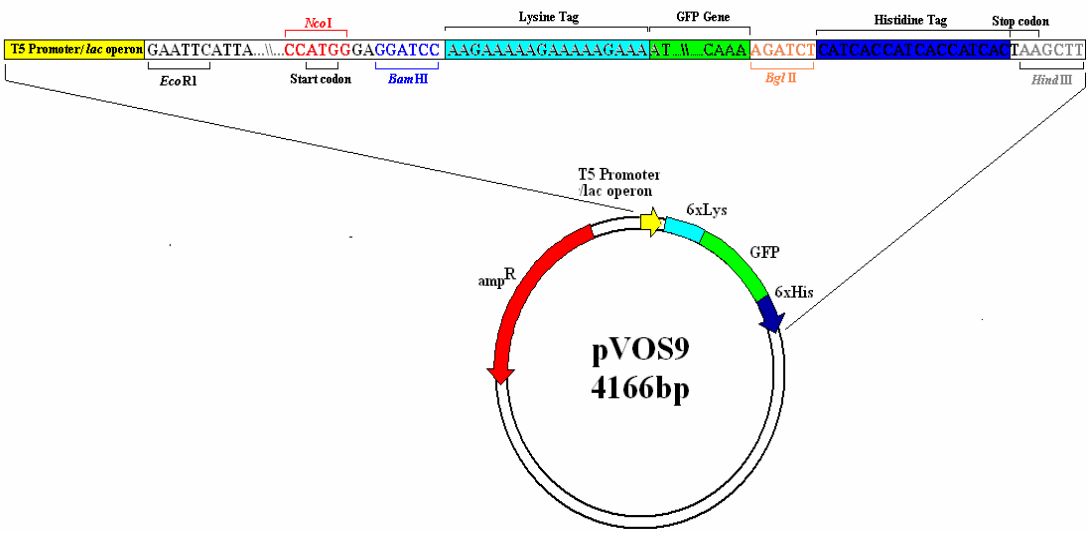

Figure 3.1.24: Illustration of vector pVOS9. An *E.coli* expression vector which will express an N-terminal lysine tagged and C-terminal histidine tagged GFP. GFP was amplified by PCR as a *BamH*I /*Bgl*II fragment and ligated with the *BamH*I /*Bgl*II digested vector fragment of pQE60 to generate pVOS9

The GFP expression vectors pVOS10 and pVOS11 were generated by using the relevant forward primer illustrated in figure 3.1.22. The cloning strategy was identical to that described in figure 3.1.23.

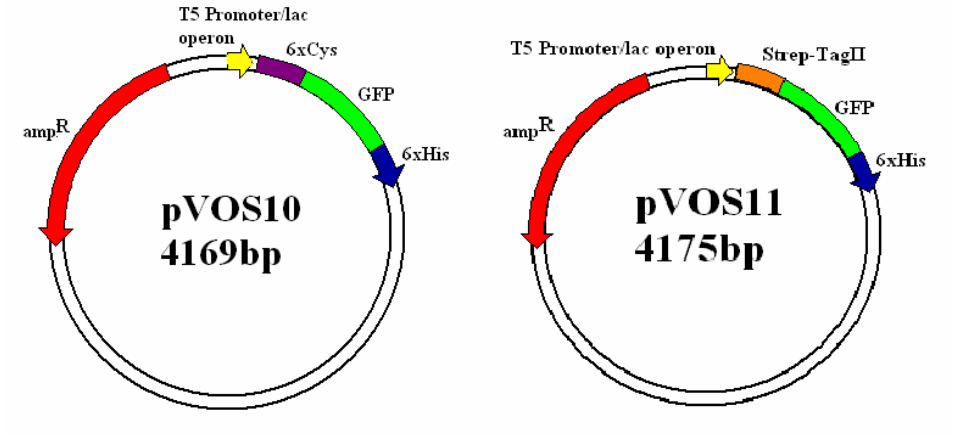

Figure 3.1.25: Schematic of vectors; pVOS10 and pVOS11

E.coli vectors for the expression of C-terminal purification and N-terminal immobilisation tagged GFP. GFP was amplified by PCR using unique forward primers and identical reverse primers. PCR products and the pQE60 vector were restricted with *BamH*I-*Bgl*II and ligated.

Each ligation was transformed into XL10-Gold competent *E.coli* cells. Following transformation, clones were initially screened by examining for fluorescence. Plasmid DNA was prepared from fluorescing colonies; vectors were verified by restriction analysis and subsequently by sequencing.

3.1.9: Cloning of GFP with a single C-terminal cysteine residue:

A single C-terminal cysteine residue was added to GFP by PCR amplification. It was found during protein expression and purification protocols (Section 3.2), that the expression of hexa-cysteine tagged GFP was problematic due to multimer formation, as noted by a large increase in the volume of high molecular weight bands present on SDS-PAGE gels. This was assumed to be caused by the addition of the cysteine immobilisation tag to the termini of GFP. This tagging protocol increased the instances of disulfide bond formation between multiple GFP proteins. The tagging of GFP with a single cysteine residue at the C-terminal of the GFP protein was developed to overcome this issue. Full vector PCR amplification using complementary phosphorylated primers carrying the desired additional residue was used for PCR amplification. The amplified plasmid, with the incorporated cysteine residue, is circularised by ligation which was facilitated by the use of phosphorylated primers. The high fidelity of Phusion *Taq* polymerase is of vital importance to this PCR cloning method as it facilitates full vector amplification. The primers used for this PCR amplification are illustrated in figure 3.1.26.

pVOS12 Forward Primer:

5' P' TAG AAG CTT AAT TAG CTG AGC TTG 3'

pVOS12 Reverse Primer:

5' P' ACA TTT GTA TAG TTC ATC CAT GCC 3'

Added Cysteine Residue

Figure 3.1.26: Primers for the creation of pVOS12, an *E.coli* expression vector which places a single cysteine residue at the C-termini of the protein. The addition of phosphorylation groups at the 5' of both the forward and reverse primers allows for the circularisation by ligation of PCR products.

The expression vector pVOS2, which added a purification tag to the N-terminus of GFP, was used as the template DNA for PCR reactions. The completed PCR reaction

was run on an agarose gel to confirm the amplification of the PCR product. The linearised PCR product pVOS12 was excised from the agarose gel and was re-circularised by ligation. The ligation was transformed into competent *E.coli* XL10-Gold or BL21 cells.

Following transformation, colonies were initially screened by examining for fluorescence. Plasmid DNA was prepared from fluorescing colonies; vectors were verified firstly by restriction analysis and subsequently by sequencing. Figure 3.1.27 illustrates the cloning protocol for the creation of this *E.coli* expression vector which expresses GFP with an N-terminal purification tag, and a single C-terminal cysteine residue immobilisation tag.

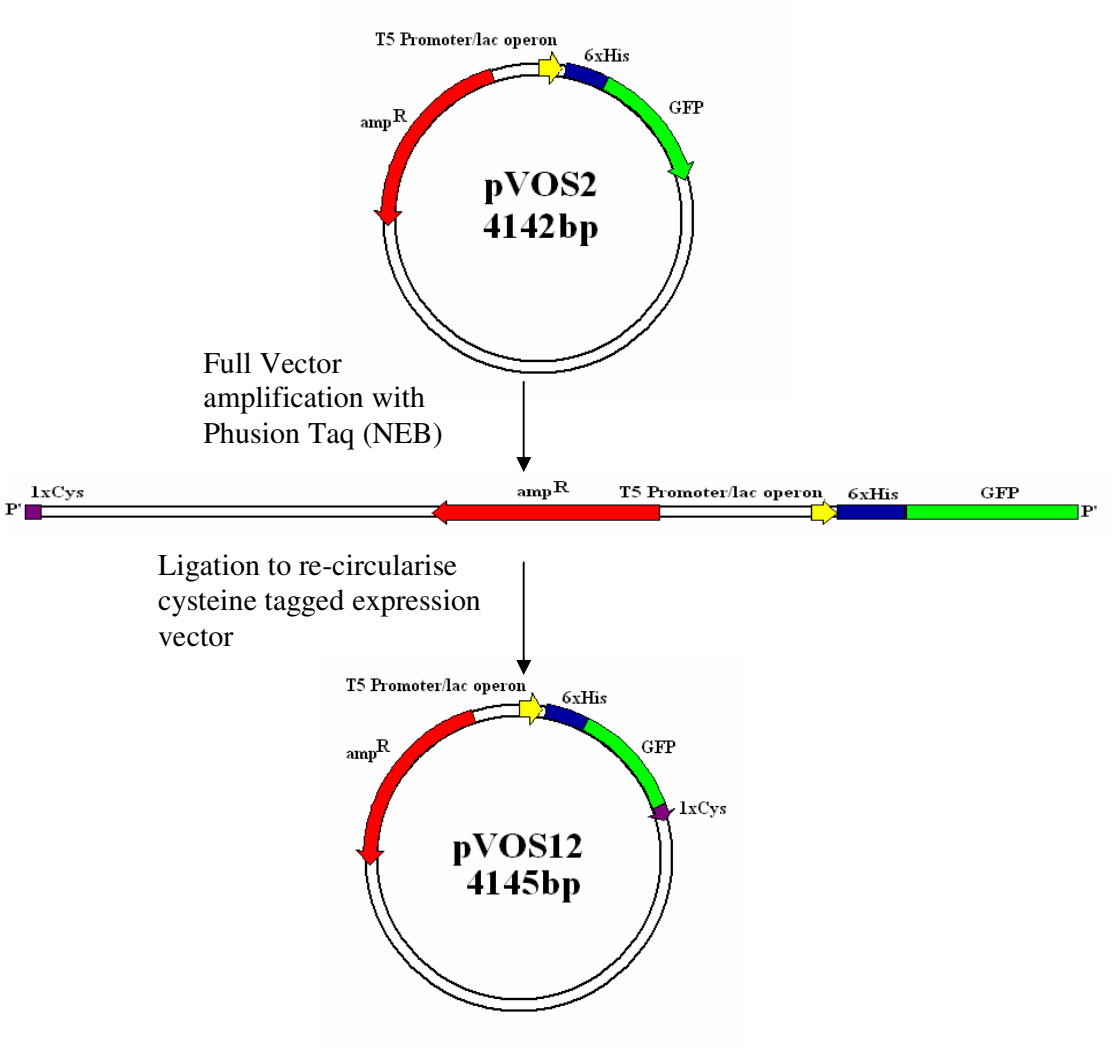

Figure 3.1.27: Cloning strategy for the creation of pVOS12 by full vector PCR amplification. This expression vector adds a single cysteine residue to the C-terminal of GFP. High fidelity Phusion *Taq* DNA polymerase allows for the complete vector amplification.

3.1.10: Summary

A range of *E.coli* expression vectors have been successfully produced by a variety of cloning strategies. These expression vectors were used to express GFP with a selection of different immobilisation tags. As outlined in the overview of this section, two covalent immobilisation tags and the bio-affinity immobilisation tag have been placed both N and C-terminally on the GFP protein. The six histidine amino acid purification tag has also been placed at both protein termini. Protein immobilisation and purification tags have also been placed in tandem at the N-terminus of GFP. Table 2.3 outlines the expression vectors generated during this study and the tagged GFP protein expressed from these vectors.

The wide range of composition and placement of immobilisation and purification tags allows for the study of the effect of such added tags on protein purification and immobilisation. The study of tagging effects will be outlined in more depth in future sections of this chapter.

3.2 Protein Expression and Purification

3.2.1 Overview:

The study of protein expression within a bacterial system is a complex field. Many factors affect the expression of proteins including the addition of purification and immobilisation tags, their location and the amino acid composition of these tags. A large range of tagged proteins was produced as outlined in Section 3.1., and studies were undertaken to determine the effects of these protein tags on protein expression levels. While incorporated tags can affect protein expression levels, external factors such as the bacterial strain, temperature of expression and induction and harvest have also been investigated to optimise protein production.

3.2.2 Growth Conditions in XL10-Gold:

Each of the sequenced clones were transformed in both XL10-Gold and BL21(DE3) *E. coli* strains. Initial expression work was performed with pVOS1 in XL10-Gold, to give an indication of expression. A 1ml aliquot from a 5ml overnight LB broth culture was used to inoculate two 100ml LB broths supplemented with ampicillin. After inoculation, both cultures were incubated at 30°C until an OD_{600} of 0.5 was reached. One of the two cultures was then induced by addition of IPTG to a final concentration of 50μM. The second 100ml culture remained uninduced. Both cultures were then incubated with shaking at 220rpm at 30°C. Immediately following induction with IPTG a 2ml sample was withdrawn from both cultures. This was noted as the time zero sample (T0). A 1ml aliquot was used to measure the optical density of the sample. The second 1ml aliquot was retained at -20°C for protein analysis by SDS-PAGE. Additional 2ml samples were taken every subsequent hour for five hours (designated T1 to T5) and a final sample withdrawn after overnight culturing (T-Ov). Each subsequent sample was processed in the same manner as the time zero sample. The samples retained for analysis by SDS-PAGE were lysed by sonication, and insoluble cell debris removed by centrifugation. Soluble fractions (prepared as described in section 2.19.3) from both the induced and uninduced samples at each time point were run on 12% SDS-PAGE. When GFP is run on SDS-PAGE small amounts of dimerised GFP were noted running at the 66.4kDa protein marker. The effect of temperature on protein expression within the XL10-Gold *E.coli* strain was studied.

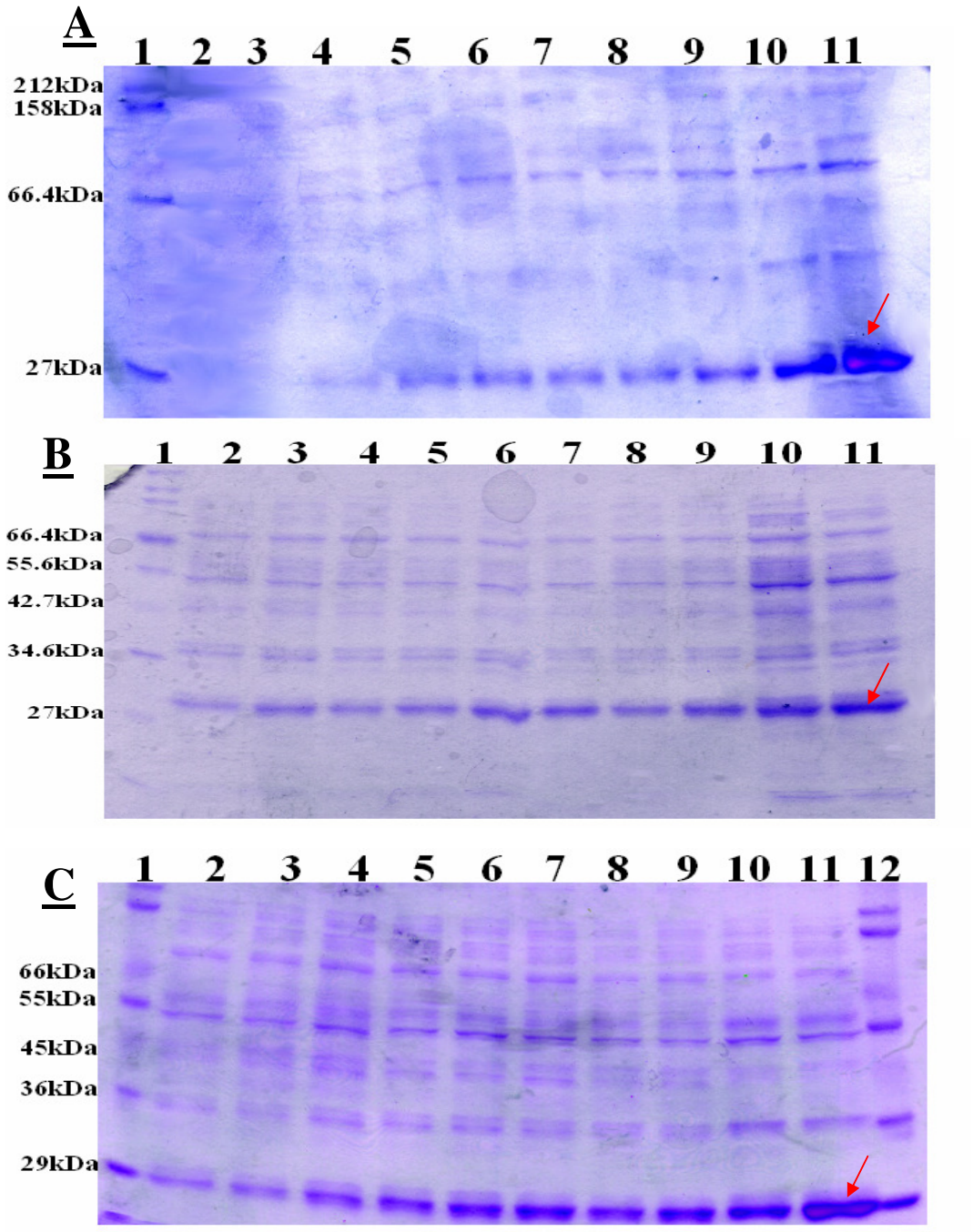

Figure 3.2.1: Analysis of pVOS1 expression levels in *E.coli* strain; XL10-Gold at a range of temperatures. **Gel A:** Soluble fractions of VOS1 (GFP with a C-terminal His^6 tag) expressed in XL10-Gold at 30°C. **Gel B:** Soluble fractions of VOS1 expressed in XL10-Gold at 37°C. **Gel C:** Soluble fractions of VOS1 grown in XL10-Gold at 37°C, induced and expressed at 30°C. Samples present in lanes across the three gels contain identical samples. **(1)** NEB Broad Range Protein Marker (**Gel C:** Sigma Wide Range Marker) **(2)** Time point 2 uninduced, **(3)** Time point 2 induced, **(4)** Time point 3 uninduced, **(5)** Time point 3 induced, **(6)** Time point 4 uninduced, **(7)** Time point 4 induced, **(8)** Time point 5 uninduced, **(9)** Time point 5 induced, **(10)** Overnight uninduced, **(11)** Overnight induced. **(12)** Sigma Wide Range Protein Marker. Expressed overnight (24hrs) protein is highlighted by a red arrow.

Figure 3.2.1 shows three 12% SDS-PAGE gels of protein expression levels at three separate temperatures from the *E.coli* XL10-Gold strain. Gel A outlines induced and uninduced T0 to T-Ov samples of VOS1 grown in XL10-Gold at 30°C. Gel B describes induced and uninduced T0 to T-Ov samples of VOS1 grown in XL10-Gold at 37°C. The final SDS-PAGE; Gel C, illustrates induced and uninduced T0 to T-Ov samples of VOS1 which were grown in XL10-Gold to induction at 37°C as outlined previously. Following induction, time zero samples were immediately taken and the cultures were incubated with shaking at 220rpm at 30°C.

Early time point samples at all temperatures, show initial GFP concentrations in both induced and uninduced samples to be low. GFP concentrations increase over time to a maximum concentration in the overnight samples. The protein is expressed in both uninduced and induced samples at all temperature levels, but is expressed at a higher levels in the overnight induced cultures based on SDS-PAGE. It was expected that temperature of expression would not have a significant effect, however the levels of protein expression within XL10-Gold, appear to be marginally greater at 30°C. The effect of the *E.coli* strain on protein expression was also studied, and is outlined in the next section.

3.2.3: Growth Conditions in BL21:

The optimum over-expression of soluble proteins in bacterial systems as outlined in section 3.2.1 relies on several factors. One of the most important factors is the bacterial expression strain used. To study this effect GFP was over-expressed at different temperatures in the BL21 *E.coli* bacterial strain.. The effect of temperature on levels of protein expression in BL21 was studied. The over expression of VOS1 in BL21 was performed identically as described for the over expression of VOS1 in XL10-Gold. The soluble fractions of the uninduced and induced time samples were separated on 12% SDS-PAGE gels.

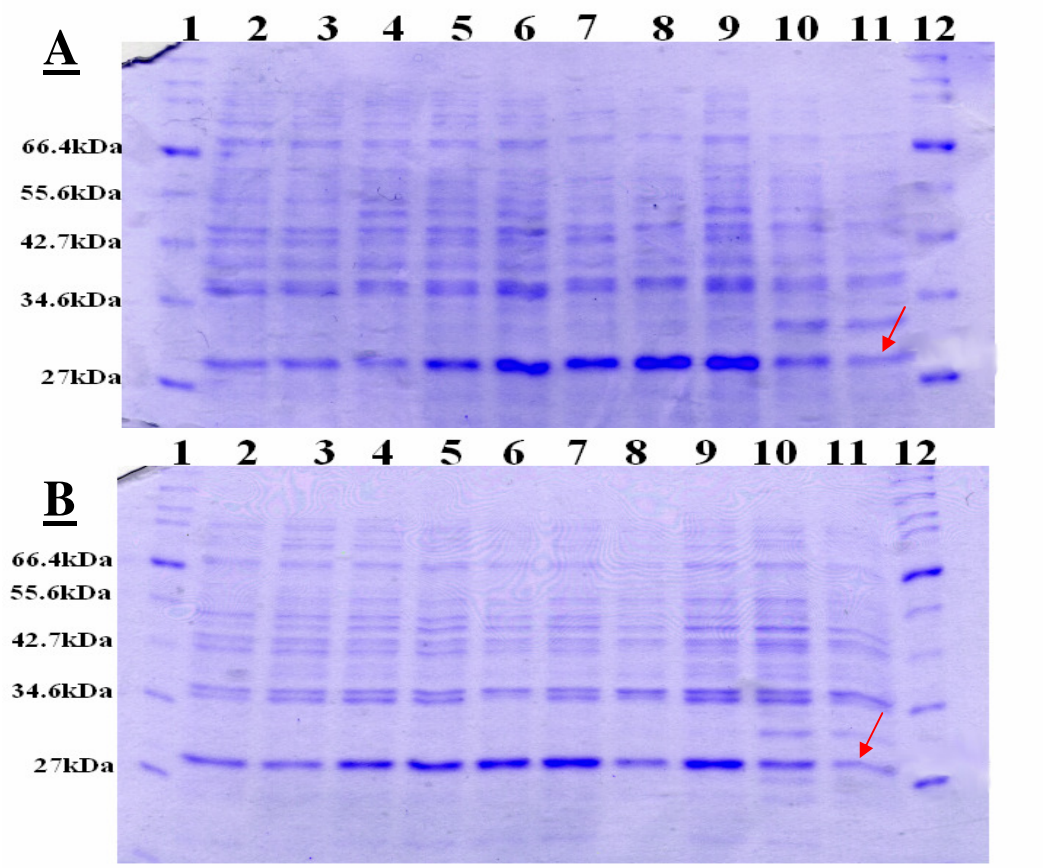

Figure 3.2.2: Analysis of pVOS1 expression levels in *E.coli* strain; BL21 at a range of temperatures. **Gel A:** Soluble fractions of VOS1 (GFP with a C-terminal His^6 tag) expressed in BL21 at 30°C. **Gel B:** Soluble fractions of VOS1 grown in BL21 at 37°C, induced and expressed at 30°C. Samples present in lanes across the two gels contain identical samples. **(1)** NEB Broad Range Protein Marker, **(2)** Time point 2 uninduced, **(3)** Time point 2 induced, **(4)** Time point 3 uninduced, **(5)** Time point 3 induced, **(6)** Time point 4 uninduced, **(7)** Time point 4 induced, **(8)** Time point 5 uninduced, **(9)** Time point 5 induced, **(10)** Overnight uninduced, **(11)** Overnight (24hrs) induced, **(12)** NEB Broad Range Protein Marker. Expressed overnight protein is highlighted by a red arrow

The optimum temperature for expression of GFP within XL10-Gold proved to be 30°C. The overnight induced and uninduced VOS1 within BL21 at 30°C was not optimum for achieving large levels of expressed protein within soluble fractions. All protein concentration levels in the soluble fractions of BL21 viewed on 12% SDS-PAGE gels showed lower levels of expression than those within XL10-Gold. The difference in overnight expression levels of BL21 shows the greatest difference between the strains. The greater levels of protein expression visible in the XL10-Gold *E.coli* strain compared to the BL21 strain at all time points allowed for the use of the XL10-Gold strain in all future expression protocols.

3.2.4: Effect of protein tags on expression.

To determine the effect of additional tags added to GFP on protein expression, VOS5 (N-terminal His6, C-terminal Strep-TagII) was expressed in an identical manner as VOS1 in XL10-Gold and at a temperature of 30°C. The soluble fraction retained was run on a 12% SDS-PAGE to determine relative amounts of expressed protein. VOS5 was also expressed in XL10-Gold at 37°C to determine if the same temperature effect observed in the expression of VOS1 at different temperatures was present in a different GFP clone.

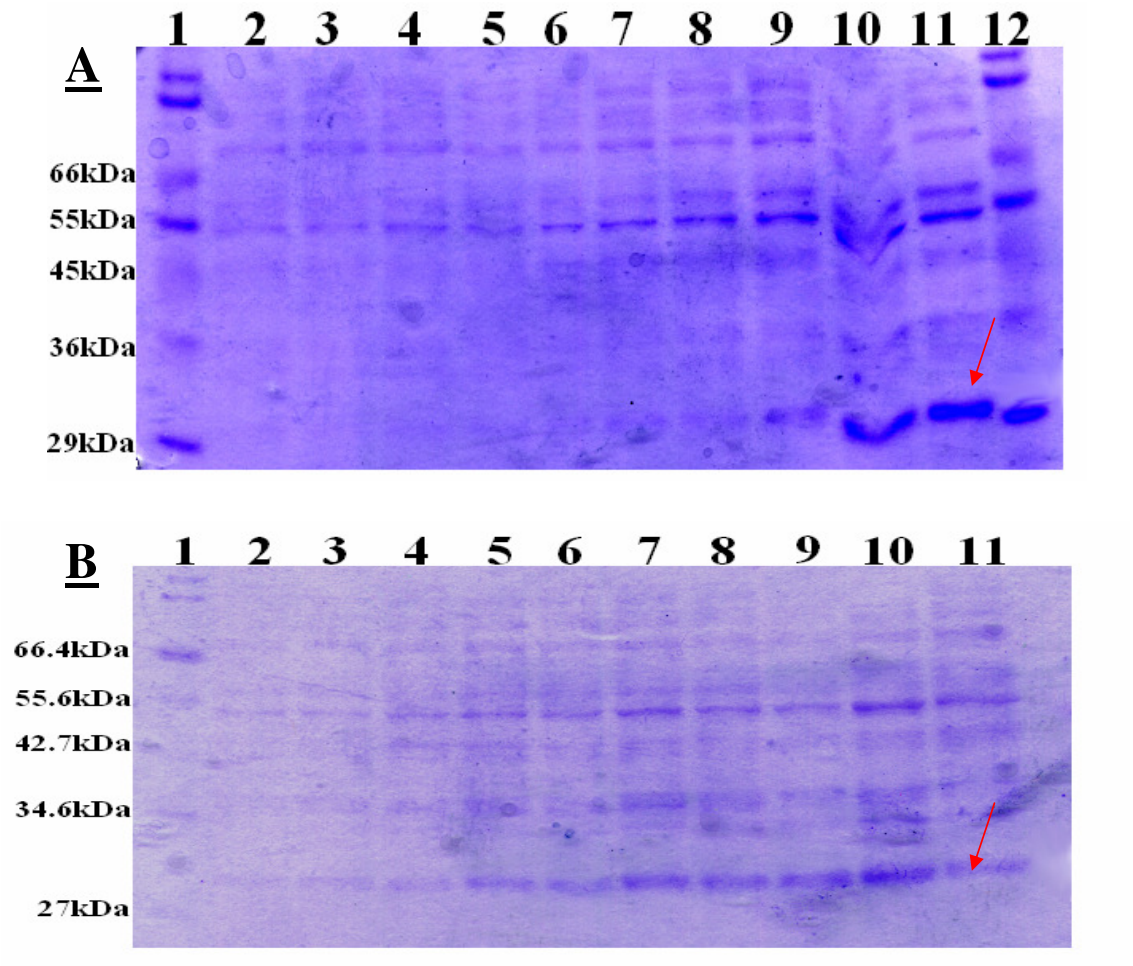

Figure 3.2.3: Analysis of pVOS5 expression levels in *E.coli* strain; XL10-Gold at a range of temperatures. **Gel A:** Soluble fractions of VOS5 (N-terminal His^6 tag, C-terminal Strep-TagII) expressed in XL10-Gold at 30°C. **Gel B:** Soluble fractions of VOS5 grown in XL10-Gold at 37°C. Samples present in lanes across the two gels contain identical samples. **(1) Gel A:** Sigma Wide Range Protein Marker, **Gel B:** NEB Broad Range Protein Marker, **(2)** Time point 2 uninduced, **(3)** Time point 2 induced, **(4)** Time point 3 uninduced, **(5)** Time point 3 induced, **(6)** Time point 4 uninduced, **(7)** Time point 4 induced, **(8)** Time point 5 uninduced, **(9)** Time point 5 induced, **(10)** Overnight uninduced, **(11)** Overnight induced, **(12)** Sigma Wide Range Protein Marker. Expressed overnight protein is highlighted by a red arrow

From figure 3.2.3 it can be seen that the temperature of expression of VOS5 in XL10-Gold was found to have a significant effect on GFP expression, with clearly better expression at 30°C than 37°C. This mirrors the expression levels seen of VOS1 at this temperature. Interestingly, when we examine expression at 37°C, GFP expression was best after overnight growth in the uninduced sample, however at 30°C the best expression was in the induced culture five hours after induction. Figure 3.2.3 illustrates that the addition of a tag to the C-terminus appears to have an effect on protein expression at 37°C.

These studies on the temperature, has outlined the importance of temperature on protein expression levels. The most efficient temperature for GFP protein expression in XL10-Gold was clearly shown to be at 30°C. The expression levels of C-terminal GFP tagged protein at 37°C (Figure 3.2.3), indicates that the addition, composition and location of protein tags can have an effect on the level of protein expression. To determine if this is the case in tagged GFP clones, all proteins were expressed and the soluble fraction ran on 12% SDS-PAGE gels. From the initial expression work performed in sections 3.2.2. and 3.2.3 optimum expression protocol was determined. Tagged GFP clones expressing in XL10-Gold were grown at 37°C with shaking at 220rpm to the induction point, immediately after induction the culture was incubated at 30°C with shaking at 220rpm. The cultures were then harvested after overnight incubation. This method allowed the cultures to reach an induction point quickly, yet produce greater levels of over-expressed proteins.

To study the effect the addition of protein immobilisation tags had on protein expression all tagged GFP proteins were over-expressed according to the conditions determined in this section. The soluble fractions were run on 12% SDS-PAGE gels (Section 2.19). Results are shown in Figures 3.2.4 to 3.2.7.

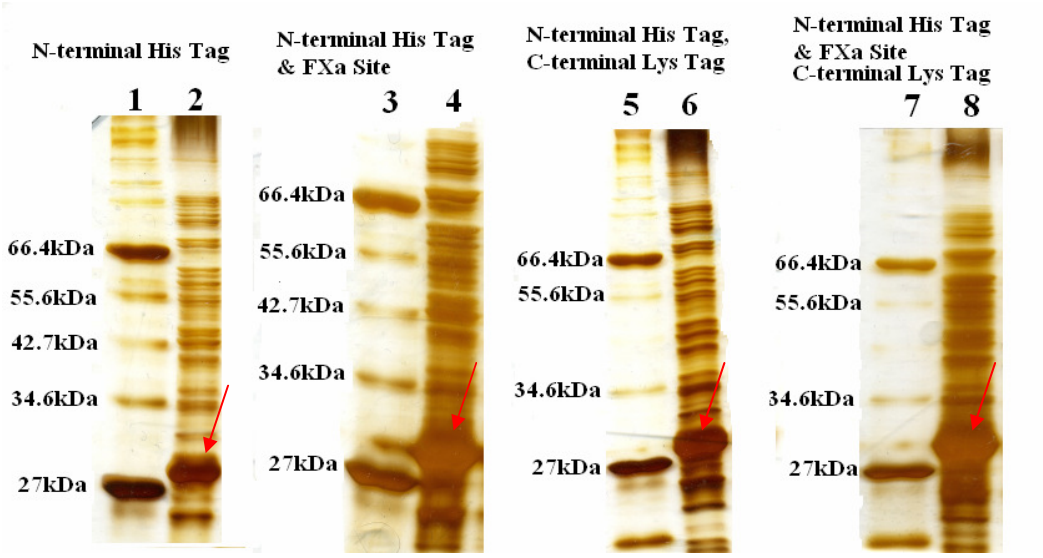

Figure 3.2.4: Expression levels of tagged GFPs; VOS2, VOS2Xa, VOS3 and VOS3Xa. **(Lanes 1, 3, 5 & 7)** NEB Broad Range Protein Marker, **(2)** Soluble fraction of VOS2 (N-terminal His^6 tag), **(4)** Soluble fraction of VOS2Xa (N-terminal His^6 tag with FXa protease site), **(6)** Soluble fraction of VOS3 (N-terminal His^6 tag, C-terminal $Lysine^6$ tag), **(8)** Soluble fraction of VOS3Xa (N-terminal His^6 tag and FXa protease site, C-terminal $lysine^6$ tag) Overexpressed tagged GFP is highlighted by a red arrow.

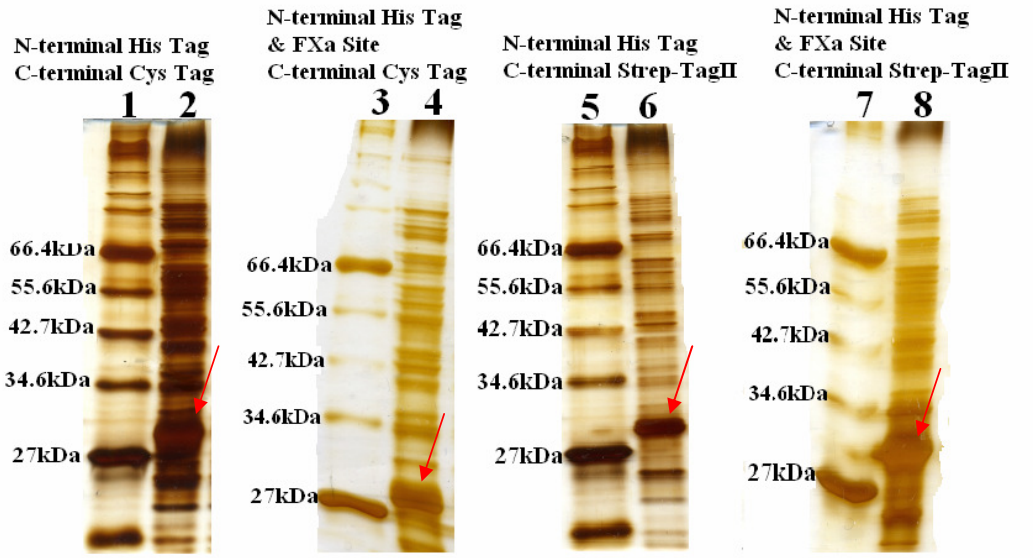

Figure 3.2.5: Expression levels of tagged GFPs; VOS4, VOS4Xa, VOS5, VOS5Xa **(Lanes 1, 3, 5 & 7)** NEB Broad Range Protein Marker, **(2)** Soluble fraction of VOS4 (N-terminal His^6 tag, C-terminal $cysteine^6$ tag), **(4)** Soluble fraction of VOS4Xa (N-terminal His^6 tag with FXa protease site, C-terminal $cysteine^6$ tag), **(6)** Soluble fraction of VOS5 (N-terminal His^6 tag, C-terminal Strep-TagII), **(8)** Soluble fraction of VOSXa (N-terminal His^6 tag and FXa protease site, C-terminal Strep-TagII). Overexpressed tagged GFP is highlighted by a red arrow.

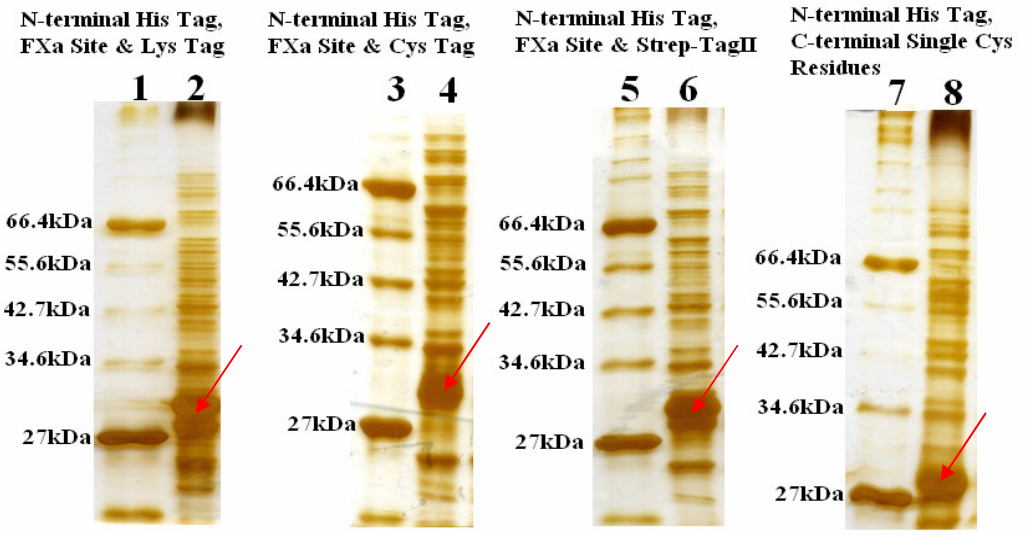

Figure 3.2.6: Expression levels of tagged GFPs; VOS6Xa, VOS7Xa, VOS8Xa and VOS12. **(Lanes 1, 3, 5 & 7)** NEB Broad Range Protein Marker, **(2)** Soluble fraction of VOS6Xa (N-terminal His^6 tag, FXa protease site and $lysine^6$ tag), **(4)** Soluble fraction of VOS7Xa (N-terminal His^6 tag with FXa protease site and $cysteine^6$ tag), **(6)** Soluble fraction of VOS8Xa (N-terminal His^6 tag, FXa protease site and Strep-TagII), **(8)** Soluble fraction of VOS12 (N-terminal His^6 tag, C-terminal single cysteine residue). Overexpressed tagged GFP is highlighted by a red arrow.

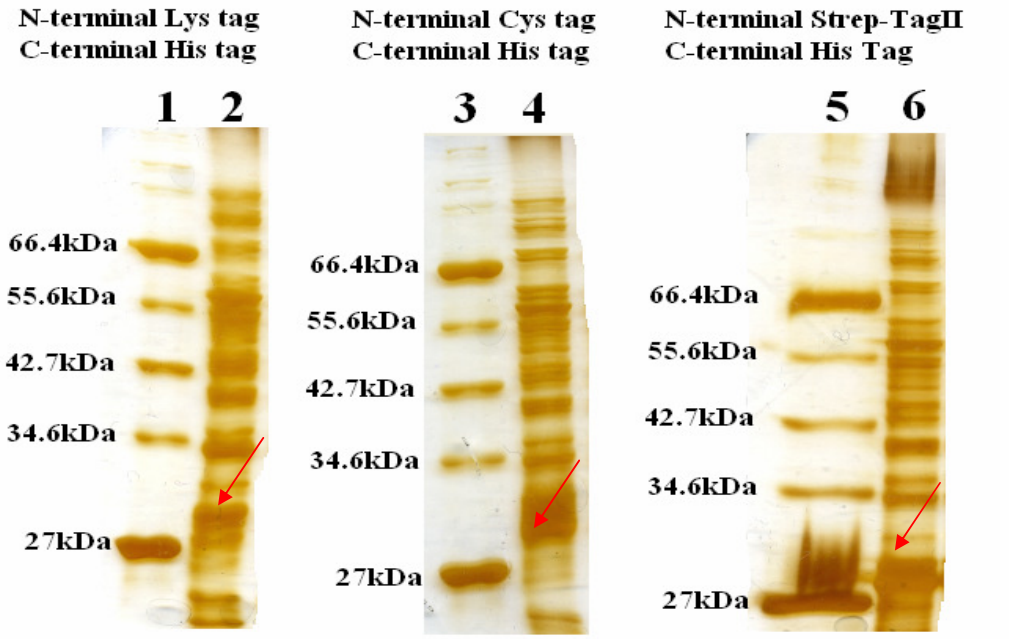

Figure 3.2.7: Expression levels of tagged GFPs; VOS9, VOS10 and VOS11. **(Lanes 1, 3, 5)** NEB Broad Range Protein Marker, **(2)** Soluble fraction of VOS9 (N-terminal lysine5 tag, C-terminal His^6 tag), **(4)** Soluble fraction of VOS10 (N-terminal cysteine6 tag, C-terminal His^6 tag), **(6)** Soluble fraction of VOS11 (N-terminal Strep-TagII and C-terminal His^6 tag) Overexpressed tagged GFP is highlighted by a red arrow.

Figures 3.2.4 to 3.2.7 shows an important result, which validates the amount of protein expression optimisation undertook. The placement of the immobilisation tag has a vital effect on the levels of protein expression. It was found that the addition of an immobilisation tag directly downstream from the promoter region greatly reduced the level of protein expression (Figure 3.2.7). Protein expression levels illustrated in figure 3.2.6 are high, these proteins are expressed with both purification and immobilisation tags at the N-terminus. The only difference between the clones expressed in figure 3.2.6 and figure 3.2.7, is that the histidine tag is located directly downstream from the promoter region rather than the immobilisation tag. It may be that the presence of the immobilisation tag in such close proximity to the promoter region has a negative effect of DNA polymerase transcription levels leading to lower expression protein concentrations.

The figures 3.2.4, 3.2.5 and 3.2.6 outline the expressed GFP protein levels within the soluble fraction. All of these GFP proteins have the histidine tag for protein purification at the N-terminal of the protein. There are some differences between these expressed proteins. The soluble fractions outlined in figures 3.2.4 and 3.2.5 are of expressed GFP, which present the histidine tag on the N-terminus and the immobilisation tags on the C-terminus. The soluble fractions shown in figure 3.2.6 are of proteins which contain no tag on the C-terminus, but instead have all the added tags on the N-terminus downstream from the histidine tag.

Figure 3.2.7 illustrates the soluble fractions produced from cultures which have the histidine tag present at the C-terminus of the expressed protein. The immobilisation tags were added to the N-terminus of these proteins. These immobilisation tags comprised of repeated lysine and cysteine residues or the Strep-TagII. The addition of immobilisation tags at the N-terminus of the protein results in a significant reduction in the quantities of protein expressed in XL10-Gold. This was an important result, which outlines the significance of performing expression optimisation studies.

3.2.5 Purification Overview

The incorporation of six histidine residues at either the N or C-terminal enables purification using IMAC columns, described in section 2.16.1. The optimisation of this purification is outlined in this section.

3.2.6 Protein Purification Protocol Overview

As outlined in Section 2.16.1, five column volumes of the soluble fraction of VOS1 containing the over-expressed protein was applied to GE Healthcare nickel sepharose resin and a step wise gradient of increasing imidazole concentration was applied to determine the minimum imidazole concentration at which the GFP protein begins to elute from the resin.

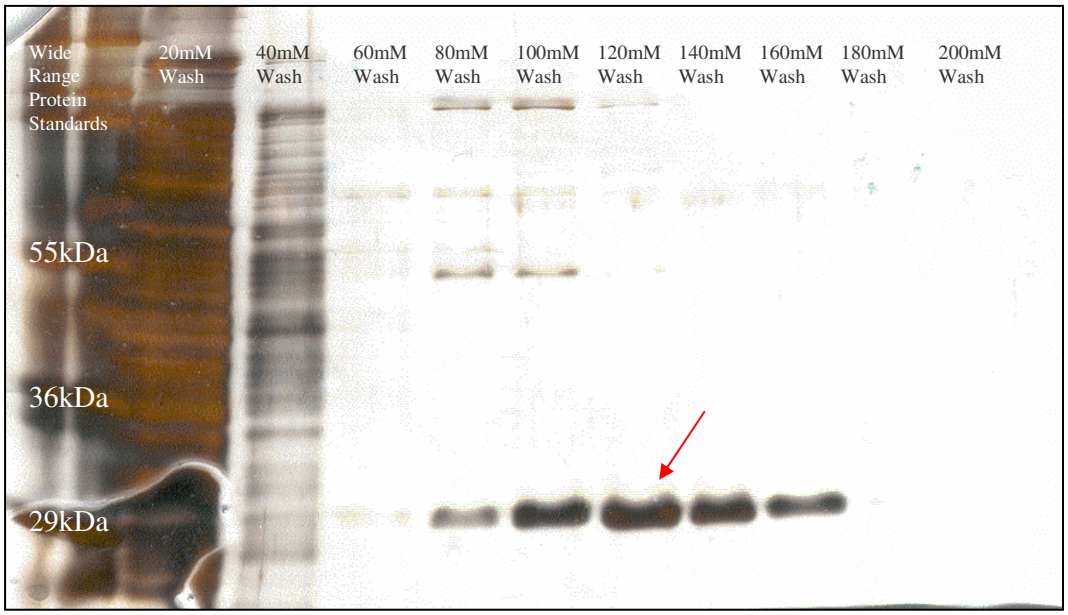

Figure 3.2.8: Initial imidazole gradient of VOS1 (C-terminal His^6 tag) purification. Five column volumes of the soluble fraction were passed over the IMAC resin, seven column volumes of each imidazole concentration was passed over the resin and the elution fractions captured. These fractions were run on a 12% SDS-PAGE gel and stained by the silver stain method (Section 2.19.4). Purified GFP bands are highlighted by a red arrow.

The imidazole gradient in Figure 3.2.8 shows GFP beginning to elute at 80mM imidazole. At both this concentration and at 100mM imidazole several higher molecular weight bands are visible. At 120mM imidazole, the larger bands have been eluted. It was decided to sacrifice some of the protein yield, which is eluted at 80mM to ensure the purity of the final product by removing the larger containment bands.

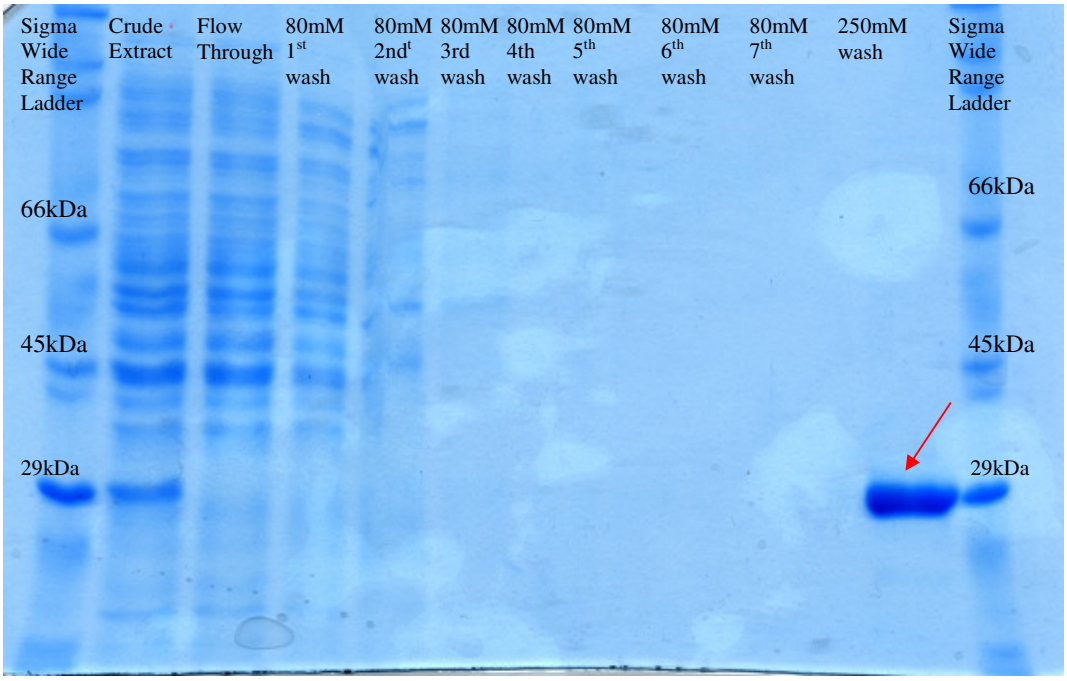

Figure 3.2.9: An optimised purification protocol for VOS1 (C-terminal His^6 tag). All GFP from the crude sample is captured by the resin as shown by the lack of a GFP band in the flow-through lane. Purified GFP bands are highlighted by a red arrow.

Figure 3.2.9 outlines the optimised purification protocol of the five column volumes of C-terminally histidine tagged GFP. From the flow-through lane it was seen that the IMAC resin completely captured the histidine tagged GFP. This column was washed with several column volumes of 80mM imidazole to ensure the thorough removal of any containment proteins. An elution buffer wash of 250mM was used to elute the VOS1 protein and as shown in figure 3.2.9, the protein was obtained in a highly purified form as assessed by SDS-PAGE. This optimised method was transferred to all other expressed GFP clones. It was found during continuing purification protocols that five columns volumes of all washes was sufficient for optimum purity of the expressed protein. From a 100ml of protein expression culture a typical yield of between 1 and 2mg per ml of purified protein was produced. Protein concentration was determined by the BCA method. (Section 2.18)

All protein expression clones were expressed as detailed in section 2.15, to determine the efficiency of protein production. Protein purification was carried out as outlined in section 2.16.1 and protein purification samples were run on 12% SDS-PAGE gels. These gels were stained by the silver staining method. (Section 2.19.4)

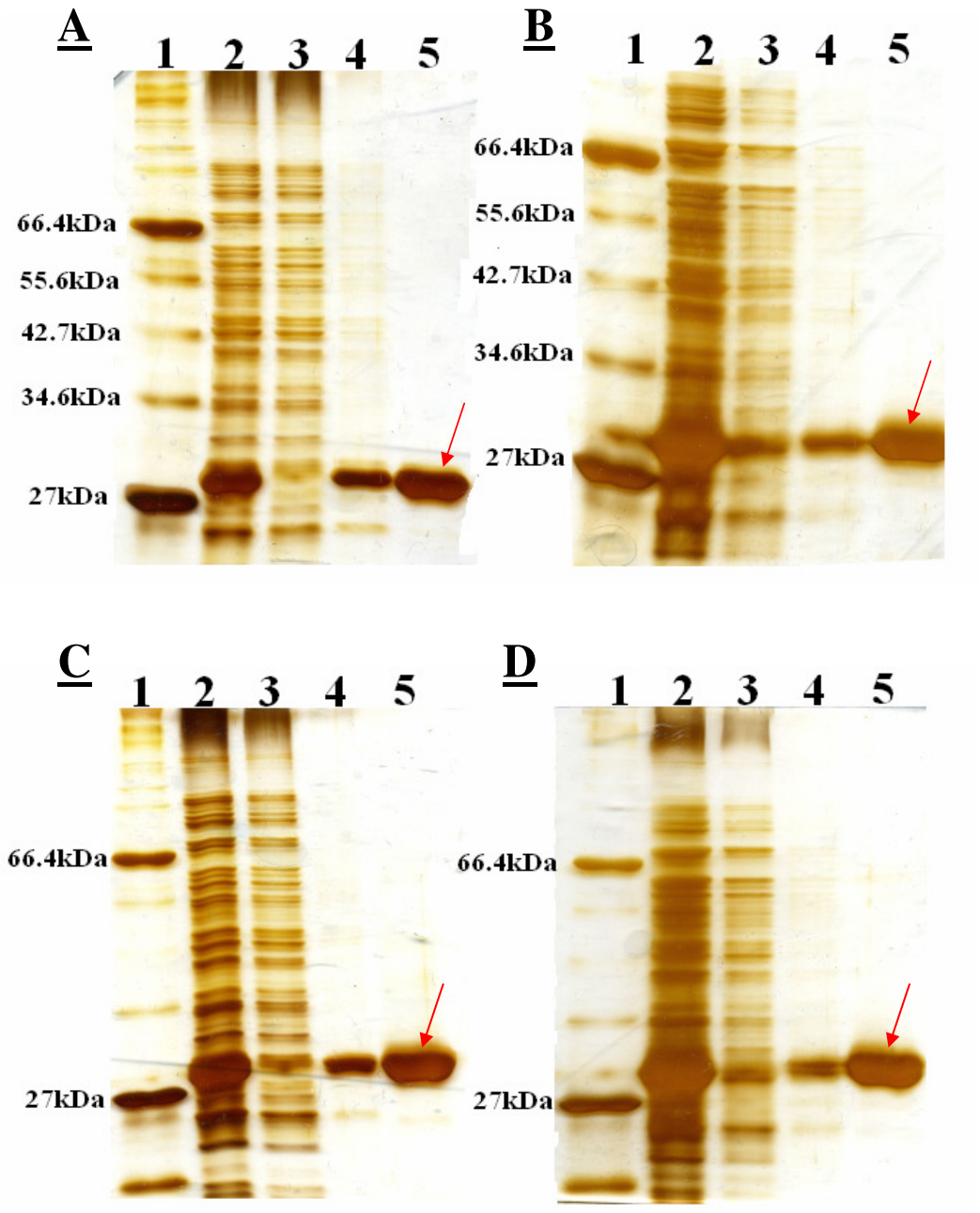

Figure 3.2.10: The purification of tagged GFPs; **Gel A:** VOS2 (N-terminal His^6 tag), **Gel B:** VOS2Xa (N-terminal His^6 tag with FXa protease site), **Gel C:** VOS3 (N-terminal His^6 tag, C-terminal $Lysine^6$ tag) and **Gel D:** VOS3Xa (N-terminal His^6 tag and FXa protease site, C-terminal $Lysine^6$ tag) **Lane 1:** NEB Broad Range Protein Marker, **Lane 2:** Protein Soluble Fractions, **Lane 3:** Protein Flow Through, **Lane 4:** 80mM Imidazole Wash, **Lane 5:** 250mM Imidazole elution. Arrows are highlighting purified monomeric GFP.

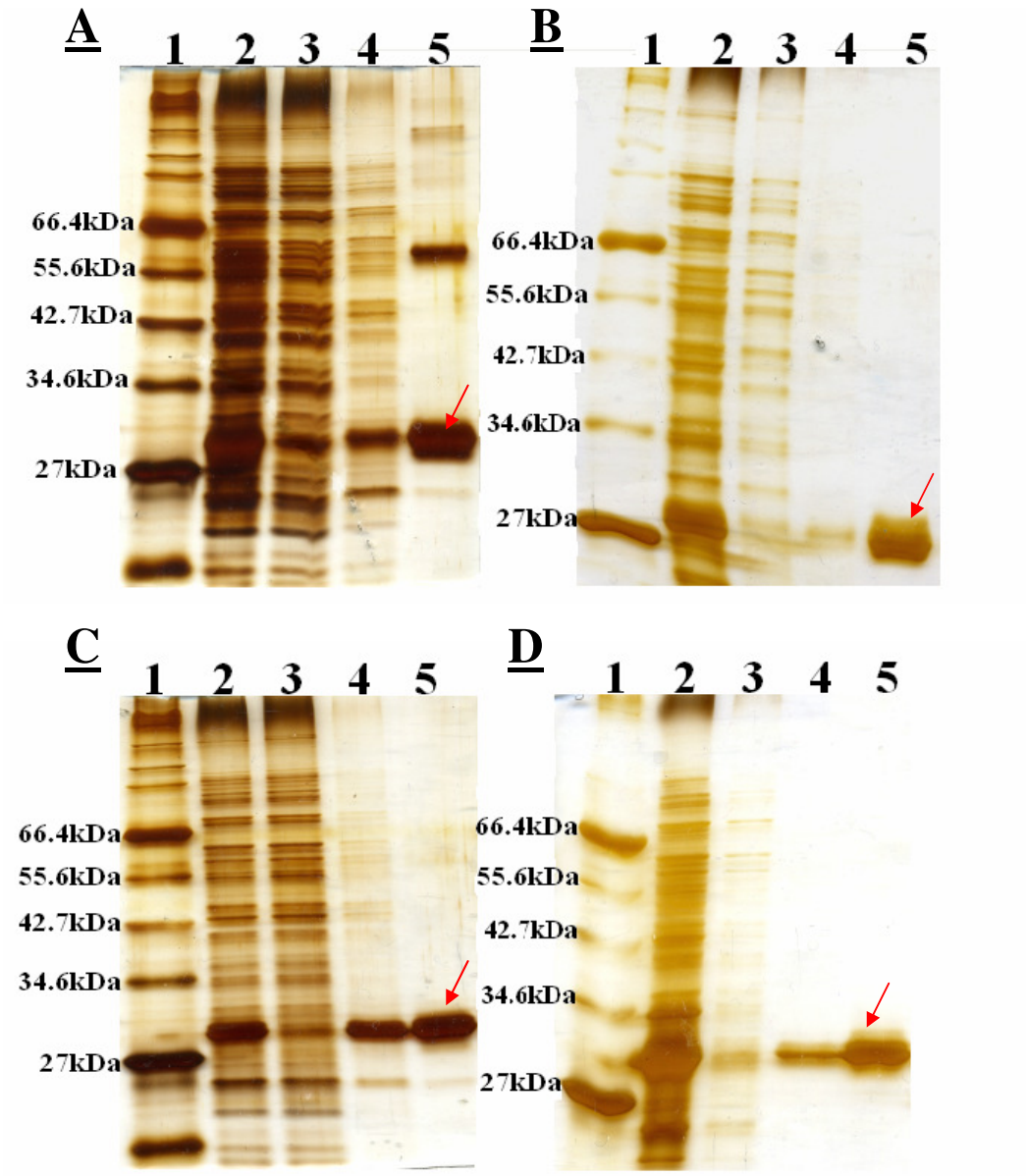

Figure 3.2.11: The purification of tagged GFPs; **Gel A:** VOS4 (N-terminal His^6 tag, C-terminal $Cysteine^6$ tag), **Gel B:** VOS4Xa (N-terminal His^6 tag and FXa protease site, C-terminal $Cysteine^6$ tag), **Gel C:** VOS5 (N-terminal His^6 tag, C-terminal Strep-TagII) and **Gel D:** VOS5Xa (N-terminal His^6 tag and FXa protease site, C-terminal Strep-TagII) **Lane 1:** NEB Broad Range Protein Marker, **Lane 2:** Protein Soluble Fraction, **Lane 3:** Protein Flow Through, **Lane 4:** 80mM Imidazole Wash, **Lane 5:** 250mM Imidazole protein elution. Arrows are highlighting purified monomeric GFP.

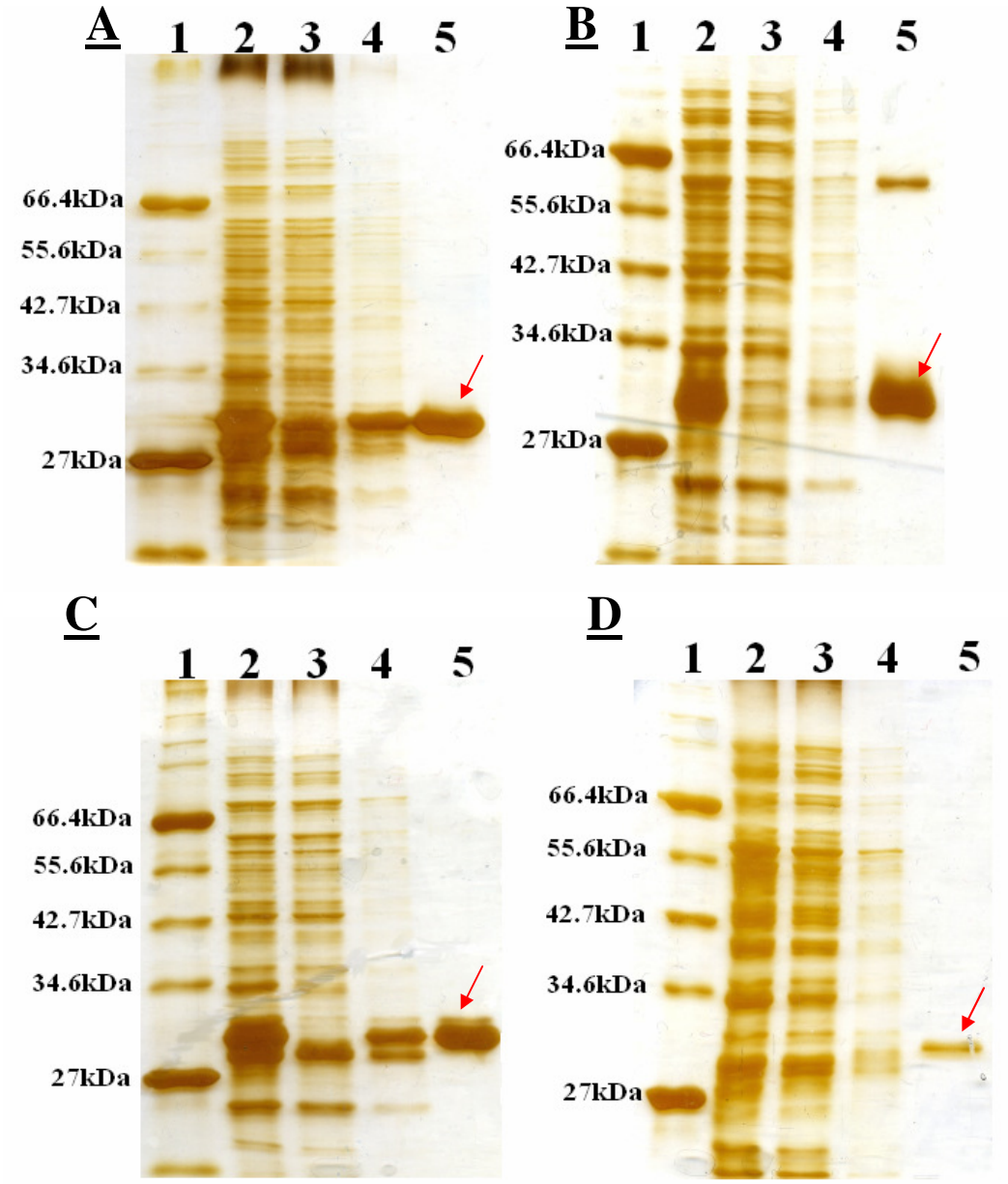

Figure 3.2.12: The purification of tagged GFPs; **Gel A:** VOS6Xa (N-terminal His^6 tag, FXa protease site and $lysine^6$ tag), **Gel B:** VOS7Xa (N-terminal His^6 tag. FXa protease site and $cysteine^6$ tag), **Gel C:** VOS8Xa (N-terminal His6 tag, FXa protease site and Strep-TagII) and **Gel D:** VOS9 (N-terminal $Lysine^5$ tag, C-terminal His^6 tag) **Lane 1:** NEB Broad Range Protein Marker, **Lane 2:** Protein Soluble Fraction, **Lane 3:** Protein Flow Through, **Lane 4:** 80mM Imidazole Wash, **Lane 5:** 250mM Imidazole elution. Arrows are highlighting purified monomeric GFP.

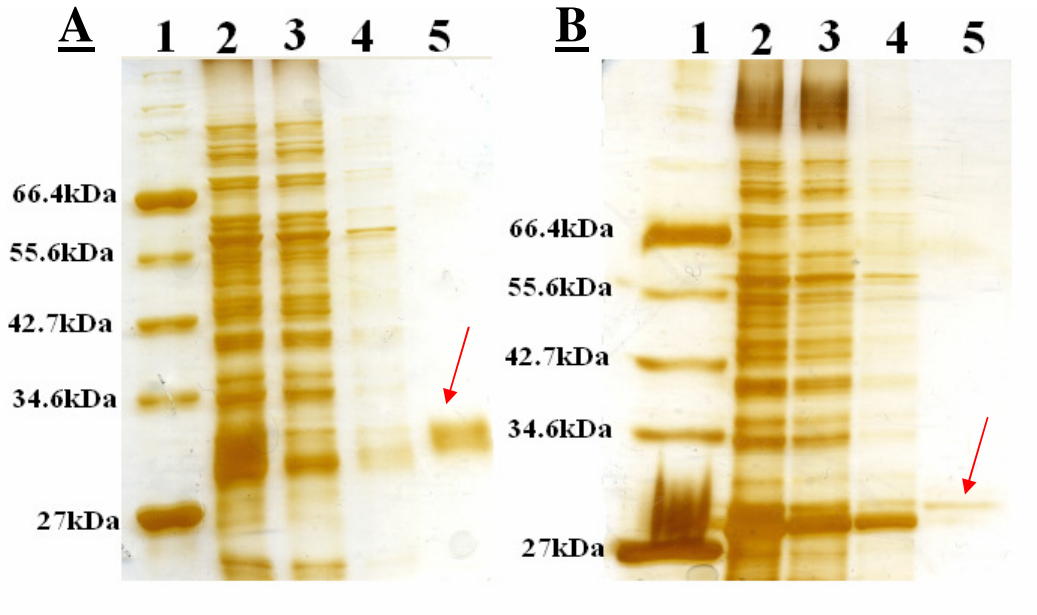

Figure 3.2.13: The purification of tagged GFPs; **Gel A:** VOS10 (N-terminal Cysteine^{6} tag and C-terminal His^{6} tag) and Gel B: VOS11 (N-terminal Strep-TagII and C-terminal His^{6} tag) **Lane 1:** NEB Broad Range Protein Marker, **Lane 2:** Protein Soluble Fraction, **Lane 3:** Protein Flow Through, **Lane 4:** 80mM Imidazole Wash, **Lane 5:** 250mM Imidazole elution. Arrows are highlighting purified monomeric GFP.

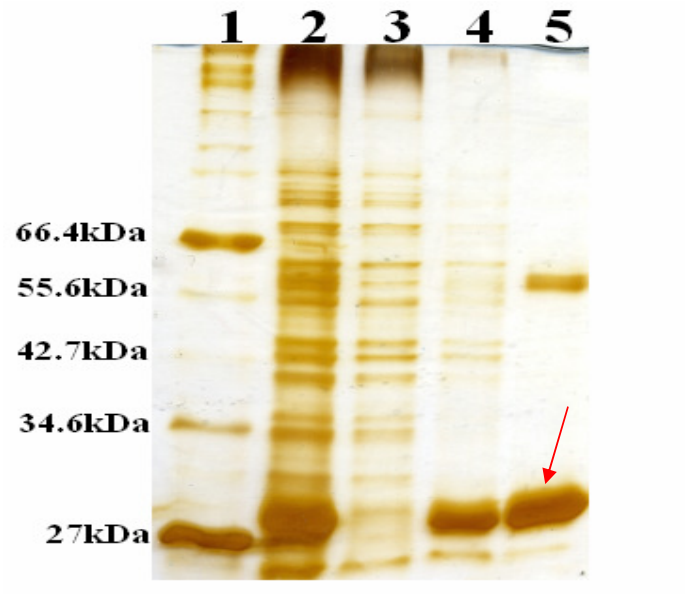

Figure 3.2.14: The purification of VOS12 (N-terminal His^{6} tag, Single C-terminal Cysteine residue) **(1)** NEB Broad Range Protein Marker, **(2)** VOS12 Soluble Fraction, **(3)** VOS12 Flow Through, **(4)** VOS12 80mM Imidazole Wash, **(5)** VOS12 250mM Imidazole elution. Arrow is highlighting purified monomeric GFP.

A gel band running just above the 27kDa protein marker band in the purification gels signifies the purification of the monomeric protein (Figures 3.2.10-3.2.14). The expression and purification of the majority of clones was successful using the methods outlined in Chapter 2. The expression and purification the N-terminal tagged GFPs, VOS9 (N-terminal Lysine^5 tag, C-terminal His^6 tag), VOS10 (N-terminal Cysteine^6 tag and C-terminal His^6 tag) and VOS11 (N-terminal Strep-TagII and C-terminal His^6 tag) was considerably less efficient than other purifications. The immobilisation tags placed on the N-terminus as previously described had an effect on the volume of expressed protein (Figures 3.2.12 & 3.2.13). As levels of purified protein achieved by IMAC, directly relates to the concentration of expressed proteins the three described clones were not purified efficiently. Due to the reduced levels of purified protein produced, these proteins, were discarded from further studies.

From the purification gels outlined of all the produced clones, it can be seen that certain clones have dimer bands in their purification lanes. While GFP can form dimers in solution it occurs rarely and is probably due to interactions between hydrophobic zones (Tsien, 1998). It was found during purification of clones which had added cysteine residues the presence of dimers was greatly increased. The presence of protein bands between 66.4kDa and 55.6kDa NEB protein markers in VOS4, VOS7Xa and VOS12 is indicative of the presence of a dimer. These dimers are formed by the oxidisation of cysteines to form cystines with other GFP molecules containing a cysteine tag. In an effort to reduce this effect, pVOS12 with a single C-terminal cysteine was constructed (Figure 3.1.14). GFP has only two inherent cysteine residues which are buried within the tertiary structure. By the addition of this single extra cysteine residue it was thought a single point for immobilisation reactions would be provided. This would reduce the volume of high molecular weight containment bands. The purification lane of VOS4 within Figure 3.2.11 (Gel A, Lane 5) is indicative of the large molecular weight molecules generated by the addition of this cysteine tag.

All purification gels outlined in this section were run in a reducing environment achieved by adding mercaptoethanol to the protein samples, the electrophoresis gel and the running buffer (Section 2.4). By removing SDS and 2-mercaptoethanol from the SDS-PAGE sample buffer as outlined in section 2.4, and boiling for five minutes the molecular weight of the expressed protein and the degree of aggregation can be revealed. (Figure 3.2.15) This gel outlines the banding pattern differences between samples of a cysteine tagged GFP clone in both reducing and non-reducing buffers. By

adding the reducing agent DTT to the protein sample in a gradient of increasing concentrations, an increase in the quantity of banding of monomeric protein and conversely a reduction the higher molecular weight bands can be seen as in figure 3.2.16.

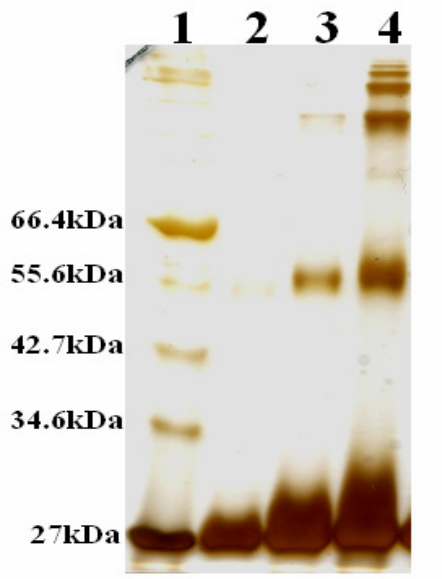

Figure 3.2.15: The effect of a reducing agent on the protein banding of cysteine tagged GFP. **(1)** NEB Broad Range Marker, **(2)** VOS1 (C-terminal His^6 tag) in reducing buffer, **(3)** VOS4 (N-terminal His^6 tag, C-terminal $Cysteine^6$ tag) in reducing buffer, **(4)** VOS4 (N-terminal His^6 tag, C-terminal $Cysteine^6$ tag) in non-reducing buffer.

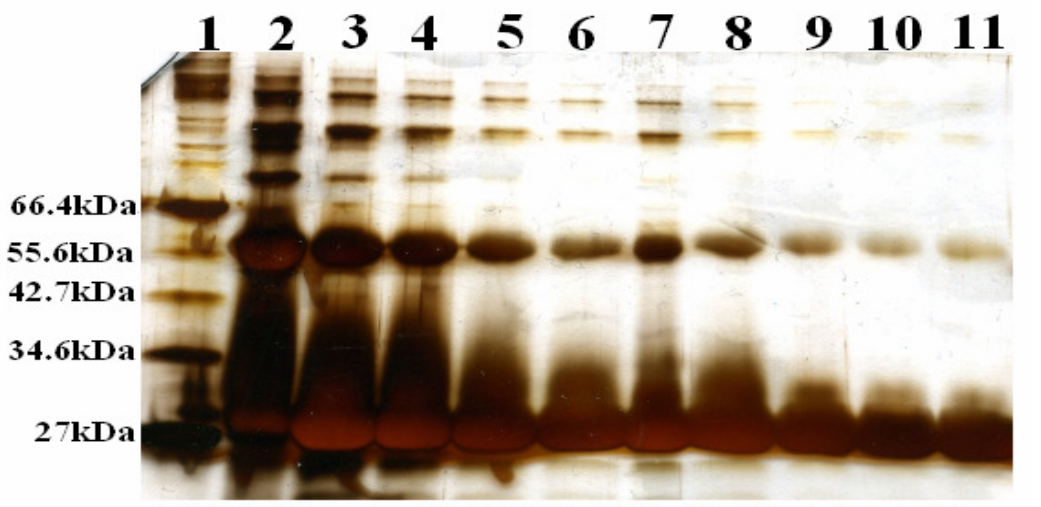

Figure 3.2.16: The effect of a DTT Gradient on the banding pattern of cysteine tagged VOS12 (N-terminal His^6 tag, Single C-terminal Cysteine residue), **(1)** NEB Broad Range Marker, **(2)** VOS12 No DTT, **(3)** VOS12 10mM DTT, **(4)** VOS12 15mM DTT, **(5)** VOS12 20mM DTT, **(6)** VOS12 25mM DTT, **(7)** VOS12 30mM DTT, **(8)** VOS12 35mM DTT, **(9)** VOS12 40mM DTT, **(10)** VOS12 45mM DTT, **(11)** VOS12 50mM DTT

The addition of 50mM DTT highlighted in Figure 3.2.16 shows the reduction of the quantity of high molecular weight proteins. This compound is only required for cysteine tagged expressed proteins as all other clones do not form multimers. The purification of monomeric protein is required for efficient immobilisation. By reducing the number of cysteine residues available for immobilisation from a six residue tag, to a one residue tag, it was attempted to reduce the amount of high molecular weight aggregates.

3.2.7: Summary

The expression of GFP in *E.coli* cells was studied to determine the effect of temperature, cell strain, location, composition and type of tags, on the expression levels of GFP. Due to these studies it was clearly seen that the most efficient method for the production of large scale quantities of protein was at 30°C in XL10-Gold *E.coli* strain. The addition of specific tags resulted in a pronounced detrimental effect on protein expression. When immobilisation tags were added to the N-terminus of GFP immediately after the vectors promoter region, the levels of protein expression was significantly reduced. Therefore, these clones were deemed unsuitable for further study. The application of a single protein purification protocol to the range of tagged GFP proteins proved successful. Highly purified GFP was obtained by the silver staining method as judged by SDS-PAGE (See figures 3.2.10 to 3.2.14). The purification of GFP with an N-terminus immobilisation tag yielded low concentrations of protein due to poor expression levels. Higher molecule weight bands were visible on SDS gels for proteins which contained added cysteine residues. The optimisation of a reducing environment by the addition of DTT was successful.

3.3 Biotinylated GFP Immobilisation on NUNC MaxiSorp Plates

3.3.1. Overview

The immobilisation of the tagged model protein GFP was the major focus of this study. The majority of covalent protein immobilisation methods rely on the side chain of amino acids. The most commonly used amino acids used for this purpose are lysine and cysteine. This is due to their nucleophilic R-groups, an amine moiety in the case of the lysine amino acid and a thiol moiety in the case of cysteine. Through cloning, additional lysine and cysteine residues have been added to the termini of GFP in an effort to increase the volume of immobilised and orientated proteins (Section 3.1). GFP was used as a model protein as its inherent fluorescence provided an easy and accurate method to measure quantities of immobilised protein. The study of immobilisation surfaces is a vital process for the correct orientation and presentation of immobilised biomolecules.

Pierce chemicals supply hetero-functional biotin linking reagents, which can be used to functionalise proteins with biotin (Figure 1.14). This process relies on the reactions that occur between an NHS moiety and the ε-amine within lysine amino acids and the maleimide group with the thiol moiety within cysteines. By the addition of additional lysine and cysteine residues to the N or C-termini of proteins, it is anticipated that the proportion of correctly orientated immobilised proteins can be increased. The addition of Strep-TagII to GFP does not require any additional modification for immobilisation, as this tag is already known for its specific reaction with streptactin, a mutated form of streptavidin. Streptavidin or streptactin were immobilised on NUNC MaxiSorp 96-well Plates and used to capture biotinylated lysine and cysteine tagged GFP as well as StrepII tagged GFP.

3.3.2: Hetero-functional Biotin Linkers:

Biotin linkers were purchased from Pierce Chemicals. (www.piercenet.com) Lysine residues are common on the surface of most proteins. Therefore the biotinylation of proteins can be achieved without the addition of additional lysine residues. But the addition of a lysine tag increases the likelihood that the protein of interest will be immobilised in an orientated fashion.

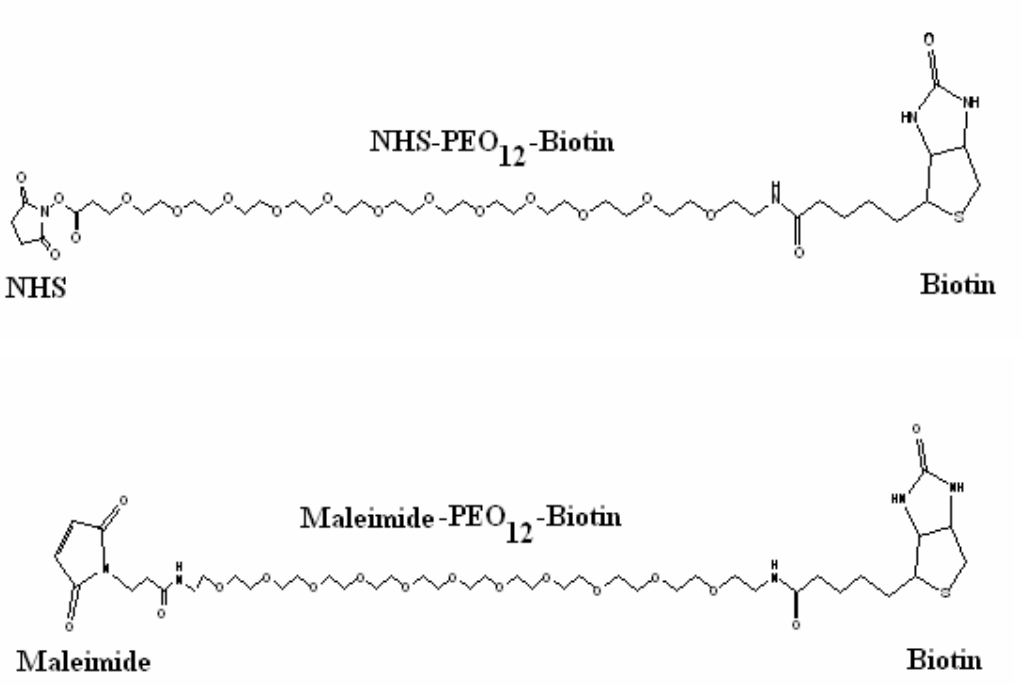

Figure 3.3.1: Hetero-functional Linkers. The NHS functionality reacts with lysine amino acids within target proteins. Maleimide functionality reacts with cysteine amino acids. Biotin functionality is used for immobilisation by its interaction with strept(avidin)/tactin. Linkers purchased from Pierce Chemicals. (**www.piercenet.com**)

Protein immobilisation protocols are often based on the thiol moiety of cysteine. Due to thiol side chain of cysteine, the amino acid is often found in pairs within the structure of proteins in its oxidised form, cystine. An exposed single cysteine residue or group of residues added by cloning methodology (Section 3.1), might allow for a more focused maleimide linker reaction, as those residues may be more sterically available. The natural fluorescence of GFP was exploited to examine the effect of adding additional lysine and cysteine residues on protein immobilisation.

3.3.3 NUNC MaxiSorp 96-well Plates

Initial studies were undertaken to determine whether white or black NUNC MaxiSorp 96-well Plates should be used for this study. White and black MaxiSorp 96-well Plates are commonly used in fluorescence protocols, as they reduce the amount of background fluorescence. Biotinylated GFP was immobilised in a 96-well plates as describe in Section 2.20. Fluorescence was read in a fluorescent plate reader.

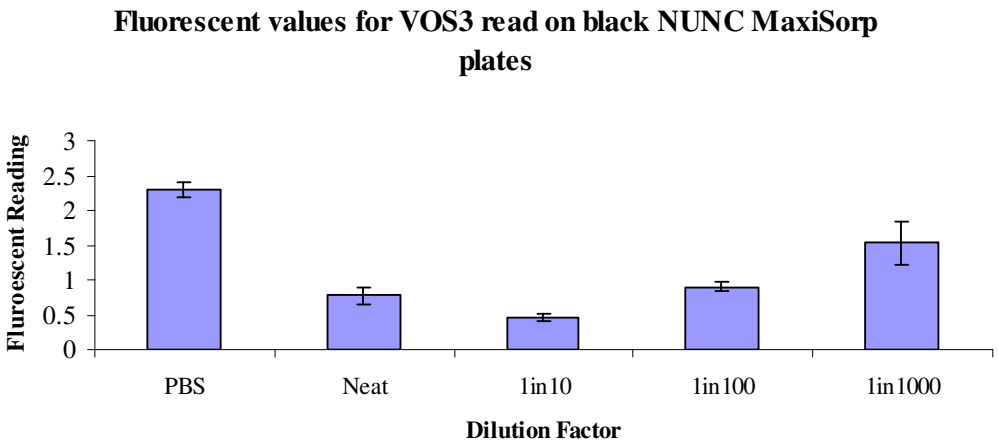

Figure 3.3.2: Fluorescence values of VOS3 (N-terminal His^6 tag, C-terminal $Lysine^6$ tag) triplicate dilutions on black NUNC MaxiSorp 96-well plates. The PBS value is shown to highlight the background fluorescence for this study. PBS negative control values have not been subtracted from protein dilutions. Samples read in triplicate at an excitation wavelength of 475nm and an emission wavelength of 509nm.

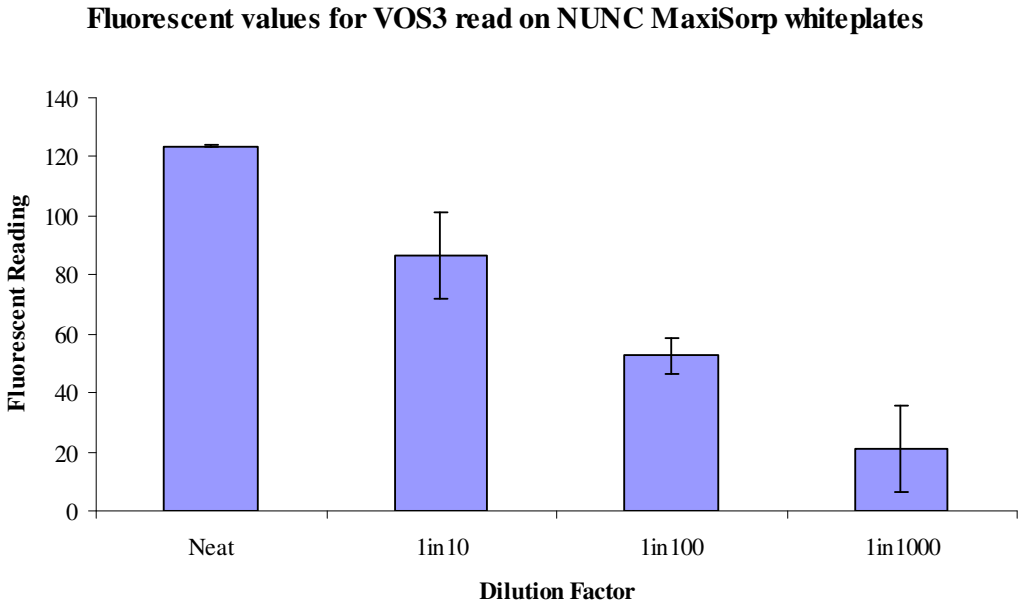

Figure 3.3.3: Fluorescent results for VOS3 (N-terminal His^6 tag, C-terminal $Lysine^6$ tag) triplicate dilutions read on NUNC Maxisorp 96-well white plates. Negative control values (PBS) have been subtracted from data. Samples read in triplicate at an excitation wavelength of 475nm and an emission wavelength of 509nm. The fluorescent readings of GFP follow the dilution curve. The scale of fluorescence readings on white plates are up to a 100 times greater than that of black plates as outlined in figure 3.3.2

From figures 3.3.2 and 3.3.3 it is apparent that white flat-bottom 96-well plates were the most reproducibly reliable immobilisation platform. Black plates from the same supplier showed large background fluorescence, which masked the fluorescent signal of the immobilised GFP. The signal achieved was over 100-fold greater for white plates when compared to 96-well plates. Therefore NUNC white MaxiSorp 96-well plates were used in all subsequent work.

3.3.4: Streptavidin and Streptactin Concentration Optimisation:

In the experiment outlined in section 3.3.3, lysine tagged GFP was immobilised directly onto the plate. In subsequent studies streptavidin or streptactin was immobilised on white MaxiSorp plates to capture biotin labelled proteins. Tagged model protein GFP was biotinylated as outlined in Section 2.21. Studies were undertaken to determine the optimum concentration of streptavidin to immobilise to achieve the optimum fluorescent signal range.

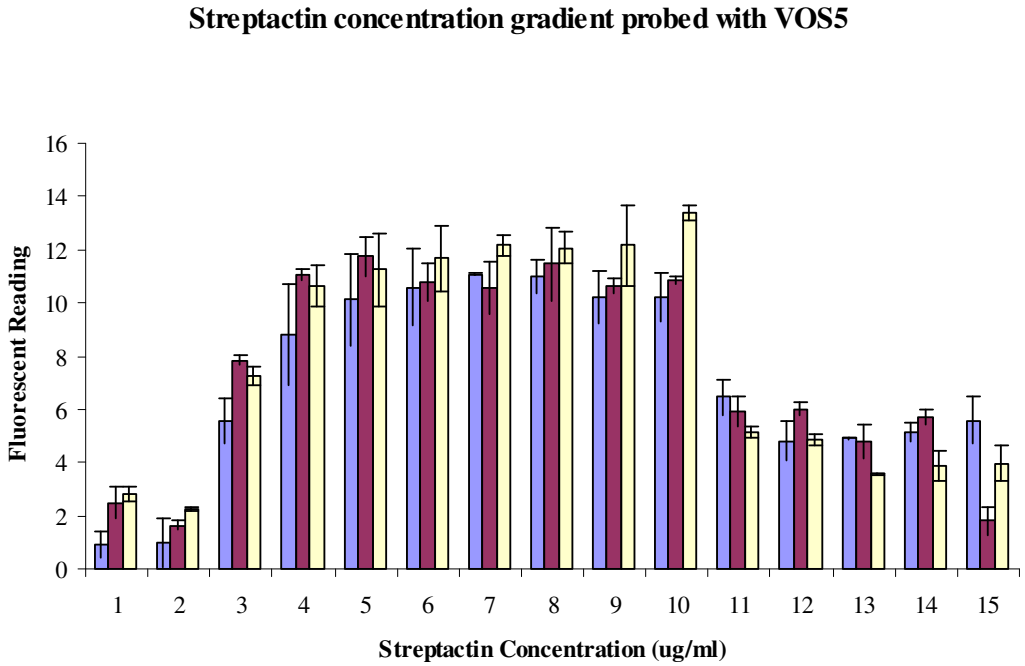

Figure 3.3.4: The effect of streptactin concentration on VOS5 (N-terminal His^6 tag, C-terminal Strep-TagII) capture. Streptactin was immobilised on white MaxiSorp plates and used to capture VOS5. Samples were read in triplicate at an excitation wavelength of 475nm and an emission wavelength of 509nm. The optimum concentration of streptactin for the most efficient capture of Stre-TagII protein was determined to be 5µl/ml.

An increasing concentration of streptavidin was immobilised on white MaxiSorp plates to determine the optimum concentration to use in subsequent experiments. Figure 3.3.4 shows that the optimum concentration of immobilised streptactin is in the range of 4µg/ml to 10µg/ml. Immobilisation time was also studied to test if this would have an effect on the amount of capture protein immobilised within the wells of the MaxiSorp 96-well Plates.

Streptavidin immobilisation times of one hour and overnight were chosen to determine if the length of immobilisation time had an effect on biotinylated protein capture. The figures 3.3.5 and 3.3.6 show that the length of time of immobilisation seems to have little to no effect on the quantity of capture protein immobilisation. All subsequent experiments were performed after strept(avidin)/tactin was immobilised for an hour at room temperature in MaxiSorp white plates. Like streptactin the optimum concentration of immobilised streptavidin was found to be 5µg/ml.

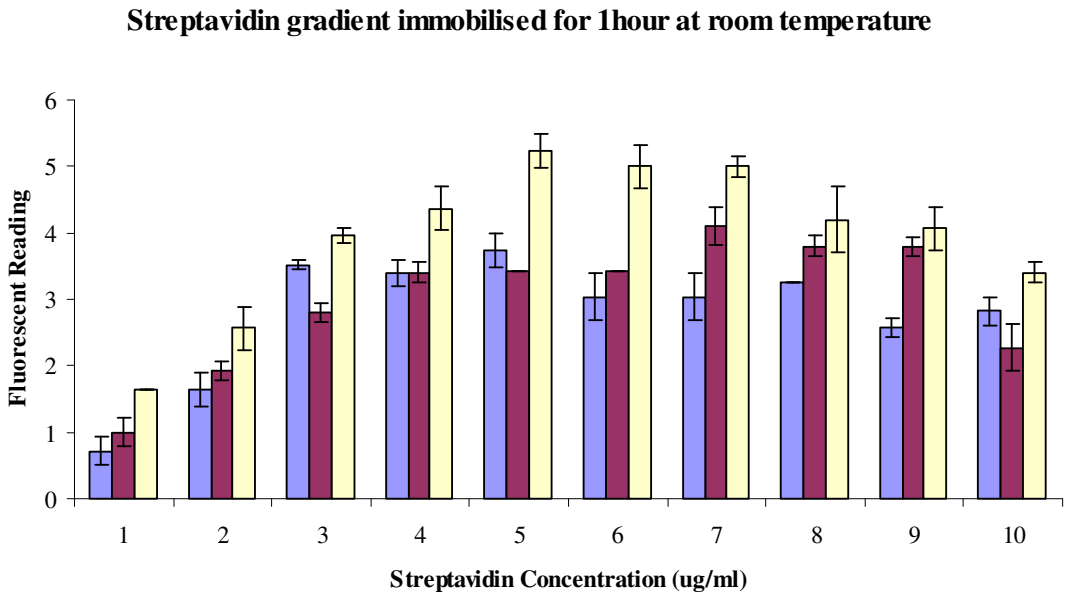

Figure 3.3.5: A concentration gradient of streptavidin immobilised on NUNC white 96-well plate for an hour at room temperature. This was probed with biotinylated VOS12 (N-terminal His^6 tag, C-terminal single cysteine residue). Samples were read in triplicate at an excitation co-efficient of 475nm and an emission co-efficient of 509nm. The optimum concentration of streptavidin immobilised was 5µg/ml.

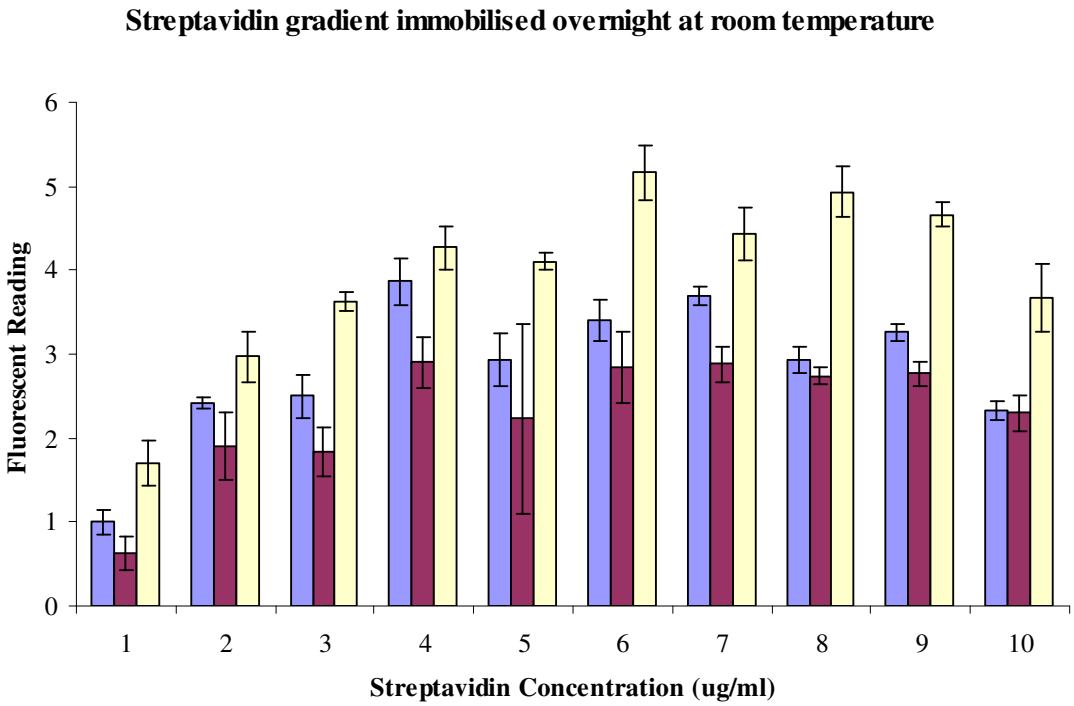

Figure 3.3.6: A concentration gradient of streptavidin immobilised on NUNC 96-well white plate overnight at room temperature. The streptavidin was probed with biotinylated VOS12 (N-terminal His6 tag, C-terminal single cysteine residue) Samples were read in triplicate at an excitation wavelength of 475nm and an emission wavelength of 509nm. The optimum concentration of streptavidin after overnight immobilisation is 6µg/ml.

3.3.5: Optimisation of Plate Reader Settings

The importance of the excitation and emission wavelengths, at which fluorescent plates are read, is considerable. These settings are an unique property of the fluorescent molecule under investigation. GFP has a well defined emission peak of 509nm but has two excitation peaks, a major peak at 395nm, and a minor peak at 475nm. Therefore, to determine the correct excitation wavelength for measurement of GFP fluorescence, a range of excitation wavelengths were chosen. Biotinylated GFP was captured by immobilised streptavidin and the fluorescence measured at each excitation wavelength. The fluorescence reader used in this experiment allows for the control of the light used to probe the samples by adjustable slit widths. The effect of slit width size on the fluorescent reading was also studied.

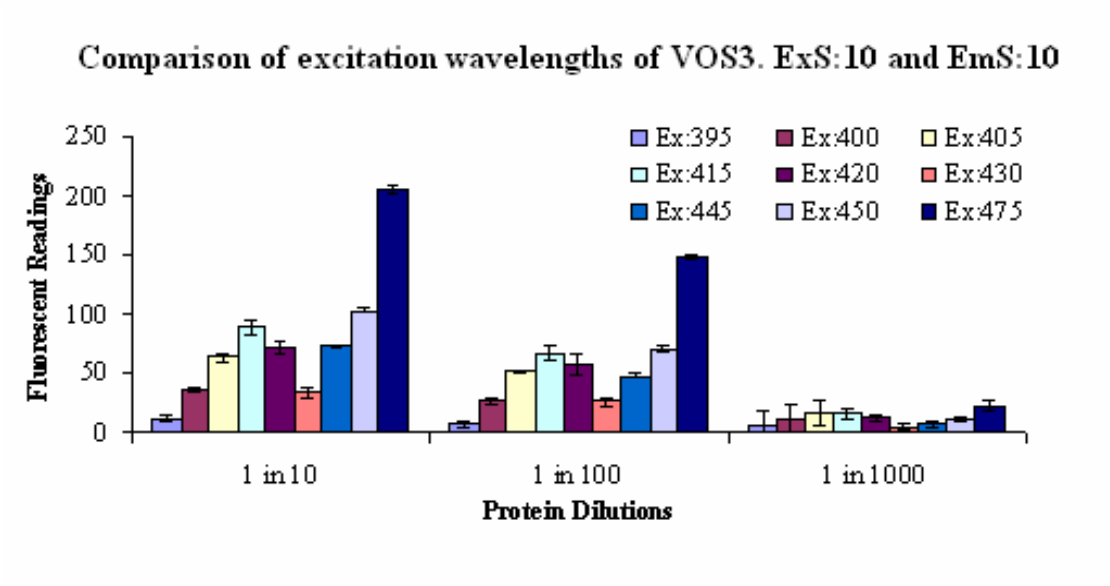

Figure 3.3.7: Comparison of excitation wavelengths with an excitation slit of 10 and emission slit of 10. 5µg/ml of streptavidin was immobilised on white MaxiSorp 96 well plates for an hour at room temperature. Biotinylated VOS3 (N-terminal His^6 tag, C-terminal $lysine^6$ tag) was captured by the immobilised streptavidin. The plate was read in triplicate at an emission wavelength of 509nm and a variable excitation wavelength. (Ex=excitation wavelength, ExS=Excitation Slit width, EmS= Emission Slit width). The 475nm excitation wavelength gave the highest level of fluorescence signal.

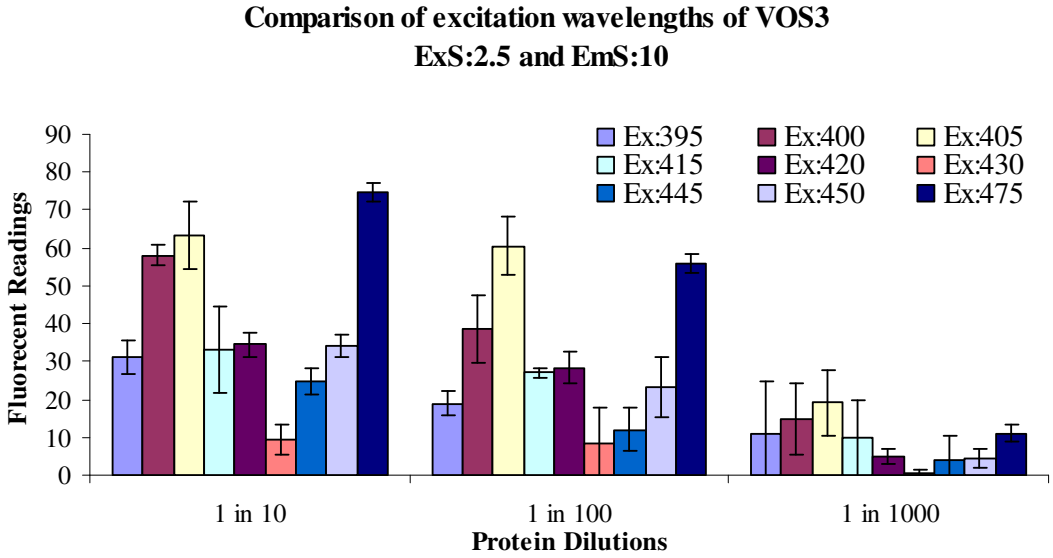

Figure 3.3.8: Comparison of excitation wavelengths with an excitation slit of 2.5 and an emission slit width of 10. 5µg/ml of streptavidin was immobilised on white MaxiSorp 96 well plates for an hour at room temperature. Biotinylated VOS3 (N-terminal His^6 tag, C-terminal $lysine^6$ tag) was captured by the immobilised streptavidin. The plate was read in triplicate at an emission wavelength of 509nm. (Ex=excitation wavelength, ExS=Excitation Slit width, EmS= Emission Slit width) For this slith width setting the 475nm excitation wavelength gave the highest fluorescent signal.

Figures 3.3.7 and 3.3.8 indicate that the most efficient excitation wavelength for the study of the efficiency of protein immobilisation was 475nm. This excitation wavelength was used in all subsequent protocols. An emission wavelength of 509nm was used in all studies. It was apparent that the excitation slit width had a major effect on sensitivity. The larger excitation slit width was found to have at least a two-fold increase in signal, across a wide range of excitation wavelengths. Unfortunately, it was found that reading certain fluorescent proteins at excitation wavelength of 475nm and slit width of 10, led to samples being off-scale. To remedy this all subsequent work was undertaken with a excitation slit width of 2.5 and emission slit width of 10. The emission wavelength was 475nm and an excitation wavelength of 509nm.

3.3.6: Immobilisation of biotinylated GFP by Streptactin

Tagged GFP	**Maleimide-Biotin tagged clone**	**NHS-Biotin tagged clone**
VOS2	VOS2ML	VOS2NL
VOS3	N/A	VOS3NL
VOS4	VOS4ML	N/A
VOS5	N/A	N/A
VOS12	VOS12ML	N/A

Table 3.3.1: Outline of biotinylated GFP proteins. Cysteine tagged GFP's (VOS4 and VOS12) were biotinylated with maleimide-biotin linker. Lysine tagged GFP (VOS3) was biotinylated with NHS-biotin linker. VOS2 was used as a control protein and was biotinylated with both the maleimide and NHS linker

A section of biotinylated tagged GFPs were constructed (Section 2.21) and outlined in table 3.3.1. This set of tagged proteins was then captured on streptactin immobilised in the wells of 96 well plates. Five GFP proteins were chosen as a sample range to study

protein immobilisation. VOS2 was a control wild type GFP protein as it features only a histidine purification tag. VOS2 was tagged with both biotin linkers, to show baseline biotinylation levels. VOS3 (N-terminal His^6 tag, C-terminal $lysine^6$ tag) was tagged by the NHS-biotin linker. Similarly VOS4 (N-terminal His^6 tag and C-terminal $Cysteine^6$ tag) and VOS12 (N-terminal His^6 tag, C-terminal single cysteine residue) were biotinylated using the Maleimide-Biotin linker. Finally VOS5 was tagged with Strep-tagII, which is recognised by streptactin. Biotinylated GFP was immobilised as outlined in Section 2.20

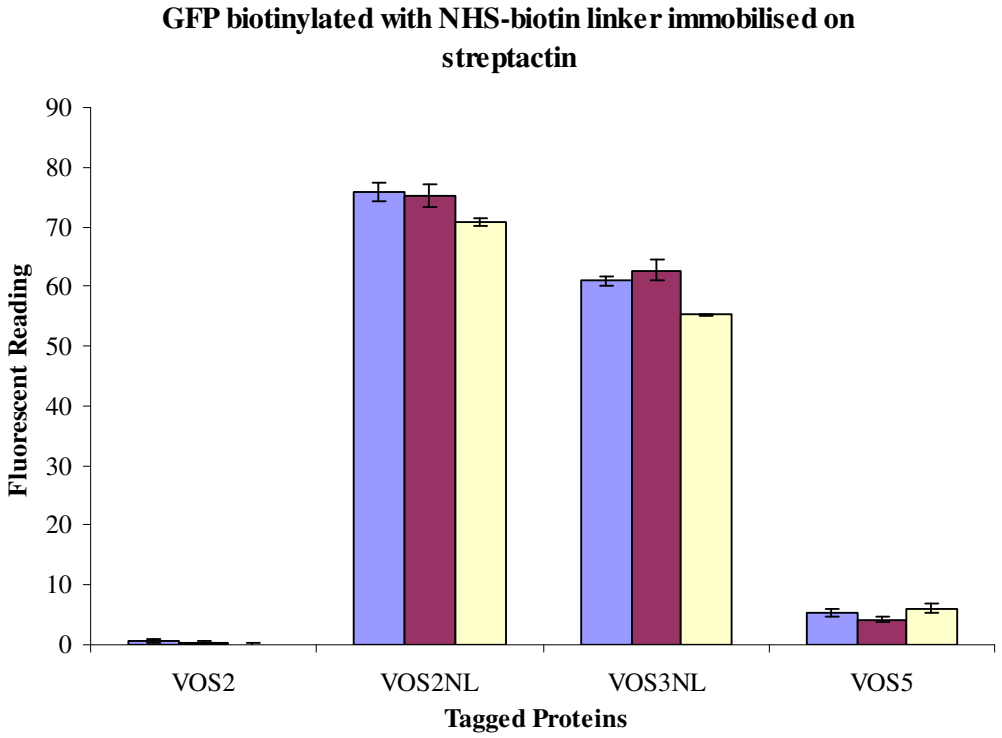

Figure 3.3.9: NHS-Biotin and Strep-tagII tagged GFP proteins captured by streptactin. 50µg/ml of each biotinylated GFP proteins, VOS2 (N-terminal His^6 tag, no biotinylation), VOS2NL (N-terminal His^6 tag, biotinylated by NHS-biotin linker), VOS3NL (N-terminal His^6 tag, C-terminal $Lysine^6$ tag, biotinylated by NHS-biotin linker) and VOS5 (N-terminal His^6 tag, C-terminal Strep-TagII) were captured by 5µg/ml immobilised streptactin. Fluorescence was read in triplicate on a white MaxiSorp 96-well plate at an excitation wavelength of 475nm and an emission wavelength of 509nm.

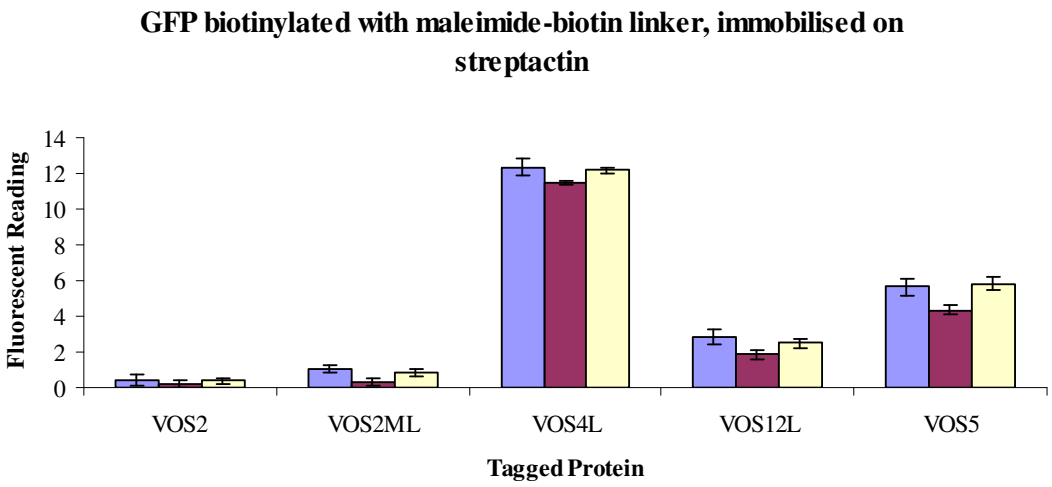

Figure 3.3.10: Maleimide-Biotin linked cysteine tagged GFP clones, captured by streptactin. 50ug/ml of biotinylated GFP, VOS2 (N-terminal His6 tag, not biotinylated), VOS2ML (N-terminal His6 tag, biotinylated with maleimide-biotin linker), VOS4 (N-terminal His6 tag, C-terminal cysteine6 tag, biotinylated with maleimide-biotin linker), VOS12L (N-terminal His6 tag, C-terminal single cysteine residue, biotinylated with maleimide-biotin linker), VOS5 (N-terminal His6 tag, C-terminal Strep-TagII) were captured on 5µg/ml of immobilised streptactin. Fluorescence was measured in triplicate in a NUNC MaxiSorp white plate at an excitation wavelength of 475nm and an emission wavelength of 509nm.

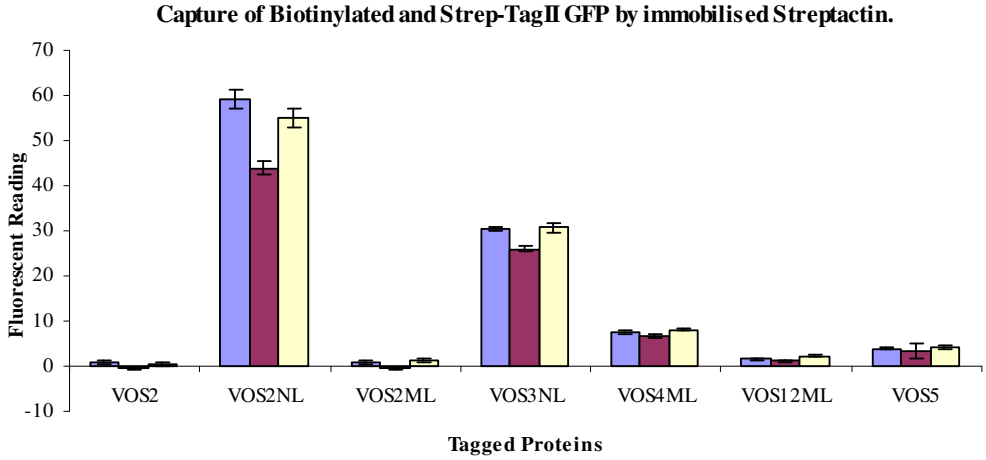

Figure 3.3.11: Comparison of NHS and Maleimide biotinylation tagging with Strep-TagII immobilisation on NUNC MaxiSorp white plates. 50ug/ml of biotinylated GFP proteins, VOS2 (N-terminal His^6 tag, no biotinylation), VOS2NL (N-terminal His^6 tag, biotinylated by NHS-biotin linker), VOS2ML (N-terminal His6 tag, biotinylated with maleimide-biotin linker), VOS3NL (N-terminal His^6 tag, C-terminal $Lysine^6$ tag, biotinylated by NHS-biotin linker), VOS4ML (N-terminal His6 tag, C-terminal cysteine6 tag, biotinylated with maleimide-biotin linker), VOS12ML (N-terminal His6 tag, C-terminal single cysteine residue, biotinylated with maleimide-biotin linker) and VOS5 (N-terminal His^6 tag, C-terminal Strep-TagII) were captured by 5µg/ml immobilised streptactin and read in triplicate at excitation wavelength of 475nm and emission wavelength of 509nm.

Figures 3.3.9 to 3.3.11 outline the effect of biotinylation reactions on the quantity of GFP immobilisation. The unbiotinylated wild type control VOS2 (N-terminal His^6 tag) shows the least amount of fluorescence as would be expected. Surprisingly the highest fluorescent value achieved for all biotinylated clones was the NHS biotinylated VOS2 (N-terminal His^6 tag), which has no additional lysine tags. This was compared to the hexa-lysine tagged GFP clone (VOS3) (Figure 3.3.10). The lysine tagged GFP protein exhibited half the fluorescence of the wild type GFP in figure 3.3.11. The maleimide biotinylated wild type GFP, VOS2ML exhibited low immobilisation since unlike the NHS linker, the reactive residues are buried within the tertiary structure of the protein. The biotinylation of the other cysteine tagged GFPs with the maleimide linker were more successful. VOS4 (N-terminal His^6 tag and C-terminal $Cysteine^6$ tag) and VOS12 (N-terminal His^6 tag and C-terminal single cysteine residues) exhibited a ten times larger fluorescence reading than the biotinylated and non-biotinylated wild type (Figure 3.3.10) The addition of six extra cysteine residues was more efficient than the addition of a single cysteine residue. VOS4 (N-terminal His^6 tag and C-terminal $Cysteine^6$ tag) exhibited four times more fluorescence than VOS12 (N-terminal His^6 tag and C-terminal single cysteine residues). It is possible that the VOS12 immobilisation was more orientated as there was only one cysteine residue available for biotinylation by the maleimide-biotin linker.

Despite streptactin being developed as a highly efficient capture molecule for Strep-TagII, the fluorescence values of VOS5 (N-terminal His^6 tag and C-terminal Strep-TagII) were lower than the values for biotinylated VOS3 or VOS4. The fluorescence value of immobilised VOS5 was half the value of immobilised biotinylated VOS4ML, but twice the fluorescence of VOS12, which had only a single cysteine residue available for biotinylation (Figure 3.3.10). The fluorescence of wild type and lysine tagged biotinylated GFP was seven times greater than VOS5 (Figure 3.3.9). The immobilisation of VOS5 can be considered to be more orientated, as the Strep-TagII is not inherent to the protein unlike lysine. Therefore, streptactin binds specifically in an orientated manner to the GFP.

The next set of immobilisations were performed using streptavidin as the capture protein for biotinylated GFP. The same bank of biotinylated proteins were used as the probe molecules, outlined in section 3.3.7. and captured as outlined in Section 2.20.

3.3.7: Immobilisation of biotinylated GFP on Streptavidin

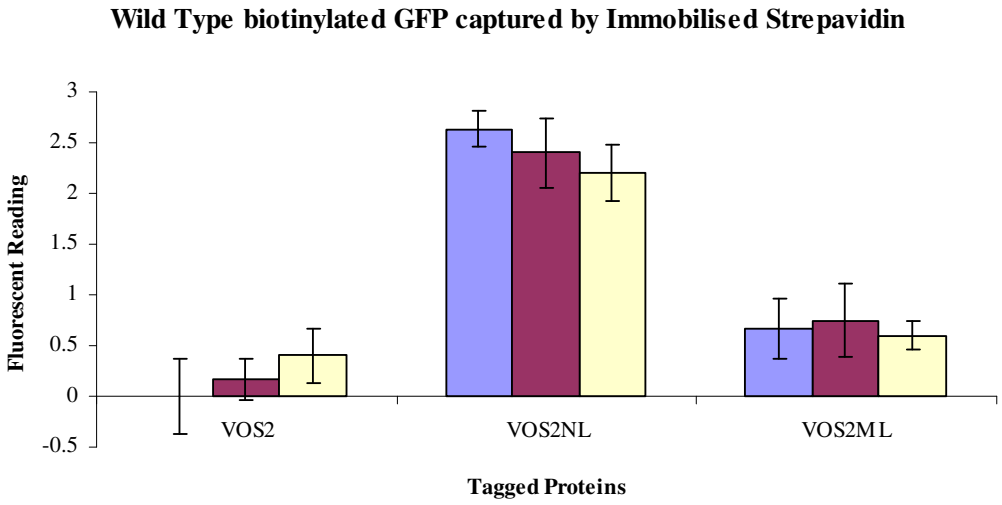

Figure 3.3.12: Immobilisation of wild type biotinylated GFP with NHS-biotin linker, VOS2 (N-terminal His^6 tag, Not biotinylated), VOS2NL (N-terminal His^6 tag) and maleimide-biotin linker, VOS2ML, (N-terminal His^6 tag) linkers. 50ug/ml of GFP was captured by 5µg/ml immobilised streptavidin. The white MaxiSorp 96-well plate was read in triplicate at an excitation wavelength of 475nm and an emission wavelength of 509nm.

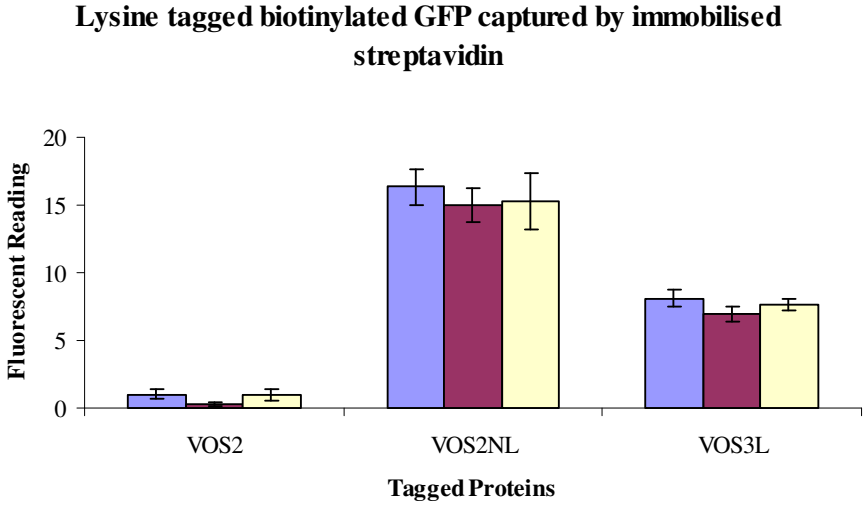

Figure 3.3.13: Triplicate readings of lysine tagged GFP, biotinylated with NHS-biotin linker, VOS2 (N-terminal His^6 tag, Not biotinylated), VOS2NL (N-terminal His^6 tag, biotinylated with NHS-biotin linker) and VOS3L, (N-terminal His^6 tag, C-terminal $lysine^6$ tag, biotinylated with NHS-biotin linker) linkers. 50ug/ml of GFP was captured by 5µg/ml immobilised streptavidin. The white MaxiSorp 96-well plate was read in triplicate at an excitation wavelength of 475nm and an emission wavelength of 509nm. The immobilisation of lysine tagged biotinylated GFP shows half the fluorescence value of the wild type biotinylated GFP values.

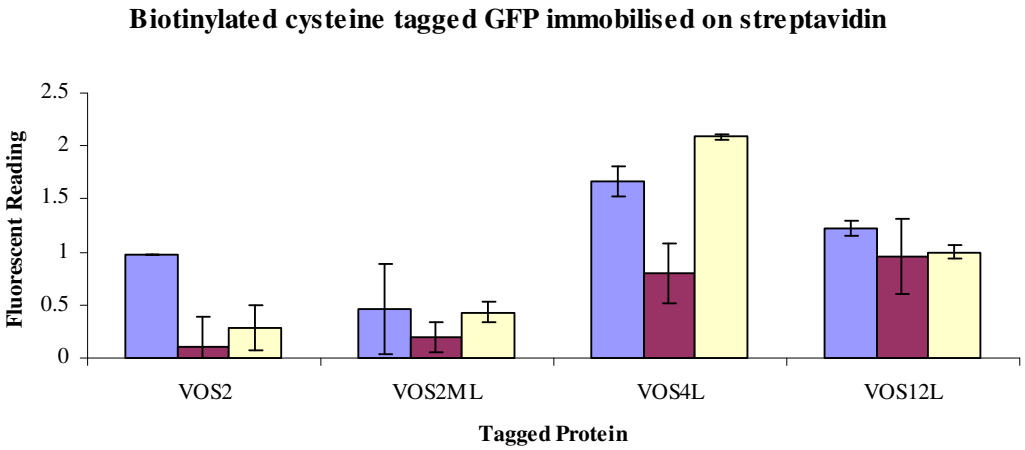

Figure 3.3.14: Triplicate readings of biotinylated cysteine tagged GFP. 50ug/ml of each biotinylated GFP, VOS2 (N-terminal His^6 tag, Not biotinylated), VOS2ML, (N-terminal His^6 tag, biotinylated by the maleimide-biotin linker), VOS4ML (N-terminal His6 tag, C-terminal cysteine6 tag, biotinylated with maleimide-biotin linker), VOS12ML (N-terminal His6 tag, C-terminal single cysteine residue, biotinylated with maleimide-biotin linker) were captured by 5µg/ml of immobilised streptavidin. The NUNC MaxiSorp white 96-well plate was read in triplicate at an excitation wavelength of 475nm and an emission wavelength of 509nm.

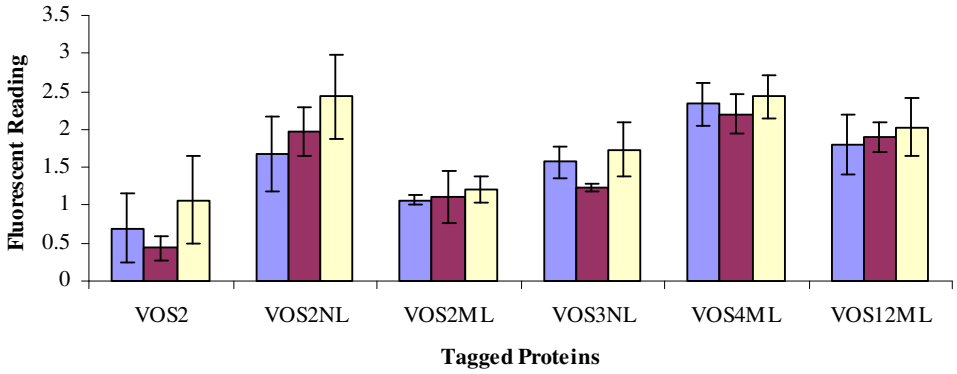

Figure 3.3.15: Cysteine and lysine tagged GFPs, biotinylated with Maleimide and NHS-biotin linkers. 50µg/ml of each biotinylated GFP; VOS2 (N-terminal His^6 tag, no biotinylation), VOS2NL (N-terminal His^6 tag, biotinylated by NHS-biotin linker), VOS2ML (N-terminal His6 tag, biotinylated with maleimide-biotin linker), VOS3NL (N-terminal His^6 tag, C-terminal $Lysine^6$ tag, biotinylated by NHS-biotin linker), VOS4ML (N-terminal His6 tag, C-terminal cysteine6 tag, biotinylated with maleimide-biotin linker), VOS12ML (N-terminal His6 tag, C-terminal single cysteine residue, biotinylated with maleimide-biotin linker) were captured by 5µg/ml immobilised streptavidin. The NUNC MaxiSorp white 96-well plate was read in triplicate at an excitation wavelength of 475nm and an emission wavelength of 509nm.

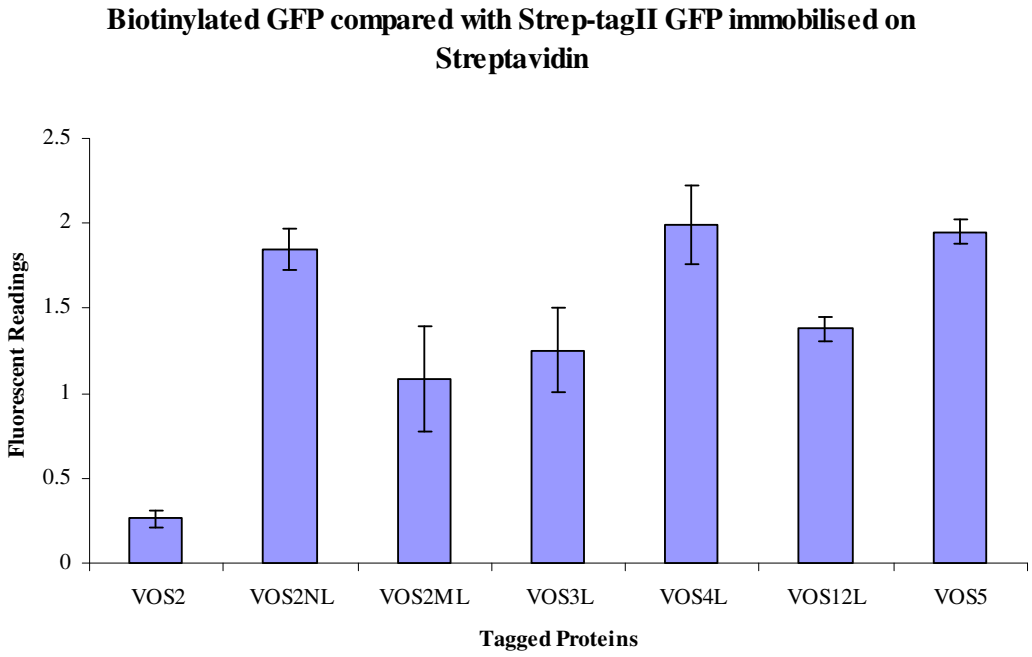

Figure 3.3.16: Combined triplicates of biotinylated immobilised GFP and Strep-TagII GFP. 50ug/ml of biotinylated GFPs; VOS2 (N-terminal His^6 tag), VOS2NL (N-terminal His^6 tag, biotinylated with NHS-biotin linker), VOS2ML (N-terminal His^6 tag, biotinylated with Maleimide-biotin linker), VOS3L (N-terminal His^6 tag, C-terminal $Lysine^6$ tag, biotinylated with NHS-biotin linker), VOS4L (N-terminal His^6 tag, C-terminal $Cysteine^6$ tag, biotinylated with Maleimide-biotin linker), VOS12L (N-terminal His^6 tag, C-terminal single cysteine residue, biotinylated with Maleimide-biotin linker), VOS5 (N-terminal His^6 tag, C-terminal Strep-TagII). were captured by 5µg/ml immobilised streptavidin. NUNC MaxiSorp white 96-well plates were read in triplicate at excitation wavelength 475nm and emission wavelength 509nm.

Figures 3.3.12 to 3.3.16 outline the immobilisation of biotinylated GFPs captured by immobilised streptavidin on white MaxiSorp 96-well Plates. It was noted that the rate of immobilisation of biotinylated proteins on to streptactin was up to five times greater than the immobilisation on streptavidin. The immobilisation of the un-biotinylated VOS2 control showed the smallest amount of fluorescence. The biotinylated wild type protein which was biotinylated via maleimide-biotin linker showed the next highest fluorescence. As with streptactin immobilisation the rate of immobilisation of the wild type biotinylated GFP (VOS2NL) is double than that of the lysine tagged GFP (VOS3NL). The highest level of immobilisation was found with the cysteine tagged GFP (VOS4L) which was biotin linked via the maleimide-biotin linker. This was followed by the Strep-TagII GFP protein. It is important to note that the rate of immobilisation via the biotinylated single cysteine residue tag immobilisation shows a

higher level of fluorescence than the biotinylated wild type protein. This indicates that the addition of the single cysteine residue acts as a single point for biotinylation with a maleimide linker resulting in a higher level of immobilisation. This single cysteine residue is not available in wild type protein. The immobilisation of the biotinylated C-terminal cysteine tagged protein (GFP4L) exhibits the highest fluorescence via capture with streptavidin.

3.3.8 Summary

The capture of biotinylated GFP via immobilised streptavidin and streptactin in 96 well plates proved successful. The immobilisation of biotinylated proteins on streptactin was ten times more efficient than immobilisation on streptavidin. When biotinylated GFP was immobilised on streptactin, the wild type NHS-biotinylated VOS2 demonstrated the highest level of immobilisation. The NHS-biotinylated lysine tagged GFP (VOS3) exhibited half the level of this wild type immobilisation. The level of protein fluorescence of lysine tagged biotinylated GFP is ten times greater than when compared to the fluorescence of cysteine tagged biotinylated GFP. This can be explained by the greater number of lysine residues in GFP available for biotinylation by the NHS-biotin linker. The addition of extra lysine residues for NHS biotinylation protocols, did not increase immobilisation levels on 96-well plates, as can be seen by the levels of immobilisation between the wild type biotinylated GFP (VOS2) and lysine tagged biotinylated GFP (VOS3). Streptactin captures double the amount of wild type biotinylated GFP than lysine tagged biotinylated GFP.

The capture of maleimide-biotin linked cysteine tagged proteins by streptavidin or streptactin also proved successful. The tagging of the model protein GFP with six cysteine residues (VOS4) increased the level of immobilisation by up to six times compared to the wild type biotinylated GFP (VOS2) (Figure 3.3.10). The tagging of GFP with a single cysteine residue (VOS12) doubled the level of immobilisation over the biotinylated wild type (VOS2). The scale of this protein immobilisation (VOS12) was six times less than the hexa-cysteine model protein (VOS4), indicating a distinct advantage of adding six cysteine residues to the GFP.

The immobilisation of these tagged model proteins was next investigated on a unique immobilisation platform. The use of monolithic columns for protein immobilisation has only recently been reported (Logan *et al.*, 2007). Section 3.4 outlines the initial work performed to immobilise GFP on to monolithic columns.

3.4: Orientation specific immobilisation of the model protein GFP within monolithic columns

3.4.1: Overview

The use of monolithic columns for the immobilisation of proteins is a relatively recent development in protein technology (Rangan Mallik, 2006). The Vinyl-azlactone immobilisation method is one of the most commonly used and is summarised in figure 1.11. and first described by Tripp *et al.* in 2000. The method for creating, functionalising and immobilising proteins within monolithic columns is outlined in detail in Section 2.23. A schematic simplified outline of this process is shown in Figure 3.4.1.

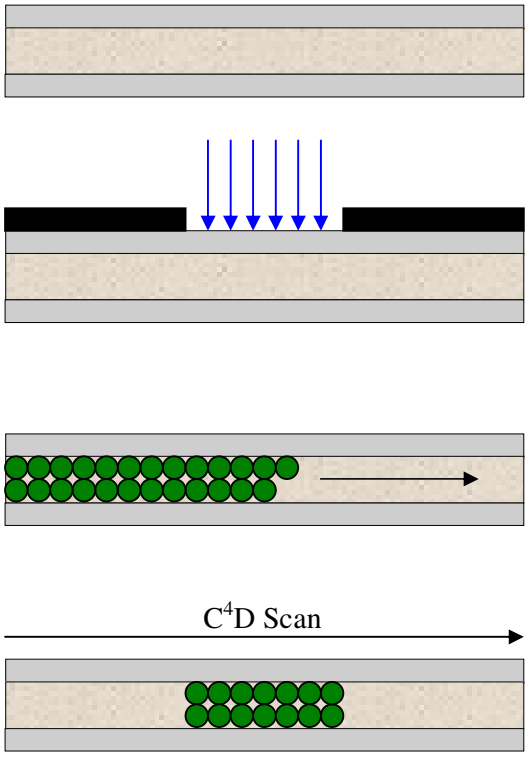

Step I: The creation of a hydrophilic monolith to reduce protein surface interactions by the immobilisation of PEGMA by UV methods. (Sections 2.23.1, 2.23.1, 2.23.3 and 2.23.4)

Step II: The monolith was filled with vinyl-azlactone. Sleeves were placed on the column to generate an 'immobilisation window' and irradiated with UV light, creating a zone of immobilised vinyl-azlactone. (Section 2.23.5)

Step III: Protein was passed over the column. This was followed by a wash of ethanolamine to block any un-reacted vinyl-azlactone functionalities. (Section 2.23.6)

Step IV: Following an overnight wash with biological buffer a conductivity scan using a C^4D detector was performed. (Section 2.23.6)

Figure 3.4.1: A summary of the protocol for the creation, immobilisation and conductivity reading of proteins within monolithic columns.

The capture of proteins by zones of reactive vinyl-azlactone relies on the reaction outlined in Figure 1.11. The amine reactive moiety, on which this reaction is dependent, is present at the N-terminus of all proteins. Additionally amine moieties are present in the R-group of lysine amino acids. By incorporating extra lysine amine acids residues

in the form of a protein tag it was theorised that the levels of protein immobilisation could be increased. By placing this tag at the N or C-terminus it was also predicted that the immobilisation of proteins could be more orientation specific.

The immobilisation of proteins on monolithic columns can be characterised by a number of benefits. The generation of reactive zones within teflon coated silica monolith columns is based on UV functionalisation. This allows for the generation of specific controllable areas of immobilised protein within the monolith. Secondly the size of monolithic columns facilitates the use of contactless conductivity detection for the study of protein immobilisation and interactions within the columns. The conductivity of the interior was detected and recorded by moving the conductivity detector millimetre by millimetre along the length monolith. Monolith size is beneficial, as the sample size required for efficient detection is reduced significantly.

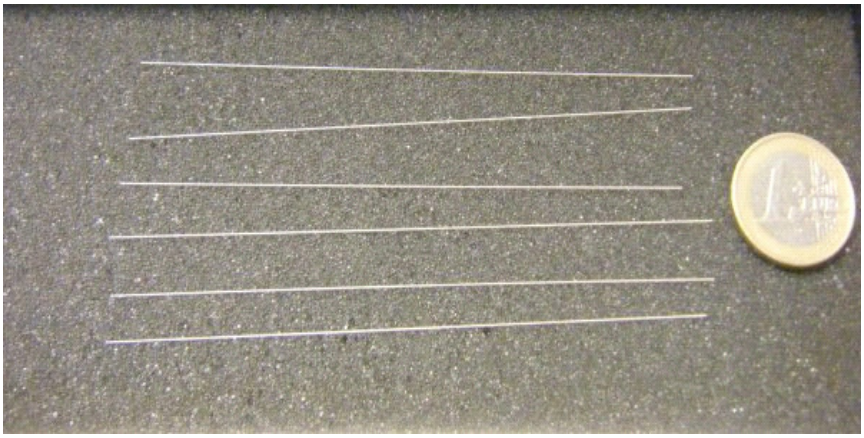

Figure 3.4.2: Six monolithic capillary columns prepared as outlined in Section 2.23. Monoliths were prepared from ethylene glycol dimethacrylate and butyl methacrylate reactive monomers.

3.4.2: Achieving a standard baseline

Initial attempts to immobilise the model protein GFP onto monolithic columns were hindered by the inability to produce an acceptable baseline conductivity reading. The immobilisation of vinyl-azlactone within monolithic columns as outlined in section 2.23.5 requires the washing of the monolithic column with methanol and water. Any contaminating amino acids present in these washes will react with the zones of immobilised vinyl-azlactone. The conductivity scan of a monolithic column in figure 3.4.3 shows two zones of contaminated immobilised vinyl-azlactone.

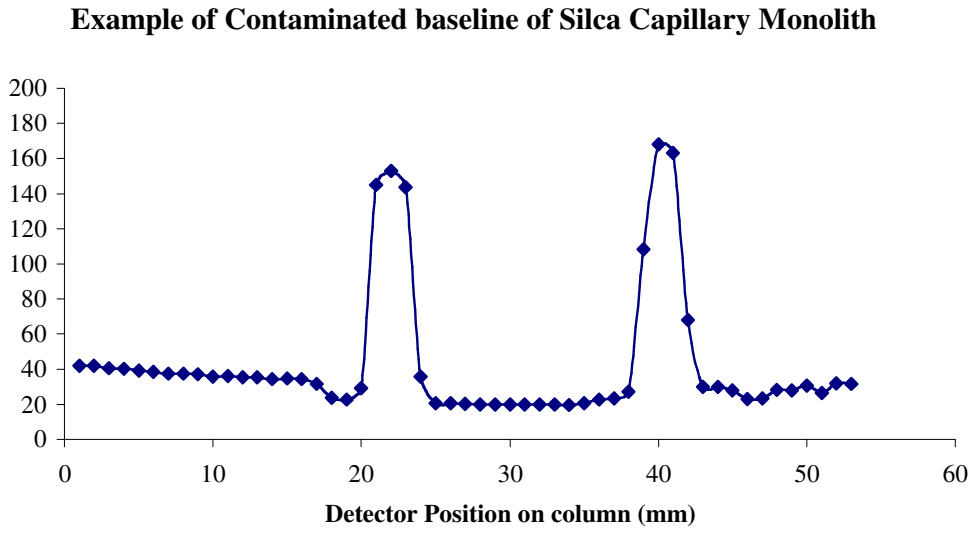

Figure 3.4.3: An example of a contaminated monolith baseline. When a monolith is being functionalised with vinyl-azlactone (Section 2.23.5), successive washes with methanol, water are required. If these washes are contaminated with proteins, peptides or amino acids, these contaminates will be captured by vinyl-azlactone as can be seen by an increase in the conductivity values for the two reactive zones.

Initial experiments undertaken to immobilise the tagged model protein GFP on monolithic columns included the optimisation of the vinyl azlactone functionalisation step to reduce this type of contamination. This included use of ultra-pure filter sterilised water, the thorough washing of the Knauer Wellchrom K-120 pump with methanol to ensure the removal of any non-specific proteins and the sealing of the buffer reservoir to reduce external containments. These experiments proved successful and an efficient protocol for the creation of functionalised monolithic columns was established.

3.4.3: The effect of protein tagging on immobilisation within monolithic columns

As described in previous sections of this chapter (Chapter 3) the model protein GFP has been tagged with additional lysine residues in an effort to increase the quantity of correctly orientated immobilised protein on a range of surfaces including monoliths. For the immobilisation of GFP on monolithic columns, a steady and uncontaminated baseline was required as outlined in section 3.4.2. The conductivity baselines of all monolithic columns were measured after the functionalisation of two distinct zones of the monolithic column with vinyl azlactone. These baseline scans were performed with ultra-pure water flowing through the monolithic column and is outlined in figure 3.4.4.

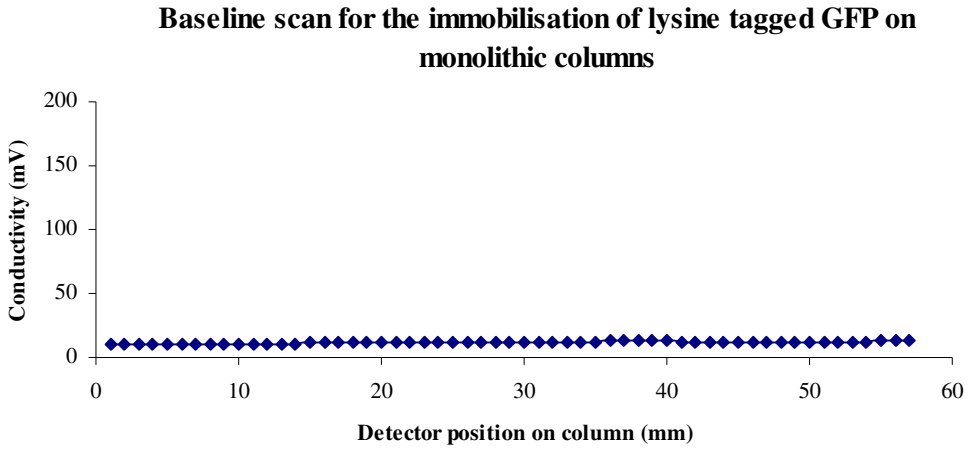

Figure 3.4.4: The initial conductivity scan of a monolithic column for the immobilisation of a lysine tagged model protein GFP. The monolith has been functionalised in two discrete zones by the photografting immobilisation of vinyl-azlactone. The baseline was achieved by moving the detector millimetre by millimetre and recording the conductivity, with water flowing through the column.

To determine the effect of the addition of a lysine tag to the immobilisation of a model protein, an untagged GFP protein was first immobilised on the monolithic column (see figure 3.4.5).

1mg/ml of the untagged GFP (VOS2-Xa) in ultra-pure water was passed over the column at 1µl/min for three hours. After the blocking of un-reacted vinyl-azlactone moieties with 1M ethanolamine the column was washed overnight with water. The conductivity scan of the monolithic column was then performed. Figure 3.4.5 shows the increase in the conductivity (compared to the baseline) of the two zones of immobilised protein. Protein immobilisation was cross-validated by placing the monolithic column on a Blue Light Transilluminator Dark Reader (Clare Chemical). This Transilluminator dark reader produces blue light, which excites the fluorophore of immobilised GFP causing it to fluoresce.

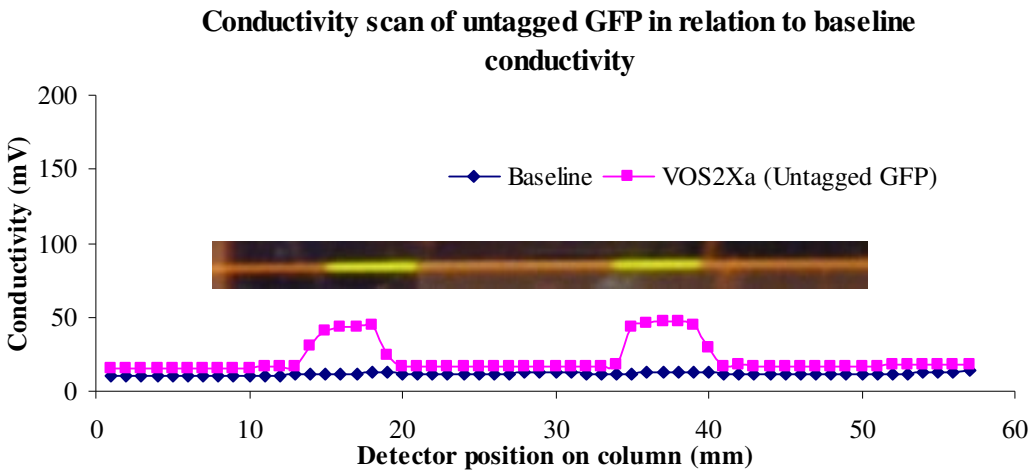

Figure 3.4.5: The conductivity scan of immobilised untagged GFP on monolithic columns. Two zones of the monolithic column were functionalised with vinyl-azlactone. 1mg/ml of untagged GFP was immobilised by reaction with vinyl-azlactone and the conductivity measured. The two zones of increased conductivity show the immobilisation of untagged GFP. This immobilisation was confirmed by visualisation of immobilised GFP using the Blue Light Transilluminator Dark Reader (Clare Chemical)

The zones of fluorescence coincided with the change in conductivity. The cross validation of conductivity and fluorescence methods clearly outline the immobilisation of untagged GFP by reaction with vinyl-azlactone.

To determine the effect of adding lysine residues to GFP, the conductivity of immobilised lysine tagged GFP within a monolithic column was studied. A second monolithic column was produced under identical conditions and at the same time as the monolith used in figure 3.4.5 (Section 2.23.2) and therefore should have identical pore sizes and distribution. This can be assumed because the formation of monolithic structures is based on the concentration of porogen and cross-linking agent within the reaction (see Section 1.4.2). Lysine tagged GFP (VOS3-Xa) was then immobilised as previously outlined for untagged GFP (VOS2-Xa) on this monolith.

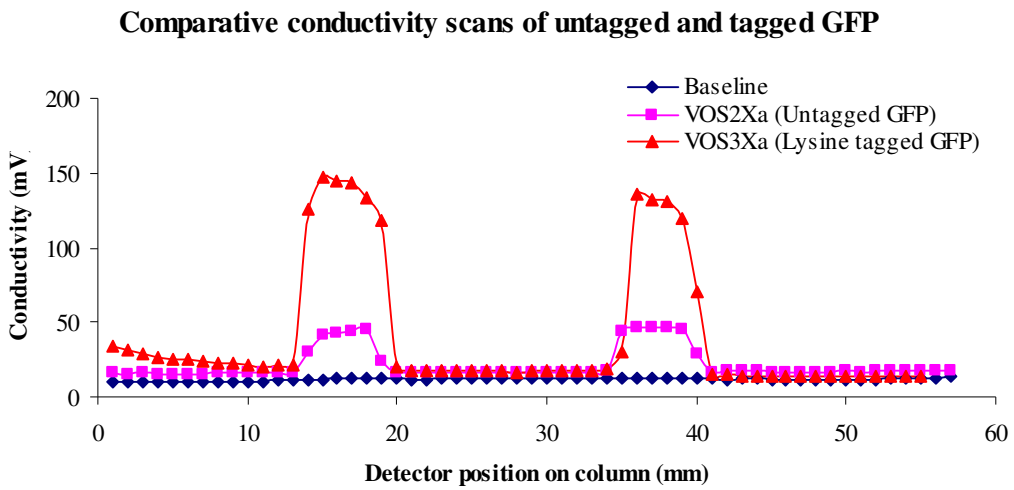

Figure 3.4.6: The comparative conductivity scans of tagged (VOS3Xa) and untagged (VOS2Xa) GFP. These conductivity scans were performed with ultra-pure H_2O flowing through the monolithic column at 1µl/min. The addition of six additional lysine residues to GFP increased the conductivity scan of the protein by almost three times.

Figure 3.4.6 clearly demonstrates the effect of the addition of lysine amino acid residues to protein immobilisation within monolithic columns. The conductivity readings of lysine tagged GFP compared to the untagged GFP, increased by roughly three fold. To determine the increase in the conductivity caused by the additional lysine residues the Peak Explorer program (http://www.soft32.com/download_187555.html) was used. The Peak Explorer program was used to calculate the peak area of tagged and untagged proteins across a range of different unique monolithic columns. This enables the determination of the scale of change in conductivity and therefore immobilisation of proteins on different monolithic columns.

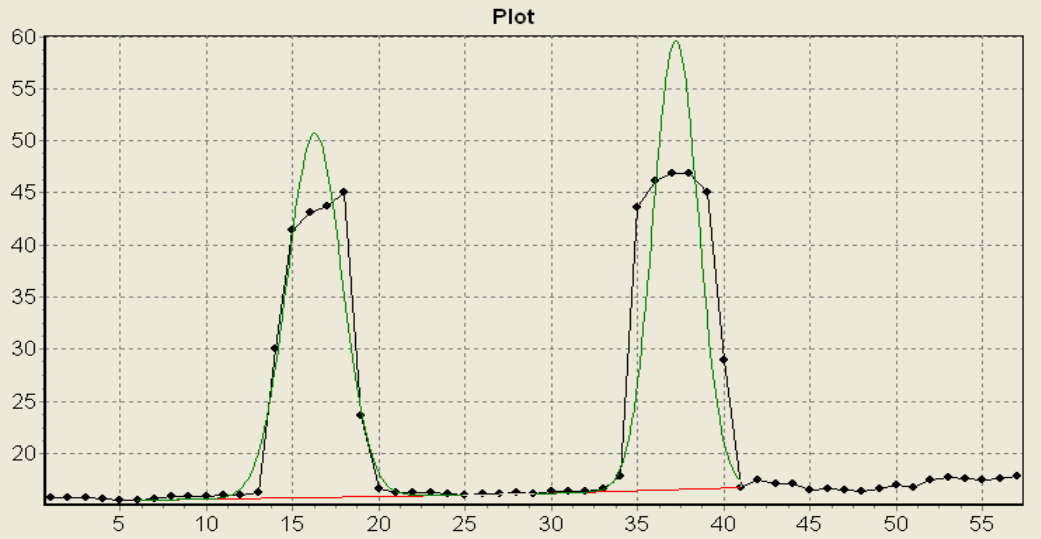

Figure 3.4.7: A representative screen capture from the Peak Explorer column. This program calculates the average area of the conductivity peaks of immobilised, tagged and untagged proteins. This allowed the comparison of the levels of immobilised proteins across different monolithic columns.

The change in the conductivity of monolithic columns can be directly related to the degree of immobilisation. By using Peak Explorer the scale of immobilisation can be compared across two zones on a single monolithic column or zones across multiple columns. The addition of six extra lysine residues increased the scale of immobilisation by over 400% for the first functionalised vinyl-azlactone zone as outlined in table 3.4.1. The increase in the scale of immobilisation in the second functionalised zone was over 200%. This difference in the percentage increase between the two zones was noted and may be explained by the first zone becoming fully saturated before the second zone.

	Area of Immobilised Protein Zone 1 (mm2)	Area of Immobilised Protein Zone 2 (mm)
VOS2-Xa	136 %	160 %
VOS3-Xa	706 %	537 %
Percentage Difference	419 %	234 %

Table 3.4.3: Percentage change in the peak areas generated by the immobilisation of tagged and un-tagged GFP within monolithic columns by vinyl-azlactone.

3.4.4: Use of Biological Buffers as stable mobile phases

Water does not provide a suitable environment for protein storage or use. This is primarily due to the many hydrophobic amino acids in proteins which may cause proteins to be denatured in such environments (Pace *et al.*, 2004). Initial studies of protein immobilisation within monolithic columns used water as a mobile phase. It was fortunate that the protein being immobilised, GFP is relatively stable in aqueous environments. These initial immobilisation protocols were used unchanged from protocols developed to capture amino acids and chemical moieties within monoliths (Connolly *et al.*, 2007).

For future experiments which involve attempting to measure protein interactions by conductivity it was important to discover a biological buffer which possessed a low level of background conductivity. A buffer with a large conductivity value may mask a change in the conductivity reading when a protein immobilisation event occurs. A range of common biological buffers were passed over a monolithic column and a conductivity scan performed to determine the buffer with the lowest background conductivity. Figure 3.4.8 demonstrates that the most commonly used biological buffers exhibit high conductivity values. The buffer which provided the lowest background conductivity scan proved to be the zwitterionic Good's buffer HEPES pH7.4. This buffer was used in all future protein immobilisation experiments on monolithic columns.

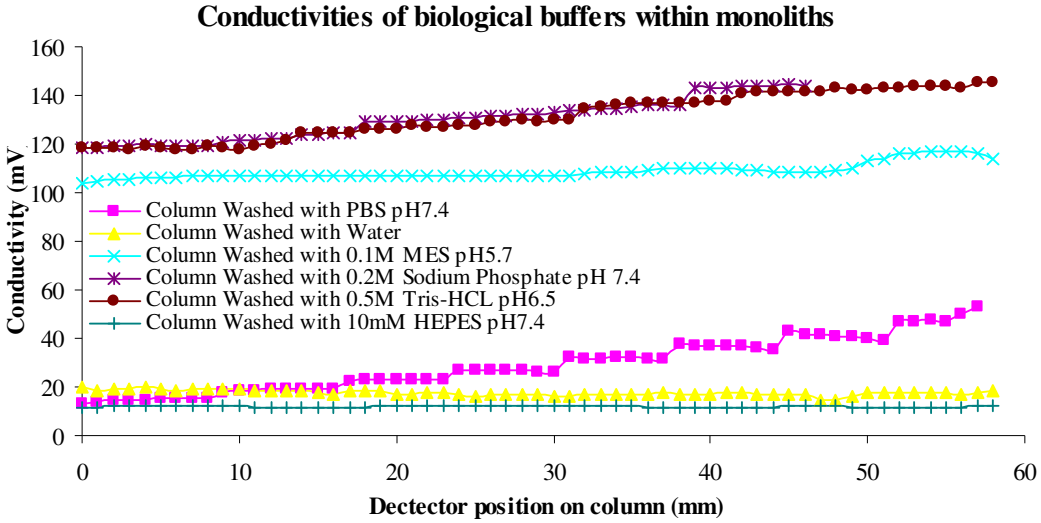

Figure 3.4.8: Relative conductivity values of a selection of biological buffers within monolithic columns. For each conductivity scan the appropriate buffers was flown through the column and the conductivity at each millimetre measured. It was found that the most appropriate buffer to give a low background conductivity was 10mM HEPES. This biological buffer was used in all future experiments.

3.4.5: Capture of biotinylated GFP on monolithic columns

The capture of proteins by vinyl-azlactone on monolithic columns is based on the reaction with the lysine residues on the surface of the protein. This is not an orientated immobilisation, as lysine is a common amino acid present on the surface of proteins. To achieve orientated protein immobilisation GFP was tagged with the Strep-tagII (Section 3.1) and was biotinylated with both the NHS and maleimide- biotin linkers (Section 2.21). Tetrameric proteins; streptavidin and streptactin have a biotin binding site within each subunit as outlined in section 1.3. Therefore, regardless of the orientation of immobilisation for these proteins on the monolith, they can retain the ability to capture biotinylated proteins. Streptavidin was immobilised on the monolithic columns by reaction with photografted vinyl-azlactone. (Section 2.23.6) Figure 3.4.9 shows the monolithic column which was prepared as described in section 2.23 and a baseline conductivity scan performed with 10mM HEPES flowing through the column. 500mgs of streptavidin was immobilised in two vinyl-azlactone functionalised zones. After immobilisation of streptavidin, unreacted vinyl-azlactone was blocked by the washing

of the column with 1M ethanolamine in 10mM HEPES buffer at pH7.4 and a second conductivity scan was performed after an overnight wash with 10mM HEPES. This scan showed an increase in the conductivity where streptavidin has been immobilised by vinyl-azlactone.

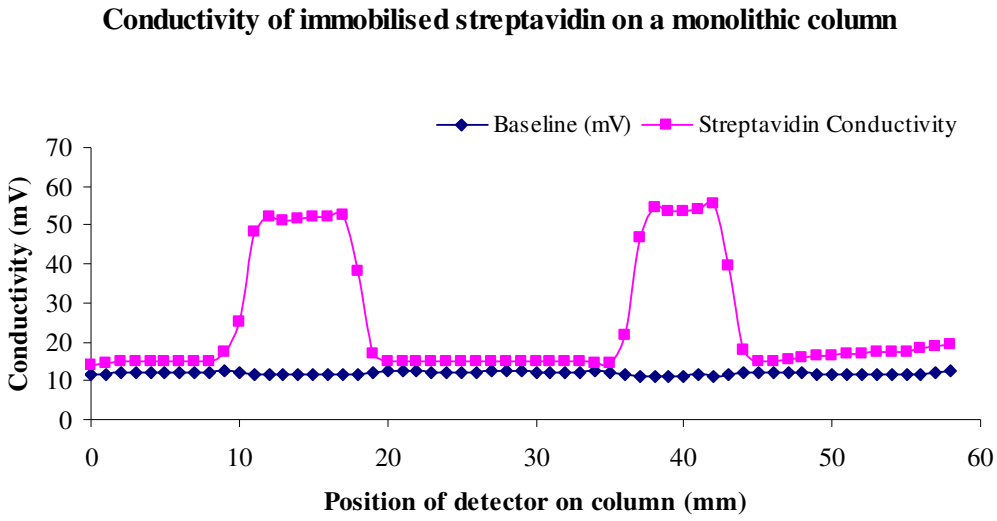

Figure 3.4.9: A conductivity scan showing the immobilisation of 500mM of streptavidin in 10mM HEPES by two vinyl-azlactone functionalised zones in a monolithic column. The baseline conductivity scan was performed with 10mM HEPES in the column. Apart from the conductivity of the immobilised zones the baseline remains low signifying localised immobilisation within the column.

To confirm that un-biotinylated GFP would not be captured by the immobilised streptavidin, 200mM of VOS3 (N-terminal Histidine^{6} tag, C-terminal Lysine^{6} tag) in 10mM HEPES, pH7.4 was passed over this column. With 10mM HEPES, p7.4 flowing through the column a conductivity scan was performed.

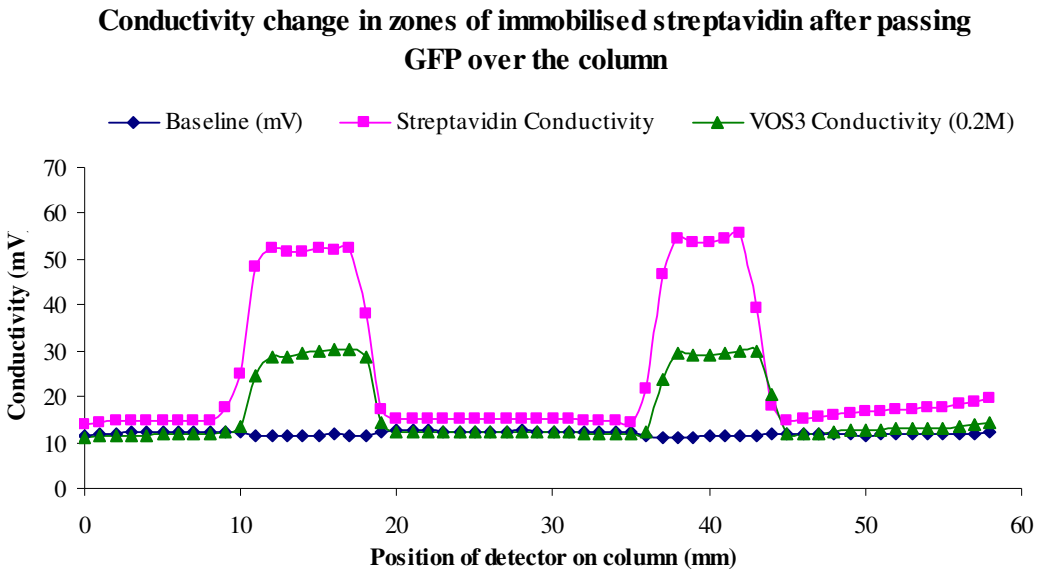

Figure 3.4.10: Conductivity change in the zones of immobilised streptavidin after passing un-biotinylated GFP through the column. The conductivity scan was performed after an overnight wash with 10mM HEPES, and with the same concentration of HEPES flowing through the column. There is a reduction of 50% in the conductivity of the zones after passing 200mM VOS3 through the column.

When initially performing conductivity scans it was thought that an increase in conductivity would be the only response to an immobilisation or protein capture event within a monolithic column. Conductivity is a measure of the ability of the solution within the monolithic columns to conduct an electrical current. The capture or immobilisation of a protein can change this ability by its net charge. When the conductivity scan of VOS3 in figure 3.4.10 was performed, it was not realised that the immobilisation of a protein on streptavidin could also reduce the conductivity values. The 50% reduction in the conductivity of the monolith could not be explained at this point. When this VOS3 conductivity scan was taken, a reliable method of visualising fluorescent zones on monolithic columns had not yet been discovered. Therefore the ability to cross confirm the change in conductivity with fluorescence visualisation was not available. Because of these factors it was decided to pass biotinylated GFP over the monolithic column despite the reduction in conductivity.

200mgs of biotinylated VOS3 in 10mM HEPES at pH7.4 was passed over the column as described in section 2.23.6. The conductivity scan was performed after washing overnight with 10mM HEPES.

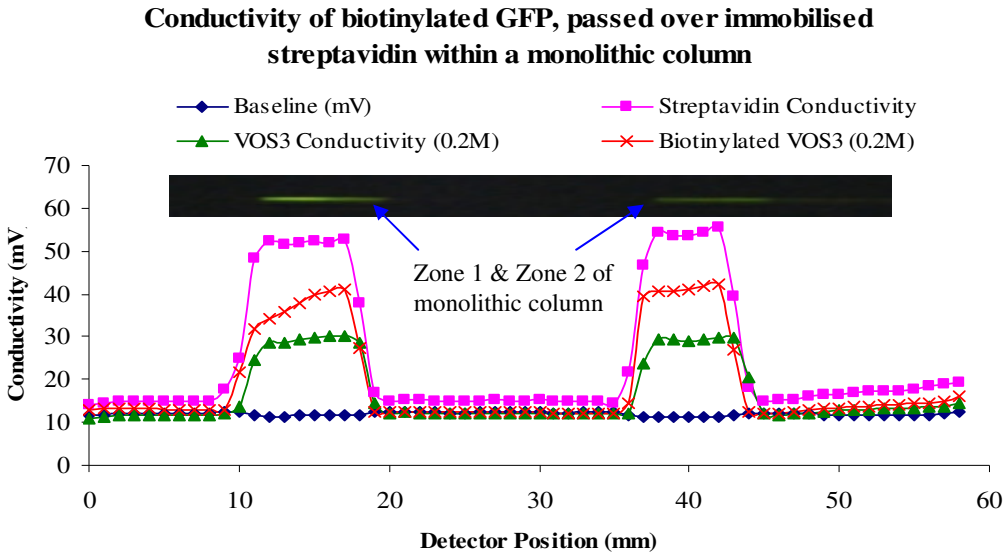

Figure 3.4.11: The conductivity change within a monolithic column after passing biotinylated GFP over two zones of immobilised streptavidin. There is an increase in the conductivity from the un-biotinylated GFP conductivity. The conductivity is still a third less than the initial streptavidin conductivity values. An efficient method of obtaining a fluorescent picture for this conductivity scan was achieved. It became apparent that the capture of proteins on monolithic columns could cause the conductivity to decrease as well as increase. The fluorescence visible was a combination of the initial un-biotinylated VOS3 protein and the biotinylated VOS3 protein.

The conductivity scans shown in figure 3.4.11 clearly demonstrate the change in the conductivity by passing biotinylated GFP over the immobilised streptavidin. The biotinylated GFP conductivity scan increased by a third over the un-biotinylated conductivity values. This biotinylated GFP conductivity scan is a third smaller than the initial streptavidin conductivity values. The development of a method to easily visualise fluorescent zones on monolithic columns using a Blue Light Transilluminator Dark Reader, enables the confirmation of the capture of GFP on immobilised streptavidin. The fluorescent zones visible in the monolithic columns comprise of a combination of the un-biotinylated and biotinylated GFP proteins. It was possible that

the un-biotinylated GFP was interacting with immobilised streptavidin by protein-protein interaction. The streptavidin is capturing the biotinylated GFP as shown by the increase in the conductivity. It is noted that the intensity of fluorescence in the first zone of immobilised protein decreases from left to right. The conductivity values of the same zone increase from left to right. This result may indicate that the greater the amount of GFP immobilised on monolithic columns the lower the conductivity. This novel result was relatively un-expected, as an increase in conductivity relative to an increase in protein immobilisation was initially expected. It also supports the previously described observation that as proteins pass along the monolith from left to right, they will saturate the first reaction zone of the column before saturating the second zone.

In order to assess whether the immobilisation of un-biotinylated GFP on streptavidin functionalised zones within monolithic columns is due to protein-protein interactions, a second monolithic column was produced with two zones of immobilised streptavidin. This second monolith was prepared at the same time as the monolith outlined in figures 3.4.9, 3.4.10 and 3.4.11. Immobilised streptavidin zones were generated as previously described. 0.2mgs un-biotinylated GFP (VOS3) in 10mM HEPES buffer was passed over this column and after an overnight wash by HEPES buffer a conductivity scan was performed.

Figure 3.4.12 shows an identical conductivity profile for the streptavidin and un-biotinylated GFP immobilisation as figure 3.4.10. The scale of streptavidin conductivity indicates an equal amount of protein immobilised by the covalent reaction with vinyl-azlactone on both columns. As in figure 3.4.10 after passing un-biotinylated GFP over the monolithic column containing immobilised streptavidin the conductivity values were reduced by 50%. The monolith column was placed on a blue light transilluminator dark reader and the presence of two distinct zones of fluorescence confirmed protein immobilisation. These results indicate that the un-biotinylated GFP protein is interacting and being captured by the immobilised zones of streptavidin.

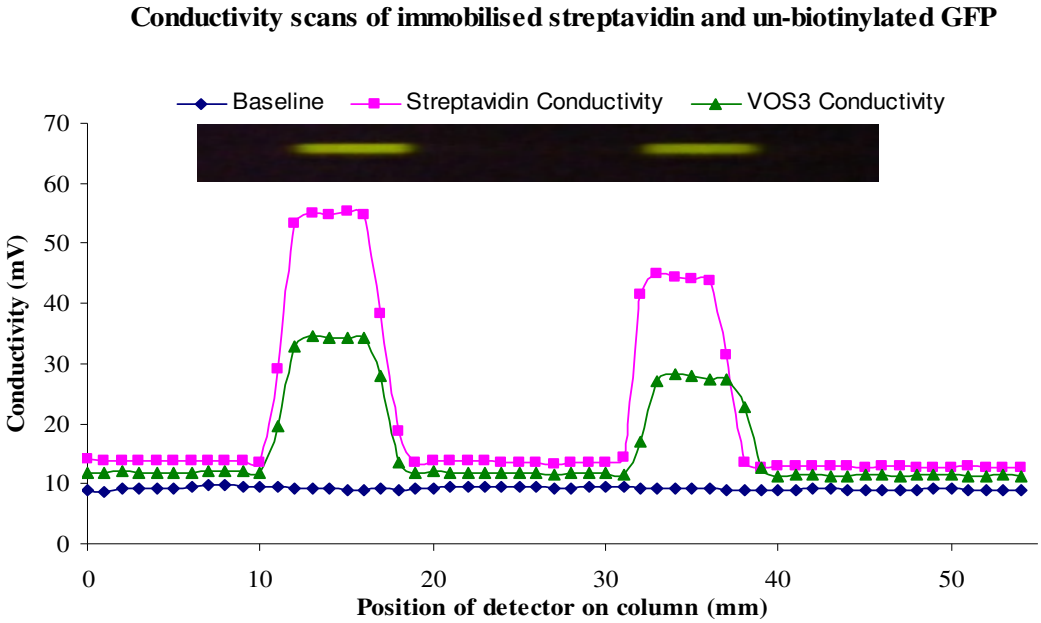

Figure 3.4.12: The baseline, streptavidin and un-biotinylated conductivity scans within a monolithic column. Confirming the results shown in figure 3.4.10, passing un-biotinylated GFP over a monolith column with two zones of immobilised streptavidin reduces the conductivity by 50% in both reactive zones. To confirm this reduction in conductivity is caused by the presence of GFP, the monolith was visualised under blue light and two fluorescent zones were present.

To determine whether GFP was interacting with streptavidin by protein-protein interactions, the column was washed for 48hours with 1M NaCl in 10mM HEPES. High salt concentrations should disrupt any protein-protein interactions. Measurements of the conductivity of monolithic columns which contain highly ionic molecules were difficult. To reduce the conductivity values and enable them to be read by the conductivity detector the monolith was washed by 10mM HEPES at pH7.4.

Figure 3.4.13 shows the conductivity scan of the column after washing for 48hrs with 1M NaCl. Sodium Chloride is a highly conductive molecule and after washing the column for 8hrs with 10mM HEPES the conductivity baseline was three times higher than the original baseline. In an attempt to bring this baseline back down to original levels the monolith was continuously washed with 10mM HEPES overnight. The column was also viewed on the blue light transilluminator dark reader to determine if any immobilised GFP was present. The intensity of fluorescence visible on the monolithic column was greatly reduced by the wash with sodium chloride. A reduced amount of fluorescence indicates that not all GFP was removed from the column. This

result clearly demonstrates that washing monolithic columns with high salt concentrations to reduce protein-protein interactions was not completely successful. A conductivity scan of monolithic columns which contained solutions with high salt concentrations proved difficult to obtain. The continuous washing of the column with 10mM HEPES buffer failed to reduce the conductivity values to the original baseline after a 48hr wash. This indicates that salt can be retained and detected within the pores of the monolithic columns for at least two days after passing the solution over the column.

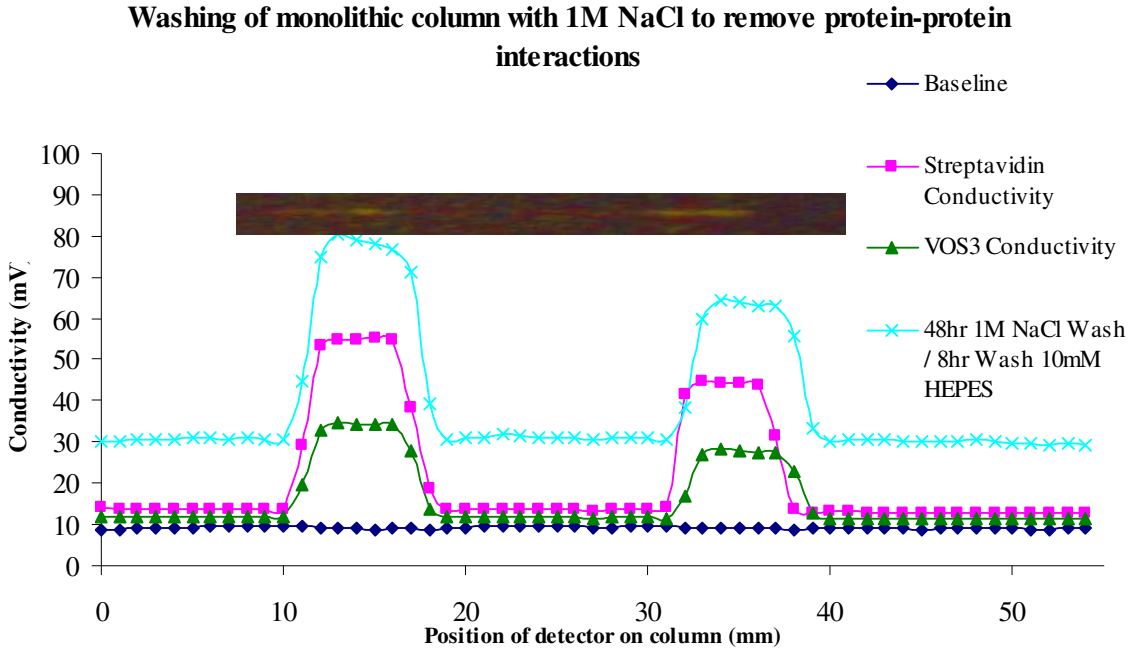

Figure 3.4.13: The conductivity scan of a monolithic containing covalently immobilised streptavidin and a un-biotinylated GFP washed for 48hrs with 1M NaCl and a further 8 hours with 10mM HEPES to equilibrate. The equilibration process is important as even after an 8 hour step the baseline is three times higher than the original baseline. The conductivity of the functionalised zones is still higher than the original streptavidin immobilisation. This is due to the highly conductive salt NaCl still being retained by the column.

The conductivity scan shown in figure 3.4.14 was the achieved after 48hours of consistent washing with 10mM HEPES. This conductivity could not be reduced by further washing with HEPES. The monolithic column was washed for a week and the conductivity scan illustrated in Figure 3.4.14 was the lowest conductivity achieved.

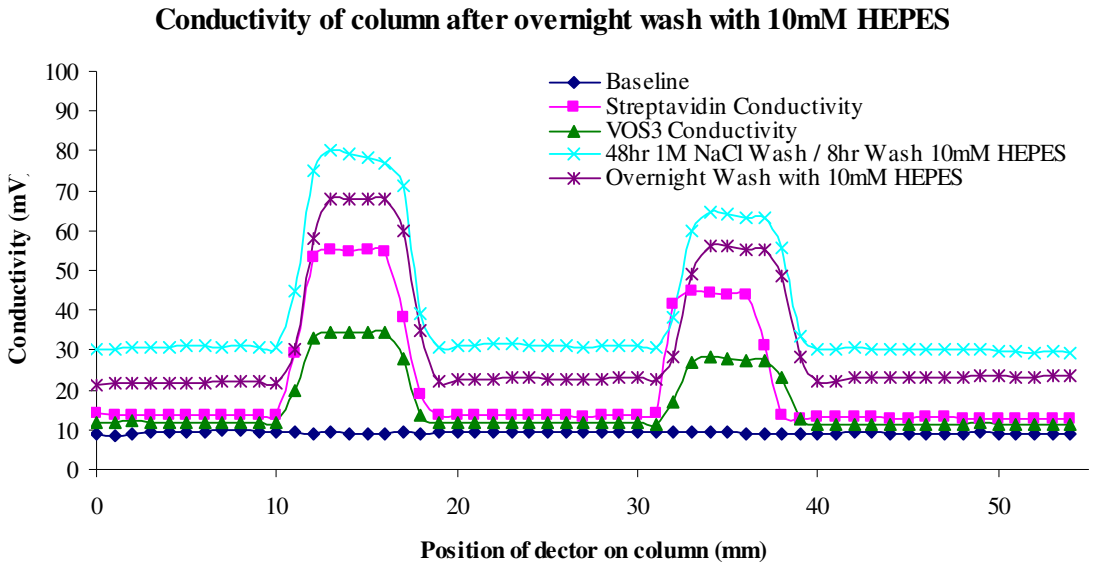

Figure 3.4.14: The conductivity of monolith after a further overnight wash with 10mM HEPES at 1µl/min. The conductivity was reduced by 10mV from the conductivity of the wash with 1M NaCl, but still not had been reduced to the conductivity of streptavidin. After washing with 10mM HEPES for 48hrs the column conductivity could not be reduced further.

The continued use of this column was no longer possible as any further conductivity scans and changes in peak area, could not be compared to the original streptavidin conductivity scan. Also one could not attempt to measure the capture of biotinylated GFP by immobilised streptavidin within monolithic columns, as the change in conductivity could be due to protein-protein interactions or the bio-affinity reaction between streptavidin and biotin. Unfortunately due to time constraints further study of this potential protein-protein effect within monolithic columns was not possible.

3.4.6: Summary

Preliminary results shown in this section clearly demonstrate that conductivity can be used to determine the degree of protein immobilisation or interactions within monolithic columns. As the model protein GFP fluoresces under blue light, conductivity and fluorescence can be used to cross-confirm protein immobilisation. Using both these non-evasive protein detection methods the addition of six extra lysine residues was shown to increase the amount of protein immobilisation within monolithic columns by over 400% in an orientation specific manner. The immobilisation of streptavidin and its capture of biotinylated proteins within monolithic columns were also studied by conductivity. The capture of biotinylated proteins by streptavidin proved to have issues, due to un-biotinylated protein being immobilised within the functionalised zones. This immobilisation was theorised to be due to protein-protein interactions. The reduction of protein-protein interactions between streptavidin and un-biotinylated GFP by washing columns with high concentrations of salt proved to be relatively successful. Unfortunately, a 1M sodium chloride wash could not totally remove the protein-protein interaction. This phenomenon was shown by fluorescence as the reduction could not be confirmed by conductivity measurement due to the high conductivity of salt, which masked any change. The removal of salt from the monolithic column by continued washing with 10mM HEPES proved difficult. The conductivity of the column was only reduced by 10mV after two days of consistent washing.

The use of GFP as a model protein for optimising immobilisation of proteins within monolithic columns proved particularly useful for initial studies due to its inherent fluorescence. The immobilisation of the vast majority of proteins can only be detected by conductivity.

Chapter 4: Model System; The capture of sialic acid by immobilised SiaP within monolithic columns and detection by C^4D

4.1 Overview

Sialic acids generally occupy the terminal position(s) in glycan chains (Varki., 1999). Sialic acid therefore has a wide range of functions within biological systems and has only recently received the attention this important molecule deserves. Their main function relates to cellular and molecular recognition. Sialic acids are antigenic determinants of blood groups and as such enable the immune system to distinguish between self and non-self structures according to their sialic acid pattern. They also serve as ligands for lectins and antibodies and therefore play an important regulatory role in many physiological processes (Traving and Schauer, 1998).

Sialic acid has also become increasingly interesting to the biopharmaceutical industry, because of its unique features. Sialylated biopharmaceuticals have exhibited an increased activity and stability *in vivo* (Fernandes and Gregoriadis, 2001). Therefore, a growing number of glycosylated pharmaceutical products are being studied with regard to their sialylation and its effects. Furthermore, an accurate estimation of the sialic acid level of a glycoprotein based drug as well as the determination of its sialylation pattern would allow for a more efficient production.

As outlined in the introduction (Section 1.6.2) the pathogen *Haemophilus influenzae* is exclusively adapted to infect humans. It evades the innate immune response of the host by sialylation of its lipoligosaccharides with the hosts own sialic acids and thus appears as-self for the hosts defence system (Mandrell *et al.*, 1992). Surprisingly then, although sialic acid is crucial for the pathogens survival within the host, *Haemophilus influenzae* is unable to synthesis sialic acid. It therefore requires an exogenous source of sialic acid (Bouchet *et al.*, 2003). It was found that sialic acid acquisition is mediated via a tripartite ATP-independent periplasmic (TRAP) transporter (Muller *et al.*, 2006). The extracytoplasmic solute receptor of this TRAP system is known as SiaP. As this protein has evolved to capture sialic acid, it was theorised that the SiaP protein could be used for sialic acid capture and detection (Severi *et al.*, 2005).

The SiaP proteins C-terminus is located on exactly the opposite side of the protein from the sialic acid binding site. C-terminal tagged SiaP protein was donated for this study by Jakub Szczepaniak who worked in our laboratory. A histidine tag was added to the C-termini of this SiaP along with an eight residue spacer sequence to aid protein purification. Downstream from this purification tag six lysine residues were added for orientation-specific protein immobilisation (Szczepaniak J., 2009).

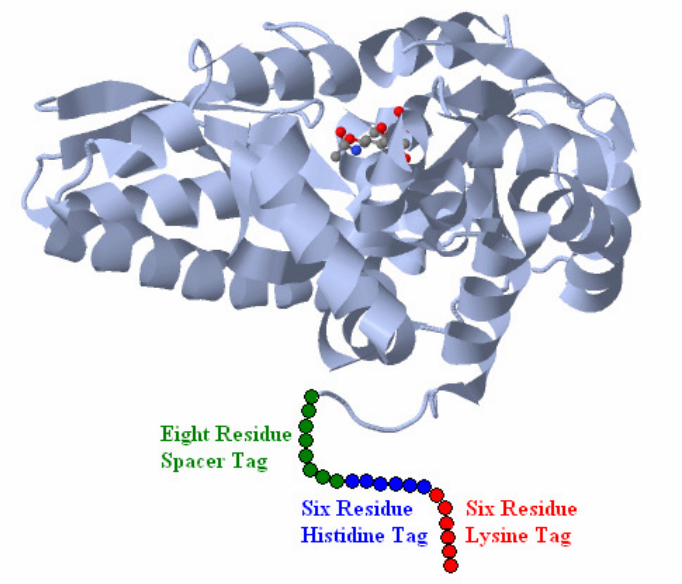

Figure 4.1: A graphic representation of the SiaP protein used in this study which was provided by Jakub Szczepaniak. This figure shows a SiaP molecule in the 'closed' position with a bound sialic acid molecule. The tags added to C-termini are shown in a coloured graphic. Eight amino acid spacer residues were added to aid protein purification. Six histidine residues were added for protein purification and six lysine residues were added to increase the amount of orientated-specific protein immobilisation.

4.2 Immobilisation of SiaP on monolithic columns.

Using the experience gained from the immobilisation of GFP on monoliths (Chapter 3), C-terminal lysine tagged SiaP was immobilised on monolithic columns. Two functionalised zones of vinyl-azlactone were generated by irradiation with UV light (section 2.23). A baseline conductivity scan was performed after washing with 10mM HEPES. A concentration of 200mM SiaP was passed over the column. In a change to the GFP monolith immobilisation protocol, the column was washed with 10mM NaOH in 10mM HEPES after SiaP immobilisation. Our laboratory had found that that our purified recombinant SiaP contained some bound sialic acid and that this could be removed with a 10mM NaoH wash (Szczepaniak J., 2009). Therefore this wash was applied to the monolith immobilisation protocol to ensure that the immobilised SiaP was free of bound sialic acid. After further washing to remove NaOH from within the monolith with 10mM HEPES a second conductivity scan was performed.

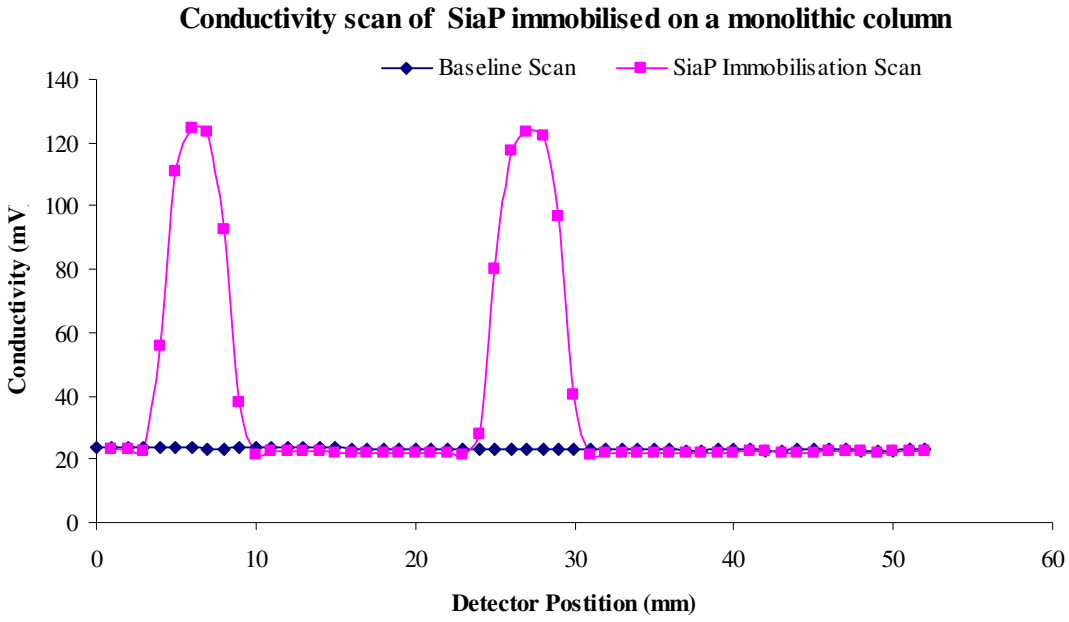

Figure 4.2: The conductivity scan of two zones of immobilised SiaP. After protein immobilisation the monolithic column was washed with 10mM NaOH in 10mM HEPES to remove any bound sialic acid. Two clear increases in the conductivity indicate a focused immobilisation of SiaP on the monolithic column.

The addition of six lysine residues to the C-termini of SiaP was expected to increase the level of immobilised protein based on the results discussed in chapter 3. It was also expected that the immobilisation was more orientation specific with the lysine residues at the C-termini. It was an important factor as SiaP requires steric space to capture sialic acid, changing from an 'open' confirmation to a 'closed' (Johnston *et al.*, 2008)**.** Tagging the protein at the N-terminus would remove the proteins ability to capture sialic acid.

4.3: The detection of Sialic Acid capture within monolithic columns by conductivity

Initial experiments were performed to determine if the capture of sialic acid by SiaP immobilised on monolithic columns could be detected by conductivity measurements. A 5mM concentration of sialic acid was initially passed over the monolith column functionalised with immobilised SiaP. Surface plasmon resonance results achieved by

our laboratory indicated that the capture of 5mM sialic acid by SiaP can be detected (Szczepaniak J., 2009).

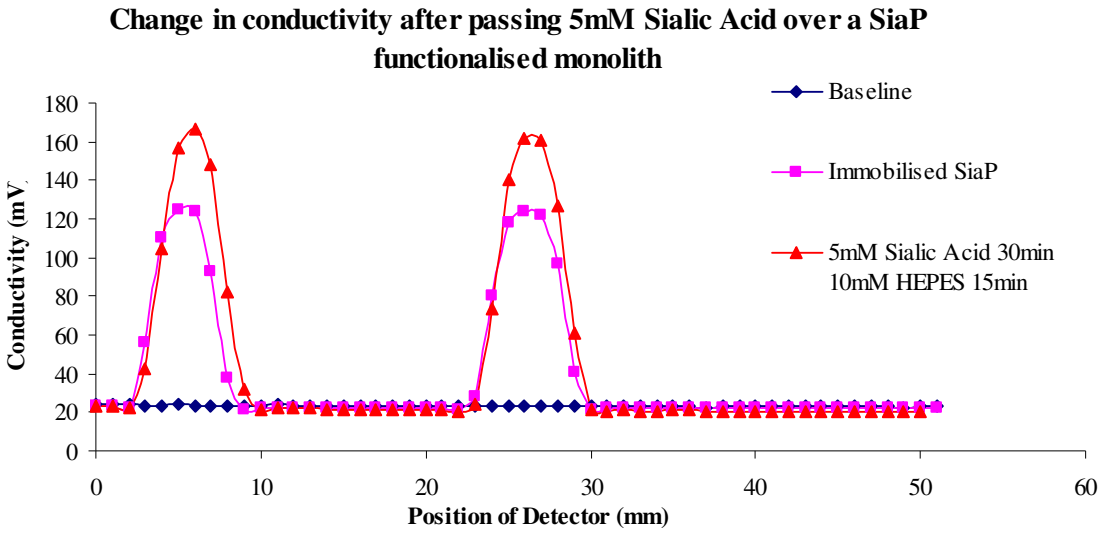

Figure 4.3: A conductivity scan of a monolithic column after passing 5mM sialic acid over two zones of immobilised SiaP. An increase in conductivity may indicate the capture of sialic acid. Sialic acid in 10mM HEPES was passed over the column for 30 minutes. This was followed by a wash with 10mM HEPES for fifteen minutes before a conductivity scan was performed.

A sample of 5mM sialic acid in 10mM HEPES was passed over the SiaP functionalised monolith for half an hour. This column was then washed for fifteen minutes with 10mM HEPES to remove any free sialic acid and a conductivity scan performed. An increase in conductivity of approximately 40% was observed as illustrated in figure 4.3. This column was continually washed with 10mM HEPES and a conductivity scan was performed after 90 minutes to observe the effect on conductivity within the monolithic column.

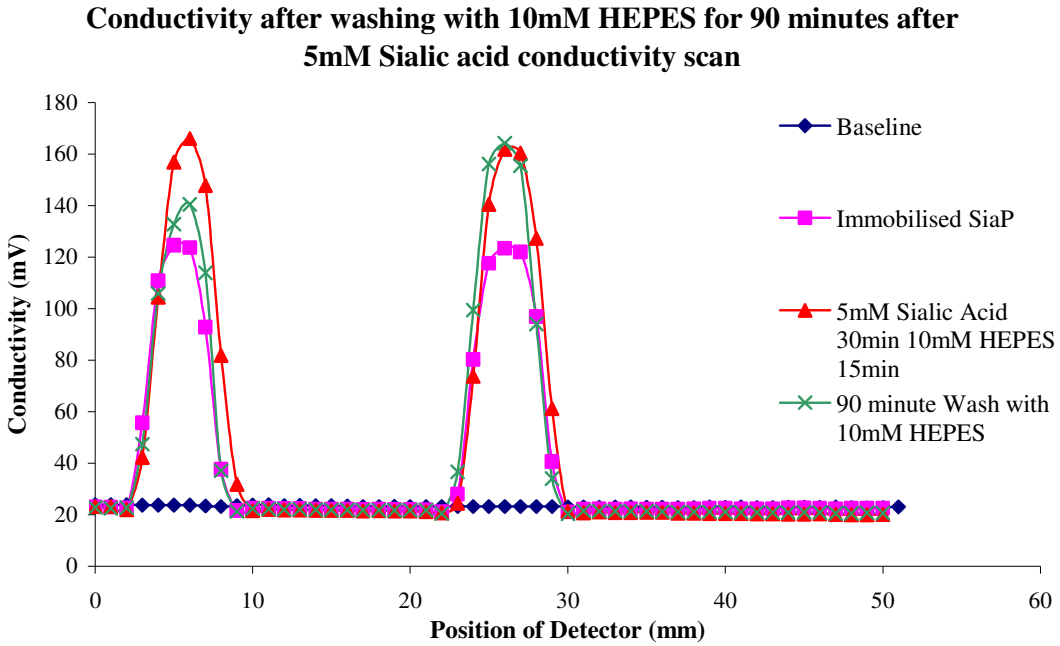

Figure 4.4: The change in conductivity after washing the monolithic column with 10mM HEPES for 90 minutes after capture of 5mM Sialic acid by immobilised SiaP. The conductivity of the first zone of immobilised SiaP reduced by approximately 20%. The second zone of immobilised protein retained the same conductivity profile.

As can be seen in figure 4.4 the conductivity profile of the first zone of immobilised SiaP was reduced by approximately 20%. This change is contrasted by the stability of conductivity in the second zone of immobilised protein. It was theorised that as HEPES flows through the monolith, it reaches and therefore washes sialic acid from the first zone of immobilised SiaP. The free sialic acid is then captured by the second zone of SiaP, which causes it to maintain its conductivity profile. This monolith column was washed continuously for the rest of the day and a conductivity scan performed every hour to measure changes in conductivity. The conductivity scan illustrated in figure 4.4 clearly demonstrates a reduction in conductivity in the first zone of immobilised protein. It is not until the conductivity of the first zone has been reduced to the original SiaP immobilisation conductivity that the conductivity of the second zone begins to decline (Figure 4.5).

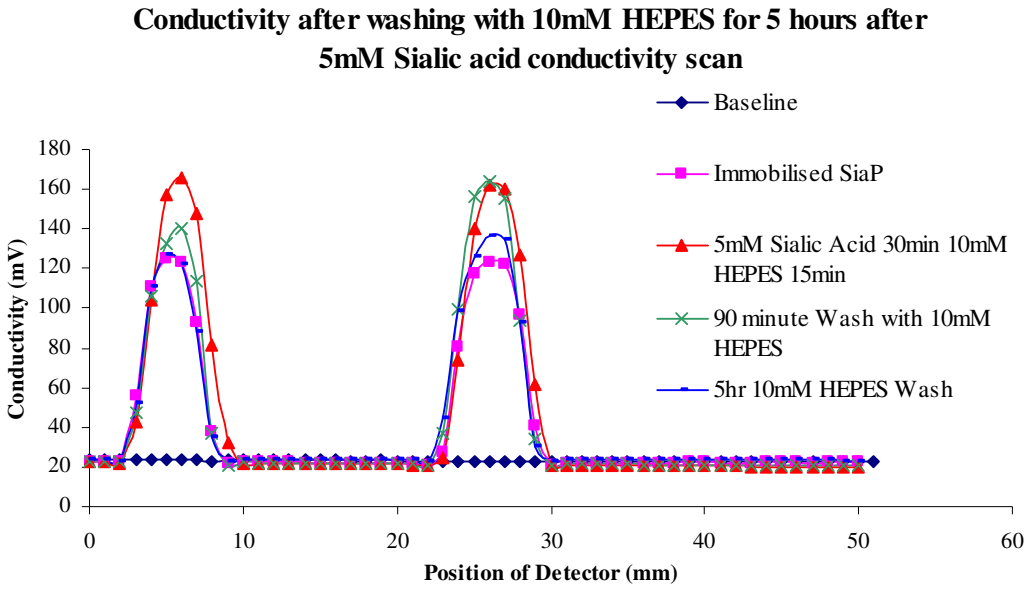

Figure 4.5: The change in conductivity after washing a SiaP functionalised monolith which had captured 5mM sialic acid for 5 hours with 10mM HEPES. The conductivity of the first immobilised zone of SiaP was reduced to the original immobilised SiaP conductivity. The second zone of immobilised SiaP was reduced by approximately 20%.

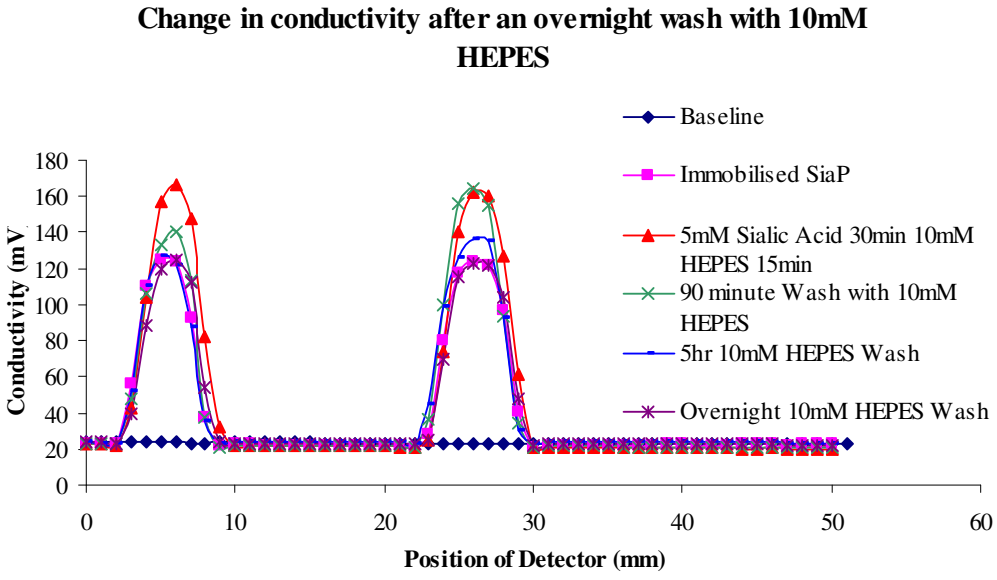

Figure 4.6: The change in conductivity after washing a SiaP functionalised monolith which had captured 5mM sialic acid, overnight with 10mM HEPES. The conductivity of both immobilised zones of SiaP has been reduced to the original immobilised SiaP conductivity.

The reduction of conductivity to the original SiaP values illustrated in figure 4.5 demonstrated the effect of overnight washing of the column. Before this experiment was performed it was thought that a wash of 10mM NaOH would be required to remove captured sialic acid from immobilised SiaP, as had been required for surface plasmon resonance (Szczepaniak J., 2009). The results outlined for the capture of 5mM Sialic acid by immobilised SiaP indicate that this restoration step may not be necessary. A period of extended washing may recharge the immobilised SiaP monolith. This would provide a distinct advantage over the surface plasmon resonance method of interaction detection. The conductivity of the immobilised zones of SiaP after 5mM sialic acid removal was used as the baseline for the application of 2.5mM sialic acid. This concentration of sialic acid was chosen to try and determine the detection limit of this detection method.

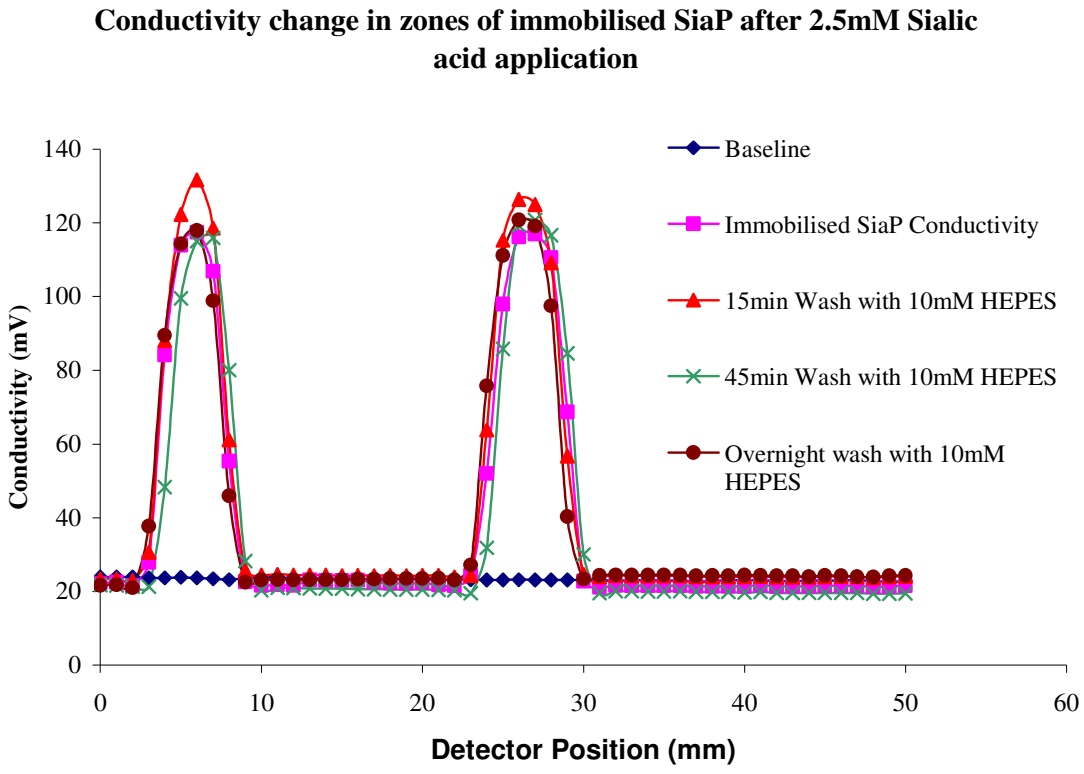

Figure 4.7: The conductivity change of the monolith after the application of 2.5mM to the zones of immobilised SiaP. There is an approximate 10% increase in the level of conductivity in the first functionalised zone. The change in conductivity of the second SiaP functionalised zones was approximately 5%

As can be seen in figure 4.7 the conductivity of the monolithic column after the application of 2.5mM Sialic acid displayed a lower change in conductivity compared to 5mM sialic acid. The reduced conductivity change in the second functionalised zone was thought to be due to the majority of the sialic acid being captured by the first zone of immobilised SiaP. After 45 minutes of washing with 10mM HEPES the conductivity scan both conductivity peaks were reduced to the background SiaP conductivity profile. This column continued to be washed with 10mM HEPES overnight and a final conductivity scan was performed. The conductivity scan produced by this overnight scan remained the same as the original SiaP conductivity. A second 5mM application of sialic acid was passed over the monolithic column this was to determine if the capture of sialic acid was reproducible. The application and washing times were kept consistent with the previous time 5mM sialic acid was applied to the column.

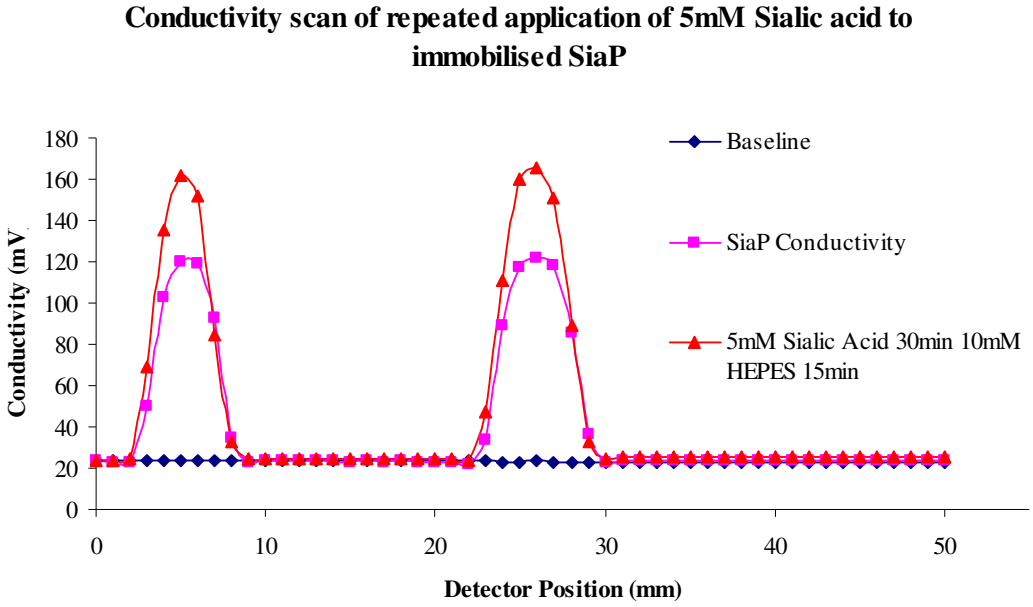

Figure 4.8: The conductivity scan for the repeat application of 5mM Sialic acid to a monolith with SiaP functionalised zones. The increase in the conductivity of both zones of immobilised SiaP was approximately 40%. This increase in conductivity mirrors the increase which was observed the first time 5mM Sialic acid was applied to the monolith.

The conductivity scan illustrated in figure 4.8 closely mirrors the conductivity profiles achieved in figure 4.3. This indicates that the conductivity detection method is a

reproducible method to determine interactions within monolithic columns. The monolith was once again washed with 10mM over the course of the day and conductivity scans performed at time intervals mirroring the time intervals outlined for the first application of sialic acid to the column.

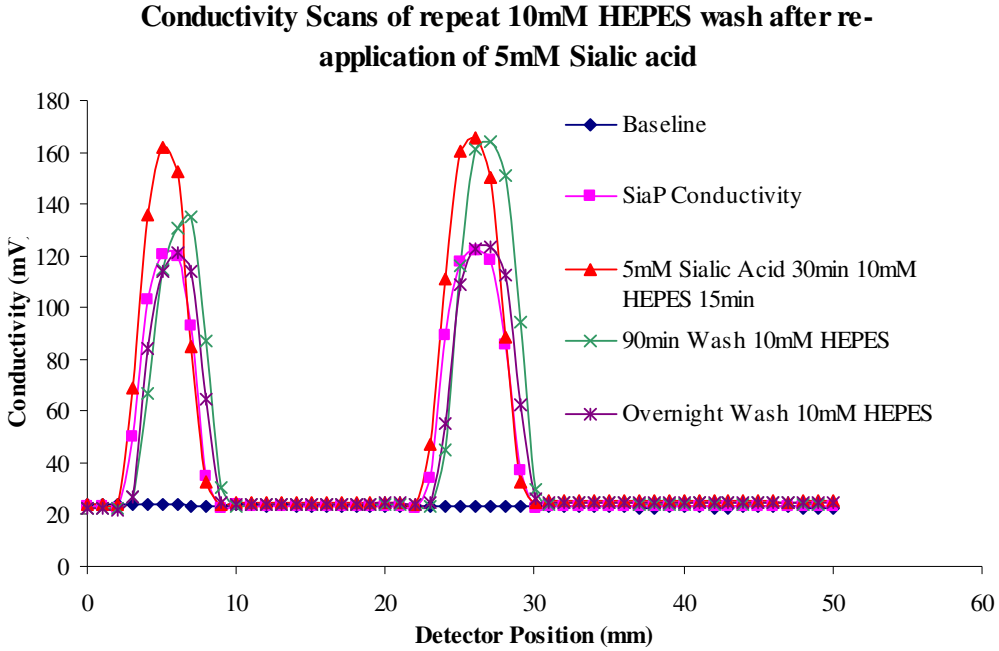

Figure 4.9: Conductivity scans of repeat application of 5mM Sialic acid to SiaP functionalised monolithic column. Conductivity scans were performed at set intervals and following overnight wash with 10mM HEPES. The conductivity scan profiles closely mirror those illustrated in figure 4.6.

The conductivity scans outlined in figure 4.9 closely mirror the conductivity scans outlined in figure 4.6. The reproducibility of the conductivity method for detecting SiaP-sialic acid interaction on monolithic columns was further studied by calculating the change in the peak areas of both SiaP immobilised zones after passing 5mM Sialic acid over the column. The peak area change as the column is washed with 10mM HEPES was also noted and compared between the two columns; the initial 5mM sialic acid application and the repeat application. Figure 4.9 illustrates the change in both peak areas for both monolithic columns after 15minutes, 90 minutes and overnight washes with 10mM HEPES. The peak areas in the first and second SiaP zones of immobilisation for both applications of sialic acid after a 15minute wash show an area increase of between 25 to 40%. After washing for 90 minutes the peak area of the first zone of immobilisation for both columns had reduced dramatically to approximately a

10% increase in peak area. The second zone of SiaP immobilisation though retained the increase in peak area after washing for 90 minutes, as observed after washing for 15 minutes. These changes were thought to be due to sialic acid being removed by washing from the first zone of immobilised SiaP, but being recaptured by the second immobilised zone. This in turn caused it to exhibit a peak area change of 30% over the peak generated by SiaP immobilisation alone. After overnight washing with 10mM HEPES all peak areas, from the original and repeat application of sialic acid to the SiaP functionalised monolith showed a peak area change of approximately 1%. Indicating that sialic acid has been removed from immobilised SiaP protein within a monolithic column.

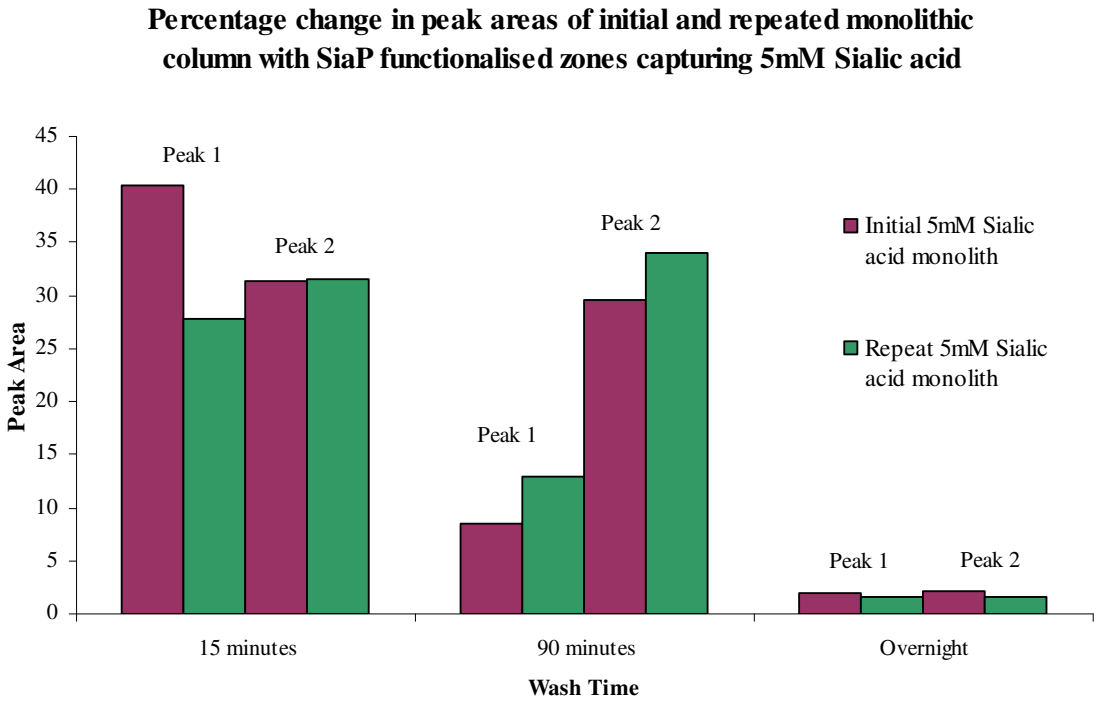

Figure 4.10: The difference in peak areas between the original monolithic capture of 5mM Sialic acid and the repeat application. The peak areas between both monoliths and the two functionalised zones on both monoliths show similarities. The peak area for both zones after each 5mM sialic acid capture after 15minutes of washing with 10mM HEPES show an increase in peak areas of between 25 and 40%. After 90 minutes of washing the initial zone in both monoliths was greatly reduced. The second functionalised zones on each monolith retained the increase in the peak area. After an overnight wash with 10mM HEPES all functionalised zones over the two columns reduced the change in peak area to less than 5%.

As the repeat application of 5mM sialic acid appeared reproducible it was deemed that the immobilised SiaP protein was not affected by the continuous washing with buffer.

The reduced change in the conductivity reading for 2.5mM sialic acid application was due to the lower amounts of sialic acid being captured by immobilised SiaP.

In order to determine if an increased conductivity signal could be achieved by increasing the concentration of sialic acid applied to the monolithic column. 7.5mM and 10mM Sialic acid concentrations were applied to the same monolithic column and conductivity scans performed after identical wash times as those outlined for the application of 5mM Sialic acid.

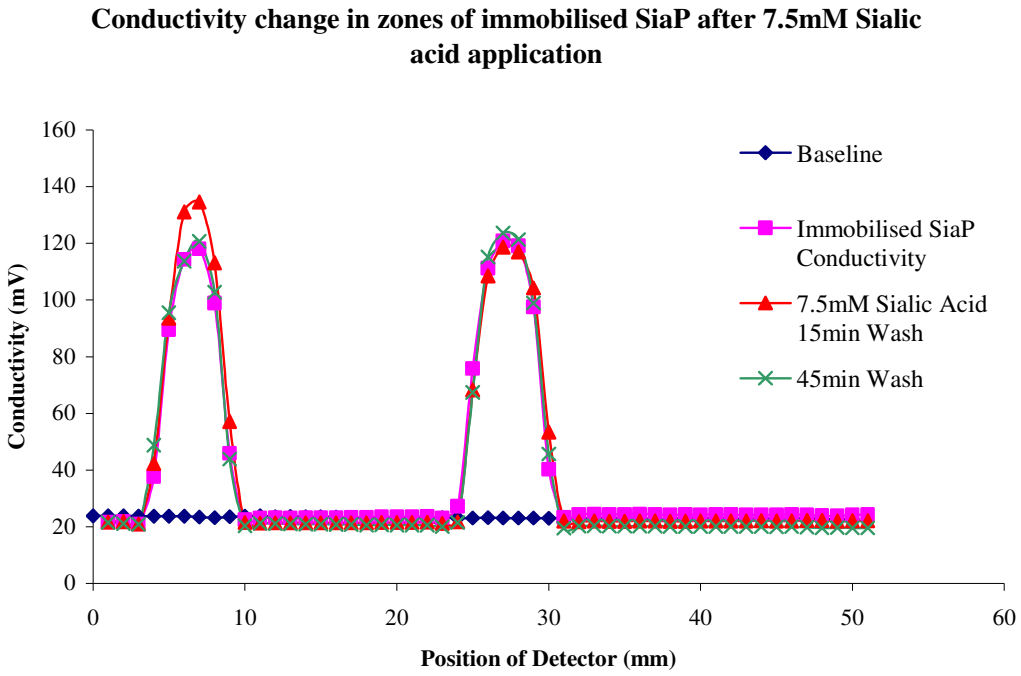

Figure 4.11: The change in conductivity after the application of 7.5mM Sialic acid to a SiaP functionalised monolithic column. There was an approximate 10% increase in conductivity in the first zone of immobilised SiaP. There was no change in the conductivity of the second immobilised SiaP zone.

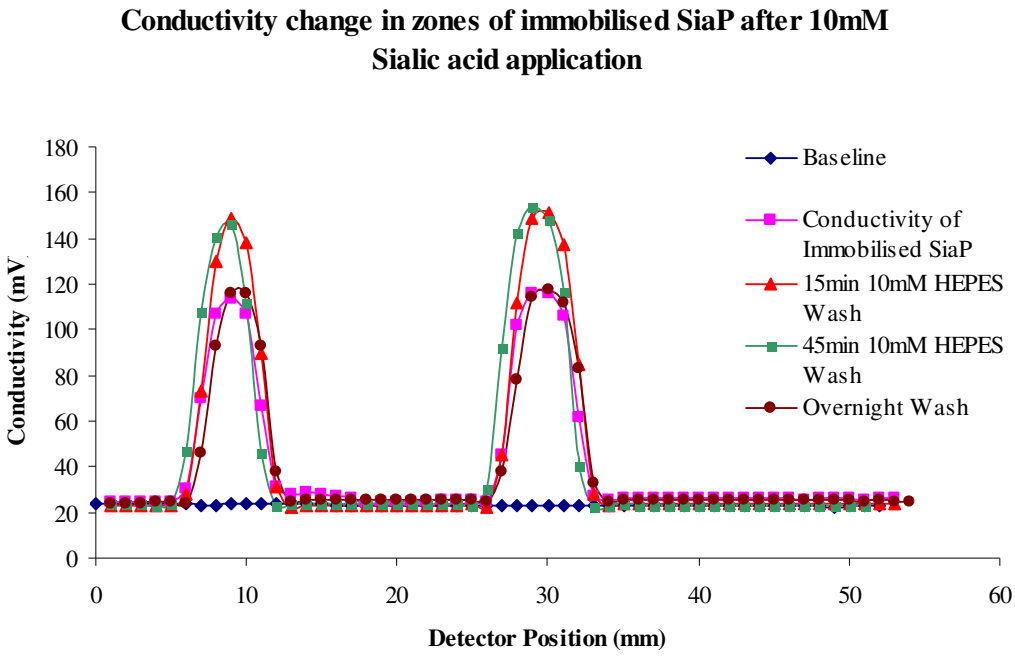

Figure 4.12: The change in conductivity after the application of 10mM Sialic acid to a SiaP functionalised monolithic column. There was an approximate 20% increase in the conductivity values of both immobilised SiaP zones. The conductivity was reduced to the conductivity of the SiaP immobilisation after continuous washing with 10mM HEPES.

As can be seen in figures 4.11 and 4.12 the application of different concentrations of sialic acid to the monolith column did result in a change in conductivity. However, the increase in conductivity did not appear to be concentration specific. The addition of 7.5mM Sialic acid to the SiaP functionalised monolith elicited a change in conductivity in only the first zone of immobilised protein. This conductivity change outlined in figure 4.11 was an increase of 10%. This was a reduced conductivity change when compared to the addition of 5mM sialic acid. The lack of change of the conductivity in the second protein zone , could not be readily explained , but does indicates that no sialic acid was captured by the functionalised zone. Once again, as observed in the washing protocols with 5mM sialic acid, the conductivity may be reduced to the observed SiaP conductivity with continuous washing with 10mM HEPES buffer. The application of 10mM sialic acid to the SiaP functionalised monolith produced an increase in conductivity of 20% over the 'background' SiaP conductivity reading.

Figure 4.12 illustrates that the conductivity could be reduced to the original SiaP reading with washing by 10mM HEPES.

The difference in conductivity readings between the application of 7.5mM sialic acid and 10mM sialic acid to the monolithic column was a concern. The increase in sialic acid concentration did not produce a corresponding increase in the conductivity. The overall reduction of conductivity by washing with buffer was seen as an indication that SiaP may not be capturing the free sugar within the monolith. To determine if this was the case an un-related sugar was applied to the functionalised monolith.

4.4: Effect of Glucose on conductivity

To determine if the change in conductivity was due to the specific interaction between sialic acid and SiaP, an unrelated sugar molecule (glucose) was applied to the SiaP functionalised monolith. A solution of 5mM Glucose was applied to the monolithic column for thirty minutes. After washing with 10mM HEPES for fifteen minutes a conductivity scan was performed. As illustrated in figure 4.13, there was an increase in conductivity of 20% in the two zones of immobilised SiaP within the monolith. This increase in conductivity could be reduced by continuous washing with 10mM HEPES which mirrored all previous sialic acid applications. This result indicated that the increase in the conductivity seen with sialic acid may not be due to a specific interaction between the free sialic acid and the immobilised SiaP protein. It was theorised that the observed increase in conductivity in all previous sialic acid applications were due to non-specific interactions between the sialic acid and protein.

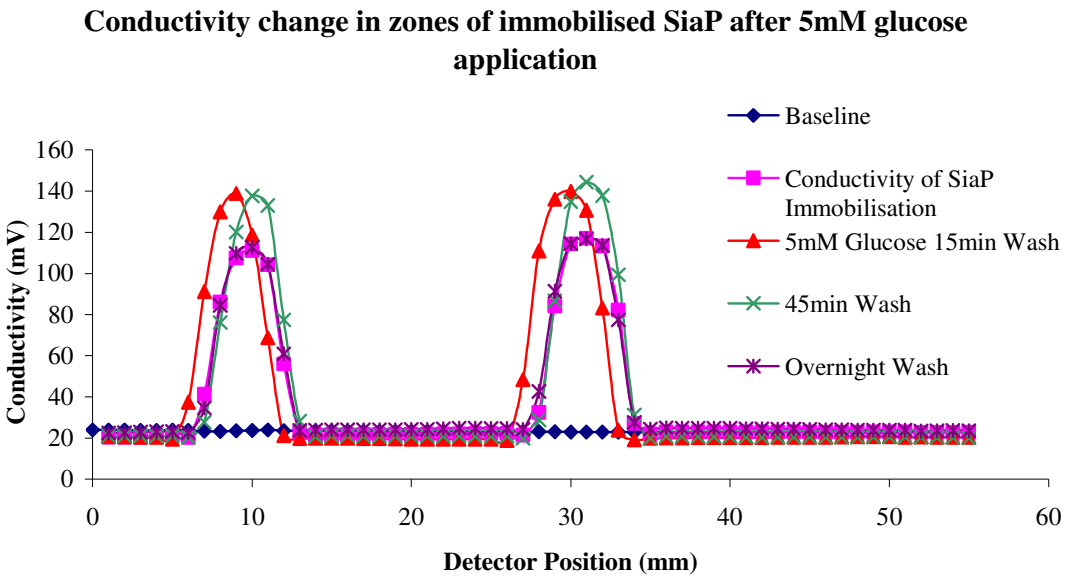

Figure 4.13: The change in conductivity after the application of 5mM glucose to the monolithic column. There was a 20% increase in both SiaP immobilised zones after the addition of glucose. The conductivity scan was performed after set periods of time and the change in conductivity observed. The conductivity had reduced to the original SiaP conductivity after an overnight wash of 10mM HEPES buffer.

4.5: Summary

The preliminary results outlined in this section provide an insight into the future work required for the successful creation of a novel free sialic acid detector. The conductivity measurement allowed for the determination of the extent of capture of the SiaP protein within two distinct functionalised zones within a monolithic column. The effect on conductivity of the addition of differing concentrations of free sialic acid was then studied. An increase in conductivity signified that there was a capture of free sugar by immobilised protein. The increase in conductivity was significantly less for 2.5mM sialic acid than for 5mM sialic acid, indicating a potentially accurate method to measure concentrations of free sugar. The similarity of the changes in the areas of conductivity peaks for two separately applied samples of 5mM Sialic acid indicated a method which had reasonable levels of reproducibility.

When higher concentrations of sialic acid were applied to the monolithic column the increases in conductivity did not match the increase in sialic acid concentration. The conductivity scan for both 7.5mM and 10mM sialic acid applications to the monolithic column showed a lower increase in conductivity than the 5mM application. Also of concern was the fact that the conductivity of the sialic acid applications could be relatively easily reduced to the SiaP conductivity levels by washing with buffer. The affinity between SiaP and sialic acid is known to be high with a Kd of 28nM (Johnston *et al.*, 2008), and a more stringent wash protocol was initially thought to be required.

To examine if the bindings observed were sugar specific free glucose was applied to the monolithic column and conductivity scans performed. The conductivity scan profile achieved for glucose was identical to the scans achieved for the sialic acid application. This indicated that the conductivity profiles of the various concentrations of sialic acid was not due to the specific capture of free sialic acid by immobilised SiaP, but rather a non-specific interaction between the free sugars and the immobilised protein.

This novel method of free sialic acid detection is in a very early stage of development but initial experiments have shown that an interaction between immobilised SiaP protein and a free sugar may be detected by conductivity. It is expected that with further optimisation of protein immobilisation within monoliths coupled with the determination of optimum buffer conditions that an efficient, simple to use, fast and sensitive free sialic acid detector could be developed.

Chapter 5: Discussion and Conclusions

5.1: General Discussion

The aim of this work was (i) the production of a range of specifically tagged model proteins and (ii) to study their effects on protein expression, purification and ultimate immobilisation. It was expected that by studying the variation of the placement and composition of immobilisation tags a more orientation specific immobilisation could be achieved. The experience gained from the tagging and immobilisation of the model protein Green Fluorescent Protein (GFP) was transferred to immobilisation protocols for the specific bio-ligand protein SiaP. In nature this protein captures free sialic acid (Severi *et al.*, 2005). As well as defining an efficient tagging protocol for protein immobilisation, the generation and study of a novel immobilisation activated surface and associated detection method was of vital importance. Monolithic columns have already been described for trypsin immobilisation (Peterson *et al.*, 2003). Monolithic formation took place in a nanoelectrospray needle which was plumbed to a mass spectrometer to detect immobilised trypsin activity. Myoglobin digested by the immobilised trypsin within a monolith was found to give a 80% coverage by mass spectrometry (Peterson *et al.*, 2003)**.** It has also been reported that the activity of immobilised trypsin is not affected by organic solvents (Slysz and Schriemer, 2003). Trypsin activity is not representative of most proteins as it is particularly solvent resistant (Klibanov, 1997). Therefore, the activity of any protein immobilised within monolithic columns can be solvent dependent**,** and will require optimisation for each unique biomolecule.

Achieving qualitative and quantitative information of immobilised protein on monolithic surfaces enclosed within a capillary column presents a challenge. One of the most common techniques used for these measurements is surface plasmon resonance (Homola *et al.*, 1999). This detection technique however can only measure amounts of proteins immobilised on flat planar surfaces and is not applicable to protein immobilisation within monolithic columns. Therefore, a novel detection method was required. Following work previously reported from this group (Connolly *et al.*, 2007) the ability of C^4D detection to measure an immobilisation and interaction event within monolithic columns was studied and assessed.

5.2 Cloning and Tagging of Green Fluorescent Protein

The GFP utilised in this study was a mutated version of the wild type, namely, GFPmut3. This protein was originally generated by selection for increased fluorescence by FACS (Fluorescence-activated cell sorting) (Cormack *et al.*, 1996). This mutant is significant for its increased fluorescence observed in the FACS system, but more importantly it exhibits an increased folding efficiency in *E.coli* bacteria. This ensures that any irregularities in expression were due to the addition of purification and immobilisation tags.

The pQE-30 and pQE-60 expression vectors were utilised for the cloning of GFP with an N or C terminal histidine tags. Both cloning vectors contained six histidine residues, either upstream or downstream of the multiple cloning site, facilitating the translation of a purification tag to the protein of interest. The addition of a second tag by PCR allowed for a highly controllable tagging system, which in turn enabled the generation of a large set of diversely tagged proteins.

Three specific immobilisation tags were added to GFP, which can be split into two distinct groups. The first group, containing a six residue lysine or cysteine tag, relies on covalent chemistry for immobilisation (see Section 1.2.3) (Ichihara *et al.*, 2006, Wong *et al.*, 2009), (Xu and Lam, 2004). The second group contained, a Strep-TagII which is an eight amino acid tag developed as a biological mimic for biotin (Schmidt *et al.*, 1996). This tag allows proteins to be immobilised by the well characterised reaction between streptavidin or streptactin and biotin (Weber *et al.*, 1989).

During the course of this study, it was discovered that the addition of six cysteine residues to GFP resulted in the formation of large protein multimers. This was due to the formation of disulfide bonds which were generated by the oxidation reaction between cysteine residues of the tag. Therefore, GFP was tagged with a single C-terminal cysteine amino acid to remove the majority of reactive cysteine residues from the tag. This tagging approach has already been described. The addition of a single cysteine residue to GFP in place of six residues was found to significantly reduce the formation of high molecular weight multimers. This allowed for a more accurate measurement of the amount of protein immobilised on activated surfaces. The protein expression levels of a number of diversely tagged GFP proteins were then further investigated.

5.3 Protein expression and purification

E.coli is one of the most commonly used hosts of recombinant protein expression (Baneyx, 1999). It facilities protein expression by its relative simplicity, rapid high density growth rate on inexpensive substrates and well characterised genetics which allow for large scale protein production. The optimal *E.coli* strain and temperature conditions for the over-expression of GFP from pVOS1 was investigated. XL10-Gold is a commonly used *E.coli* strain that contains the *lac*I^q allele. This genotype results in a high expression level of the LacI repressor protein, which in turn strongly represses the activity of the P*tac* promoter in the absence of IPTG. BL21 is a commonly used expression strain that is OmpT and Ion protease deficient, which should allow for higher recovery of recombinant proteins (Sørensen and Mortensen, 2005).

The GFP expression vector pVOS1 was transformed into the above *E.coli* strains. The optimal expression temperature and harvest time for both of these strains was investigated. The temperature ranges chosen for the study of protein expression was 30°C, 37°C and a combination of both temperatures. This combination involved growth to the point of induction at 37°C, following induction by IPTG expression**,** carried out at 30°C. The importance of the optimisation of protein expression within *E.coli* has previously been outlined (Georgiou and Valax, 1996). Cultures were allowed to incubate for a defined period, sampling two millilitres routinely at hourly intervals.

SDS-PAGE was utilised to determine an optimum temperature for protein expression (Laemmli, 1970). Control samples were taken from an uninduced culture and run alongside the induced samples to compare protein expression levels. The expression of tagged GFP from the XL10-Gold *E.coli* strain exhibited high levels of expression at all temperatures after overnight incubation (see Figure 3.2.1). XL10-Gold was found to be a leaky expresser due to the presence of GFP in the overnight un-induced sample (see Figure 3.2.1, Lane 10)**.** However, GFP is a non-toxic protein and therefore should not have an effect on cell growth. The folding of GFP in *E.coli* systems is so well defined it is commonly used as a fusion protein to measure the expression and folding of troublesome proteins (Cha *et al.*, 2000). The highest yield of expressed protein was found after overnight expression at 37°C/30°C. GFP was discovered and initially purified from the jellyfish *Aequorea Victoria* (Tsien, 1998)

and evolved to be expressed at the lower temperatures found in a maritime environment. Incubation at 37°C allows for rapid high density growth to the point of induction, while protein expression at 30°C mimics natural expression conditions for GFP.

The greatest yield of over expressed protein in BL21 was found to be present five hours after induction at each temperature. The levels of overnight expression in BL21 were significantly reduced when compared to the five hour sample. During the course of this study GFP was found to be present in the media after overnight expression from BL21. This indicates GFP is released from the cells but further studies are required to investigate this effect which could be due to cell lysis or protein export from the cell. The level of expressed protein in BL21 appeared to be less than the levels of expressed protein in XL10-Gold by visualisation of SDS-PAGE analysis. Due to this finding all future proteins were expressed overnight at 37°C/30°C from XL10-Gold. During the course of the study all expressed protein was purified from the soluble fraction, with insoluble fractions exhibiting little fluorescence.

The established optimal protein expression protocol for pVOS1 was used for the expression for all subsequent GFP clones (see Figures 3.2.4 to 3.2.7). GFP was over expressed from twelve clones successful. Three clones (pVOS9, pVOS10 and pVOS11) showed a distinct reduction in the levels of protein expression over the average expression levels exhibited by the other over-expressing clones. These three clones were tagged at their N-termini with a protein immobilisation tag and at their C-termini with a histidine tag. This result correlates with results achieved previously (Ichihara *et al.*, 2006). This group studied the effect of tagging on the expression of eGFP (enhanced Green Fluorescent Protein). When a five residue cysteine tag was added to the N-terminal the levels of protein expression fell when compared to eGFP which was cysteine tagged at the C-terminus. Interestingly, a second group added a hexa-arginine to the N-termini of GFP and reported no effect in protein expression levels (Nock *et al.*, 1997).

Therefore, it was concluded that the addition of poly-lysine/cysteine tag or a Strep-TagII to the N-termini of this protein severely affected the levels of expressed protein within the soluble fraction (see Figure 3.2.7). The fusion of these three tags, in particular the lysine and cysteine with six repeat residues, directly downstream from the promoter region of the vector, may have affected the initial transcription process, and lead to the reduction in overall protein expression. When both the purification

and immobilisation tags were placed at the N-termini the level of protein expression was not affected. As illustrated in figure 3.2.6 the placement of the protein purification tag immediately downstream from the promoter region did not effect protein expression. This result indicates that the specific location of the immobilisation tag was the cause of the observed reduction in expression levels.

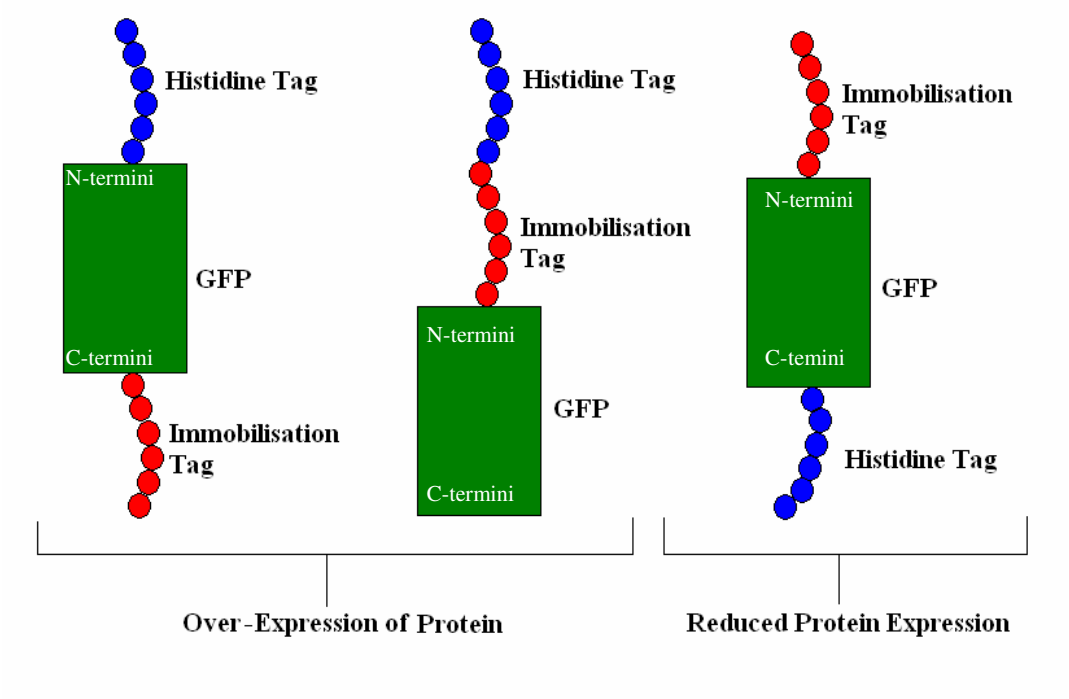

Figure 5.1: Graphical representation of tagged GFP and the tags effect on protein expression levels

The result illustrated in figure 5.1 justified the work undertaken to produce a number of differently tagged proteins and to study their effects on protein expression. The three clones (pVOS9, pVOS10 & pVOS11) were then deemed unsuitable for future work.

Once the optimal conditions of recombinant protein expression were evaluated a purification strategy was investigated to maximise the recovery of recombinant protein from the soluble cell extract while maintaining a high level of purity. The expression plasmid pVOS1 was used to establish an optimal protein purification protocol. Expression of GFP with this plasmid included an addition of six histidine residues to the C-terminus to the expressed protein. IMAC purification strategies were employed for the purification of the expressed protein utilising nickel sepharose resin coupled with step wise elution with imidazole (Porath *et al.*, 1975, Nilsson *et*

al., 1997). The imidazole gradient (see figure 3.2.8) found that histidine tagged GFP remained bound to the resin at concentrations of imidazole up to 80mM. After several column volumes of washing with 80mM imidazole an elution buffer wash of 250mM imidazole was found to elute histidine tagged protein from the nickel resin column (see figure 3.2.9)**.** This optimal protein purification protocol was successfully applied to the remaining clones (see Figures 3.2.10 to 3.2.14)**.** The exception to this purification method was the clones which were not over-expressed in the soluble fraction (see Figure 3.2.12, Gel D and Figure 3.2.13).

Samples of hexa-cysteine tagged purified proteins, when examined on SDS-PAGE gels, were found to contain high molecular weight contaminant bands. To investigate if these high molecular weight bands were due to possible disulfide bond formation between cysteine residues, proteins were examined on SDS-PAGE gels in a non-reducing environment. Figure 3.2.16 showed that a DTT concentration of 50mM greatly reduced the amount of high molecular weight protein bands visible in the SDS-PAGE gel (Cleland, 2002). This indicates that the larger protein bands were multimeric GFP products produced by the oxidisation of cysteines between immobilisation tags to form cystine residues. This finding led to the creation of an additional clone for the expression of GFP with a single cysteine residue on the C-terminus. SDS-PAGE analysis of expressed GFP purified from this clone reveals dimer formation. By limiting the number of cysteine residues within the immobilisation tag to one, the formation of large multimers is significantly reduced. Dimer formation persists due to the single cysteine residue being available for oxidation by a second identically tagged protein.

5.4 Biotinylated GFP immobilisation onto 96 well plates

Biotinylated GFP was captured on 96 well NUNC MaxiSorp plates by immobilised streptavidin or its mutant streptactin. This mutant streptactin has been reported to have a higher affinity for the Step-TagII (Voss and Skerra, 1997). The capture and immobilisation of GFP which has been tagged with Strep-TagII can be directly monitored by fluorescence (as outlined in section 3.3). The GFP proteins which were tagged with the covalent immobilisation tags (hexa-lysine and cysteine) require further modification to be captured by streptavidin/tactin. Both cysteine and lysine tagged GFPs were tagged with heterofunctional biolinkers based on the respective

chemistries of their added immobilisation tags (see Figure 3.3.1) (Wong *et al.*, 2009). The lysine tagged protein was biotinylated with a linker which contained a NHS reactive moiety, while the cysteine tagged protein was biotinylated with a linker which contained a maleimide moiety as discussed in section 3.3.2. In this way, the effectiveness of the addition of these immobilisation tags can be directly related to the amount of biotinylated GFP captured by immobilised streptavidin or streptactin. Optimum immobilisation and excitation and emission wavelength conditions were initially determined. Both wavelength values were identical to the values originally described in the creation of the GFPmut3 mutant (Cormack *et al.*, 1996). It was found that the highest fluorescence values achieved were after immobilisation of 5µg/ml streptavidin/tactin for an hour at room temperature before probing with 50µg/ml of biotinylated GFP. The capture of biotinylated GFP by immobilised streptactin was found to be five-fold greater than that bound by streptavidin (see Figure 3.3.9)**.** This was mirrored across all tagged proteins whether they were biotinylated with the NHS-biotin linker, the maleimide-biotin linker or the Strep-TagII. The significant increase in the levels of protein capture may be attributed to the changes in the binding pockets between streptavidin and its mutant streptactin (Korndorfer and Skerra, 2002). It was theorised by our group that the mutated flexible loop of the streptactin protein outlined in the previous report, allows for greater availability of the binding site for the biotin moiety.

The level of fluorescence seen with the immobilisation of the GFP tagged with Strep-TagII was significantly lower than the proteins which were biotinylated with the biotinylation linkers. The immobilisation of the tetrameric streptavidin and streptactin proteins can theoretically bind up to four biotinylated proteins (Diamandis and Christopoulos, 1991). The linker used for the biotinylation of both the cysteine and lysine tag acts as a spacer between the biotin moiety and GFP. As the added Strep-TagII is in close proximity to the point of capture of GFP by a subunit of the multimeric streptavidin/tactin it may obstruct binding at other subunits. Due to time constraints a GFP protein which contained a linker separating the GFP and Strep-TagII could not be generated. This protein would establish whether steric hindrance played a role in the amount of biotinylated protein captured by immobilised streptavidin or streptactin.

The levels of captured biotinylated tagged proteins demonstrated unexpected result. The biotinylated GFP which contained no additional lysine residues showed up to a

33% higher level of capture/immobilisation when compared to the biotinylated GFP which contained the added lysine tag. This effect was found when the protein was captured by either streptavidin or streptactin indicating it is capture molecule independent.

When comparing the fluorescence levels of cysteine tagged biotinylated GFP there was a 500% increased capture by the biotinylated GFP with a six residue cysteine tag when compared to the GFP with a single cysteine residue at the C-terminus and an 1100% increase when compared to the untagged GFP protein which was biotinylated with the same linker. Wild type GFP contains two cysteine residues within the amino acid sequence and both are buried within the structure of the protein (Tsien, 1998)**.** These cysteine residues are not available for the biotinylation reaction. Wild type GFP was not biotinylated with the maleimide linker and therefore was not found to be captured by immobilised streptavidin/tactin.

5.5 Orientation specific immobilisation of the model protein GFP within monolithic columns

The immobilisation of proteins within a monolithic column is a relatively recent development (Rangan Mallik, 2006). There are examples of the use of immobilised proteins within monolithic column for protein mapping (Frantisek, 2006). Similarily the use of conductivity for detection within capillary electrophoresis is a commonly used method (Zemann, 2003). To date, there has not been an attempt to detect protein immobilsation or interactions within monolithic columns using this conductivity method.

The use of GFP for this experiment allowed for cross-confirmation of protein immobilisaiton within the monolithic column by both fluorescence and conductivity. Significant optimisation was carried out in this work to develop protocols which allowed for the reproducible and controllable creation of monoliths. The immobilisation of proteins within the monolithic columns also required a significant degree of optimisation to account for possible non-specific changes in conductivity.

Experiments were performed to determine if the addition of six extra lysine residues to the C-terminus increased the amount of protein specifically immobilsed within the monolith. The level of protein immobilisation was determined by the change in the

conductivity due to a change in the monoliths abilty to conduct a current. The ability to conduct a current is altered by a proteins net charge. The addition of six extra lysine residues to a GFP protein causes a 200% increase in the conductivity where the protein is immobilised in the of the functionalised zones within a monolith (see figure 3.4.6). Therefore in all subsequent experiments proteins were tagged with additional lysine residues for immobilisation within monolithic columns. The method of immobilisation used for the capture of lysine tagged GFP within monolithic columns made use of the inherent or added lysine residues. The increase in the conductivity of lysine tagged GFP in comparsion to non-tagged GFP suggests that the majority of the immobilised protein is orientation specific.

However, due to the presence of inherent lysine residues, all immobilised protein may not be specifically orientated. Therefore, in an attempt to achieve a more reliable orientation specific protein immobilisation, biotinylated GFP was captured by immobilised streptavidin. As previously outlined the tetrameric protein, strepavidin was immobilised by its inherent lysines within two zones of vinyl-azlactone functionalised monolithic column (see Section 3.4.5). Initial studies indicated that the optimium buffer used for the capture of biotinylated proteins by immobilised streptavidin was the low conductivity HEPES buffer. The low conductivity of this buffer was vital as it would not mask any changes in conductivity within the functionalised zones. Biotinylated and un-biotinylated GFP proteins were passed over streptavidin functionalised zones of the monolithic column. When GFP was passed through the column, the conductivity values of the two functional zones increased for both biotinylated or un-biotinylated proteins by approximately 66%. The capture of both forms of tagged GFPs by immobilised streptavidin was confirmed by fluorescence measurement. The capture of un-biotinylated GFP indicated that the interaction between streptavidin and GFP was not due to biotinylation. This was theorised to be due to protein protein interactions (Jones and Thornton, 1996). To confirm this theory, 1M NaCl solution was passed over the column in an attempt to disrupt the interaction (Phizicky and Fields, 1995). The high salt conconcentration wash reduced the level of fluorescence which could be visulised within the monolithic column but did not remove it completely. The conductivity of the washed column however increased due to the high conductivity of the salt. After two days of continious washing with 10mM HEPES the conductivity was reduced by 12.5% (see Figure 3.4.14).

These results indicate that it is possible to measure protein immobilisation in monolithic columns by measuring changes in conductivity. Furthermore , the addition of a six residue lysine tag was found to increase protein immobilisation within monolithic columns, most likely, in an orientation specific manner. Finally to achieve an orientated immobilisation of biotinylated proteins with monolithic column requires further optimisation as there are non-specific protein-protein interactions involved.

5.6 Model System; The capture of sialic acid by immobilised SiaP within monolithic columns and detection by C4D

Utilising optimised protocols a protein with a high affinity for free sialic acid (SiaP) was immobilised within vinyl-azlactone functionalised zones of a monolithic column. The change in conductivity of the SiaP functionalised zones with the addition of 5mM sialic acid was measured. The conductivity of the column increased in both immobilised protein zones by approximately 33% (see Figure 4.3). Hourly conductivity scans were performed during continous washing of the monolith with 10mM HEPES. The conductivity of the immobilised SiaP zones were found to ultimately reduce over time by 33% to the original SiaP conductivity baseline. Reproducability of the system was confirmed by re-application of 5mM sialic acid to this column. The resulting change in conductivity mirrored previous 5mM sialic acid conductivity readings. This indicates that measureing changes in conductivity of immobilised SiaP is potentially a possible method for the determination of free sialic acid concentration.

Continuous washing with buffer reduced the conductivity of the first zone to the SiaP conductivity baseline prior to the reduction of the conductivity in the second zone. It was theorised that the free sialic acid removed from the first zone by washing is recaptured by the second zone of immobilised SiaP. A concentration of 2.5mM sialic acid was applied to the column to determine the detection limit of this method. When half the concentration of free sialic acid (5mM to 2.5mM) was appied to the monolith, a fifty percent reduction in the conductivity change was observed (see Figure 4.7). However, when 7.5mM and 10mM of sialic acid was applied to this column the change in conductivity did not mirror corresponding increase in sialic acid concentration (see Figures 4.11 and 4.12).

It was theorised that the capture of sialic acid was not a specific capture by SiaP but rather a non-specific interaction. In an attempt to determine whether this binding was sugar-specific, glucose was applied to the column. This application of glucose was found to increase the level of conductivity within the two zones of immobilsed SiaP (see Figure 4.13) indicating that the changes in the conductivity found with sialic acid, may not be due to specific capture of sialic acid by the immobilised SiaP. Further study is required to determine if this 'system' can specifically measure the level of free sialic acid in solution.

5.7 Conclusions and Future Work

This study has described results that clearly show the effects of adding different affinity and immobilisation tags to protein expression, purification and immobilisation.

The potential use of conductivity detection to determine the capture of biotinylated protein to streptavidin has been confirmed. This detection method cannot however distinguish between protein to protein interactions and biotin-streptavidin interactions. More experimentation will be required to optimise the capture of biotinylated proteins by immobilised streptavidin within monolithic columns. These experiments should include changing the buffering conditions to favour biotin-streptavidin reactions while inhibiting protein to protein interactions. The optimisation of this immobilisation method will allow for the development of an extremely novel functionalised surface, which will allow for the immobilisation of orientation specific proteins.

The protein SiaP, exhibits a high affinity for free sialic acid (Severi *et al.*, 2005). Preliminary results indicate that the capture of sialic acid by immobilised SiaP within monolithic columns can be detected by a change in conductivity. The change in conductivity observed may not be due to the capture of sialic acid by SiaP but may be due to non-specific sugar-protein interactions. Further experiments should be performed to determine how to reduce the level of these non-specific interactions while increase binding of sialic acid by SiaP. The optimisation of this protocol is also required, such as the determination of the detection limits, sample application times

and regeneration of the immobilised SiaP 'surface'. The development of a rapid and reliable free sialic acid monitor would generate an extremely novel on-line detector.

The correct degree of sialylation of glycoproteins can significantly improve their activity, immunogenetic characteristics and blood retention time (Byrne *et al.*, 2007). The development of a method which can measure the concentration of free sialic acid during the cell culture process would prove an important development in the optimisation of the biopharmaceutical processes.

The level of protein immobilisation within monolithic columns has to be compared to levels of protein immobilisation on other surfaces such as glass slides, resins, and nitrocellulose. As previously outlined the immobilisation of proteins on such surfaces can be achieved by many different methods, most commonly through absorption, covalent immobilisation or bio-affinity methods (Wong *et al.*, 2009).

A disadvantage of using monolithic columns is this surface cannot match the quantity of unique proteins immobilised on commonly used surfaces such as glass slides, due to current methods of monolithic column functionalisation. For example over 10,000 unique proteins have been immobilised on functionalised glass slides. (Macbeath and Schreiber, 2000).

One of the major challenges for this conductivity detection method is to increase its sensitivity. Biosensors which have been generated with immobilised proteins exhibit impressive detection limits. A biosensor for the detection of PSA (prostate-specific antigen) has been generated which can detect levels of 0.2 to 60ng/ml from a background of human serum albumin (Wu *et al.*, 2001). Even more impressively 40ρg/ml of B-type natriuretic peptide, which is a biomarker for heart failure, has been detected by a biosensor (Mizutani, 2008). These detection limits compare extremely well when compared to the 2.5mM limit of sialic acid detection which has been currently achieved by the conductivity method. Though detection limit comparisons between the different biosensors are not entirely accurate due to the different surfaces used in biosensor creation.

Monoliths which were developed originally for liquid chromatography (Svec and Frechet, 1992), have in recent times achieved notice as potential surfaces for biosensors (Logan *et al.*, 2007, Frantisek, 2006, Peterson *et al.*, 2003). To date no 'on-column' detection method has been outlined, with all monoliths being attached to MALDI-MS or MALDI-TOF to determine reactions which have taken place with the column (Peterson *et al.*, 2002). It has been found that the levels of bio-molecules

immobilised with monolithic columns have been difficult to quantify. Normal procedures involve destroying the monolith and performing standard protein quantification assays on the destroyed column. The development of a protein detection method for monolithic columns therefore is a timely and necessary method and conductivity has already been described to detect immobilised protein within monoliths (Connolly *et al.*, 2007).

Finally the well characterised advantages of monolithic columns such as low sample volumes and high throughput coupled with a sensitive and easy to use detection method such as C^4D would allow for the creation of extremely novel bio-surfaces. If the few remaining scientific limitations can be over-come a new vista of protein immobilisation surfaces and detection will become visible.

Chapter 6: References

A

Allen, S., Zaleski, A., Johnston, J. W., Gibson, B. W. & Apicella, M. A. 2005. Novel Sialic Acid Transporter of Haemophilus influenzae†. *Infect Immun,* **73,** 5291-300.

Argarana, C. E., Kuntz, I. D., Birken, S., Axel, R. & Cantor, C. R. 1986. Molecular cloning and nucleotide sequence of the streptavidin gene. *Nucleic Acids Res,* **14,** 1871-82.

Arvidsson, P., Plieva, F. M., Savina, I. N., Lozinsky, V. I., Fexby, S., Bülow, L., Yu. Galaev, I. & Mattiasson, B. 2002. Chromatography of microbial cells using continuous supermacroporous affinity and ion-exchange columns. *Journal Of Chromatography A,* **977,** 27-38.

B

Baneyx, F. 1999. Recombinant protein expression in Escherichia coli. *Current Opinion in Biotechnology,* **10,** 411-421.

Bauer, S. H. J., Månsson, M., Hood, D. W., Richards, J. C., Moxon, E. R. & Schweda, E. K. H. 2001. A rapid and sensitive procedure for determination of 5-N-acetyl neuraminic acid in lipopolysaccharides of Haemophilus influenzae: a survey of 24 non-typeable H. influenzae strains. *Carbohydrate Research,* **335,** 251-260.

Bedair, M. & Oleschuk, R. D. 2006. Lectin affinity chromatography using porous polymer monolith assisted nanoelectrospray MS/MS. *Analyst,* **131,** 1316-21.

Blum, H., Beier, H. & Gross, H. J. 1987. Improved silver staining of plant proteins, RNA and DNA in polyacrylamide gels. *Electrophoresis,* **8,** 93-99.

Bouchet, V., Hood, D. W., Li, J., Brisson, J.-R., Randle, G. A., Martin, A., Li, Z., Goldstein, R., Schweda, E. K. H., Pelton, S. I., Richards, J. C. & Moxon, E. R. 2003. Host-derived sialic acid is incorporated into Haemophilus influenzae lipopolysaccharide and is a major virulence factor in experimental otitis media. *Proceedings of the National Academy of Sciences of the United States of America,* **100,** 8898-8903.

Bujard, H., Gentz, R., Lanzer, M., Stueber, D., Mueller, M., Ibrahimi, I., Haeuptle, M. T. & Dobberstein, B. 1987. A T5 promoter-based transcription-translation system for the analysis of proteins in vitro and in vivo. *Methods Enzymol,* **155,** 416-33.

Byrne, B., Donohoe, G. G. & O' Kennedy, R. 2007. Sialic acids: carbohydrate moieties that influence the biological and physical properties of biopharmaceutical proteins and living cells. *Drug Discovery Today,* **12,** 319-326.

C

Cabantous, S., Rogers, Y., Terwilliger, T. C. & Waldo, G. S. 2008. New molecular reporters for rapid protein folding assays. *PLoS One,* **3,** e2387.

Cabantous, S., Terwilliger, T. C. & Waldo, G. S. 2005. Protein tagging and detection with engineered self-assembling fragments of green fluorescent protein. *Nat Biotechnol,* **23,** 102-7.

Cha, H. J., Wu, C. F., Valdes, J. J., Rao, G. & Bentley, W. E. 2000. Observations of green fluorescent protein as a fusion partner in genetically engineered Escherichia coli: monitoring protein expression and solubility. *Biotechnol Bioeng,* **67,** 565-74.

Chalfie, M., Tu, Y., Euskirchen, G., Ward, W. & Prasher, D. 1994. Green fluorescent protein as a marker for gene expression. *Science,* **263,** 802-805.

Cheeks, M. C., Kamal, N., Sorrell, A., Darling, D., Farzaneh, F. & Slater, N. K. H. 2009. Immobilized metal affinity chromatography of histidine-tagged lentiviral vectors using monolithic adsorbents. *Journal Of Chromatography A,* **1216,** 2705-2711.

Cleland, W. W. 2002. Dithiothreitol, a New Protective Reagent for SH Groups*. *Biochemistry,* **3,** 480-482.

Cody, C. W., Prasher, D. C., Westler, W. M., Prendergast, F. G. & Ward, W. W. 1993. Chemical structure of the hexapeptide chromophore of the Aequorea green-fluorescent protein. *Biochemistry,* **32,** 1212-8.

Connolly, D., O'Shea, V., Clarke, P., O'Connor, B. & Paull, B. 2007. Evaluation of photografted charged sites within polymer monoliths in capillary columns using

contactless conductivity detection. *Journal of Separation Science,* **30,** 3060-3068.

Cordiano, I., Steffan, A., Randi, M. L., Pradella, P., Girolami, A. & Fabris, F. 1995. Biotin-avidin immobilization of platelet glycoproteins (BAIPG): a new capture assay for the detection of anti-platelet antibodies. *J Immunol Methods,* **178,** 121-30.

Cormack, B. P., Valdivia, R. H. & Falkow, S. 1996. FACS-optimized mutants of the green fluorescent protein (GFP). *Gene,* **173,** 33-38.

Crameri, A., Whitehorn, E. A., Tate, E. & Stemmer, W. P. 1996. Improved green fluorescent protein by molecular evolution using DNA shuffling. *Nat Biotechnol,* **14,** 315-9.

Cubitt, A. B., Heim, R., Adams, S. R., Boyd, A. E., Gross, L. A. & Tsien, R. Y. 1995. Understanding, improving and using green fluorescent proteins. *Trends in Biochemical Sciences,* **20,** 448-455.

D

David A. Zacharias & Roger Y. Tsien 2005. Molecular Biology and Mutation of Green Fluorescent Protein. *In:* MARTIN CHALFIE, S. R. K. (ed.) *Green Fluorescent Protein (Second Edition).*

Diamandis, E. P. & Christopoulos, T. K. 1991. The biotin-(strept)avidin system: principles and applications in biotechnology. *Clin Chem,* **37,** 625-36.

Duckworth, B. P., Xu, J., Taton, T. A., Guo, A. & Distefano, M. D. 2006. Site-Specific, Covalent Attachment of Proteins to a Solid Surface. *Bioconjugate Chemistry,* **17,** 967-974

E

Ericson, C., Liao, J.-L., Nakazato, K. & Hjertén, S. 1997. Preparation of continuous beds for electrochromatography and reversed-phase liquid chromatography of low-molecular-mass compounds. *Journal of Chromatography A,* **767,** 33.

F

Fernandes, A. I. & Gregoriadis, G. 2001. The effect of polysialylation on the immunogenicity and antigenicity of asparaginase: implication in its pharmacokinetics. *International Journal of Pharmaceutics,* **217,** 215-224.

Fleischmann, R., Adams, M., White, O., Clayton, R., Kirkness, E., Kerlavage, A., Bult, C., Tomb, J., Dougherty, B., Merrick, J. & Al., E. 1995. Whole-genome random sequencing and assembly of Haemophilus influenzae Rd. *Science,* **269,** 496-512.

Fracassi Da Silva, J. A. & Do Lago, C. L. 1998. An Oscillometric Detector for Capillary Electrophoresis. *Anal. Chem.,* **70,** 4339-4343.

Frantisek, S. 2006. Less common applications of monoliths: I. Microscale protein mapping with proteolytic enzymes immobilized on monolithic supports. *Electrophoresis,* **27,** 947-961.

G

Georgiou, G. & Valax, P. 1996. Expression of correctly folded proteins in Escherichia coli. *Current Opinion in Biotechnology,* **7,** 190-197.

Geyer, H. & Geyer, R. 2006. Strategies for analysis of glycoprotein glycosylation. *Biochimica et Biophysica Acta (BBA) - Proteins & Proteomics,* **1764,** 1853-1869.

Gonzalez, M., Bagatolli, L. A., Echabe, I., Arrondo, J. L., Argarana, C. E., Cantor, C. R. & Fidelio, G. D. 1997. Interaction of biotin with streptavidin. Thermostability and conformational changes upon binding. *J Biol Chem,* **272,** 11288-94.

Gorokhovatsky, A. Y., Rudenko, N. V., Marchenkov, V. V., Skosyrev, V. S., Arzhanov, M. A., Burkhardt, N., Zakharov, M. V., Semisotnov, G. V., Vinokurov, L. M. & Alakhov, Y. B. 2003. Homogeneous assay for biotin based on Aequorea victoria bioluminescence resonance energy transfer system. *Anal Biochem,* **313,** 68-75.

Griesbeck, O., Baird, G. S., Campbell, R. E., Zacharias, D. A. & Tsien, R. Y. 2001. Reducing the Environmental Sensitivity of Yellow Fluorescent Protein. Mechanism and Applications. *J. Biol. Chem.,* **276,** 29188-29194.

Guijt, R. M., Evenhuis, C. J., Macka, M. & Haddad, P. R. 2004. Conductivity detection for conventional and miniaturised capillary electrophoresis systems. *Electrophoresis,* **25,** 4032-4057.

Gupalova, T. V., Lojkina, O. V., Pàlàgnuk, V. G., Totolian, A. A. & Tennikova, T. B. 2002. Quantitative investigation of the affinity properties of different recombinant forms of protein G by means of high-performance monolithic chromatography. *Journal Of Chromatography A,* **949,** 185-193.

H

Hartmuth C. Kolb, M. G. Finn & K. Barry Sharpless 2001. Click Chemistry: Diverse Chemical Function from a Few Good Reactions. *Angewandte Chemie International Edition,* **40,** 2004-2021.

Heim, R., Prasher, D. C. & Tsien, R. Y. 1994. Wavelength mutations and posttranslational autoxidation of green fluorescent protein. *Proc Natl Acad Sci U S A,* **91,** 12501-4.

Heim, R. & Tsien, R. Y. 1996. Engineering green fluorescent protein for improved brightness, longer wavelengths and fluorescence resonance energy transfer. *Curr Biol,* **6,** 178-82.

Homola, J., Yee, S. S. & Gauglitz, G. 1999. Surface plasmon resonance sensors: review. *Sensors and Actuators B: Chemical,* **54,** 3-15.

Hood, D. W., Makepeace, K., Deadman, M. E., Rest, R. F., Thibault, P., Martin, A., Richards, J. C. & Moxon, E. R. 1999. Sialic acid in the lipopolysaccharide of *Haemophilus influenzae*: strain distribution, influence on serum resistance and structural characterization. *Molecular Microbiology,* **33,** 679-692.

I

Ichihara, T., Akada, J. K., Kamei, S., Ohshiro, S., Sato, D., Fujimoto, M., Kuramitsu, Y. & Nakamura, K. 2006. A Novel Approach of Protein Immobilization for Protein Chips Using an Oligo-Cysteine Tag. *J. Proteome Res.,* **5,** 2144-2151.

Inoue, H., Nojima, H. & Okayama, H. 1990. High efficiency transformation of Escherichia coli with plasmids. *Gene,* **96,** 23-8.

J

Jiang, T., Mallik, R. & Hage, D. S. 2005. Affinity Monoliths for Ultrafast Immunoextraction. *Analytical Chemistry,* **77,** 2362-2372.

Johnston, J. W., Coussens, N. P., Allen, S., Houtman, J. C. D., Turner, K. H., Zaleski, A., Ramaswamy, S., Gibson, B. W. & Apicella, M. A. 2008. Characterization of the N-Acetyl-5-neuraminic Acid-binding Site of the Extracytoplasmic Solute Receptor (SiaP) of Nontypeable Haemophilus influenzae Strain 2019. *Journal of Biological Chemistry,* **283,** 855-865.

Jones, S. & Thornton, J. M. 1996. Principles of protein-protein interactions. *Proceedings of the National Academy of Sciences of the United States of America,* **93,** 13-20.

K

Kalia, J., Abbott, N. L. & Raines, R. T. 2007. General method for site-specific protein immobilization by Staudinger ligation. *Bioconjug Chem,* **18,** 1064-9.

Khan, F., He, M. & Taussig, M. J. 2006. Double-Hexahistidine Tag with High-Affinity Binding for Protein Immobilization, Purification, and Detection on Ni–Nitrilotriacetic Acid Surfaces. *Analytical Chemistry,* **78,** 3072-3079.

Klibanov, A. M. 1997. Why are enzymes less active in organic solvents than in water? *Trends in Biotechnology,* **15,** 97-101.

Koch, B., Jensen, L. E. & Nybroe, O. 2001. A panel of Tn7-based vectors for insertion of the gfp marker gene or for delivery of cloned DNA into Gram-negative bacteria at a neutral chromosomal site. *Journal of Microbiological Methods,* **45**, 187-195.

Korndorfer, I. P. & Skerra, A. 2002. Improved affinity of engineered streptavidin for the Strep-tag II peptide is due to a fixed open conformation of the lid-like loop at the binding site. *Protein Sci,* **11,** 883-93.

L

Laemmli, U. K. 1970. Cleavage of Structural Proteins during the Assembly of the Head of Bacteriophage T4. *Nature,* **227,** 680-685.

Laitinen, O. H., Hytonen, V. P., Nordlund, H. R. & Kulomaa, M. S. 2006. Genetically engineered avidins and streptavidins. *Cell Mol Life Sci,* **63,** 2992-3017.

Laitinen, O. H., Nordlund, H. R., Hytonen, V. P. & Kulomaa, M. S. 2007. Brave new (strept)avidins in biotechnology. *Trends Biotechnol*.

Lee, D., Svec, F. & Fréchet, J. M. J. 2004. Photopolymerized monolithic capillary columns for rapid micro high-performance liquid chromatographic separation of proteins. *Journal of Chromatography A,* **1051,** 53.

Li, X., Zhang, G., Ngo, N., Zhao, X., Kain, S. R. & Huang, C. C. 1997. Deletions of the Aequorea victoria green fluorescent protein define the minimal domain required for fluorescence. *J Biol Chem,* **272,** 28545-9.

Logan, T. C., Clark, D. S., Stachowiak, T. B., Svec, F. & Frechet, J. M. J. 2007. Photopatterning Enzymes on Polymer Monoliths in Microfluidic Devices for Steady-State Kinetic Analysis and Spatially Separated Multi-Enzyme Reactions. *Analytical Chemistry,* **79,** 6592-6598.

Luo, Q., Zou, H., Zhang, Q., Xiao, X. & Ni, J. 2002. High-performance affinity chromatography with immobilization of protein A and L-histidine on molded monolith. *Biotechnology and Bioengineering,* **80,** 481-489.

M

Macbeath, G., Koehler, A. N. & Schreiber, S. L. 1999. Printing Small Molecules as Microarrays and Detecting Protein-Ligand Interactions en Masse. *J. Am. Chem. Soc.***,** 7967-7968.

Macbeath, G. & Schreiber, S. L. 2000. Printing proteins as microarrays for high-throughput function determination. *Science,* **289,** 1760-3.

Mandrell, R. E., Mclaughlin, R., Aba Kwaik, Y., Lesse, A., Yamasaki, R., Gibson, B., Spinola, S. M. & Apicella, M. A. 1992. Lipooligosaccharides (LOS) of some Haemophilus species mimic human glycosphingolipids, and some LOS are sialylated. *Infect. Immun.,* **60,** 1322-1328.

Mather, B. D., Viswanathan, K., Miller, K. M. & Long, T. E. 2006. Michael addition reactions in macromolecular design for emerging technologies. *Progress in Polymer Science,* **31,** 487-531.

Matz, M. V., Fradkov, A. F., Labas, Y. A., Savitsky, A. P., Zaraisky, A. G., Markelov, M. L. & Lukyanov, S. A. 1999. Fluorescent proteins from nonbioluminescent Anthozoa species. *Nat Biotechnol,* **17,** 969-73.

Mizutani, F. 2008. Biosensors utilizing monolayers on electrode surfaces. *Sensors and Actuators B: Chemical,* **130,** 14-20.

Morise, H., Shimomura, O., Johnson, F. H. & Winant, J. 1974. Intermolecular energy transfer in the bioluminescent system of Aequorea. *Biochemistry,* **13,** 2656-2662.

Muller, A., Severi, E., Mulligan, C., Watts, A. G., Kelly, D. J., Wilson, K. S., Wilkinson, A. J. & Thomas, G. H. 2006. Conservation of Structure and Mechanism in Primary and Secondary Transporters Exemplified by SiaP, a Sialic Acid Binding Virulence Factor from Haemophilus influenzae. *J. Biol. Chem.,* **281,** 22212-22222.

N

Nilsson, J., Ståhl, S., Lundeberg, J., Uhlén, M. & Nygren, P.-Å. 1997. Affinity Fusion Strategies for Detection, Purification, and Immobilization of Recombinant Proteins. *Protein Expression and Purification,* **11,** 1-16.

Nock, S., Spudich, J. A. & Wagner, P. 1997. Reversible, site-specific immobilization of polyarginine-tagged fusion proteins on mica surfaces. *FEBS Lett,* **414,** 233-8.

O

Olli, H. L., Kari, J. A., Ari, T. M., Tikva, K., Eevaleena, P., Edward, A. B., Meir, W. & Markku, S. K. 1999. Mutation of a critical tryptophan to lysine in avidin or streptavidin may explain why sea urchin fibropellin adopts an avidin-like domain. *FEBS Letters,* **461,** 52-58.

Ormo, M., Cubitt, A. B., Kallio, K., Gross, L. A., Tsien, R. Y. & Remington, S. J. 1996. Crystal structure of the Aequorea victoria green fluorescent protein. *Science,* **273,** 1392-5.

Osamu Shimomura, Frank H. Johnson & Yo Saiga 1962. Extraction, Purification and Properties of Aequorin, a Bioluminescent Protein from the Luminous Hydromedusan, *Aequorea. Journal of Cellular and Comparative Physiology,* **59,** 223-239.

Ostryanina, N. D., Vlasov, G. P. & Tennikova, T. B. 2002. Multifunctional fractionation of polyclonal antibodies by immunoaffinity high-performance monolithic disk chromatography. *J Chromatogr A,* **949,** 163-71.

P

Pace, C. N., Treviño, S., Prabhakaran, E. & Scholtz, J. M. 2004. Protein structure, stability and solubility in water and other solvents. *Philosophical Transactions of the Royal Society of London. Series B: Biological Sciences,* **359,** 1225-1235.

Palm, G. J., Zdanov, A., Gaitanaris, G. A., Stauber, R., Pavlakis, G. N. & Wlodawer, A. 1997. The structural basis for spectral variations in green fluorescent protein. *Nat Struct Mol Biol,* **4,** 361-365.

Patterson, G. H., Knobel, S. M., Sharif, W. D., Kain, S. R. & Piston, D. W. 1997. Use of the green fluorescent protein and its mutants in quantitative fluorescence microscopy. *Biophysical Journal,* **73,** 2782-2790.

Peterka, M., Jarc, M., Banjac, M., Frankovic, V., Bencina, K., Merhar, M., Gaberc-Porekar, V., Menart, V., Strancar, A. & Podgornik, A. 2006. Characterisation of metal-chelate methacrylate monoliths. *Journal Of Chromatography A,* **1109,** 80-85.

Peterson, D. S., Rohr, T., Svec, F. & Frechet, J. M. J. 2002. Enzymatic Microreactor-on-a-Chip: Protein Mapping Using Trypsin Immobilized on Porous Polymer Monoliths Molded in Channels of Microfluidic Devices. *Analytical Chemistry,* **74,** 4081-4088.

Peterson, D. S., Rohr, T., Svec, F. & Frechet, J. M. J. 2003. Dual-Function Microanalytical Device by In Situ Photolithographic Grafting of Porous Polymer Monolith: Integrating Solid-Phase Extraction and Enzymatic Digestion for Peptide Mass Mapping. *Anal. Chem.,* **75,** 5328-5335.

Phizicky, E. & Fields, S. 1995. Protein-protein interactions: methods for detection and analysis. *Microbiol. Rev.,* **59,** 94-123.

Porath, J., Carlsson, J., Olsson, I. & Belfrage, G. 1975. Metal chelate affinity chromatography, a new approach to protein fractionation. *Nature,* **258,** 598-599.

Prasher, D. C., Eckenrode, V. K., Ward, W. W., Prendergast, F. G. & Cormier, M. J. 1992. Primary structure of the Aequorea victoria green-fluorescent protein. *Gene,* **111,** 229.

R

Rangan Mallik, D. S. H. 2006. Affinity monolith chromatography. *Journal of Separation Science,* **29,** 1686-1704.

Reid, B. G. & Flynn, G. C. 1997. Chromophore Formation in Green Fluorescent Protein. *Biochemistry,* **36,** 6786-6791.

Reznik, G. O., Vajda, S., Cantor, C. R. & Sano, T. 2001. A streptavidin mutant useful for directed immobilization on solid surfaces. *Bioconjug Chem,* **12,** 1000-4.

Riccardi Cdos, S., Dahmouche, K., Santilli, C. V., Da Costa, P. I. & Yamanaka, H. 2006. Immobilization of streptavidin in sol-gel films: Application on the diagnosis of hepatitis C virus. *Talanta,* **70,** 637-43.

Rieux, L., Niederländer, H., Verpoorte, E. & Bischoff, R. 2005. Silica monolithic columns: Synthesis, characterisation and applications to the analysis of biological molecules. *Journal of Separation Science,* **28,** 1628-1641.

Rusmini, F., Zhong, Z. & Feijen, J. 2007. Protein Immobilization Strategies for Protein Biochips. *Biomacromolecules,* **8,** 1775-1789.

Rybak, J. N., Scheurer, S. B., Neri, D. & Elia, G. 2004. Purification of biotinylated proteins on streptavidin resin: a protocol for quantitative elution. *Proteomics,* **4,** 2296-9.

S

Salih, A., Larkum, A., Cox, G., Kuhl, M. & Hoegh-Guldberg, O. 2000. Fluorescent pigments in corals are photoprotective. *Nature,* **408,** 850-853.

Sano, T. & Cantor, C. R. 1990. Expression of a cloned streptavidin gene in Escherichia coli. *Proc Natl Acad Sci U S A,* **87,** 142-6.

Saxon, E. & Bertozzi, C. R. 2000. Cell surface engineering by a modified Staudinger reaction. *Science,* **287,** 2007-10.

Scaronolínová, V., Kascaroni, V., Ccaron & Ka 2006. Recent applications of conductivity detection in capillary and chip electrophoresis. *Journal of Separation Science,* **29,** 1743-1762.

Schauer, R. 2004. Sialic acids: fascinating sugars in higher animals and man. *Zoology,* **107,** 49-64.

Schmidt, T. G., Koepke, J., Frank, R. & Skerra, A. 1996. Molecular interaction between the Strep-tag affinity peptide and its cognate target, streptavidin. *J Mol Biol,* **255,** 753-66.

Schmidt, T. G. M. & Skerra, A. 1993. The random peptide library-assisted engineering of a C-terminal affinity peptide, useful for the detection and purification of a functional Ig Fv fragment. *Protein Eng.,* **6,** 109-122.

Schweda, E. K. H., Richards, J. C., Hood, D. W. & Moxon, E. R. 2007. Expression and structural diversity of the lipopolysaccharide of Haemophilus influenzae: Implication in virulence. *Quorum sensing in human pathogens,* **297,** 297-306.

Severi, E., Hood, D. W. & Thomas, G. H. 2007. Sialic acid utilization by bacterial pathogens. *Microbiology,* **153,** 2817-22.

Severi, E., Randle, G., Kivlin, P., Whitfield, K., Young, R., Moxon, R., Kelly, D., Hood, D. & Thomas, G. H. 2005. Sialic acid transport in Haemophilus influenzae is essential for lipopolysaccharide sialylation and serum resistance and is dependent on a novel tripartite ATP-independent periplasmic transporter. *Mol Microbiol,* **58,** 1173-85.

Severinov, K. & Muir, T. W. 1998. Expressed protein ligation, a novel method for studying protein-protein interactions in transcription. *J Biol Chem,* **273,** 16205-9.

Sheridan, D. L. & Hughes, T. E. 2004. A faster way to make GFP-based biosensors: two new transposons for creating multicolored libraries of fluorescent fusion proteins. *BMC Biotechnol,* **4,** 17.

Shimomura, O. 1979. Structure of the chromophore of Aequorea green fluorescent protein. *FEBS Letters,* **104,** 220-222.

Siemering, K. R., Golbik, R., Sever, R. & Haseloff, J. 1996. Mutations that suppress the thermosensitivity of green fluorescent protein. *Current Biology,* **6,** 1653-1663.

Slysz, G. W. & Schriemer, D. C. 2003. On-column digestion of proteins in aqueous-organic solvents. *Rapid Communications in Mass Spectrometry,* **17,** 1044-1050.

Smith, P. K., Krohn, R. I., Hermanson, G. T., Mallia, A. K., Gartner, F. H., Provenzano, M. D., Fujimoto, E. K., Goeke, N. M., Olson, B. J. & Klenk, D. C. 1985. Measurement of protein using bicinchoninic acid. *Anal Biochem,* **150,** 76-85.

Soellner, M. B., Dickson, K. A., Nilsson, B. L. & Raines, R. T. 2003. Site-specific protein immobilization by Staudinger ligation. *J Am Chem Soc,* **125,** 11790-1.

Sørensen, H. P. & Mortensen, K. K. 2005. Advanced genetic strategies for recombinant protein expression in Escherichia coli. *Journal of Biotechnology,* **115,** 113-128.

Stachowiak, T. B., Svec, F. & Frechet, J. M. J. 2006. Patternable Protein Resistant Surfaces for Multifunctional Microfluidic Devices via Surface Hydrophilization of Porous Polymer Monoliths Using Photografting. *Chem. Mater.,* **18,** 5950-5957.

Steinhauer, Christer Wingren, Farid Khan, Mingyue He, Michael J. Taussig & Carl A. K. Borrebaeck 2006. Improved affinity coupling for antibody microarrays: Engineering of double-(His)6-tagged single framework recombinant antibody fragments. *Proteomics,* **6,** 4227-4234.

Stulik, K., Pacakova, V., Suchankova, J. & Coufal, P. 2006. Monolithic organic polymeric columns for capillary liquid chromatography and electrochromatography. *Journal of Chromatography B,* **841,** 79.

Svec, F. & Frechet, J. M. J. 1992. Continuous rods of macroporous polymer as high-performance liquid chromatography separation media. *Anal. Chem.,* **64,** 820-822

Szczepaniak J. (2009) Ph.D Thesis. Dublin City University, Ireland

T

Traving, C. & Schauer, R. 1998. Structure, function and metabolism of sialic acids. *Cell Mol Life Sci,* **54,** 1330-49.

Tripp, J. A., Stein, J. A., Svec, F. & Frechet, J. M. J. 2000. "Reactive Filtration": Use of Functionalized Porous Polymer Monoliths as Scavengers in Solution-Phase Synthesis. *Org. Lett.,* **2,** 195-198.

Tsien, R. Y. 1998. The green fluorescent protein. *Annu Rev Biochem,* **67,** 509-44.

Tsumoto, K., Umetsu, M., Kumagai, I., Ejima, D. & Arakawa, T. 2003. Solubilization of active green fluorescent protein from insoluble particles by guanidine and arginine. *Biochemical and Biophysical Research Communications,* **312,** 1383.

V

Varki A. (1999) Essentials of glycobiology. Cold Spring Harbour, NY. :Cold Spring Harbour Laboratory Press, c1999.

Vass R. (2005) Ph.D Thesis. Dublin City University, Ireland

Vimr, E., Lichtensteiger, C. & Steenbergen, S. 2000. Sialic acid metabolism's dual function in Haemophilus influenzae. *Mol Microbiol,* **36,** 1113-23.

Vlakh, E. G., Tappe, A., Kasper, C. & Tennikova, T. B. 2004. Monolithic peptidyl sorbents for comparison of affinity properties of plasminogen activators. *Journal of Chromatography B,* **810,** 15-23.

Voss, S. & Skerra, A. 1997. Mutagenesis of a flexible loop in streptavidin leads to higher affinity for the Strep-tag II peptide and improved performance in recombinant protein purification. *Protein Eng,* **10,** 975-82.

W

Wallen, M. J., Laukkanen, M. O. & Kulomaa, M. S. 1995. Cloning and sequencing of the chicken egg-white avidin-encoding gene and its relationship with the avidin-related genes Avr1-Avr5. *Gene,* **161,** 205-9.

Walters, R. R. 2008. Affinity chromatography. *Analytical Chemistry,* **57,** 1099A-1114A.

Wang, Q., Chan, T. R., Hilgraf, R., Fokin, V. V., Sharpless, K. B. & Finn, M. G. 2003. Bioconjugation by Copper(I)-Catalyzed Azide-Alkyne [3 + 2] Cycloaddition. *Journal of the American Chemical Society,* **125,** 3192-3193.

Watzke, A., Kohn, M., Gutierrez-Rodriguez, M., Wacker, R., Schroder, H., Breinbauer, R., Kuhlmann, J., Alexandrov, K., Niemeyer, C. M., Goody, R. S. & Waldmann, H. 2006. Site-selective protein immobilization by Staudinger ligation. *Angew Chem Int Ed Engl,* **45,** 1408-12.

Weber, P. C., Ohlendorf, D. H., Wendoloski, J. J. & Salemme, F. R. 1989. Structural origins of high-affinity biotin binding to streptavidin. *Science,* **243,** 85-8.

Wilchek, M., Bayer, E. A. & Livnah, O. 2006. Essentials of biorecognition: the (strept)avidin-biotin system as a model for protein-protein and protein-ligand interaction. *Immunol Lett,* **103,** 27-32.

Wong, L. S., Khan, F. & Micklefield, J. 2009. Selective Covalent Protein Immobilization: Strategies and Applications. *Chemical Reviews*.

Wood, T. I., Barondeau, D. P., Hitomi, C., Kassmann, C. J., Tainer, J. A. & Getzoff, E. D. 2005. Defining the Role of Arginine 96 in Green Fluorescent Protein Fluorophore Biosynthesis. *Biochemistry,* **44,** 16211-16220.

Wu, G., Datar, R. H., Hansen, K. M., Thundat, T., Cote, R. J. & Majumdar, A. 2001. Bioassay of prostate-specific antigen (PSA) using microcantilevers. *Nat Biotechnol,* **19,** 856-60.

X

Xu, Q. & Lam, K. S. 2004. Protein and Chemical Microarrays: Powerful Tools for Proteomics. *ChemInform,* **35**.

Y

Yang, F., Moss, L. G. & Phillips, G. N., Jr. 1996. The molecular structure of green fluorescent protein. *Nat Biotechnol,* **14,** 1246-51.

Yang, Q., Liu, X. Y., Ajiki, S., Hara, M., Lundahl, P. & Miyake, J. 1998. Avidin-biotin immobilization of unilamellar liposomes in gel beads for chromatographic analysis of drug-membrane partitioning. *J Chromatogr B Biomed Sci Appl,* **707,** 131-41.

Youvan, D. C. & Michel-Beyerle, M. E. 1996. Structure and fluorescence mechanism of GFP. *Nat Biotech,* **14,** 1219.

Yu, C., Davey, M. H., Svec, F. & Frechet, J. M. J. 2001. Monolithic Porous Polymer for On-Chip Solid-Phase Extraction and Preconcentration Prepared by Photoinitiated in Situ Polymerization within a Microfluidic Device. *Analytical Chemistry,* **73,** 5088-5096

Z

Zacharias, D. A., Violin, J. D., Newton, A. C. & Tsien, R. Y. 2002a. Partitioning of Lipid-Modified Monomeric GFPs into Membrane Microdomains of Live Cells. *Science,* **296,** 913-916.

Zacharias, D. A., Violin, J. D., Newton, A. C. & Tsien, R. Y. 2002b. Partitioning of lipid-modified monomeric GFPs into membrane microdomains of live cells. *Science,* **296,** 913-6.

Zemann, A. J. 2003. Capacitively coupled contactless conductivity detection in capillary electrophoresis. *Electrophoresis,* **24,** 2125-2137.

Zemann, A. J., Schnell, E., Volgger, D. & Bonn, G. K. 1998. Contactless Conductivity Detection for Capillary Electrophoresis. *Anal. Chem.,* **70,** 563-567.